Brunel UNIVERSITY LONDON

Expression of Shelterin and Shelterin-associated Genes in Breast Cancer Cell lines

A thesis submitted for the degree of Doctor of Philosophy

By

Azadeh Motevalli

Division of Biosciences

School of Health Sciences and Social Care

January 2014

Declaration

I hereby declare that the research presented in this thesis is my own work, except where otherwise specified, and has not been submitted for any other degree.

Azadeh Motevalli

ABSTRACT

Mammalian telomeric DNA consists of tandem repeats of the sequence TTAGGG associated with a specialized set of proteins, known collectively as Shelterin. These telosomal proteins protect the ends of chromosomes against end-to-end fusion and degradation. The objective of this project was to investigate whether expression of Shelterin and Shelterin-associated proteins are altered, and influence the protection and maintenance of telomeres, in breast cancer cells. Initial findings showed that most of the Shelterin and Shelterin-associated genes were significantly down-regulated (at the mRNA expression level) in a panel of ten breast cancer cell lines. Epigenetic alterations to DNA (methylation at CpG Islands) and histones can result in altered expression of genes. Further investigations showed that the promoter region of *POT1* was partially methylated in the breast cancer cell line, 21NT. To support these observations, a DNA methylation inhibitor, 5-aza-CdR, and a histone deacetylation inhibitor, TSA, were used in an attempt to reactivate the expression of silenced genes. This work generated novel findings. Treatment with 5-aza-CdR and TSA resulted in the highest recovery of *TIN2* and *POT1* mRNA levels at both short-term (48 and 72 hours) and long-term (3 weeks) treatment of the breast cancer cell line, 21NT cells. In addition, *POT1* promoter methylation was analysed before and after treatment of 21NT cells. Bisulphite sequencing data were consistent with the mRNA expression results, showing up-regulation of *POT1*, as all methylation sites were demethylated after the treatment of 21NT cells with 5-aza-CdR. These studies also showed for the first time that both the short-term (72 hours) and 3 weeks treatment of 21NT cells with 5-aza-CdR was able to increase telomere lengths (using four measurement methods, i.e. TRF, q-PCR, flow-FISH and iQFISH).

Breast cancer cell lines expressed low levels of several telosomal mRNAs and that this down-regulation was found to be due in part to promoter methylation. Methylation was shown to be relieved through treatment of the cells with 5-aza-CdR and TSA; specifically, *POT1* was shown to be up-regulated to a higher extent compared with other Shelterin genes. Given that previous studies involved over-expression of *POT1* in telomerase-positive cells to demonstrate telomere length elongation, we addressed the possibility that over-expression of *POT1* may affect telomere length in 21NT breast cancer cells. The results showed that the average telomere length of the *POT1* over-expressing clones was increased by 2 to 3 kb compared with 21NT non-transfected and empty vector controls. The study also demonstrated that increased telomere length (by ectopic over-expression of *POT1*) is not due to a direct effect of telomerase enzyme activity. One explanation for this could be that *POT1* may induce a negative regulator of telomerase activity to maintain telomere length. Taken together, the results generated in this project suggest that *POT1* may control a localised activation of telomerase enzyme at the telomere end, and regulate stability of the Shelterin complex.

ACKNOWLEDGEMENTS

This thesis is the end of my journey in obtaining my PhD and has been kept on track and been seen through to completion with the support and encouragement of numerous people including my friends and colleagues. At the end of my thesis I would like to thank all those people who made this thesis possible and an unforgettable experience for me.

At this moment of accomplishment, first and foremost special thanks go to my supervisors, Professor Robert Newbold and Dr Terry Roberts; without their knowledge and guidance this thesis would not have been completed. Thank you for helping to develop my critical thinking and writing skills and introducing me to the exciting worlds of telomeres and Shelterin. My gratitude also goes to Dr Hemad Yasaei who always had excellent ideas and whose expertise has helped a lot with the design and interpretation of my experiments. I would also like to thank Dr Predrag Slijepcevic for all the advice and help he has given me in the field of cytogenetic.

I would like to express special thanks to Dr Sahar Al-Mahdawi and Mrs Alison Marriott for their expert advice and those little skills that have made a huge difference in my research. Additionally, I would like to express my eternal appreciation to my best friend, Dr Sara Anjomani Virmouni, whose dedication and persistent confidence in me, has taken the load off my shoulders most of the times.

I must say a special thanks to my colleagues Hannah Linne and Jessica Chiara Pickles for providing support and being there for me whenever I needed.

I would like to take the opportunity to offer my thanks to my friends Sepideh Aminzadeh Gohari, Dr Sheba Zahir, Dr Punam Bhullar, Dr Vahid Ezzatizadeh, Dr Maryam Ojani and Julie Davies who have given me their support and help throughout my PhD.

Last but not the least; my parents deserve special mention for their devoted support and prayers. My mother, in the first place is the person who gave me the fundamentals for my learning character, showing me the joy of intellectual pursuit ever since I was a child. My father is the one, who sincerely raised me with his caring and gentle love, and my brothers and my lovely sister for their sincere support in every way during my thesis.

And finally, to my dearest; Alireza Mohammadi who has and continues to be an endless source of encouragement, grounding and support; there is no doubt that I could not have done this without him.

TABLE OF CONTENTS

LIST OF FIGURES

LIST OF TABLES

LIST OF ABBREVIATIONS

ALT	Alternative Lengthening of Telomere
ANK	Ankarin
AP	Alkaline phosphate
ATM	Ataxia Telangiectasia Mutated
BCA	Bicinchoninic acid
BCAC	Breast cancer association consortium
BFB	Breakage-Fusion-Bridge
B-ME	β-Mercaptoethanol
BMI	Body mass index
Bp	Base pair
BRCA1	Breast cancer susceptibility genes 1
BRCA2	Breast cancer susceptibility genes2
BSA	Bovine serum albumin
BRIP1	BRCA1 interacting protein C-terminal helicase 1
C	Cytosine
CBP	CRB-binding protein
CDP-*Star*	Substrate solution
ChIP	Chromatin Immunoprecipitation
CLL	Chronic lymphocytic leukaemia
COSMIC	Catalogue of somatic mutations in cancer
CRUK	Cancer research UK
C_t	Threshold cycle
C5	Fifth carbon
DBD	DNA-binding domain
DCIS	Ductal carcinoma *in situ*
cDNA	Complementary DNA
DDR	DNA damage response
DIG	Digoxigenin
DKC	Dyskeratosis congenita
D loop	Displacement loop
DMEM	Dulbecco's modified eagle medium
DMSO	Dimethylsulphoxide
DNA	Deoxyribonucleic acid
DNMTs	DNA methyltransferases
DNMT1	DNA methyltransferase 1
DNMT2	TRDMT1
DNMT3L	DNA cytosine-like 5-methyltransferase
dNTPs	Deoxynucleotide triphosphate
DSBs	Double-strand breaks
ECL	Enhanced chemiluminescence
ECTR	Extra-chromosomal linear and circular telomeric DNA
EDTA	Ethylene diamine tetra-acetic acid
EGF	Epithelial growth factor
ER	Estrogen receptor
ES	Stem cells
FISH	Fluorescence *in site* hybridization
FITC	Fluorescein isothiocynate
EST1A	Ever shorter telomere 1
FCS	Fetal calf serum
FXLXP	TRF-binding motif
GAPDH	Glyceraldehyde-3-phosphate dehydrogenase
GAR domain	Gly/Arg-rich domain
G	Guanine

HATs	Acetyl transferase
HCC	Hepatocellular carcinoma
HCl	Hydrochloric acid
HER2	Human epidermal growth factor receptor 2
HMECs	Normal mammary epithelial cell strains
HR	Homologous Recombination
HRT	Hormone replacement therapy
HPA	Hybridisation protection assay
HPS	Histidine, proline and serine
IARC	The international agency for research on cancer
IDC	Infiltrating ductal carcinoma
ILC	Infiltrating lobular carcinoma
IPA	Isopropyl alcohol
IQ-FISH	Interphase Q-FISH
Kb	Kilobase
KCL	Potassium chloride
kDa	Kilo dalton
LCIS	Lobular carcinoma *in situ*
LOH	Loss of heterozigosity
LY-R	Radio-resistant mouse lymphoma cells
LY-S	Radio-sensitive mouse lymphoma cells
M1	Mortality stage 1
M2	Mortality stage 2
MeCP1	Methyl -CpG binding protein 1
MEF	Mouse embryonic fibroblast
MEM	Modified eagle medium alpha
MgCl2	Magnesium chloride
Ml	Millilitre
Ml	Microlitre
MRI	Magnetic resonance Imaging
MSP	Methylation specific PCR
NaCl	Sodium chloride
NaOH	Sodium hydroxide
NHEJ	Non-homologous end Joining
NTC	No template control
Nt	Nucleotides
OB-fold	Oligonucleotide/oligosaccharide binding domain
OD	Optical densitometry
PARP	Poly (ADP-ribose) polymerase
PBS	Phosphate buffer solution
PC3	Prostate cancer cell line
PCR	Polymerase chain reaction
PI	Propidium iodide
PinX1	PIN2/TRF1-interacting, telomerase inhibitor 1
PNA	Peptide nucleic acid
POT1	Human protection of telomeres 1
Q-FISH	Quantitative *in situ* hybridization
RAP1	Repressor activator protein 1
RNA	Ribonucleic acid
RNAi	RNA interference
RNP	Ribonucleoprotein
RPA	Replication protein A
Rpm	Revolutions per minute
RPMI	Roswell park memorial institute
RT	Room temperature
RT	Reverse transcriptase

RT-PCR	Reverse Ttanscriptase polymerase chain reaction
RUNX3	Runt-related transcription factor 3
RQ	Relative quantification
SAM	S-adenosyl-L-methionine
SCG	Single copy gene
Sec	Seconds
SEM	Standard error of the mean
SNPs	Single nucleotide polymorphisms
Ss	Single-stranded
SSC	Saline-sodium citrate
ssDNA	Single strand DNA
STELA	Single telomere length analysis
SV	Splice variants
T	Thymidine
TBE	Tris-Borate EDTA
TBPs	Telomere binding proteins
TE	Tris-EDTA
TEP1	Telomerase- associated protein 1
TERT	Telomerase reverse transcriptase
TFI	Telomeric fluorescence intensity
Telomere loop	T-loop
TIN2	TRF1-interacting nuclear protein2
TNKS1/2	Tankyrase1 and 2
TR	Telomerase RNA
TRAP	Telomere-repeat amplification
TRDMT1	tRNA aspartic acid methyltransferase 1
TRF	Terminal restriction fragment
TRF1	Telomeric repeat binding Factor 1
TRF2	Telomeric repeat binding Factor 2
TSA	Trichostatin A
T-SCE	Telomere-sister chromatid exchanges
TSG	Tumour suppressor gene
5-aza-CdR	5-aza-2'-deoxycytidine

CHAPTER I

GENERAL INTRODUCTION

1.1-Structure and function of the breast

The female breast is an assemblage of mammary glands and fatty tissue in conjunction with nerves, veins, arteries and connective tissues known as the fascia (American cancer Society 2013, Cancer research UK). The glands are placed on the subcutaneous layer of the anterior and a portion of the lateral thoracic wall. The breast is made up of the secretory glandular tissue which is located in the upper portion of the breast and surrounding adipose tissues (Figure 1.1). The glandular tissues are separated by septa of connective tissues and organized into 15 to 20 sections which are called lobules. Each lobule contains its own duct systems and interacts with a lactiferous duct to course via the breast towards the nipple/areolar part. Additionally, during lactation, lobules produce milk which is transported to the nipple by the ducts (Rakha, El-Sayed *et al.* 2008) (Figure 1.1). Before puberty, functional and structural differences between the male and female breast cannot be distinguished. In women, however the production of hormones such as estrogen and progesterone results in the proliferation of ductal cells and the development of a network of lobes and lobules in preparation for lactation. In male, there are a small number of ducts just behind the nipple. However because men do not produce any milk there is no lobule development (Rakha, El-Sayed *et al.* 2008) (Figure 1.1).

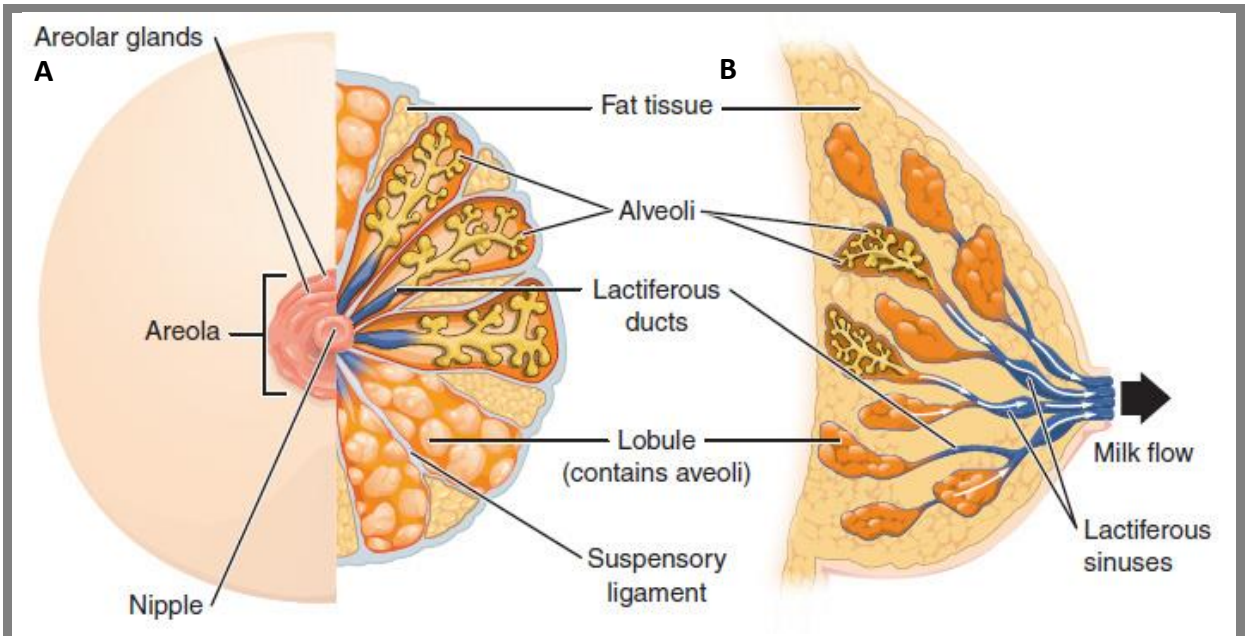

Figure 1.1-Schematic diagram showing the anatomy and physiology of the male **(A)** and female **(B)** breast (Image obtained from http://cnx.org/content/m46392/latest/ website).

1.2-Breast cancer

1.2.1-Epidemiology, incidence and mortality rates

Breast cancer is the most common type of cancer in women in developed countries (Cancer Research UK, 2008) (Figure 1.2). It is estimated that in the 1990s, breast cancer accounted for approximately 1 in 3 of all female cancers in the UK and Ireland. Indeed, current trends have shown a rise in incidence such that 1 in 8 women will develop breast cancer in the UK at some time in their lives (Cancer Research UK, 2010). Based on current estimated data in 2010, 49,564 females and 397 males were diagnosed with breast cancer, which also caused 11,556 women and 77 male deaths in the UK (Cancer research UK 2010).

Universally, the incidence and mortality rates of breast cancer vary around the world. As shown in Figure 1.2, in less-developed countries, the incidence and mortality rates

were lower in 2008 in comparison with those in Europe (Cancer Research UK, 2008). In the USA, newly estimated data obtained in 2013 showed that over 232,340 females and 2,240 males were diagnosed with breast cancer and it caused 39,620 female and 410 male deaths (National Statistics, 2013). In contrast, the mortality rates in the US have decreased since 1980, due to earlier detection methods and improved treatments (Chu, Tarone *et al.* 1996).

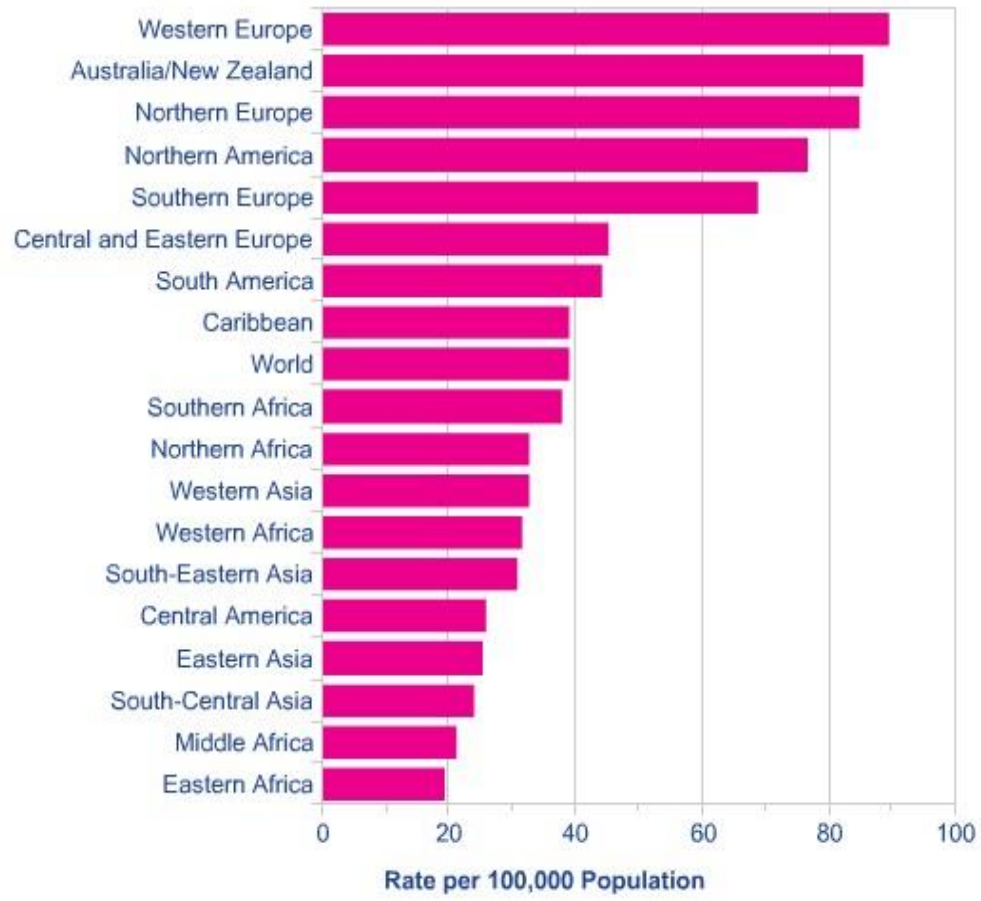

Figure 1.2-Standardized mortality for breast cancer in different countries. The estimated data show that female breast cancer incidence is highest in Western European countries with the lowest rate observed in Middle and Eastern Africa (Cancer Research UK, 2008 http://www.cancerresearchuk.org/cancer-info/cancerstats/types/breast/incidence/).

The International Agency for Research on Cancer (IARC) revealed that the highest male breast cancer incidence rates occurred in Israel with an age-adjusted rate of 1.24 per 100,000. Interestingly, the lowest incidence rates for both males (0.16/100,000) and females (18.0/100,000) were reported in Thailand. In 2013, so far, breast cancer caused 88,886 deaths in females in European countries representing a 7% decrease since 2009. In Southern and Eastern European countries, the highest incidence rates (among women and men) have been reported in Italy (Ly, Forman *et al.* 2013). However, the lowest breast cancer incidence rates were reported in the Russian Federation and Ukraine in comparison with the rest of European countries (Ly, Forman *et al.* 2013).

Like most epithelial cancers, breast cancer is strongly related to age. As shown in Figure 1.3, breast cancer accounted for approximately 17% of cancer-related deaths in females in European countries (Ferlay, Steliarova-Foucher *et al.* 2013). The variation of incidence and mortality rate in industrial countries indicated that many factors such as ethnic and life style risk factors (diet, alcohol, smoking, and obesity), use of hormone replacement therapy (HRT) in post-menopausal women, and socio-economic status are implicated in increasing breast cancer development (Li, Weiss *et al.* 2000; Chen, Weiss *et al.* 2002; Rosenberg, Magnusson *et al.* 2006).

According to Cancer Research UK, in 1989, 15,625 women died from breast cancer in comparison with 12,417 in 2005. The estimated 5-year survival rates of women diagnosed with breast cancer was 50% in the UK and Wales in the 1970s, but since that time the survival rates have increased to more than 80% (National Statistics, 2007). This reduction in the number of deaths is thought to be attributed to various factors such as earlier detection of the disease due to raised awareness among females, widespread mammography

screening programs and development of more effective treatments (e.g. mastectomy or removal of lymph nodes, lumpectomy, radiotherapy, chemotherapy and hormone therapy) (Botha, Bray *et al.* 2003; Weigelt, Horlings *et al.* 2008).

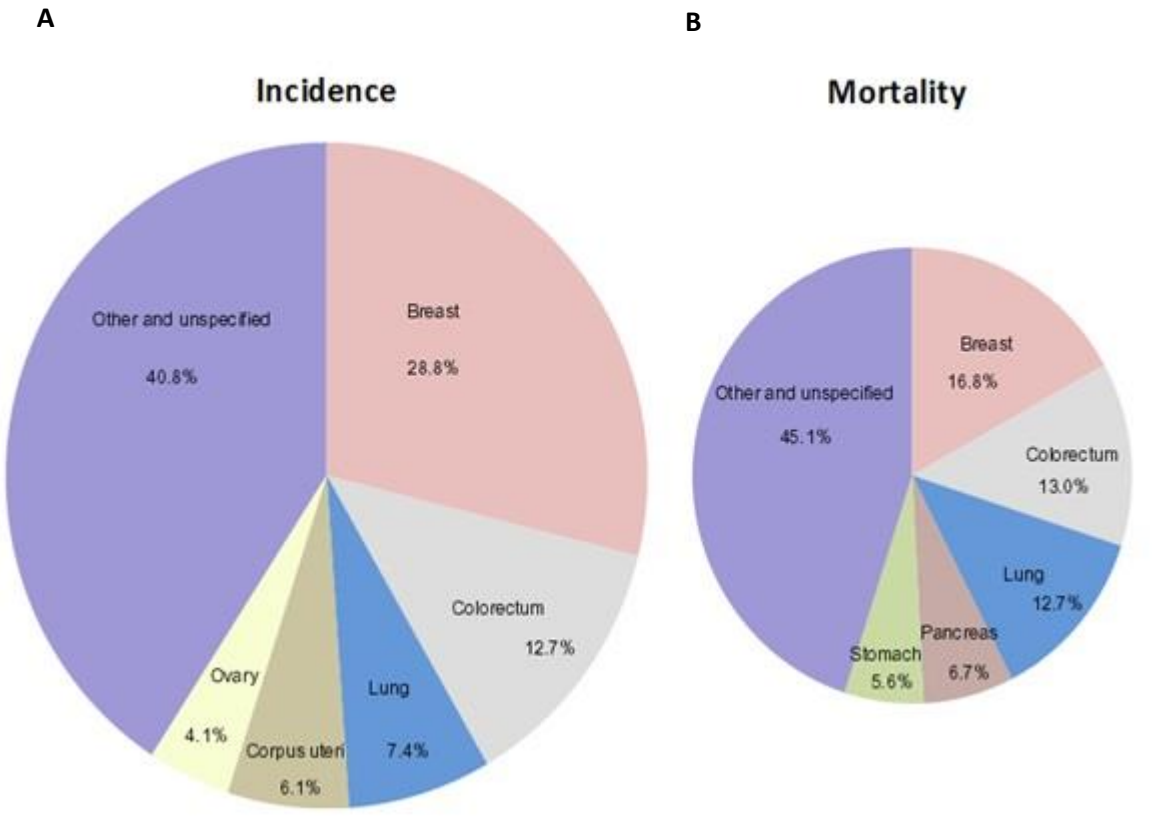

Figure 1.3-Incidences (A) and mortalities (B) of female cancers in Europe. The area of the pie chart indicates the proportion of incidence and death. Breast cancer in comparison with other cancers had the highest incidence and mortality rates (Ly, Forman *et al.* 2013).

1.2.2-Development of breast cancer

Breast cancer is characterized by uncontrolled growth of mammary epithelial cells (e.g. luminal or ductal) when they are in proliferative state. Breast cancer is classified into different stages based on the tumour phenotype i.e.; normal to hyperplasia, carcinoma *in situ*, invasive carcinoma and metastatic cancer. Many breast cancers most commonly start

to develop within the ducts or lobules and are known in the early stages as ductal or lobular carcinoma *in situ* (DCIS/LCIS) or, subsequently, as an invasive carcinoma that infiltrates connective and fatty tissues (Weidner, Semple *et al.* 1991; Simpson, Gale *et al.* 2003). Cancer Research UK reported that DCIS accounts for approximately 25% of all breast cancers. In contrast, lobular carcinoma *in situ* is a rare form of cancer which is not classified as breast cancer (Table 1.1). Ductal carcinoma *in situ* (DCIS) or intraductal carcinoma of the breast is the most common type of non-invasive breast cancer as the abnormal epithelial cells have not grown beyond adjacent fatty and connective tissues and grow slowly (Figure 1.1) (Allred 2010). Such cancers would initially not overtly affect the woman's health but can be detected by mammography. A positive mammogram would be normally confirmed by biopsy to identify the presence of malignant cells (American Cancer Society, 2013), which can then also be classified as low, intermediate or high grade. The estimated incidence rate indicates that DCIS is more common in females at age 60 and over. However, it is uncommon under the age of 35 years. The risk factors for DCIS include high body mass index (BMI), increased breast density and nullparity (Virnig, Tuttle *et al.* 2010). Lobular carcinoma *in situ,* also known as lobular neoplasia (LCIS) is a rare pre-cancerous type of cancer and is implicated as a risk factor in increasing the development of invasive breast cancer (Table 1.1) (Simpson, Gale *et al.* 2003; Arpino, Bardou *et al.* 2004). The predominant form of invasive ductal breast carcinoma is known as infiltrating ductal carcinoma (IDC) and is responsible for approximately 85% of cases. IDC originates in the milk ducts, invades into the fatty tissues and, from there, may metastasize to other parts of the body (Wiechmann and Kuerer 2008). A high Body Mass Index (BMI), nullparity or having late first child, increased breast density, early menstruation and drinking more than three alcoholic drinks

per day are all risk factors correlated with the development of IDC (Virnig, Tuttle *et al.* 2010). The lowest incidence rate of IDC is observed in females under 30 and the highest rates occur at age 75 and over (Virnig, Tuttle *et al.* 2010). Yet another form of invasive breast cancer is infiltrating lobular carcinoma (ILC) and, in comparison with LCIS, is more aggressive and accounts for 8-14% of breast cancer diagnosis (Table 1.1). ILC expands in the milk-producing glands (lobules) and often spreads to other regions of the body (Arpino, Bardou *et al.* 2004; Wiechmann and Kuerer 2008).

Table 1.1-Different stages and classification of breast cancer. The T classification of the primary tumour is based on clinical or pathological criteria or both. Tis = *in situ* disease (not fully invasive). Table obtained from National Cancer Institute, 2013: (http://www.cancer.gov/cancertopics/pdq/treatment/breast/healthprofessional/Table1)

Stages	Tumour size	Characteristic
Stage 0	Tx	Primary tumour cannot be assessed
	T0	No evidence of primary tumour
	Tis	Carcinoma *in situ*
	Tis (DCIS)	Ductal Carcinoma *in situ* (DCIS)
	Tis (LCIS)	Lobular Carcinoma *in situ* (LCIS)
	Tis (Paget)	Paget's disease of the nipple with no associated tumour mass
Stage 1	T1, Tumour size ≤20mm	Node status; clear or negative nodes
Stage 2	T1, Tumour size ≤ 1mm	Node status; clear or negative nodes, Cancerous, No spread of tumour
	T1a, Tumour size> 1mm	Node status; clear or negative nodes, Cancerous, No spread of tumour
	T1b, Tumour size> 5mm	Node status; clear or negative nodes, Cancerous, No spread of tumour
	T1c, Tumour size> 10mm	Node status; clear or negative nodes, Cancerous, No spread of tumour
	T2, Tumour size> 20mm	Node status; clear or negative nodes, Cancerous, No spread of tumour
	T3, Tumour size> 50mm	Node status; clear or negative nodes, Cancerous, No spread of tumour
Stage 4	T4, any size	Spread to chest wall or to the skin
	T4a, any size	Spread to chest wall, not includes only pectorallis muscle
	T4b, any size	Tumour has spread
	T4c, Both T4a and T4b	Both T4a and T4b
	T4d	Inflammatory carcinoma

1.2.3-Breast cancer diagnosis and treatment

Breast cancer is diagnosed by a variety of different methods, including self-examination, clinical examination, mammography, ultrasound and Magnetic Resonance Imaging (MRI) (Saslow, Boetes *et al.* 2007; Yu, Liang *et al.* 2010). The clinical examination typically reveals a lump within the breast tissue and in some cases involves the nipple or skin around the affected region (College of American Pathologists-CAP, 'Breast Cancer' 2011). Mammography, as a non-invasive method, is the most common imaging tool which is used to detect suspected breast tumours, premalignant or begin lesions, with a good degree of accuracy. In addition, mammograms are able to increase significantly the efficacy of diagnosis by detecting the detailed abnormalities of an early stage tumour including irregular densities, micro-calcification and architectural distortion progression, even before they can be recognized by clinical examination (Gotzsche and Nielsen 2011). MRI and ultrasound techniques are often used to refine diagnosis providing additional imaging information (Schmitz, Gianfelice *et al.* 2008).

The treatment of breast cancer depends on the accurate determination of the stage of the disease. For instance, tumour cells at stage IV (metastatic cancer, IDC) are more likely to have spread into surrounding stromal tissue. Therefore, initial visualisation of the tumour mass by mammography is essential for a better prognosis and survival chances. Lumpectomy which involves removal of the tumour lesion together with a margin of surrounding normal tissue is the most common treatment of DCIS (Weigelt, Horlings *et al.* 2008). However, patients at this stage of disease can decide to have removed a wide area or, alternatively, a relatively small amount of surrounding tissue. Mastectomy, involving removal of all breast tissue including skin and nipple, may be required in order to prevent

reoccurrence of the invasive ductal carcinoma (Cancer Research UK, 2013). In the case of to LCIS and ILC, malignant cells rarely form a palpable mass, and are therefore not easily detectable with mammography or by breast examination (Biglia, Mariani *et al.* 2007).

1.2.4-Molecular genetics of breast cancer

Two classical models of breast cancer exist; (i) sporadic cancer, which is caused by a combination of somatic genetic and environmental factors and (ii) familial cancer, which is a result of a predisposing mechanism of genetic alteration (Table 1.2) (Kenemans, Verstraeten *et al.* 2004). Epidemiological studies have classified familial breast cancer genes susceptible to germline mutations into high-risk and low-to moderate-risk classes (Mangia, Malfettone *et al.* 2011). *BRCA1*, *BRCA2*, *PTEN*, *TP53*, *LKB1/STK1* and *CDH1* are categorized as high risk genes, whereas *CHEK2*, *TGFβ1*, *CASP8* and *ATM* are classified as those with low-to moderate-risk (Mangia, Malfettone *et al.* 2011).

Table 1.2-Represents familial and sporadic breast cancer genes (Eisenhauer, Chaturvedi *et al.* 2001; Murata, Khattar *et al.* 2002; Mangia, Malfettone *et al.* 2011; Deb, Do *et al.* 2013).

Gene	Familial breast cancer	Sporadic breast cancer	Function
BRCA1	*		DNA damage response
BRCA2	*		DNA damage response
PALB2	*		DNA damage response
BRIP1	*		DNA damage response
ATM	*		DNA damage response
NBS1	*		DNA damage response
RAD50	*		DNA damage response
CHEK2	*		DNA damage response
P53	*		Tumor suppressor
PTEN	*		Tumor suppressor
PIK3CA	*		Coordinate a diverse range of cell functions
hMSH2		*	Tumor suppressor
hMLH1		*	DNA repair pathway
COMT		*	Enzymatic interaction in the metabolism of estrogen
YP1A1		*	Enzymatic interaction in the metabolism of estrogen
CYP1B1		*	Enzymatic interaction in the metabolism of estrogen
GSTM1		*	Enzymatic interaction in the metabolism of estrogen
GSTT1		*	Enzymatic interaction in the metabolism of estrogen

It is estimated that approximately 5% of breast cancer cases are hereditary and linked to germ-line alterations in *BRCA1* and *BRCA2* tumor suppressor genes. These genes are known to be mutated in breast cancer (Couch, Farid *et al.* 1996; Brohet, Velthuizen *et al.* 2013). In addition, it has been shown that *BRCA1* is sometimes hypermethylated at its promoter region in breast cancer (Catteau, Harris *et al.* 1999; Jacot, Thezenas *et al.* 2013). Human epidermal growth factor receptor 2 (*HER2*) is another tumor suppressor gene that plays a fundamental role in cell growth. Martin (2006) reported that over-expression of *HER2* (primarily via gene amplification) in 20% of breast cancer cases could lead to excessive cell growth and result in aggressive tumor cells (Lacey, Devesa *et al.* 2002; Martin 2006). *TP53* is a key tumor suppressor gene (TSG) that is found to be mutated in approximately 40% of sporadic breast cancers (Miller, Smeds *et al.* 2005). A high frequency of loss of heterozygosity (LOH) involving the *BRCA* and *p53* genes has been identified in many sporadic breast cancers (Johnson, Shaw *et al.* 2002). A study by Byrnes *et al.* (2008) showed that there are other genes apart from the 'key driver' genes involved in breast cancer (Byrnes, Southey *et al.* 2008). For instance, BRCA1 interacting protein C-terminal helicase 1 (*BRIP1*) plays a role in *BRCA1*-dependent DNA repair and cell cycle checkpoint function, and encodes a helicase that interacts with the BRCA1 C-terminal domain. Mutation of this gene is also linked with an increased risk of breast cancer (Levitus, Waisfisz *et al.* 2005; Litman, Peng *et al.* 2005). A partner of *BRCA2*, the *PALB2* gene is involved in the double-strand DNA repair pathway, and interacts with the BRCA2 protein which plays a role in homologous recombination (HR). In multiple populations, this gene has been screened for the presence of mutations in multiple small studies of familial and early-onset of breast cancer (Reid, Schindler *et al.* 2007; Tischkowitz, Capanu *et al.* 2012). Previous findings by Byrnes *et al.*

(2008) showed that mutations in the *BRCA2* are correlated with a high risk of breast cancer. *RAD51* paralogs or *RAD51* and the family of *RAD51*-related genes are associated with repairing DNA damage through cooperation with various DNA repair proteins such as BRCA1 and BRCA2. The RAD51 protein has a central role in single-strand annealing and is involved in responding to DNA damage (Suwaki, Klare *et al.* 2011). Six monoallelic mutations of *RAD51C*, one of the subfamily of *RAD51*-related genes, were found in breast cancer (Meindl, Hellebrand *et al.* 2010). In addition, *RAD51D* and *RAD51L1* genes were reported as having a possible association with ovarian and breast cancer risk (Loveday, Turnbull *et al.* 2011; Pelttari, Kiiski *et al.* 2012).

1.3-Telomeres

Telomeres are made up of G-rich nucleotide repeats of the sequence $(TTAGGG)_n$ bound by associated proteins at the ends of the chromosomes of eukaryotic and all mammalian cells (Griffith, Comeau *et al.* 1999; Smogorzewska and de Lange 2004). Telomeric DNA together with the associated telosomal proteins, collectively known as the Shelterin complex, are essential for the overall maintenance of genome integrity and prevent DNA degradation and chromosome end-to-end fusions (Palm and de Lange 2008). In normal mammalian chromosomes, telomeric DNA contains 5 to 15 kilobases of tandem TTAGGG repeat sequences that get critically shorter in telomerase-negative cells after each cell cycle division, due to the end replication problem (Harley, Futcher *et al.* 1990). When the terminal primer is degraded through the process of lagging strand synthesis, the 5' gap appears at both ends of linear chromosome (Levy, Allsopp *et al.* 1992). The ends of chromosomes are synthesized in a 5' to 3' direction which degrades about 130 to 210

nucleotides during each cell cycle, resulting ultimately in the telomere reaching a critically short length. The end replication problem was first suggested by Nobel prize winner, James Watson (Watson 1972). At about the same time it was proposed that short telomere length is linked to the end replication problem at the 3´ end (Olovnikov 1973) (Figure 1.4).

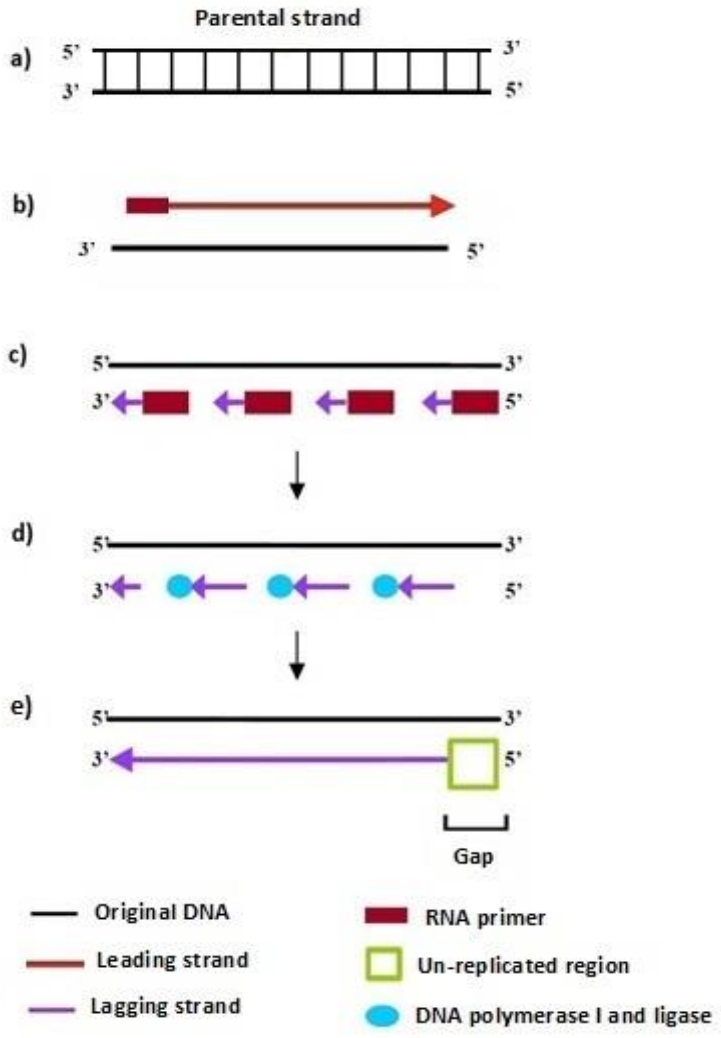

Figure 1.4-Shematic representation of the "end replication problem" during DNA replication. a) A parental DNA strands. **b)** In each cycle of DNA replication, the leading strand is synthesized. **c)** However, in the lagging strand formation of an Okazaki fragment requires an RNA primer **(d)** which leaves a gap of about 8 to 12 base pair in the 5´ end of lagging strand. **e)** Thus, the end of the lagging strand cannot be replicated and is lost after several rounds of cell division; hence results in the shortening of 5´ end and 3´ overhang. This model described by Makarov *et al.* (1997) (Makarov, Hirose *et al.* 1997).

During the process of DNA replication, telomeric DNA does not replicate properly due to the inefficiency of DNA polymerase to complete replication of the 5´ end of a linear chromosome. To prevent incomplete replication of the 5´end of a linear telomeric DNA, chromosomes are "capped" as hypothesized by McClintock and Muller (Muller 1938; McClintock 1941; Elizabeth H Blackburn 2006). Thus, the terminal nucleotides of chromosomal DNA are capped by telomeres which have evolved to protect them from enzymatic degradation and thus add stability to the chromosomes (Shampay, Szostak *et al.* 1984).

1.3.1-Telomere structure and function

The ends of telomeres contain a single-stranded 3'-guanine-rich extension (the G-strand) called the 3' overhang that is located between 50-500 nucleotide from the end of the telomere; the complementary strand is known as the cytosine-rich strand (the C-strand). The telomerase enzyme is responsible for maintaining the 3' overhang by extending its length by 100-300 base pairs beyond the C-rich strand, per division (Palm and de Lange 2008). It has been previously shown by electron microscopy that telomeres consist of two loops (Griffith, Comeau *et al.* 1999) (Figure 1.5). The telomere loop (T-loop) is a large duplex lariat structure in mammalian telomeres. The telomeric DNA folds back into itself to form T-loop and the 3' overhang binds to the 5' end of duplex strand of telomeric repeats to form a displacement loop (known as the D-loop) (Griffith, Comeau *et al.* 1999; Wright and Shay 2005) (Figure1.5).

The six-protein Shelterin complex packages telomeric DNA and helps to hide the chromosome ends from being detected as a double stranded break during the DNA

replication process. The proteins belonging to the Shelterin complex are: Telomeric Repeat binding Factor 1 (TRF1), Telomeric Repeat binding Factor 2 (TRF2), Protection of Telomeres 1 (POT1), TRF1-interacting nuclear protein 2 (TIN2), TPP1 (known as ACD, adrenocortical dysplasia homolog) and Repressor activator protein 1 (RAP1) (Figure 1.5). TRF1 and TRF2 bind to the double stranded T-loop of telomeric DNA and are implicated in maintaining the formation of the T-loop structure, while POT1 interacts with single-stranded TTAGGG repeats at the 3' overhang, as well as in the D-loop of the T-loop configuration. TRF1 and TRF2 recruit TIN2, RAP1, TPP1, and POT1 to telomeric DNA (van Leth, Andrews *et al.* 2005).

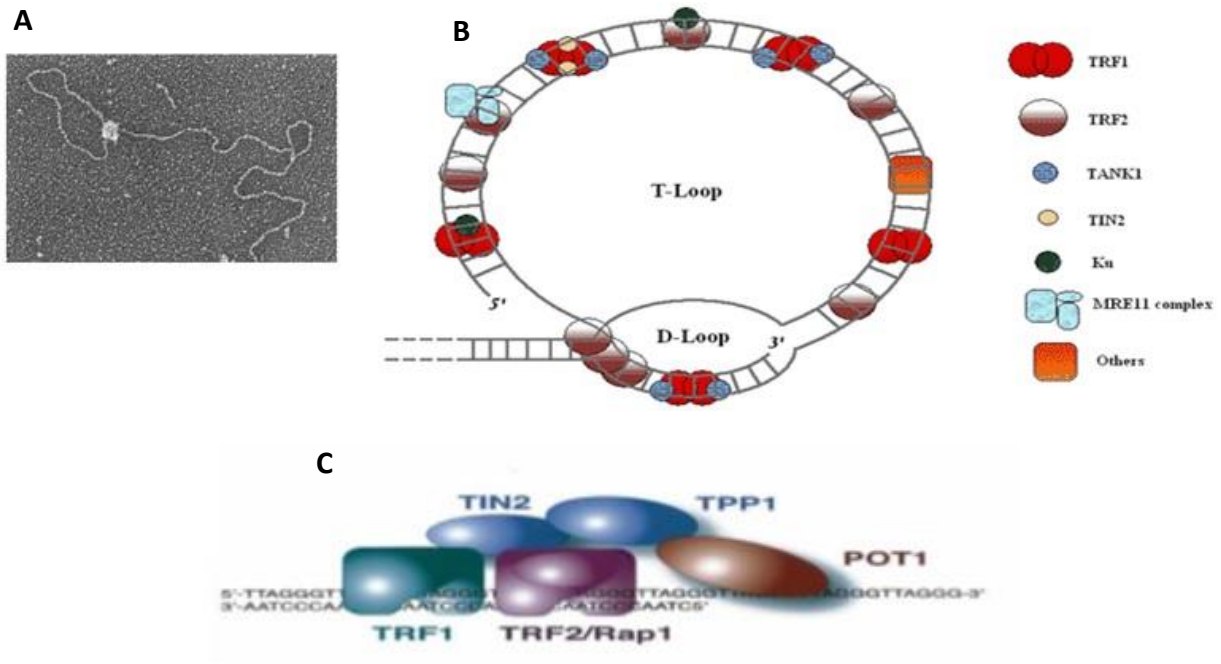

Figure 1.5-T-loop structure of the mammalian telomeric 'cap'. A) T-loop structure of human telomere imaged by electron microscopy (Griffith, Comeau *et al.* 1999). **B)** The single-stranded portion of the 3´overhang of telomeric DNA folds into the double stranded DNA and forms a larger T-loop and a smaller D-loop (de Lange T. 2006). **C) Schematic of the Shelterin complex on telomeric DNA.** POT1 is shown only at the binding site closest to the duplex telomeric DNA and binds directly to the 3´ single stranded over hang. TRF1 and TRF2 are the only Shelterin proteins that bind to double-stranded telomeric DNA (de Lange 2005).

Another vital function of telomeres is to prevent the loss of genetic information at the 5' end of a newly synthesized chromosome, by allowing the terminal ends to be replicated completely. This process can be accomplished in the presence of the telomerase enzyme. However, in the absence of telomerase, telomeres are gradually lost due to the "end replication problem" with each consecutive cell cycle (Figure 1.4). In normal cells, when the length of a telomere becomes critically short, the cells stop dividing and, having reached their Hayflick limit, undergo replicative senescence or apoptosis (Hayflick and Moorhead 1961; Makarov, Hirose *et al.* 1997). At the point when telomeres become dysfunctional, chromosomal end-to-end fusions can occur (Levy, Allsopp *et al.* 1992). Conversely, in the presence of telomerase enzyme activity (in unicellular organisms, in germline mammalian cells and in cancers) the shortening of telomeres that leads to senescence is avoided (Shippen-Lentz and Blackburn 1989).

1.3.2-Telomere shortening in breast cancer

Telomere dysfunction through telomere shortening and/or dysregulation of telomeric DNA-binding proteins (Shelterin), occurs in both the *in situ* and invasive stages of many cancers, such as breast cancer (Butler, Hines *et al.* 2012). Clinical observations have indicated that short telomere length increases a risk of developing epithelial cancers (Plentz, Wiemann *et al.* 2003).

Butler *et al.* (2012) showed that Shelterin genes play a fundamental role in regulating telomere length in breast tumours. They reported that the mRNA levels of *TRF1*, *TRF2* and *POT1* were inversely correlated with telomere length. Telomere shortening was observed in breast cancer tissues whereas the mRNA levels of aforementioned genes were up-regulated

(Butler, Hines *et al.* 2012). In addition, a recent study by Ramsay *et al.* (2013) showed that mutation of *POT1* in many carcinomas such as lung, ovarian and breast causes telomere dysfunction (Ramsay, Quesada *et al.* 2013). Therefore, dysregulation of telomere length through telomere-binding proteins suggests a common molecular mechanism that underlies clinical abnormalities. Hence, a better understanding the role of telomeres and telomere binding proteins may have a fundamental impact on breast cancer diagnosis and treatment.

1.3.3-Telomere dysfunction and senescence

Numerous recent advances in molecular and cell biology have shown that telomere dysregulation is involved in cellular senescence and cell death. Telomere dysfunction appears through diverse mechanisms such as Shelterin dysfunction and telomere shortening (Sfeir and de Lange 2012). Mutations within telomere-associated (telosomal) proteins (such as POT1) can alter the expression or function of these proteins, leading to telomere dysfunction (Ramsay, Quesada *et al.* 2013). Several studies have shown that the DNA damage response (DDR) is induced by telomere shortening via the activation of tumor suppressor proteins namely p53 and Rb proteins, and consequently p53-p21 and p16-pRb growth arrest pathways (Campisi 2005; Kuilman, Michaloglou *et al.* 2010; Rodier and Campisi 2011). Two significant blockades have been postulated to inhibit normal cells transforming into cancerous cells: Mortality stage 1 (M1) and Mortality stage 2 (M2) (Shay, Pereira-Smith *et al.* 1991). At the M1 stage, cells stop dividing via the DDR which leads to senescence. However, some cells are able to bypass the M1 stage via inactivation of p53 and pRB pathways and hence, they can continue to divide with further decreasing telomere length. When the lengths of telomeres are reduced to critical levels, cells enter into the M2 stage. At this stage, genetic abnormalities such as end-to-end chromosomal fusions,

anaphase bridges and uncapped chromosome ends occur (Newbold 2005). Chromosomal instability is triggered through increased telomeric end-to-end fusions, resulting in dicentric chromosomes via breakage-fusion-bridge (BFB) cycles. It is important to note that, during mitosis, chromosome instability can continue when the two centromeres of a dicentric chromosome are pulled to the opposite poles by spindles (so the called breakage-fusion-bridge cycle). Genomic instability is correlated with the frequency of cell death or senescence making M2 difficult to distinguish from M1 (Stewart and Weinberg 2006). However, some rare cells are able to escape from M2 through reactivation of telomerase expression and become immortal (Wright, Pereira-Smith *et al.* 1989).

It is known that the telomerase enzyme is active in germ line and stem cells, but inactive in most normal diploid somatic human cells, and it is thought that the latter has evolved as a protection against cancer. Approximately 85 to 90% of cancer cells display high telomerase activity (Kim, Piatyszek *et al.* 1994; Cong, Wright *et al.* 2002). However, a minority of cancers (~15%) and some immortalized cells can maintain telomere length via Alternative Lengthening of Telomere mechanism (ALT) (Feldser, Hackett *et al.* 2003; Newbold 2005; Shay and Wright 2005; Stewart and Weinberg 2006). ALT cell lines are characterised by several unique features including heterogeneous telomere length, presence of extra-chromosomal linear and circular telomeric DNA (ECTR), high frequency of telomere-sister chromatid exchanges (T-SCE) and ALT associated promyelocytic leukemia bodies (APBs) (Royle, Foxon *et al.* 2008; Conomos, Pickett *et al.* 2013).

1.4-Telomerase

Telomerase is a unique cellular ribonucleoprotein (RNP) complex that synthesizes TTAGGG sequence repeats onto the 3' end of chromosome terminals (Griffith, Comeau *et al.* 1999; Wyatt, West *et al.* 2010). The core enzyme contains two subunits: telomerase reverse transcriptase (TERT) and telomerase RNA (TERC) (Figure 1.6) (Meyerson, Counter *et al.* 1997). The TR molecule, complementary to the telomeric repeats, is an important element

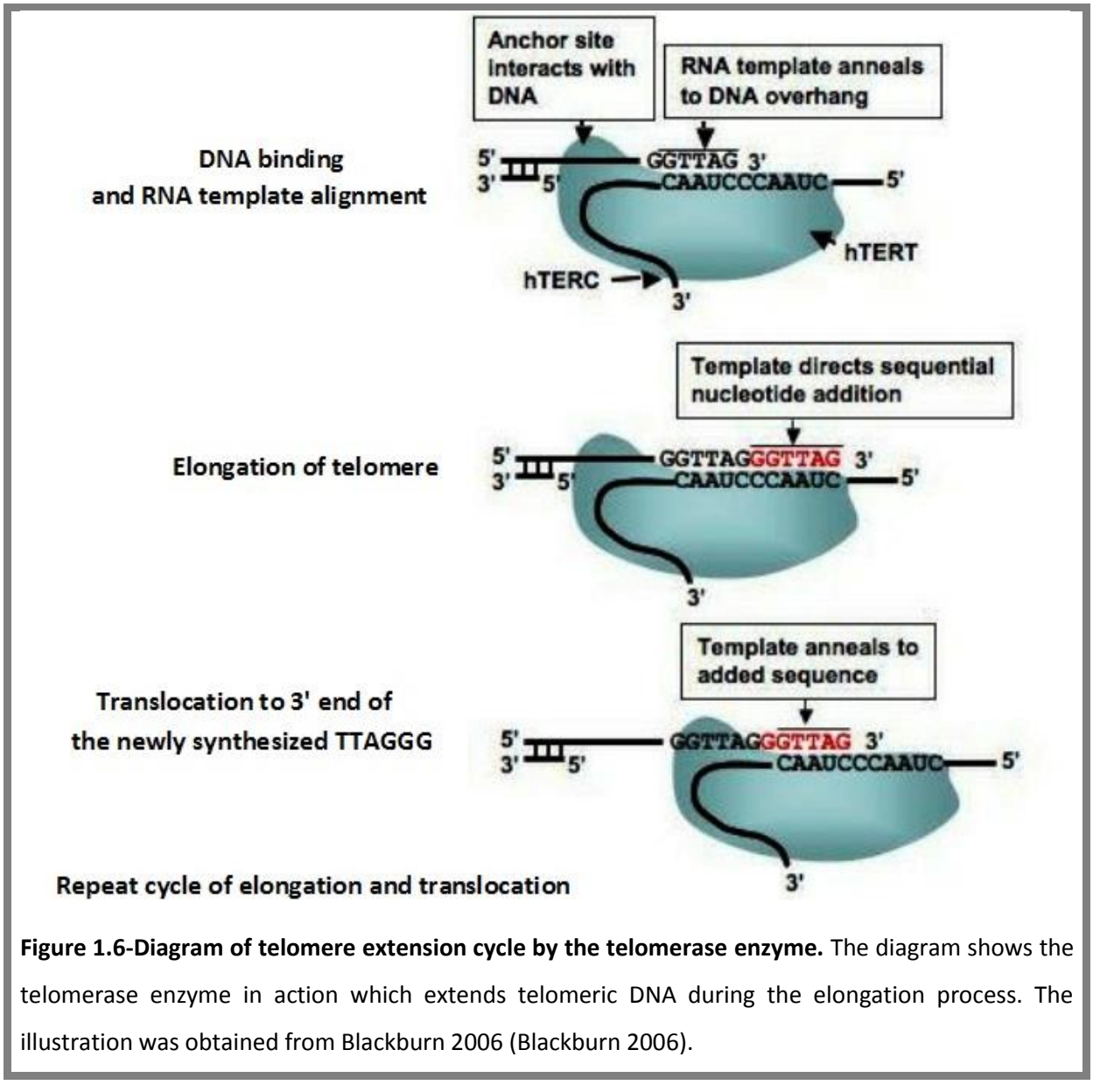

Figure 1.6-Diagram of telomere extension cycle by the telomerase enzyme. The diagram shows the telomerase enzyme in action which extends telomeric DNA during the elongation process. The illustration was obtained from Blackburn 2006 (Blackburn 2006).

of the telomerase enzyme; it consists of an RNA template region that facilitates adding telomeric repeats through the action of the reverse transcriptase catalytic subunit of telomerase (TERT) (Autexier and Lue 2006). These two subunits can bind with additional proteins that together expedite synthesis and elongation of telomeric DNA (Wyatt, West *et al.* 2010).

1.5-Shelterin genes structures and functions

1.5.1-Telomeric Repeat binding Factor 1 (TRF1)

TRF1, the first member of the Shelterin complex, was discovered in HeLa cells and is a ubiquitously expressed protein of 439 amino acids (Zhong, Shiue *et al.* 1992; Chong, van Steensel *et al.* 1995; van Steensel and de Lange 1997) (Figure 1.7). TRF1 contains a 50 amino acid C-terminal Myb DNA-binding domain that directly binds to the double stranded telomeric DNA and is localized to the nucleus. The Myb domain is one of the three helical domains that are involved in specific-protein-DNA or protein-RNA interactions (Chong, van Steensel *et al.* 1995; Bianchi, Smith *et al.* 1997). TRF1 contains a dimerisation domain which has a ~ 200 amino acid TRF-specific domain. This mediates homodimerisation which is essential for binding to TTAGGG repeat sequences. The acidic N-terminus domain of TRF1 binds to the Shelterin-associated proteins tankyrase 1 and tankyrase 2 (Palm and de Lange 2008). These two proteins are able to modify TRF1 to hinder its DNA-binding activity or remove TRF1 from telomeres and promote its degradation. The C-terminal Myb domain of TRF1 is able to induce bending, looping, and pairing of telomeric DNA, binds to the hetronucleotide repeats of DNA on both the parallel and antiparallel strands. TRF1 may be able to facilitate the folding back of the telomeric DNA in T-loop formation via other

telomeric binding protein such as TIN2, TPP1, and POT1 (Bianchi, Smith *et al.* 1997; Broccoli, Smogorzewska *et al.* 1997; Griffith, Bianchi *et al.* 1998). Therefore, TRF1 acts as a tether through which other Shelterin components interact with the 3' overhang and facilitate the protection of telomeric DNA from degradation and end-to-end fusion (Ye, Hockemeyer *et al.* 2004). The TRFH domain of TRF1 consists of a versatile peptide docking site to recruit other Shelterin proteins to telomeres. Chen *et al.* (2008) showed that TRF1 recruits TIN2 via its TRFH domain which interacts with PinX1 (Chen, Yang *et al.* 2008). PinX1 (PIN2/TRF1-interacting, telomerase inhibitor 1) is a telomerase inhibitor which maps to human chromosome 8p23 and exhibits heterozygosity in different cancers. However, whether PinX1 is inactivated in tumorigenesis is yet to be defined (Soohoo, Shi *et al.* 2011).

It has been suggested previously that TRF1 can interact with DNA-dependent RNA polymerase II to transcribe the C-strand of telomeric DNA (Schoeftner and Blasco 2008). Hence, it is important to note that the phosphorylation of threonine 122 position of TRF1 by CK2 plays a fundamental role for TRF1 binding to the telomere, thus regulating telomere length (Kim, Davalos *et al.* 2008). Preliminary observations in telomerase-positive human cells showed that TRF1 is a negative regulator of telomere length. It is believed that long term over-expression of *TRF1* even in the presence of telomerase, leads to a gradual decrease in the process of telomere shortening. However, the expression of a dominant negative *TRF1* mutant result in the inhibition of binding of endogenous TRF1 to double stranded telomeric DNA and induces abnormal telomere length elongation (van Steensel and de Lange 1997; Smogorzewska, van Steensel *et al.* 2000). All these findings support the role of TRF1 as a negative regulator of telomere length (in *cis*) to maintain the access of

telomerase to the end of telomeres (van Steensel and de Lange 1997; Ancelin, Brunori *et al.* 2002).

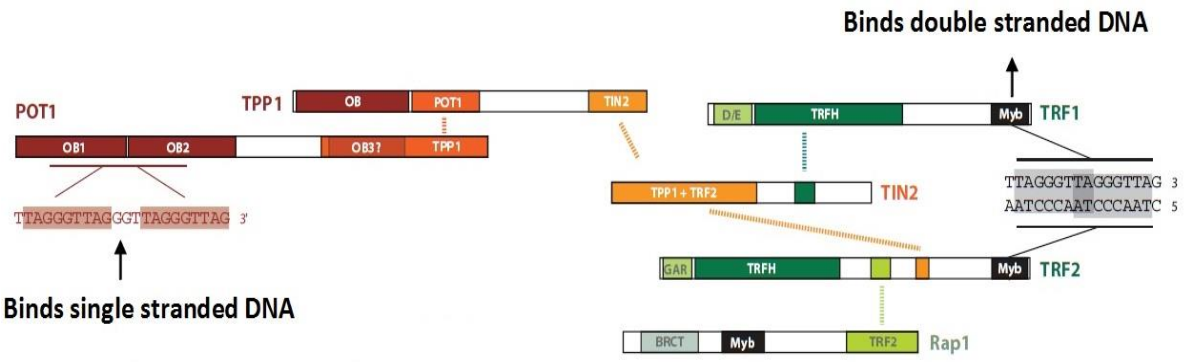

Figure 1.7- Interaction between human telomere binding proteins (Shelterin) and telomeric DNA. Binding of individual Shelterin proteins through interaction with specific sequences. TRF1 and TRF2 bind double stranded DNA, whereas POT1 and TPP1 bind single stranded telomeric DNA, therefore aiding in formation of the T-loop. TIN2 binds TPP1 and TRF1, TRF2 and RAP1. The image was obtained from Palm *et al.* (2008) (Palm and de Lange 2008).

1.5.2-Telomeric Repeat binding Factor 2 (TRF2)

Similar to TRF1, TRF2 has a TRF homology (TRFH) domain close to its amino-terminus and a C-terminal Myb DNA-binding domain which are bound via a flexible hinge domain (Bianchi A 1997; Bilaud, Brun *et al.* 1997; Fairall L 2001; Hanaoka 2005). However, unlike TRF1, the amino terminus in TRF2 contains the Gly/Arg-rich domain (GAR domain) on its N-terminus. The TRFH domain function acts as a docking site for target proteins that consists of FXLXP motifs (binding for TRF1) and YXLXP motifs (binding for TRF2) (Figure 1.7) (Bhanot and Smith 2012). Moreover, TRF2 is twice as abundant as TRF1 and the two proteins do not interact directly with each other (Diotti and Loayza 2011). TRF1 and TRF2, are closely related within their carboxyl-terminal Myb domains and both proteins bind to the double stranded

telomeric DNA as homodimers / or oligomers via homotypic interactions in the TRFH domain. Additionally, TRF2 can bind to the interstitial telomeric DNA repeated-related sequences (Smogorzewska, van Steensel *et al.* 2000). The T-loop-like structures are shaped through TRF2 when provided with a model telomere substrate and within this structure, TRF2 preferentially localizes to the junction between the single stranded and double TTAGGG repeats and prevent the ends of telomeric DNA from being detected as DNA damage (Stansel, de Lange *et al.* 2001). Over-expression of *TRF2* in HeLa and HT1080 tumor cells causes telomeres to become uncapped, which leads to the formation of chromosomal end-to-end fusions (Karlseder, Broccoli *et al.* 1999). Moreover, TRF2 can protect chromosome ends and inhibit activation of DNA damage response pathways in tumors and normal epithelial cells (Assmus, Urbich *et al.* 2003; Spyridopoulos, Haendeler *et al.* 2004; Gensch, Clever *et al.* 2007). It is important to note that TRF1 and TRF2 are required to form a T-loop-based mechanism to maintain and protect telomere length. TRF2, like TRF1, may be a negative regulator of telomere length homeostasis. It was previously reported that over-expression of *TRF2* triggers cells to lose their 3' overhang (Smogorzewska, van Steensel *et al.* 2000). Celli and de Lange (2005) showed that conditional deletion of Trf2 in p53 null mouse embryonic fibroblasts induces telomeric DNA damage (Celli and de Lange 2005). Therefore, in human cells, TRF1 and TRF2 seem to play an important role in the protection and maintenance of telomeres.

1.5.3-Human Protection of telomeres 1 (POT1)

Human POT1 was originally discovered through its homology to the alpha subunit of the TEBPα/β telomeric end-binding complex in Oxytricha nova (Smogorzewska and de Lange 2004). POT1 was also identified in mammals, Aspergillus, Arabidopsis, and Caenorhabditis

elegans and appears to play a critical role in telomere maintenance in eukaryotes (Baumann and Cech 2001; Wei and Price 2003; Raices, Verdun *et al.* 2008). Similar to TEBPα, POT1 contains an N-terminal oligonucleotide/oligosaccharide DNA-binding domain (DBD) and a C-terminal protein-protein interaction domain. The hPOT1-DBD has 340 residues and has been co-crystallized with single strand DNA. POT1 also has two OB folds which are able to recognise the single strand DNA decamer telomeric sequence 5'-TTAGGGTTAG-3' *in vitro* and may possibly have one OB fold at its C-terminus (Figure 1.7) (Diotti and Loayza 2011). The OB-fold is an oligonucleotide/oligosaccharide binding domain (about 110 residues) consists of a five-strand β-sheet, coiled to shape a blocked β-barrel and capped through an α helix located between the third and fourth β strands (Theobald, Mitton-Fry *et al.* 2003; Bochkarev and Bochkareva 2004). The OB2 of POT1 binds to and protects the 3' overhang of single stranded telomeric DNA, whereas the first N-terminal OB folds connects to the first six nucleotides (Lewis and Wuttke 2012). The interaction between the carboxyl-terminal of POT1 with TPP1 plays a key role for POT1 loading onto telomeres, while the OB fold of POT1 is essential for telomere localization (Wang, Podell *et al.* 2007). The POT1/TPP1 complex is able to interact with single stranded DNA (ssDNA) at many positions along the 3' overhang (Lei, Podell *et al.* 2004). In addition, the POT1/TPP1 3' end can bind to the displaced G-strand in the D-loop (Loayza, Parsons *et al.* 2004). It has been reported that POT1 protects telomere termini via inhibition of the ATR-mediated DNA damage response that is induced by telomere dysregulation. Co-immunoprecipitation experiments have revealed that POT1 protein interacts with TRF1, TRF2 and RAP1 along the double stranded of telomeric DNA via POT1/TPP1/ TIN2 protein bridges (Kelleher, Kurth *et al.* 2005). Extensive evidence indicates that POT1 appears to modulate telomere length through inhibiting telomerase enzyme

activity (Lei, Zaug *et al.* 2005). On the other hand, the POT1/TPP1 complex has been implicated in the recovery of telomerase activity acting as part of a telomerase processivity factor via reducing the rate of primer dissociation (Wang, Podell *et al.* 2007; Latrick and Cech 2010; Zhong, Batista *et al.* 2012). Previous studies by Kelleher *et al.* (2005) showed that binding of POT1 to the 3' overhang is essential to negatively regulate telomerase activity *in vivo*. They reported that POT1 is implicated in modulating telomerase activity through the access of telomerase to the telomere but not during the extension process. It appears that POT1 protein inhibits telomerase via steric hindrance by preventing base pairing between the telomerase RNA and the DNA primer (Kelleher, Kurth *et al.* 2005). Previous work showed that the deletion of the DNA-binding domain of POT1 with over-expression of N-terminally truncated POT1 induces telomere length (Loayza 2003; Liu, Safari *et al.* 2004; Ye, Hockemeyer *et al.* 2004). Moreover, partial deletion of POT1 affects telomere length at the 3' and 5' ends of chromosomes (Hockemeyer, Sfeir *et al.* 2005; Yang, Zheng *et al.* 2005). Furthermore, POT1/TPP1 complex covers the 3' overhang of single-stranded of telomeric DNA and inhibits binding of the telomere to telomerase (Wojtyla, Gladych *et al.* 2011). All these findings support an emerging view that POT1 can both positively and negatively regulating telomerase enzyme activities via interacting with TPP1.

1.5.4-TRF1-interacting nuclear protein 2 (TIN2)

TIN2 acts as the central component in the Shelterin protein complex. This protein is able to interact directly with the double stranded TTAGGG sequences via binding TRF1 and TRF2, thus providing a bridge between the single strand 3' overhang through connecting TPP1 and POT1 and double stranded telomeric DNA (Kim, Kaminker *et al.* 1999; Houghtaling BR 2004; Kim, Beausejour *et al.* 2004; Ye, Donigian *et al.* 2004; Ye, Hockemeyer *et al.* 2004).

The C-terminal TRF-binding motif (FXLXP) of TIN2 binds to the TRFH domain of TRF1, while TIN2 interacts with its specific site in the hinge domain in TRF2 through its N-terminal domain (Figure 1.7) (Misra, Mahajan *et al.* 2008; Bhanot and Smith 2012). TIN2 occupies a central position to form a bridge between TRF1 and TRF2. However, TIN2 does not associate with TRF2 within its TRFH domain but stabilises TRF2 at the telomere end (Houghtaling, Cuttonaro *et al.* 2004; Chen, Yang *et al.* 2008). In addition, TIN2 also binds TPP1 and POT1, using a third protein interaction site situated on its N terminus. The interaction between TIN2 and TRF2 is enhanced by TPP1 (O'Connor, Safari *et al.* 2006). Takai *et al.* (2011) showed that TIN2 disruption leads to a considerable decrease in localization of Shelterin complex at telomeres; this induces replication protein A (RPA) binding to telomere ends and increases the ATR-mediated DNA damage responses which can also affect the phenotypes in Pot1a and Pot1b in double knockout mice (Takai, Kibe *et al.* 2011). Additionally, TIN2 depletion by RNA interference (RNAi) results in telomere elongation, indicating that TIN2 is a negative regulator of telomere length (Ye and de Lange 2004). Previous studies investigating the role of TIN2 and TRF showed that these two components play a role in telomere cohesion (Canudas, Houghtaling *et al.* 2007). In mice, deletion of Tin2 results in embryonic lethality; this finding further supports the role of TIN2 in telomerase recruitment and telomere length regulation and maintenance via facilitating TRF2-dependent prevention of the ATM-mediated DDR pathway (Takai, Kibe *et al.* 2011).

1.5.5-Repressor activator protein 1 (RAP1)

RAP1 is a 399 amino-acid protein which is highly conserved with a carboxyl-terminal RCT domain homologous to the carboxyl-terminus of budding yeast Rap1 protein. RAP1 has an amino-terminal BRCT domain, a central Myb domain-(s), followed by a predicted coiled

domain, and carboxyl-terminus localization signal (Figure 1.7) (Zhu, Kuster *et al.* 2000; Celli and de Lange 2005). RAP1 binds TRF2 through its C-terminal domain and its association with telomeres depends on its interaction with TRF2. Furthermore, TRF2 maintains the localization and stability of RAP1 and deletion of TRF2 causes RAP1 to be released from the telomere component (Martinez, Thanasoula *et al.* 2010). O'Connor *et al.* (2004) discovered that DNA repair proteins such as; Rad50, Mre11, PARP1, BTBD12 and Ku86/Ku70 are found in the RAP1-TRF2 complex (O'Connor, Safari *et al.* 2004). BTBD12 complexes with RAP1-TRF2 to facilitate Holliday junction processing and the DNA damage response indicating that these complexes play a fundamental role at inhibiting homologous recombination (HR) at telomere (O'Connor, Safari *et al.* 2004).

1.5.6-TPP1 (ACD, adrenocortical dysplasia homolog)

TPP1 emerged as the last member of the Shelterin complex and was originally known as TIN2-interacting factor. This protein was found to interact with both POT1 and TIN2 (Houghtaling, Cuttonaro *et al.* 2004; Liu, Safari *et al.* 2004; Ye, Hockemeyer *et al.* 2004). As within POT1, TPP1 contains an N-terminal OB fold and is structurally similar to the homolog of *Oxytricha nova* TEBPβ. This finding suggested that the TPP1/POT1 heterodimer is the homolog of TEBPα-β heterodimer (Figure 1.7) (Wang, Podell *et al.* 2007; Xin, Liu *et al.* 2007). TPP1 binds POT1 through its interaction domain and TIN2 via its C-terminal interaction domain (Ye, Hockemeyer *et al.* 2004). The N terminus of TPP1 in the OB-fold domain can interact with telomerase. Therefore, there is a possibility that telomerase may be regulated by TPP1 (Ye, Donigian *et al.* 2004; Xin H 2007). Telomere length may be maintained by recruiting POT1 via its interaction with TPP1 and TIN2. Moreover, the complex of TPP1/ TIN2/POT1 binds to TRF1 and TRF2 and is probably the main way in which POT1 is recruited

to telomeres (Hockemeyer, Palm *et al.* 2007; Loayza D 2003). Evidence has been obtained that over-expression of *TPP1* defective in interacting with POT1, results in telomere de-protection (Houghtaling, Cuttonaro *et al.* 2004; Xin, Liu *et al.* 2007). POT1 deficient in TPP1 binding can localize to telomeres as well as form a weak interaction between POT1 and TRF2 causing telomere dysfunction (Colgin, Baran *et al.* 2003; Yang, Zheng *et al.* 2005; He, Multani *et al.* 2006; O'Connor, Safari *et al.* 2006). Additionally, the TPP1/TIN2 complex plays a fundamental role in sub-cellular localization of TPP1 and POT1. It has been reported that deletion of the *Tpp1* gene in mouse embryo fibroblasts results in chromosome end-to-end fusion and telomere dysregulation (Kibe, Osawa *et al.* 2010). Taken all of this information together, it is speculated that TPP1 plays an important role in regulating and protecting telomere length.

1.6-Shelterin-associated genes structures and functions

1.6.1-Tankyrase 1 and Tankyrase 2 (TNKS1/2)

Tankyrases are human telomere-associated poly (ADP-ribose) polymerases. Tankyrase 1 (TRF1-interacting ankyrin-related ADP-ribose polymerase 1) was first identified as a TRF1-associated factor via a yeast two-hybrid screen (Smith, Giriat *et al.* 1998). Tankyrase 1 consists of several domains such as: the N-terminal HPS domain, which comprises multiple runs of histidine, proline and serine (HPS) repeats. The large ankyrin (ANK) domain near to the N-terminus of TNKS1, contains 24 repeated ANK, and includes five functional sub-domains including the sterile α module (SAM) domain which is implicated in takyrase multimerization, and a poly (ADP-ribose) polymerase (PARP) domain which is located in the C-terminal region of tankyrase 1 (Figure 1.8) (Seimiya, Muramatsu *et al.*

2004). The PARP domain of TNKS1 belongs to the super family of PARPs proteins that are involved in numerous cellular processing, particularly DNA repair and programmed cell death (Isabelle, Moreel *et al.* 2010). *In vitro*, TNKS1 is similar to other PARPs that utilize NAD^+ as a cofactor to synthesize long linear or branched poly ADP-ribose onto protein acceptors (Kaminker, Kim *et al.* 2001; Sbodio, Lodish *et al.* 2002; Gelmini, Quattrone *et al.* 2007; Hsiao and Smith 2008). Polymers of ADP-ribose can be added to protein by post-translational modification which then changes protein function. Tankyrase 1 is a homolog of tankyrase 2 and these two homologues have similar structures and domains (ankyrin, SAM and PARP). The only structural difference between these two molecules is that TNKS2 lacks the N-terminal His-Pro-Ser rich domain (Lehtio, Collins *et al.* 2008).

TRF1 interacts with the N-terminal acidic domain of TNKS1 and TNKS2 proteins. It has been reported that poly ADP-ribosylation of TRF1, *in vitro*, inhibits its binding to telomeric DNA via tankyrase 1. Poly ADP-ribosylation is a process by which multiple groups of ADP-ribose moieties can also transferred to proteins to form long branched chains. This protein modification is carried out by PARPs. The structure of PARPs is involved in the regulation of several cellular events such as maintenance of genomic instability, DNA repair and telomere maintenance (Diefenbach and Burkle 2005). Over-expression of *TNKS1* and *TNKS2* in human cells results to release TRF1 from telomeres and TNKS1 acts as a positive regulator of telomere length (Chiang, Nguyen *et al.* 2006). Tankyrases may be involved in the removal of telomerase-inhibiting complexes from telomeric DNA to maintain telomeric ends. Therefore, it has been suggested that TNKS1 presumably regulates access of telomerase to the telomeric end (Ha, Kim *et al.* 2012). Additionally, knockdown of *TNKS1* by

interfering RNA (RNAi) in human cells showed misaligned chromosomes and aberrant spindle structure (Kim and Smith 2013).

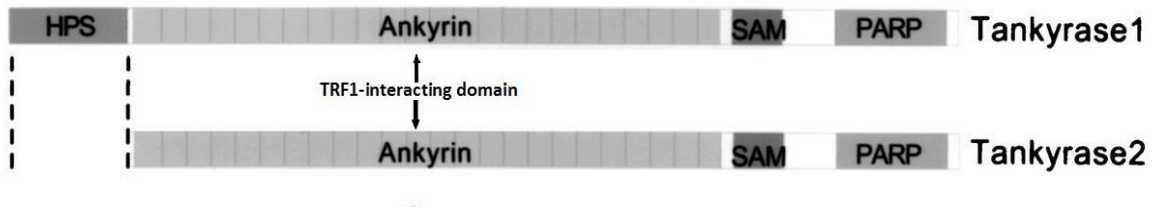

Figure 1.8-A Schematic of Tankyrase 1 and Tankyrase 2. These Shelterin-associated genes are positioned at the telomere. The ankyrin domain of tankyrase 1 and tankyrase 2 interact with TRF1 (Cook, Dynek *et al.* 2002). However, the sequences associated with binding of EST1A and TEP1 have not been elucidated thus far.

1.6.2-Ever shorter telomere 1 (EST1A)

EST1A (sometimes known as SMG6) is also considered to be a Shelterin-associated protein. Telomerase is activated by EST1A at the 3' end of the telomere. Therefore, EST1A is a positive regulator of telomerase (Salhab, Jiang *et al.* 2008). Over-expression of *EST1A* induces anaphase bridges due to chromosomal end-to-end fusion, and may affect telomere capping (Reichenbach, Hoss *et al.* 2003). It has been reported that TEP1 associates with telomerase components but the role of TEP1 in telomerase function is poorly understood (Liu, Snow *et al.* 2000).

1.7-DNA methylation status and cancer

Aberrant DNA methylation in various malignancies has become the subject of intense investigation. Malignant cells in comparison with their normal counterparts undergo major disruptions in their DNA methylation patterns. In particular, methylation of DNA

within promoter regions serves to suppress the expression of genes that could play a critical role in inhibiting tumorigenesis (Das and Singal 2004). Several tumour suppressor genes, such as the *MLH1* mismatch-repair gene are implicated in colorectal and other cancers as well as the *p16*/*CDKN2A* cell-cycle control gene involved in various malignancies, and *BRCA1* in early breast cancer, are all found to be hypermethylated (Esteller, Corn *et al.* 2001). In addition, Ottaviano *et al.* (1994) and Graff *et al.* (1995) showed that a variety of genes, including cell adhesion and steroid receptor genes play a fundamental role in the development of breast cancer, and are hypermethylated in these tumours (Ottaviano, Issa *et al.* 1994; Graff, Herman *et al.* 1995). Furthermore, Zinn *et al.* (2007) reported that the promoter region of *hTERT* was hypermethylated in lung, colon and breast cancer cell lines (Zinn, Pruitt *et al.* 2007). Since the expression of hypermethylated genes (e.g. those mentioned above) can be actively restored after treatment with DNA methylation inhibitors, such as 5-aza-2'-deoxycytidine (5-aza-CdR), therapeutic strategies have been developed to reverse critical methylation regions of DNA in breast cancer and other malignancies.

1.8-DNA Methylation and gene expression

DNA methylation patterns in normal cellular process and abnormal events associated with disease are becoming a very interesting and important field of research (Sharma, Kelly *et al.* 2010). Many studies now recognize alterations to the epigenome lie at the heart of many complex diseases such as cancer, autoimmune disease, psychiatric and behavioral disorders (Jirtle and Skinner 2007; Jones and Baylin 2007; Ballestar 2011).

In vertebrates, epigenetic alterations such as DNA methylation and histone modifications by specific enzymes play a fundamental role in regulating gene expression of

normal and disease cellular processes (Kim, Samaranayake *et al.* 2009). It has been known for many years that chromatin packages DNA in a condensed state to preserve its integrity. Epigenetic mechanisms change chromatin structure to produce different categories of epigenetic modifications such as: incorporation of histone variants, histone modifications and in mammals, cytosine-5 DNA methylation at CpG dinucleotides (Sharma, Kelly *et al.* 2010). In eukaryotic and prokaryotic cells, one of the most important epigenomic phenomena is defined by DNA methylation that plays a significant role in regulating gene expression and chromatin architecture, in cooperation with histone alterations and other chromatin associated proteins (Singal and Ginder 1999; Jurkowski and Jeltsch 2011). DNA methylation is carried out by DNA (cytosine-5) methyltransferases (DNMT). The transfer of a covalent methyl group from a donor *S*-adenosylmethionine (SAM) to the the fifth carbon (C5) of cytosine, mainly within the CpG dinucleotide, is catalysed by methyltransferases enzymes (Girault, Tozlu *et al.* 2003; Turek-Plewa and Jagodzinski 2005). Research has demonstrated that the resulting precise DNA methylation patterns can be inherited when DNA replicates by the cooperative activity of DNMTs (Holliday 1991; Kim, Samaranayake *et al.* 2009).

1.8.1-DNA methyltransferases (DNMTs)

The eukaryotic DNMT family includes five members: DNMT2, DNMT3A, DNMT3B, DNMT3L and DNMT1. The most abundant enzyme is DNA (cytosine-5) methyltransferase 1 (DNMT1) which preferentially methylates hemi-methylated DNA during replication for maintenance of the DNA methylation patterns (Bestor 2000; Robertson 2001; Turek-Plewa and Jagodzinski 2005). This enzyme has an important function in imprinting and in X-chromosome inactivation during embryogenesis (Sado, Fenner *et al.* 2000). TRDMT1

(formally known as DNMT2) is the smallest mammalian DNA methyltransferase and does not show major *de novo* or maintenance methyltransferase activity in embryonic stem cells (ES) or adult somatic tissue (Okano, Xie *et al.* 1998; Yoder and Bestor 1998). However, the structure of TRDMT1 has shown that this enzyme methylates at position 38 in aspartic acid tRNA (tRNA aspartic acid methyltransferase 1) (Squires, Patel *et al.* 2012). DNMT2 is involved in recognition of DNA damage, DNA recombination and mutation repair (Turek-Plewa and Jagodzinski 2005). Other known functional methyltransferases are DNMT3A and DNMT3B, which mainly methylate CpG dinucleotides without preference for hemimethylated DNA, and so have been classified as *de novo* methyltransferases predominantly during embryogenesis (Okano, Xie *et al.* 1998; Turek-Plewa and Jagodzinski 2005). The DNA cytosine-like 5-methyltransferase (DNMT3L) protein does not have methyltransferase active site motifs and must assist other *de novo* DNMTs (Aapola, Kawasaki *et al.* 2000). It has been considered that it may antagonize functional methyltransferase activity (Robertson 2001).

1.8.2-How does DNA methylation repress transcription?

Gene expression can be prevented by DNA methylation through multiple mechanisms. DNA methylation can significantly inhibit transcription factors for some genes. However, it does not account for the general repression of gene expression usually associated with DNA methylation (Kass, Pruss *et al.* 1997). The methyl group of 5-methyl-cytosine protrudes out into the major groove of the DNA helix and it is here that the main contacts are formed with various DNA binding proteins. Consequently, the most direct mechanism of transcriptional inhibition by DNA methylation is by direct interference with transcription factor binding (Maldonado, Hampsey *et al.* 1999). Alternatively, the presence

of a methylation-specific binding protein may possibly act as a repressor (Mossman, Kim *et al.* 2010).

1.8.3-DNA demethylating agents

DNA methylation inhibitors are a class of substances that can demethylate DNA, resulting in re-expression of silenced genes. DNA demethylating agents can be used for cancer therapy. The CpG-rich regions of normal mammalian genomes are usually non-methylated, with the exception of imprinted genes. These regions, within which genes activity are transcribed, become heavily methylated and inactivated or silenced in the genome of tumour cells (Ghoshal, Datta *et al.* 2005). Among many agents with DNA methylation-modifying capability, 5-azacytidine (5-aza-CR) or its analogue 5-aza-2'-deoxycytidine (5-aza-CdR) are DNA methyltransferase inhibitors (Figure 1.9).

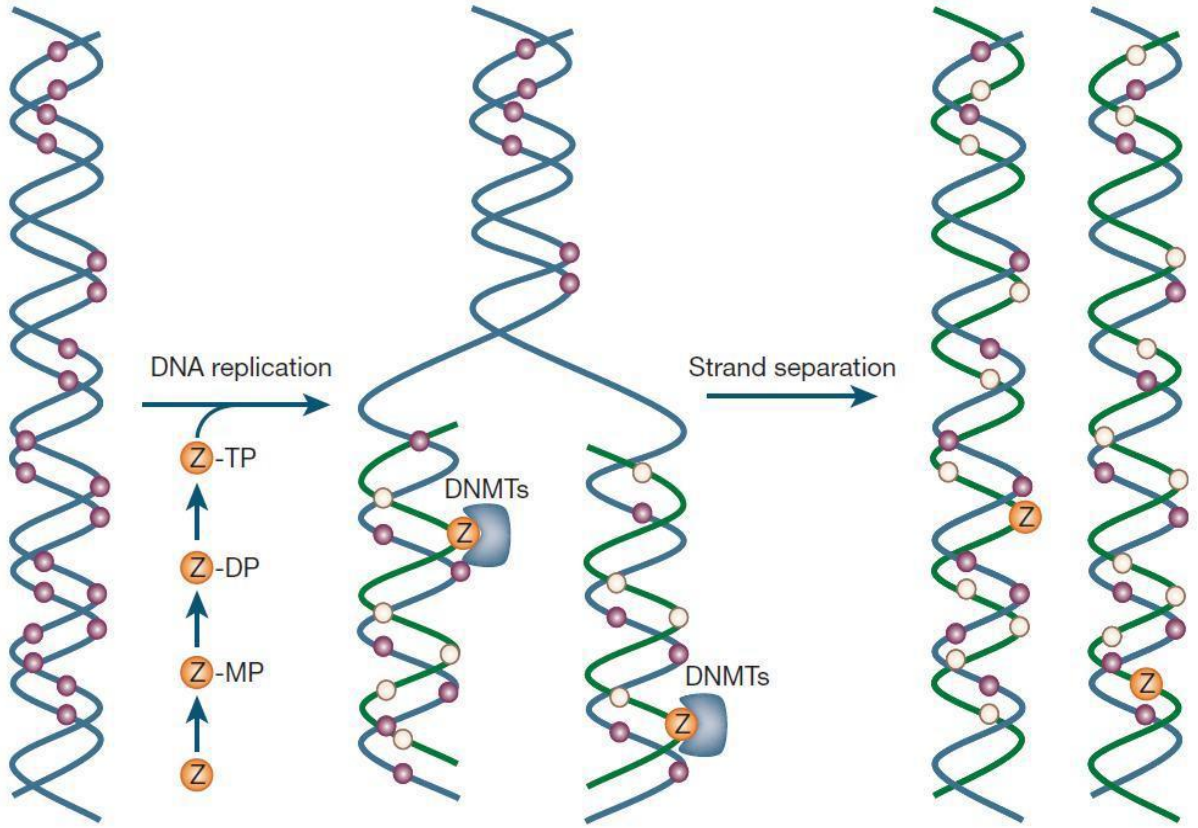

Figure 1.9-Mechanism of action of nucleoside analogue inhibitors. Deoxynucleoside analogues, 5-aza-CdR (indicated by Z) is converted into the triphosphate inside S-phase cells and is incorporated in place of cytosine into DNA (Egger, Liang *et al.* 2004).

These inhibitors were initially shown to have significant cytotoxic and antineoplastic activities in many experimental tumors. However, it was subsequently discovered that they are strong inducers of DNA demethylation (Lin, Shaw *et al.* 2011). 5-aza-CdR is an analogue of cytosine that has more potent therapeutic effects than 5-aza-CR in human leukaemia, myelodysplastic syndromes and hemoglobolinopathies. Following cellular uptake and sequential phosphorylation, 5-aza-CdR is incorporated into DNA but not RNA or protein whereas 5-aza-CR is incorporated into both RNA and DNA (Zhu, Hileman *et al.* 2004). Once incorporated into DNA, both compounds as are would expect, have related mechanisms of action; they irreversibly bind the methyltransferase enzymes (DNMTs) while they attempt to methylate the cytosine analogue. This depletion of DNMTs in the cells results in hypomethylation of DNA, and induction of DNA damage (Zhu, Hileman *et al.* 2004; Stresemann, Brueckner *et al.* 2006; Flotho, Claus *et al.* 2009). In addition, other potential compounds have been recently developed that are able to reduce the level of DNA methylation, such as zebularine (Zhou, Cheng *et al.* 2002), hydralazine, procaine (Rubin 2005; Sarzi-Puttini, Atzeni *et al.* 2005), an anti-sense oligonucleotide MG98 (Goffin and Eisenhauer 2002) and procainamide (Lin, Shaw *et al.* 2011). However, the detailed mechanisms of these compounds need to be assessed where hypermethylation-induced gene silencing plays an important role in disease pathology, especially in breast cancer.

1.9-Mechanism of Histone modifications and gene expression

Many post-transcriptional modifications of histones, such as phosphorylation, ubiquitinations, acetylation, deacetylation and methylation, have been revealed as epigenetic tags (Kouzarides 2007).

Histone deacetylase (HDACs) enzymes are responsible for removing the acetyl groups from N-terminal lysine/arginine residues in the amino-terminal tails of core histones, specifically the core histones of H2A, H2B, H3 and H4. Histone acetylation is catalysed by histone acetyl transferases (HATs) enzymes (Bannister and Kouzarides 2011). Deacetylation of histones is carried out to maintain the balance between silent and transcriptionally active chromatin. Removal of acetyl groups by HDACs leads to chromosome compaction and prevents transcription (Zhang 2008). HDACs classified as Class I HDACs include 1, 2, 3, and 8. Class IIa HDACs include 4, 5, 7 and 9 and Class IIb consists of HDAC6 and 10. HDACs Class I and II are zinc-dependent enzymes whereas Class III, sirtuins (sir 1-7) need NAD^+ for their enzyme activity. Class IV HDAC is exemplified by HDAC11 (Blander and Guarente 2004). Histone acetyl transferase (HATs) enzymes are classified into two types including A HATs and B HATs. The class A HATs enzymes are located in nucleus and are involved in regulating gene expression via acetylation of nucleosomal histones (Roth, Denu *et al.* 2001). Type B HATs are positioned in the cytoplasm and are required for acetylating new synthesized histones before their aggregation into nucleosomes (Roth, Denu *et al.* 2001). In addition, the transcriptional co-activators such as CRB-binding protein (CBP) are involved to catalyse acetylation of core histones, which activate the HAT enzyme. Therefore, the acetylation of histones functions to modulate gene expression. Importantly, transcription is regulated by the interaction of HATs with a large number of transcription factors (Abel and Zukin 2008).

Of all known histone modifications, it has been shown that disruption of HATs or HDACs activity can contribute several cancers (Zhang 2008). For example several studies have been reported that inhibition of HDACs by Trichostatin A (TSA) results in the expression of key tumour suppressor genes such as *p53*, *RB1*, *EGFR* in HeLa cells (Zhang

2008). Trichostatin A, a microbial metabolite, is a potent inhibitor of mammalian HDAC Class I and II enzymes. This drug can be utilized to modify gene expression by preventing histone deacetylases and the access of DNA transcription factors to DNA molecules inside chromatin. For this reason inhibition of histone acetylation by TSA has been used successfully as an anticancer drug for cancer treatment (Drummond, Noble *et al.* 2005; Meng, Dai *et al.* 2008).

1.10-Aims of the Project

In the last few years, several studies have indicated that maintenance of telomere length can be influenced by the regulation of Shelterin proteins. Therefore, the first aim of this project (Chapter III) was to determine if there are any changes in the expression patterns of Shelterin and Shelterin-associated genes in breast cancer cells. Ten independently derived breast cancer cell lines were investigated and Shelterin gene expression compared with that in normal diploid breast epithelial cell strains (HMECs). The underlying mechanisms behind any changes in expression patterns were then studied by means of epigenetic analysis and mutational studies (Chapter IV). Because it has been demonstrated that the expression of Shelterin and Shelterin-associated genes is correlated with reduced telomere lengths, the effect of up-regulation of Shelterin gene expression, using 5-aza-CdR and TSA, on telomere length was investigated (Chapter V). For this purpose, 21NT, a breast ductal carcinoma cell line was studied (using four telomere measurement methods, i.e. TRF, q-PCR, flow-FISH and iQFISH). The aforementioned techniques were compared in terms of reliability and accuracy. Finally, (Chapter VI) based on previous studies demonstrating that over-expression of one of the Shelterin component, *POT1*, induces telomere lengthening, the final aim of the project was to examine whether over-expression of *POT1* could affect telomere length elongation in the 21NT breast cancer cell line.

CHAPTER II

GENERAL MATERIALS AND METHODS

2.1-Cell lines and cell culture methodology

2.1.1-Cell culture complete growth media

- **Modified Eagle's medium alpha (MEM):** 1x MEM stock, 1µl/ml hydrocortisone (1:1000), 1µl/ml insulin (1:1000), 10% fetal calf serum (FCS), 1% glutamax, 1% HEPES and 1% NEAA and 1µl/ml Epithelial Growth Factor (EGF)
- **DMEM/F12:** 1x DMEM/F12, 10% FCS and 1% glutamax, 0.5 µg/ml hydrocortisone
- **RPMI-1640:** 1x RPMI/1640, 1% glutamax, 10% FCS, 0.1mM Na Pyruvate, 1% HEPES.
- **F12:** 1x F12, 1% glutamax, 7% FCS
- **RPMI 1640:** 1x RPMI/1640, 10% FCS

Table 2.1 shows a summary of the cell lines that were used during the project, along with details of growth media.

Table 2.1-Description of different cell lines and normal mammary cell strains (HMECs)

Cell lines	Patient Age	Histopathological Diagnosis	Tumour Stage	Primary Site	Growth Media	References
21NT	36	*PDC	Primary	Breast	MEM	(Band, Zajchowski *et al.* 1990; Cuthbert, Bond *et al.* 1999)
21MT-2	36	PDC	Metastatic	Breast	MEM	(Band, Zajchowski *et al.* 1990; Cuthbert, Bond *et al.* 1999)
GI101	57	*IDC	III	Breast	DMEM/F12 without hydrocortisone	---
BT-20	74	IDC	---	Breast	DMEM/F12 without hydrocortisone	(Lasfargues and Ozzello 1958)
HS578-T	74	IDC	---	Breast	DMEM/F12 without hydrocortisone	(Hackett, Smith *et al.* 1977)
BT474	60	IDC	---	Breast	DMEM/F12 without hydrocortisone	(Lasfargues, Coutinho *et al.* 1978)
MCF-7	69	IDC	IV	Pleural effusion	DMEM/F12 without hydrocortisone	(Soule, Vazguez *et al.* 1973)
HCC1143	52	PDC	II	Breast	RPMI/1640	(Gazdar, Kurvari *et al.* 1998)
MTSV1-7	**---**	Normal immortalized mammary gland	---	Breast	DMEM/F12 With hydrocortisone	(D'Souza, Berdichevsky *et al.* 1993)
PB1	36	PDC	Primary	Breast	MEM	(Band, Zajchowski *et al.* 1990; Cuthbert, Bond *et al.* 1999)
PC3	62	Prostatic adenocarcinoma	IV	Prostate	F12	(Kaighn, Narayan *et al.* 1979)
LY-R	---	Mouse Lymphoma, Radiosensitive	---	Lymphoma	RPMI/1640	Dr Andrzeg Wojcik University of Warszawa,Poland
LY-S	---	Mouse Lymphoma, Normal Radiosensitive	---	Lymphoma	RPMI/1640	Dr Andrzeg Wojcik University of Warszawa,Poland
HMEC1	---	Normal human mammary epithelial cell strain	---	Breast	Grown by Dr. H. Yasaei	(Labarge, Garbe *et al.* 2013)
HMEC2	19	Normal human mammary epithelial cell strain	---	Breast	Grown by Dr. H. Yasaei	(Garbe, Bhattacharya *et al.* 2009)
***Normal commercial**	78	FirstChoice® Human breast total RNA	---	Breast	---	AM6952 (Applied Biosystems)
PC3/hTERT	62	Prostatic adenocarcinoma	---	Derived from PC-3 telomerised	F12	Professor Newbold group (Brunel University)

***Infiltrating ductal carcinoma (IDC),*Primary ductal carcinoma (PDC), *Normal mammary epithelial tissue.

2.1.2- Cell culture procedure

All cell culture was carried out in a LaminAirHB2448 (Heraeus Instrument) cabinet (hood). The culture medium was pre-warmed at 37^{o}C in a water-bath for 10 minutes. Then the cell lines were taken out of liquid nitrogen and thawed in a water-bath for 3 minutes. Cells were transferred into a p100 tissue culture dish containing 15ml of warm culture medium and transferred to fully humidified incubators (HeraCell, Heraeus) set at 5% CO_2 and 37°C. After 24 hours, the medium in p100 dish was aspirated to wash away residual DMSO and fresh media added. Healthy cells were fed with fresh culture medium every 2 days. An inverted phase contrast microscope (Olympus CK40) was utilized for visualizing the cells. Digital images of cells were captured using an Olympus IX71 microscope attached to a coolSNAP cf camera (Photometrics). Cells were monitored every day and deemed suitable for cryostorage once 80-90% confluence was reached. All cell lines were sub-cultured with trypsin-EDTA (Gibco/Invitrogen) 1:3 at 80 % confluence. 15 minutes prior to trypsinization, the required culture medium, versene (0.04% EDTA in 1XPBS) and trypsin-EDTA were all pre-warmed to 37^{o}C in a water-bath. The external container surfaces, cabinet hood and all equipments were sterilized using 70% IMS to avoid any fungus or bacterial infection. Cell culture medium was aspirated from plates and the adherent cell monolayer washed once with 10ml of versene. After gentle swirling and aspiration of versene, 3ml of warm trypsin-EDTA was added to p100 dish and incubated for 5 minutes. Next, the detached cells in trypsin-EDTA were neutralized with 10ml complete cultured medium and the cells spun down at 15000*rcf* for 5 minutes in a Sorvall Legend T bench centrifuge. Supernatants were aspirated and the cell pellets re-suspended by gentle flicking to disperse the cells before re-

suspending them into appropriate volume of complete medium. Finally, 1ml of suspended cells was then put in a new p100 dish with the fresh medium.

2.1.3-Cryopreservation of cells

Before freezing, the cells were monitored for growth state and contamination. All healthy cell lines growing in log-phase in p100 tissue culture dish were fed with fresh medium 24 hours before freezing. The culture medium was removed and the cells were trypsinized as described above. The cell suspension was then transferred to a falcon tube and the pellet centrifuged at 15000*rcf* for 5 minutes. The supernatant was aspirated off and the pellet gently flicked and re-suspended in 1ml freezing mixture containing 90% FCS and 10% DMSO (dimethylsulfoxide, Sigma). Cell suspensions were aliquoted into 1.5 or 2ml ampoules for storage in liquid nitrogen. Prior to transfer to liquid nitrogen, the vials were kept in Nalgene Nunc cooler at -80^{o}C for 24 hours. This allows a controlled rate of cooling to prevent the formation of intra-cellular ice crystals that may rupture cell membranes. The plastic holder was filled with Isopropyl alcohol (IPA). The ampoules were finally transferred into liquid nitrogen for long-term storage. Cells were routinely frozen down at 3-5x10^{6} per ml from P-100 tissue culture dishes and 1-2x10^{6} from p60.

2.2-RNA extraction

2.2.1-RNA extraction using RNeasy Mini Kit (50)

RNA extraction was carried out utilizing an RNeasy Mini kit (QIAGEN), which provided fast processing and effective purification of RNA from cells. The procedure was performed according to the manufacturer's instructions. Before starting RNA extraction, β-Mercaptoethanol (β-ME) must be added to Buffer RLT. The number of pelleted cells was

approximately $5x10^6$ so 6µl β-ME was added to 600µl of Buffer RLT. The cells were washed with 10ml of sterile PBS (Phosphate Buffer Solution) twice. PBS was then removed and the appropriate amount of Buffer RLT and β-ME (600µl for a 10cm plate) was added to the plate. The surface of the plate was scraped using a scraper (Sarstedt). After transferring the cells to a tube, passed the lysate at least 5 times through 20-gauge needle (0.9mm diameter) fitted to an RNase-free syringe. Next, 600µl of 70% ethanol (1 volume) was added to the homogenized lysate, and mixed well by pipetting. 700µl of the samples were transferred to an RNeasy mini column placed in a 2ml collection tube. Samples were centrifuged for 60 seconds at ≥ 13,000*rcf*. After this, 700µl of Buffer RW1 was added to the RNeasy column. Tubes were centrifuged for 60 seconds at ≥ 13,000*rcf* to wash the column. The RNeasy column was transferred into a new 2ml collection tube and 500µl Buffer RPE added. Tubes were centrifuged for 2 minutes at ≥ 13,000*rcf* to dry the RNeasy silica-gel membrane. This step was repeated to eliminate any chance of possible Buffer RPE carryover. The RNeasy column was placed in a new 2ml collection tube, centrifuged at full speed for 1 minute, and the column then transferred to a new 1.5ml collection tube. Finally, 50µl RNase-free water was added directly onto the RNeasy silica-gel membrane. Samples were then centrifuged for 1 minute at ≥ 13,000*rcf*. RNA concentrations were measured at 260/280 nm to ensure a ratio of > 1.7, indicating the RNA is free of contaminants. The samples were stored at -80°C for further analysis.

2.2.2-RNA extraction using TRIZOL reagent

Briefly, cells at approximately 80% confluence, was trypsinized and washed twice with 5ml of cold PBS. 1ml of Trizol reagent (Sigma) was added to the cells and left for at least 2 minutes at room temperature. The cell lysate was gently pipetted two or three times

and immediately stored at -80^{o}C for long-term storage. All collected samples were incubated at room temperature for 5 minutes. 200µl of molecular biology grade chloroform (Sigma) was added per 1ml of Trizol. Then the tubes were shaken vigorously by hand for at least 15 seconds and centrifuged at 13000*rcf* for 30 minutes at 4^{o}C in a bench centrifuge (Eppendorf centrifuge 5415R). The clear upper-aqueous phase containing RNA was carefully pippetted into a fresh microcentrifuge tube. 750µl of isopropyl alcohol per ml of Trizol was added to each sample and mixed gently prior to incubation for 10 minutes at room temperature. The tubes were centrifuged at 12000*rcf* for 15 minutes at 4^{o}C. RNA precipitate forms a gel-like pellet normally on the side of the tube. The isopropyl alcohol was poured off and the RNA pellets were washed once with 75% ethanol. The pellets were washed thoroughly by vortexing about 10 seconds and centrifuged at 75000*rcf* for 5 minutes at 4^{o}C. The 75% ethanol was carefully removed and the RNA pellets left to air dry at room temperature for 10 to 15 minutes. The RNA pellets were dissolved in 20µl of DEPC-treated water and retropipetted several times. The samples were left on ice for at least one hour. The absorbance of RNA was read at 260 and 280 nm.

2.3-cDNA synthesis

2.3.1-DNAse treatment of RNA

1µl of 10x DNase I Reaction Buffer and 1µl DNase I (Amp Grade) were added to 1µg of RNA and DEPC-treated water to make a total volume of 10µl. Tubes were incubated for 15 minutes at room temperature. Then DNase I was inactivated by the addition of 1µl of 25 mM EDTA solution to the reaction mixture. The samples were heated 10 minutes at 65^{o}C.

2.3.2-Reverse transcriptase

250ng/µl random primers and 1µl 10mM dNTP Mix (10 mM each dATP, dGTP, dCTP, and dTTP at neutral pH) were added to the DNAse-treated RNA. Samples were incubated at 65^{o}C for 5 minutes and cooled on ice for at least 1 minute. 4µl 5x First-Strand Buffer, 1µl 0.1 M DTT, 1µl RNaseOUT Recombinant RNase Inhibitor, and 1µl of SuperScript III were added to the tubes. The samples were mixed by pipetting gently up and down. The tubes were incubated at 25^{o}C for 5 minutes, 50^{o}C for 60 minutes, and 70^{o}C for 15 minutes. The cDNA was ready to use as a template for amplification in PCR.

2.4-Primer design

Primers were designed for PCR and RT-qPCR using three different primer design program. These were the primer-BLAST (primer3) at: www.ncbi.nlm.nih.gov, CLC main workbench 6.1 (CLC bio) and primer express version 2.0 (Applied Biosystems). Some genes had different isoforms, for instance: *TRF1*, *TIN2* genes had two isoforms, *POT1* had 5 isoforms and *SMG6* had 4 isoforms. Therefore, CLC main workbench was used to design primers to these splice variants as you can download each individual splice variant and design primers form specific defined regions of the gene. Primer parameters were set as follows:

- Primer Tm (melting temperature): min (57°C) – max (63°C), optimum (60°C)

- Primer length: min (18bp) – max (22) bp, optimum (20)

- Primer GC% content: min (45%) – max (55%)

- Amplicon product size: min (50bp) – max (200bp)

2.4.1-Primer optimization study

The Shelterin and Shelterin-associated primers were designed using NCBI primer blast software to check for specificity of each primer (Table 2.2).

Table 2.2-This table below shows Shelterin and Shelterin-associated primer sequences for use in Real-Time PCR

Primer name	Primer Sequence (5' ⟶ 3')	Product length (bp)	Accession Number
TIN2, SV1-F	CAAGACTGAGAAATCCACATGC	52	NM_001099247
TIN2, SV1-R	AACCATTCCCTGAACCCTCT		
TIN2, SV2-F	TTCTGGCTGCCATGGAAAAG	108	NM_012461
TIN2, SV2-R	GCTGCATCCAACTCAGCACAT		
TPP1, F	TTAGCGCTGTGTGTGTGCTCTT	101	NM_001082486
TPP1, R	CCGAACGGTTCAGCACATATTT		
POT1, SV2-F	GAGAACAAGCGACTATGCCCA	104	NR_003102
POT1, SV2-R	ACCCTAGGAAGAGTTTAGGCGG		
POT1, SV1-F	TTGTTCGCTTTCACAGGCTG	101	NM_015450
POT1, SV1-R	TCCCAAAGTTCCCTCAAACG		
TRF1, SV2-F	ATGCTCGATTTCCTCTGCCTC	101	NM_003218
TRF1, SV2-R	CCATGAATAATAGCCTCTGCGC		
TRF1, SV1-F	ATGGAACCCAGCAACAAGACC	215	NM_017489
TRF1, SV1-R	CGGCTGACTCTTTGAAACAGGT		
TRF2, F	AAAACGAAAGTTCAGCCCCG	101	NM_005652
TRF2, R	GCTGTCCTCCTCCAAGACCAAT		
RAP1, F	ACCCTGCTCTTTGGCTGTTCT	101	NM_018975
RAP1, R	TGTGTGCGCGTTTTAAGGAA		
TNKS1, F	TCAGTGTCTCTCCCAATGGCAC	103	NM_003747
TNKS1, R	TGTTTGCAAGGCCATTTACAGG		
TNKS2, F	CCCAACACTGCTCAATTGTCAC	101	NM_025235
TNKS2, R	GCAACGAGTGGCCTTTAAATTC		
TEP1, F	TGCCAGGCCGCACTGTCTTG	136	NM_7110
TEP1, R	ACCTGCTCCGCCCTCGTGAT		
SMG6, SV1-F	TCCCAGCAACCCCTTACATCT	115	NM_173156
SMG6, SV1-R	AAGCCGGCACAGCTTTTGTAG		
GAPDH-F	GAAGGTGAAGGTCGGAGT	226	N/A
GAPDH-R	GAAGATGGTGATGGGATTTC		

F: Forward, **R**: Reverse

2.5-Real Time Polymerase Chain Reaction (RT-PCR)

2.5.1-Optimizing primer concentration

Before carrying out qPCR, primers were tested using conventional PCR to make sure they gave the correct PCR product size. Primer concentrations were also optimised so that no primer dimmers or secondary products would be produced that could interfere with qPCR data. Three different concentrations (10µM, 5µM and 2.5µM) of forward and reverse primers were tested to find the optimized primer concentration. 10µl of 1.1x Reddy Mix (Thermofisher) (containing tracking dyes) was added to 1µl Forward primer, 1µl Reverse primer, 7µl sterile water, and 1µl cDNA. The reaction mixture volume was 20µl and was incubated in a thermo cycler at 94°C for 5 minutes, followed by 35 cycles of 94°C for 45 seconds, 60°C for 45 seconds, and 72°C for 10 minutes. After that, PCR products were ready for agarose gel electrophoresis.

2.5.2-Agarose gel electrophoresis

A 2% agarose gel was made in 1x TBE buffer solution (Sigma-Aldrich) (1.0M Tris, 0.9M Boric Acid, and 0.01M EDTA). 5µl ethidium bromide (10mg/ml) was added to the 100ml of molten gel and the gel poured into a tray (final concentration, 0.5µg/ml). Once the agarose gel was set, the gel was covered with 300ml of 1x TBE buffer and 20µl of PCR products were loaded into the wells. 7µl of 1kb ladder (Invitrogen) was used as a marker to estimate the size of PCR products. The gel was run at 70 V for approximately 1.5 hours. To visualise the PCR products, an Alphaimager under U.V. light was used. A single band should be seen in a positive lane, and no band should be seen in a negative control lane. The size of the PCR product must match the expected product size.

2.6-Real-Time quantitative RT-PCR (qRT-PCR)

SYBR® green master mix and the ABI Prism 7900HT (Applied Biosystems) was used to perform quantitative real-time reverse transcriptase PCR (qRT-PCR). qRT-PCR reactions were carried out in 96-well plates (Microamp, Applied Biosystems) and each sample was run in triplicate. A final volume of 10µl pre-mix was prepared containing 5µl of 2x SYBR® green master mix, 1µl of 5µM of forward and reverse primers (See Table 2.2 for primers used), 1µl of cDNA, and distilled water to make the final volume up to 10µl. Target and endogenous pre-mixes were prepared separately and 9µl of reaction pre-mix was aliquoted into each of 96-well plate; 1µl of cDNA was immediately added and the plate was sealed utilizing an optical adhesive film (MicroAmp® Optical Adhesive Film, Applied Biosystems). Samples were minimized to light exposure. After that, 96-well plate was centrifuged at 13000*rcf* for 1 minute at room temperature. All samples were analysed in triplicate and control reactions (where no cDNA was added in the 96-wells, only dH_2O) were included in the study design. The default PCR conditions are as listed below:

50°C .....2 min 1 cycle

95°C .....10 min 1 cycle

95°C..... 15 sec 40 cycles

60°C .....1 min 40 cycles

Finally the dissociation curve was constructed immediately after the PCR run to check and verify results. Relative quantification values were determined by the $2^{-\Delta\Delta Ct}$ method using SDS 2.3 software (Applied Biosystems). Dissociation curves were useful to detect nonspecific amplification, and primer dimmers that may affect the quality of the data.

In this way, the mRNA expression level of each gene was detected by using qRT-PCR normalized to GAPDH. Both β-actin and GAPDH was evaluated as endogenous controls and GAPDH was found to be more reliable endogenous control.

2.7- Genomic DNA extraction using Wizard ™Genomic DNA Kit protocol

Genomic DNA (gDNA) was extracted from cancer cell lines and normal mammary epithelial cell strains (See Table 2.1) using the Wizard ™Genomic DNA Kit protocol (Promega). Briefly, plates containing approximately $3x10^6$ cells were trypsinized and transferred to a labelled 1.5ml Eppendorf tubes. The cell pellets were centrifuged at 13,000*rcf* for 20 seconds. The supernatant was removed and cells were lysed by adding 600µl Nuclei Lysis solution. After removing all clumps by pipetting up and down, 3µl RNase A solution was added to the nuclear lysate. The samples were incubated for 30 minutes at 37°C. After adding 200µl of Protein Precipitating Solution, the tubes were shaken vigorously for 20 seconds. After that, proteins were precipitated by centrifugation for 5 minutes at 13,000*rcf*. The supernatant was transferred to a 1.5ml clean Eppendorf tube containing 600µl of (room temperature) isopropanol (2-Propanol) and gently mixed by inverting tubes. Following the precipitation of genomic DNA (gDNA), the samples were centrifuged at 13,000*rcf* for 5 minutes. After removing the supernatant, the resulting pellet was washed with 600µl of ice cold 70% ethanol and centrifuged for 1 minute at 13,000*rcf*. The pellets were dried for 10-15 minutes at room temperature. Pellets were re-suspended in 50µl of Rehydration Solution by incubating at overnight at 4°C. The isolated gDNAs were stored at -20°C until required. The concentration purity of DNA was read at 260 and 280 nm.

2.8-Western blotting

2.8.1-Protein isolation

After culturing cell lines to 80% confluence, the medium was removed and the plate was rinsed six times with 5ml of sterile ice-cold PBS and trypsinized as described above. The cell suspension was then transferred to a Falcon tube and centrifuged at 15000*rcf* for 5 minutes. The supernatant was aspirated off and the pellet washed three times with sterile ice-cold PBS. All the excess liquid was removed and 500µl of RIPA buffer (Radioimmunoprecipitation assay buffer, Sigma) and 10µl of 25x protease inhibitor (Thermo) was added to the tube and left for 5 minutes. After transferring cells to the fresh tube, samples were sheared by passing it through a 1ml syringe and a 23g needle 10 times (0.9 mm diameter). Samples were then collected into fresh Eppendorf tubes and centrifuged at 16,000*rcf* for 15 minutes at 4°C. The supernatant was aliquoted and transferred to clean Eppendorf tubes and stored at -80°C.

2.8.2-Determination of protein concentration

The protein concentration of samples was determined using the Pierce™ BCA Protein Assay Kit (Thermo Scientific). Pierce BCA Protein Assay is a detergent-compatible formulation based on bicinchoninic acid (BCA) for the colorimetric detection and quantitation of total protein. The assay was performed according to manufacturer's guidelines. A standard calibration curve was set up using bovine serum albumin (BSA) diluted in RIPA buffer, ranging from concentrations 0-5µg/ml (Figure 2.1). All unknown sample protein concentrations were measured against the standard curve (Table 2.3).

Table 2.3-Preparation of diluted BSA standards for BCA analysis

Tube	Volume of dH_2O	Volume of BSA	Final BSA concentration (µg/ml)
A	100	0	0
B	90	10	0.25
C	80	20	0.5
D	60	40	1
E	40	60	1.5
F	25	75	3
G	0	100	5

200µl of working reagent (BCA protein assay reagent A/B diluted 50:1) was prepared for each aliquot of protein extract and BSA protein standard concentration. To each 5µl of protein lysate, 200µl of the Working Reagent was added and the samples were vortexed thoroughly on a shaker for 30 second. The tube was incubated at 37°C for 30 minutes in a water bath and then allowed to cool at room temperature. Subsequently, 100µl of each sample was added to the 96-well plate. The A562 of the standards and protein lysates was then measured using a plate reader (BP800, BioHit). A standard curve was prepared by plotting the blank-corrected measurement for each BSA standard against its concentration. The standard curve was then used to determine the protein concentration of each study sample.

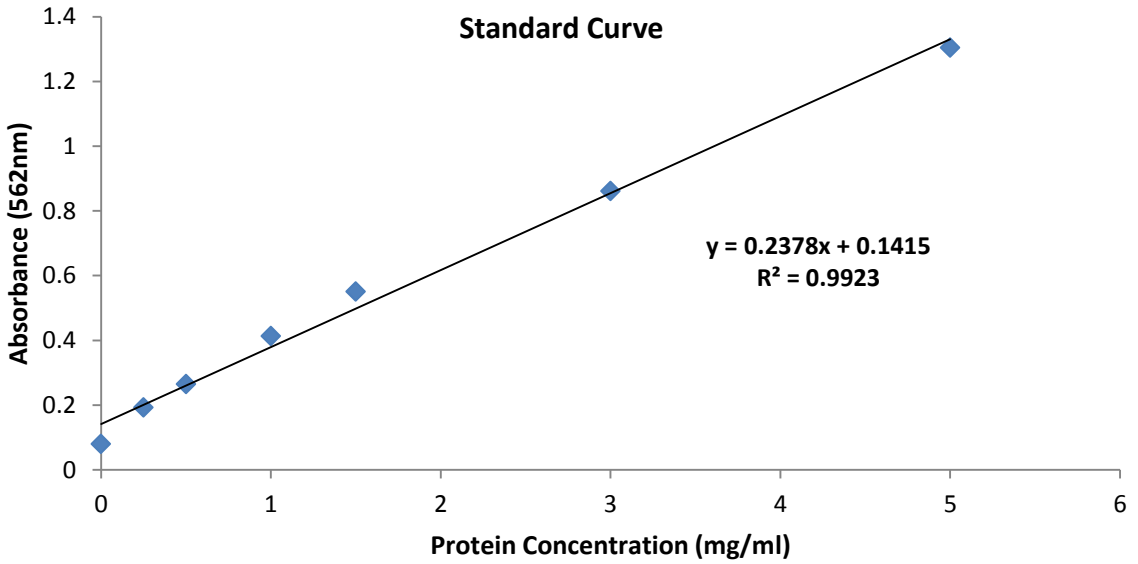

Figure 2.1-Standard curve used in protein quantification.

2.8.3-Protein gel electrophoresis

Protein lysates were prepared from breast cancer cell lines and a normal human mammary epithelial cell strain. The protein concentration was determined utilizing the BCA assay as previously described. For each sample, approximately 30µg of protein was prepared in 4x Laemmle buffer (1.5M Tris-Cl pH 6.8, glycerol, β-mercaptoethanol, SDS, 1% bromophenol blue) to a total volume of 30µl. The lid of the Eppendurf tube was pierced and samples were placed at 95°C for 10 minutes to denature the globular structure of the proteins and then centrifuged at high speed for 30 seconds and the tubes were left on ice until used. 30µl of samples were loaded carefully onto each well of a ready-made 12**%** precast acrylamide gel (Bio-Rad). The protein marker (Sigma) was loaded in the first and last wells of the gel. The interior and exterior of the tank was filled with 1x ready-made running buffer (Bio-Rad). After that, the samples were initially run at 100 volts until proteins entered

the gel and the power was switched to 250 volts for approximately 45 minutes. The samples were checked regularly to prevent running off of the protein samples.

2.8.4-Blotting and transfer

Acrylamide gels were blotted onto Mini PVDF Transfer ready-made membrane (Bio-Rad) using the Trans-Blot® Turbo™ apparatus (Bio-Rad) according to the manufacturer's protocol.

2.8.5-Blocking and antibody incubation

Once the transfer of protein from gel onto the ready-membrane was completed the membranes were blocked with 5% blocking solution. The blocking reagent contains 5g (w/v) of semi-skimmed milk (Marvel) in 100ml of Tris buffer saline-Tween (TBST) made with 16g (w/v) of NaCl, 0.2g (w/v) KCl, 3g (w/v) of Tris base, 0.1% (v/v) Tween-20 added to 800ml of distilled water adjusted pH to 7.6, and distilled water added to 1 litre. The membrane was incubated in 20ml of blocking solution for one hour on a shaker at room temperature. The milk mixture blocks the non-specific binding of an antibody to the membrane. Following one hour of blocking, the membrane was rinsed with TSBT and the primary antibody was added. The primary antibody was diluted down according to the manufacturer's recommendation and was further optimized by the user. Table 2.4 below shows all antibodies used in this experiment with optimized dilution ranges.

Table 2.4-Primary and secondary antibodies used in western blot experiments

Antibody	Manufacturer	Source	Clonality	Dilution
POT1 Primary	Abcam	Rabbit	Monoclonal	1:5000
POT1 Secondary	Abcam	Rabbit	Polyclonal	1:10000
TPP1 Primary	Abcam	Rabbit	Polyclonal	1:7500
TPP1 Secondary	Abcam	Rabbit	Monoclonal	1:10000
β-actin Primary	Sigma	Rabbit	Polyclonal	1:10000
β-actin Secondary	Abcam	Goat Anti-rabbit	Polyclonal	1:20000

Primary antibodies were diluted in 5% blocking buffer in 1x TBST and added to the membrane overnight on a shaker set at medium pace (100rpm/minute) at 4°C. The following day the membrane was washed four times with 1x TBST for 15 minutes each and incubated with a secondary antibody diluted in 5% blocking buffer on a shaker at room temperature for one hour.

2.8.6-Protein detection with chemiluminescence

After 1 hour incubation with a secondary antibody the membrane was washed four times in 1x TBST for 15 minutes. The amount of ECL plus (Enhanced chemiluminescence) kit (GE Healthcare) required for detection was based on the size of the membrane and was recommended by the manufacturer. 1ml of reagent A was mixed with 1ml of reagent B. The ECL mixture was pipetted onto the membrane, ensuring that whole surface of the membrane was saturated with the reagent, and covered with Saran wrap and left for 5 minutes in a dark room. The excess of the ECL was tipped off onto a paper towel, wrapped with the protein containing side of the membrane facing down onto a piece of clean Saran wrap and placed in an x-ray cassette. Exposure to ECL plus hyperfilm (Amersham) was done

for between 30 seconds and 20 minutes. The x-ray films were developed using an automatic machine (CURIX 60, AGFA). The ECL chemiluminescence was active for at least one hour allowing multiple exposures.

2.9-Statistical Analysis

All statistical analysis was performed using Student's t test and the level of significance used throughout was $P \leq 0.05$.

CHAPTER III

ANALYSIS OF EXPRESSION OF SHELTERIN AND SHELTERIN-ASSOCIATED GENES IN BREAST CANCER CELL LINES

3.1- Introduction

Telomeres are made up of G-rich nucleotide repeats $(TTAGGG)_n$ that protect chromosome ends in mammalian cells. A six-protein complex called Shelterin or the telosome, comprised of TRF1, TRF2, POT1, TIN2, TPP1 and RAP1, packages telomeric DNA and helps to hide the chromosome ends from being recognized as sites of DNA damage during DNA replication (Martinez and Blasco 2010). Shelterin proteins interact with a number of other factors known as Shelterin-associated proteins that can influence chromosome-end integrity and dynamics. These Shelterin-associated genes are Tankyrase 1, Tankyrase 2, *SMG6* and *TEP1* (Smith, Giriat *et al.* 1998; Liu, Snow *et al.* 2000; Salhab, Jiang *et al.* 2008).

In the absence of telomerase, i.e., in most normal adult somatic cells, the hexanucleotide repeats decrease after each cell division; therefore cells undergo senescence or apoptosis when the lengths of telomeres are reduced to a critical level. In addition, telomere loss causes genome instability, resulting in destruction of cell-cycle control, one of the hallmarks of cancer (Lu, Zhang *et al.* 2011). The telomerase enzyme regulates telomere length elongation (Greider 1996). In most cancer cells, telomerase has been reactivated and prevents cancer cells from entering senescence or apoptosis (Lu, Zhang *et al.* 2011). Consequently, the activation of telomerase is an important step in development of human cancers (Salhab, Jiang *et al.* 2008). Previous studies reported that Shelterin genes (*TRF1*, *TRF2*, and *POT1*) were up-regulated in gastric, breast, cervix and brain cancer cell lines (Matsutani, Yokozaki *et al.* 2001; Lee, Rha *et al.* 2008) whereas another group (Yamada, Tsuji *et al.* 2002) demonstrated that the expression of Shelterin genes (*TRF1*, *TRF2* and *TIN2*) was decreased in gastric cancer cell lines. Moreover, Salhab *et al.* (2008)

quantified comprehensively the levels of mRNA expression of *hTERT*, *hTR*, Shelterin and Shelterin-associated genes in breast cancer tissue samples by real-time polymerase chain reaction. Their results showed that the expression levels of *TNKS2*, *POT1* and *TRF2* were significantly lower in malignant tissues compared with normal matched tissue samples. However, *TEP1*, *TNKS1*, and *EST1* were up-regulated (Salhab, Jiang *et al.* 2008). Furthermore, subsequent studies have confirmed that *POT1* is over-expressed in gastric cancer tissues (Gao, Zhang *et al.* 2011). Also, the transcriptional level of *TRF2* was found to be correlated with tumour size; i.e, large tumours expressed higher levels of *TRF2* (Gao, Zhang *et al.* 2011).

In order to obtain a better and clearer understanding of the exact role and function of Shelterin and Shelterin-associated proteins in protection and maintenance of telomeres in human breast cancer, the mRNA expression levels of Shelterin and Shelterin-associated genes in a panel of ten breast cancer cell lines and one prostate cancer cell line were compared with commercially (Applied Biosystems) available normal human mammary tissue (cDNA) and that from normal primary human mammary epithelial strains (controls).

3.2-Materials and methods

3.2.1- Analysis of cDNA quality

Total RNA from about $1x10^6$ human epithelial cells was isolated using RNeasy Mini Kit (50) (QIAGEN Company). Total RNA (1µg) was reverse-transcribed into cDNA using superscript III (Invitrogen). The forward and reverse primer sequences used for all Shelterin and Shelterin-associated genes are detailed in Table 2.2. Analysis of the standard Shelterin and Shelterin-associated RT-PCR products on agarose gels showed a correct size for all human breast cancer cell lines, normal mammary epithelial cell strain (HMEC) and a prostate cancer cell line (PC-3). In all cases, observation of a specific fragment in the absence of primer-dimmer band was sufficient to confirm the quality and quantity of cDNA samples to utilize subsequently for qRT-PCR.

3.3-Quantification of Shelterin and Shelterin-associated mRNA in breast and prostate cancer cell lines

To determine the level of Shelterin and Shelterin-associated mRNA transcription in breast cancer cell lines, qRT-PCR was performed. To quantify Shelterin and Shelterin-associated expression levels, the C_t values obtained for each mRNA were normalised to those for human *GAPDH* mRNA (endogenous control). Each sample was run in triplicate (Figure 3.1) and each experiment was performed at least three times to ensure the reproducibility and accuracy of the results. The mean value of each individual triplicate sample was used in further calculations utilizing the $2^{-\Delta\Delta Ct}$ method to determine relative quantification (RQ) values using the SDS 2.3 software (Applied Biosystems). Relative transcription levels of all Shelterin and Shelterin-associated genes from the panel of cancer cell lines were calibrated by calculating the RQ mean values and human breast total RNA

(Normal) was used as a calibrator. Applying the qRT-PCR amplification program, the quality of the target and endogenous (Shelterin, Shelterin-associated and GAPDH) cDNA products, with no primer-dimmer formation, was confirmed by constructing the dissociation curve analysis (Figure 3.1).

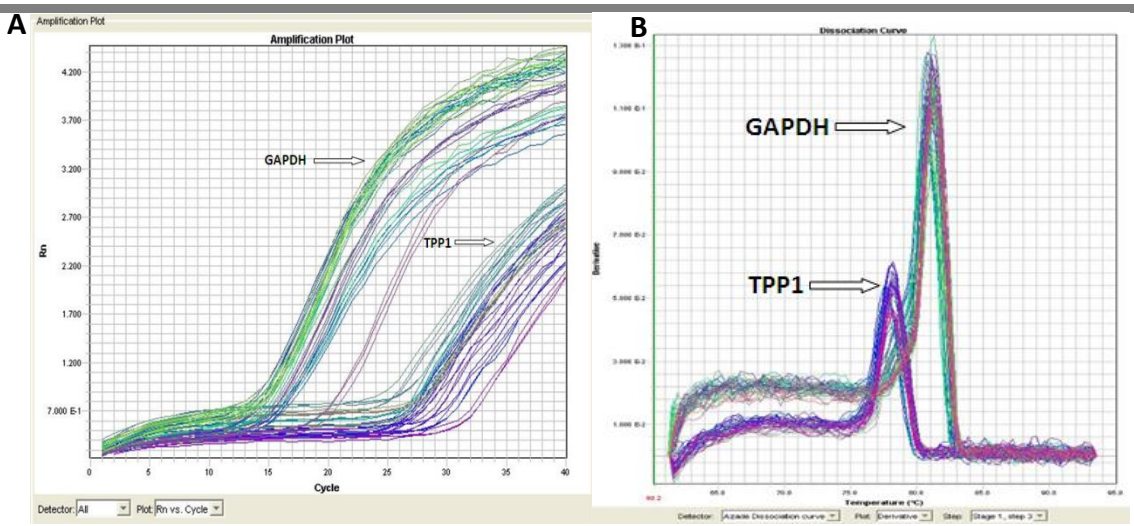

Figure 3.1-qRT-PCR analyses. The images show schematic example of **(A)** C_t of each individual triplicate sample for target gene and GAPDH cDNAs, **(B)** dissociation curve for RT-GAPDH and RT-POT1 primers.

3.4-Results

3.4.1-Determination of Shelterin, Shelterin-associated and GAPDH mRNA expression levels using real-time quantitative RT-PCR

Expression levels of Shelterin and Shelterin-associated genes were quantified in normal breast tissue, a large panel of breast cancer epithelial cell lines (MCF-7, GI101, BT474, 21MT-2, MTSV1-7, HCC1143, BT20, PB1, HS578-T, and 21NT) and a prostate cancer cell line (P-C3) by quantitative RT-PCR to compare the expression level of each gene in normal commercial tissue and cancerous cells. Some of the Shelterin genes have different splice variants; for example, there are five splice variants (SV) of *POT1* whereas *TNKS1* and *TNKS2* do not have splice variants (Table 3.1). To investigate whether there is a difference in mRNA expression level between *POT1* isoforms in cancer cell lines, two sets of primers were designed for SV1 and SV2 (Table 3.1). In addition, *TIN2* and *TRF1* genes have two splice variants which were quantified by qRT-PCR while four isoforms have been observed in *SMG6* (*EST1*) from which only one isoform was assessed (Table 3.1).

Table 3.1-Shelterin and Shelterin-associated genes that encode splice variants

Gene	No of splice variants	Size of variants (bp)	Accession Number
POT1	5	V1: 4095	NM_015450
		V2: 4215	NR_003102
		V3: 4006	NR_003103
		V4: 3964	NM_001042594
		V5: 4192	NR_003104
SMG6	4	V1: 5936	NM_173156
		V2: 5798	NM_201568
		V4: 4789	NM_201569
		V5: 6054	NM_001174061
TNKS1	----	9599	NM_003747
TNKS2	----	6274	NM_025235
TIN2	2	V1: 1869	NM_001099274
		V2: 2196	NM_012461
TRF1	2	V1: 2960	NM_017489
		V2: 2900	NM_003218
TRF2	----	2996	NM_005652
RAP1	----	2196	NM_018975
TEP1	----	10694	NM_007110
TPP1	----	3540	NM_000391

As shown in Figure 3.2, the expression of *POT1*, SV1, was lower in breast cancer cell lines than in normal breast tissue. This difference was statistically significant when comparing the levels in normal tissue with those in primary and advanced tumours ($P<0.5$). Figure 3.2-B shows that *POT1* SV2 was also down-regulated in tumour cell lines *(*$P<0.05$ and $P<0.01$ respectively). However, no substantial differences in expression between *POT1* SV1 and *POT1* SV2 were observed (See also Figure 3.9).

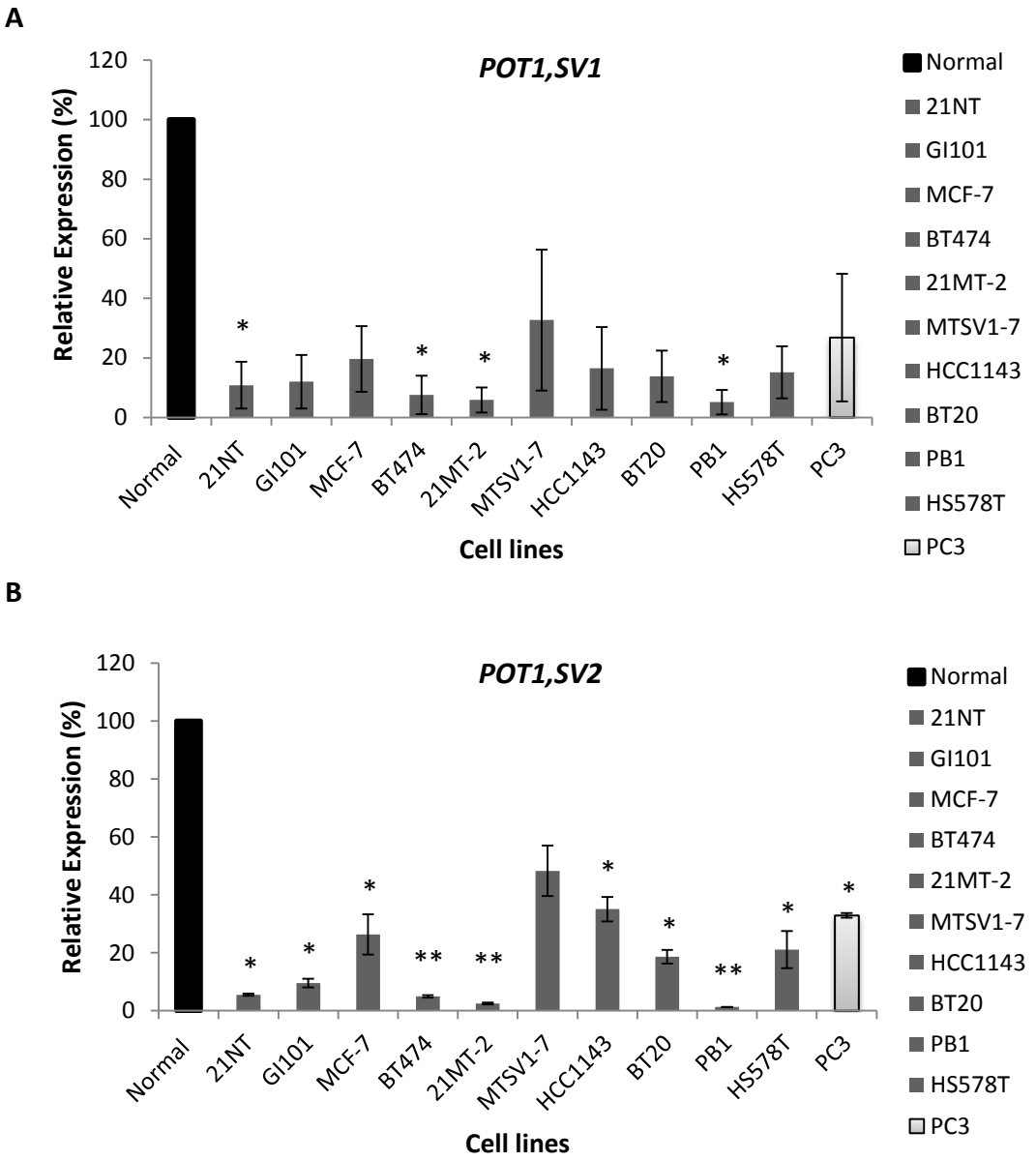

Figure 3.2-Expression of *POT1* variants 1 and 2 in tumour cell lines. The level of *POT1* normalised against *GAPDH* mRNA in breast cancer cell lines compared with prostate cancer and normal breast tissue, determined by a quantitative reverse transcription polymerase chain reaction. **A)** *POT1*, SV1 and **B)** *POT1*, SV2 expression in breast cancer samples, a normal breast tissue and a prostate cancer cell line (PC-3). The PC-3 cell line was included for comparison. Normal breast tissue (cDNA) was used as the calibrator. Error bars represent SEM,* $P<0.05$ and ** $P<0.01$.

The mRNA expression of *RAP1*, *TNKS1* and *TNKS2* were substantially decreased in all cancer cell lines compared with normal breast tissue (P<0.05, P<0.01, and P<0.001 respectively) (Figures 3.3 and 3.4). However, expression of *RAP1* was at least 2-fold higher in MCF-7 and PC-3 compared with other cancer cell lines (Figure 3.3).

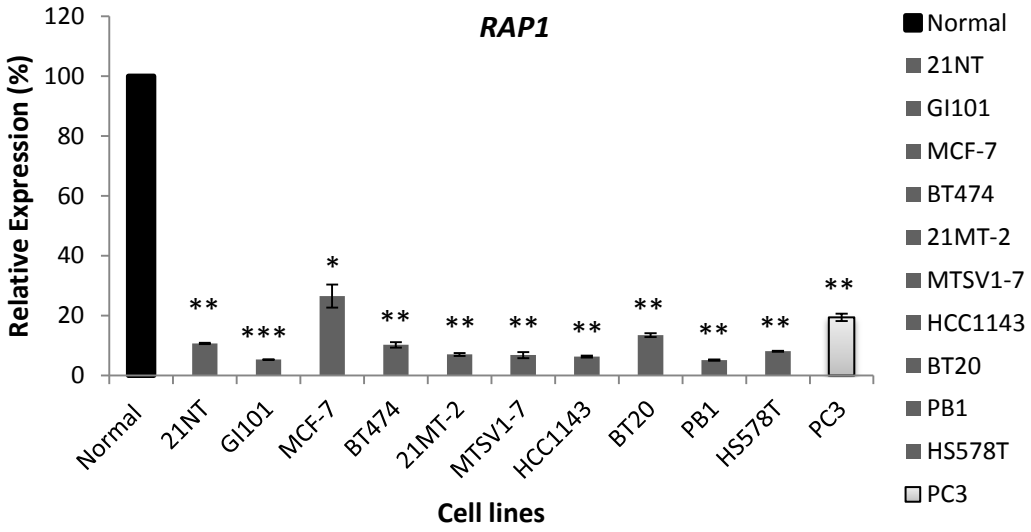

Figure 3.3-Expression of *RAP1* in tumour cell lines. Quantification of *RAP1*, mRNA levels determined by qRT-PCR in PC-3 and breast cancer cell lines. Normal breast tissue (cDNA) was used as the calibrator. Error bars represent SEM, * P<0.05, ** P<0.01, *** P<0.001.

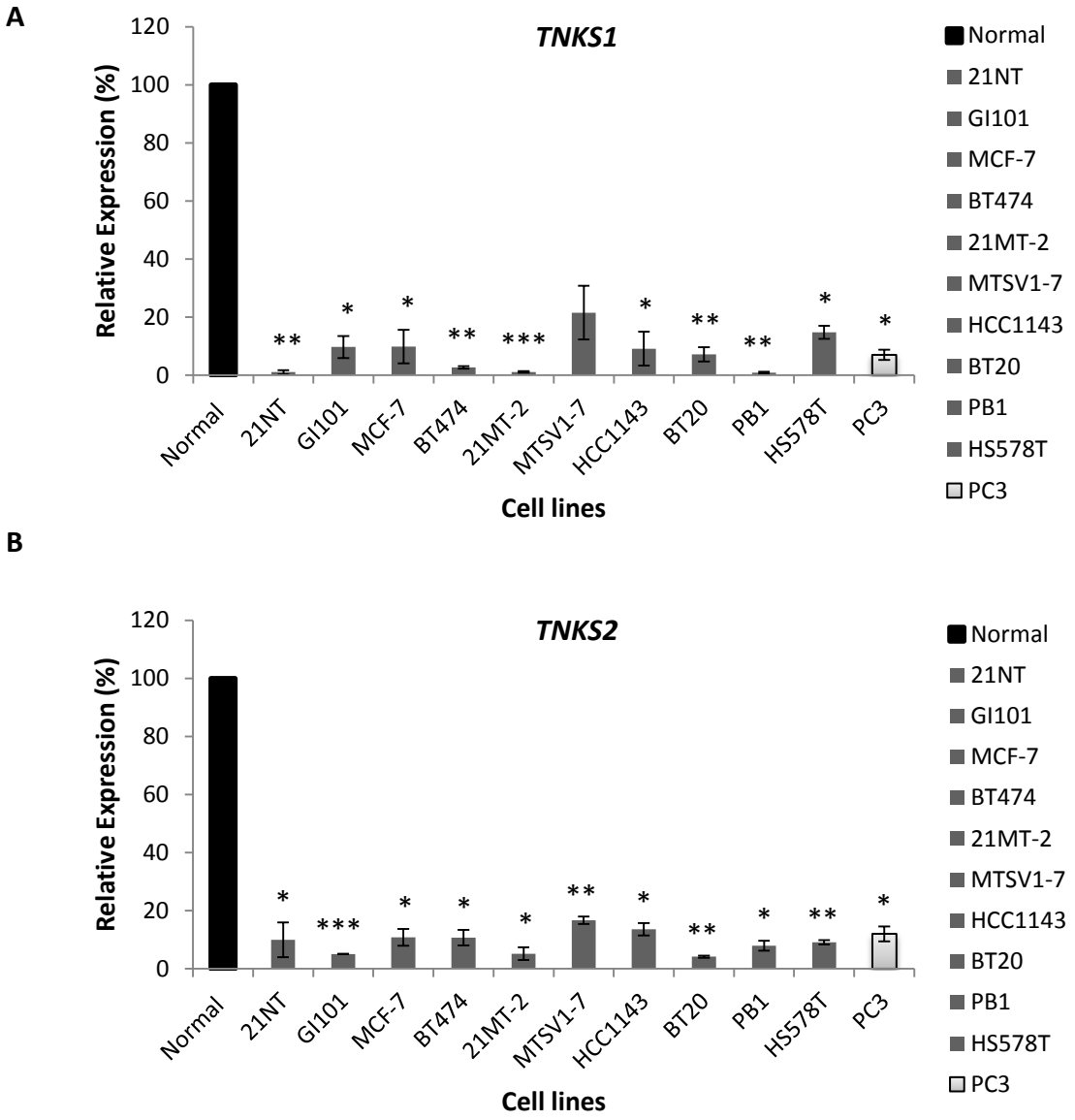

Figure 3.4-Expression of *TNKS1* and *TNKS2* in tumour cell lines. The histograms in **(A)** and **(B)** represent qRT-PCR analysis of *TNKS1* and *TNKS2* mRNA isolated from cancer cell lines. **A)** *TNKS1* and **B)** *TNKS2* expression in breast cancer, prostate cancer, and normal tissue. Normal breast tissue (cDNA) was used as the calibrator. Error bars represent SEM, **P*<0.05, ***P*<0.01, ****P*<0.001.

Figure 3.5 shows that with *TIN2* (SV1 and SV2) levels in all breast tumour cell lines and the prostate cancer cell line (PC-3) were also considerably lower than that of normal breast tissue; the most significant reductions were observed in GI101, MTSV1-7, BT20, and HS578-T cells ($P<0.05$ and $P<0.01$ correspondingly). However, no major differences have been observed between the two *TIN2* splice variants ($P<0.05$, and $P<0.01$ respectively).

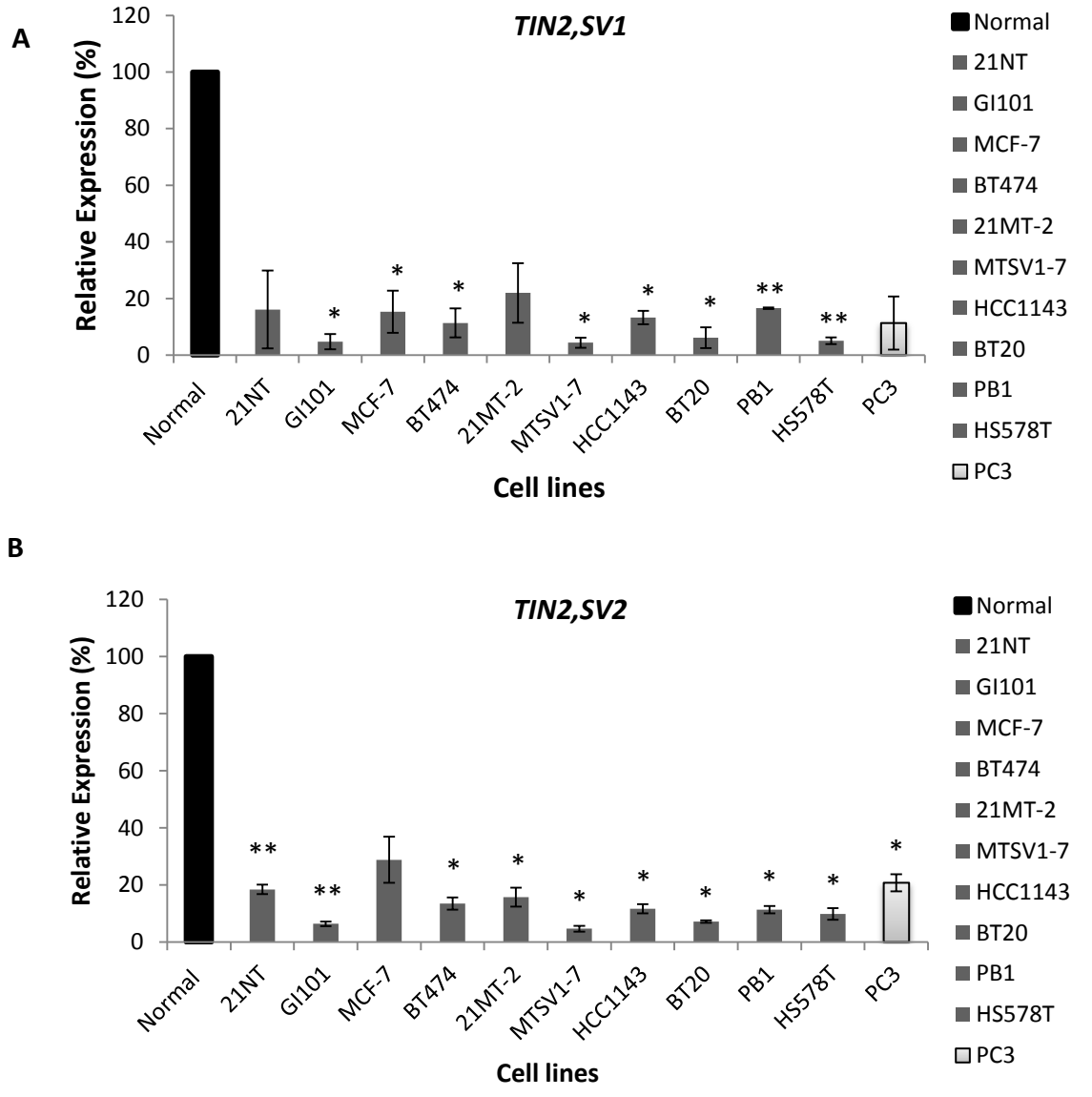

Figure 3.5-Expression pattern of *TIN2*, SV1 and SV2. The graphs (**A** and **B**) represent analysis of mRNA from the indicated human cell lines by qRT-PCR to detect the *TIN2* SV1 and *TIN2* SV2. Error bars represent SEM, * $P<0.05$, ** $P<0.01$.

As shown in Figure 3.6-A, all the breast cancer cell lines examined expressed substantially lower levels of *SMG6* ($P<0.05$, $P<0.01$, and $P<0.001$ respectively) in comparison with normal breast tissue control. In marked contrast to the other Shelterin genes, with *TPP1*, MCF-7, MTSV1-7, PB1, BT20, and PC-3 cell lines expressed high levels of *TPP1* mRNA compared with normal tissue, whereas the remainder of the breast cancer cell lines expressed low levels of *TPP1* (Figure 3.6-B) ($P<0.05$ and $P<0.01$ correspondingly).

Results are presented for *TRF1* SV1 and SV2, and *TRF2* in Figures 3.7-A, 3.7-B and 3.8-A. The mRNA expression of *TRF1* SV1, its splice variant 2 and *TRF2* was significantly lower ($P<0.05$ and $P<0.01$ correspondingly) in comparison with expression of *TRF1* and *TRF2* from normal breast tissue. However, the mRNA levels of *TRF1* SV1 and SV2 were higher in the prostate cancer cell line (PC-3) in comparison with breast cancer cell lines. *TRF2* and *TEP1* showed a trend similar to that of *TRF1* in all tumour cell lines (Figures 3.7 and 3.8). In this section, all the results indicated that, with the notable exception of *TPP1*, all Shelterin and Shelterin-associated genes were down-regulated in tumour cell lines.

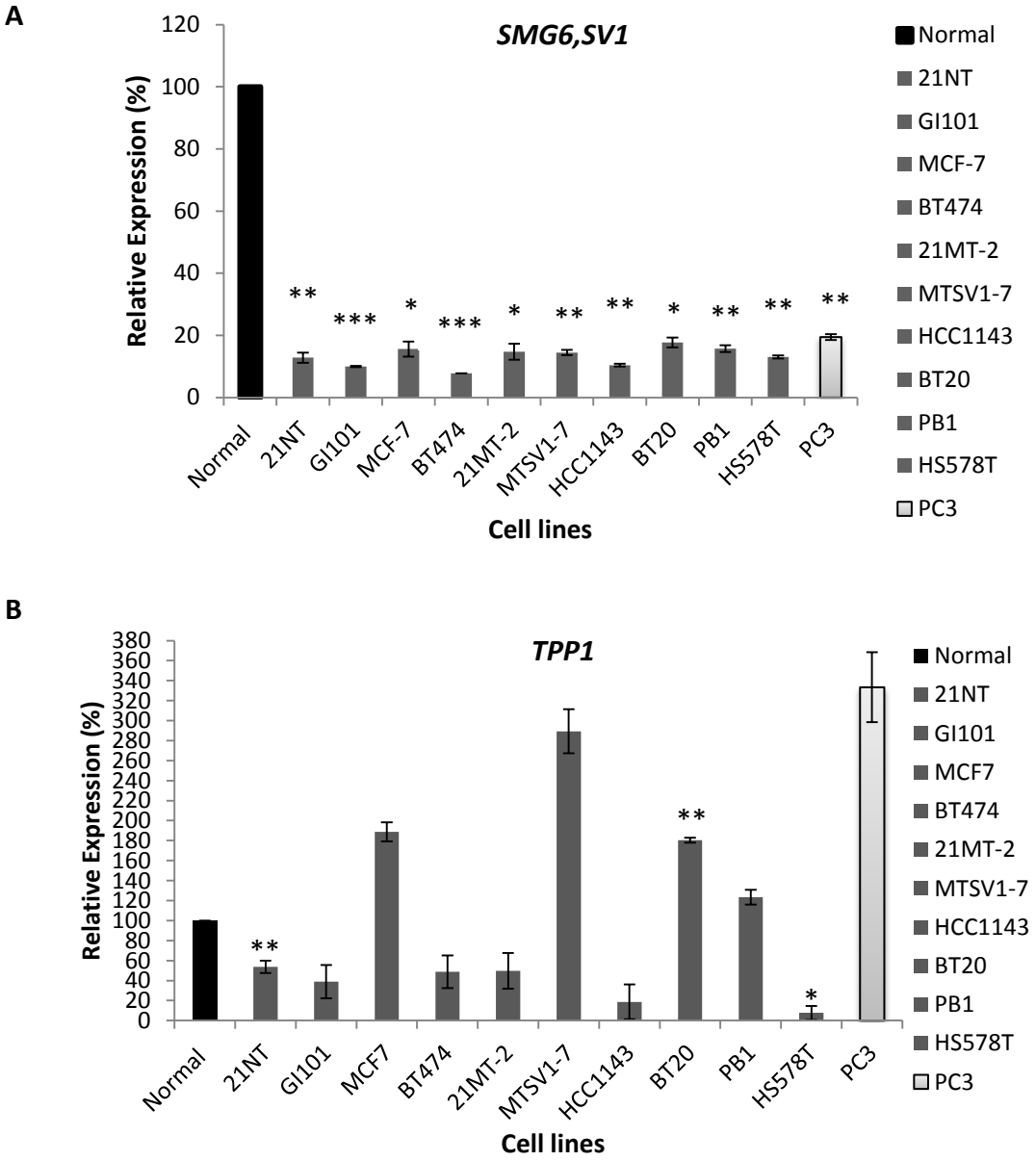

Figure 3.6-Expression patterns of *SMG6* (or *EST1*) and *TPP1*. A) Represents analysis of mRNA from the indicated human cell lines by qRT-PCR to detect SMG6 mRNA levels. **B**) The mRNA levels of *TPP1* determined by qRT-PCR in breast, prostate cancer cell lines and normal breast tissue. Normal breast tissue (cDNA) was used as the calibrator. Error bars represent SEM, **P*<0.05, ***P*<0.01, ****P*<0.001.

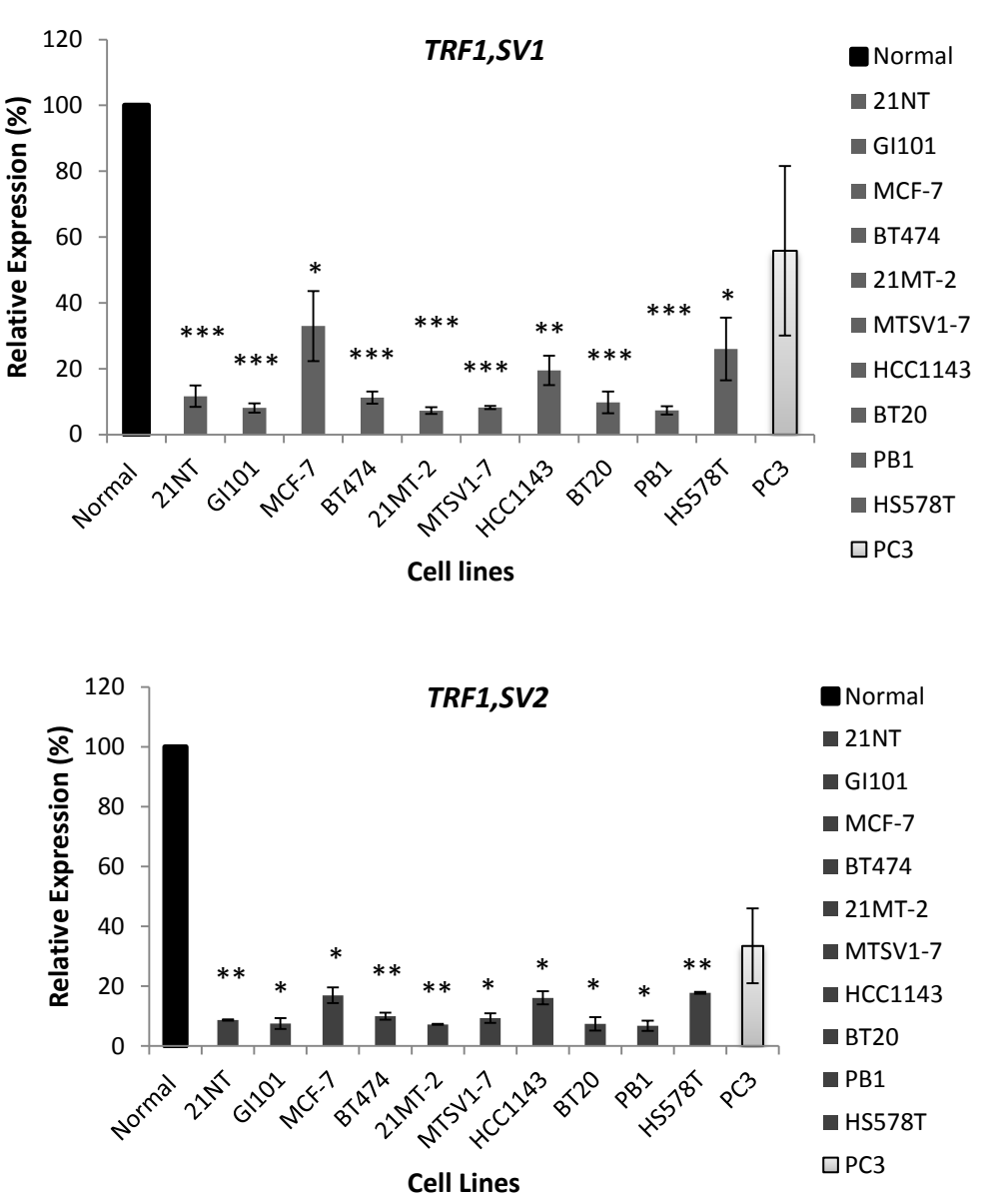

Figure 3.7-The level of *TRF1* V2 and V1 in breast and prostate cancer cell lines, determined by qRT-PCR. A) *TRF1*, SV2 and **B)** *TRF1*, SV1 expression in breast cancer, prostate cancer, and normal tissue. Normal breast tissue (cDNA) was used as the calibrator. Error bars represent SEM, **P*<0.05, ***P*<0.01, ****P*<0.001.

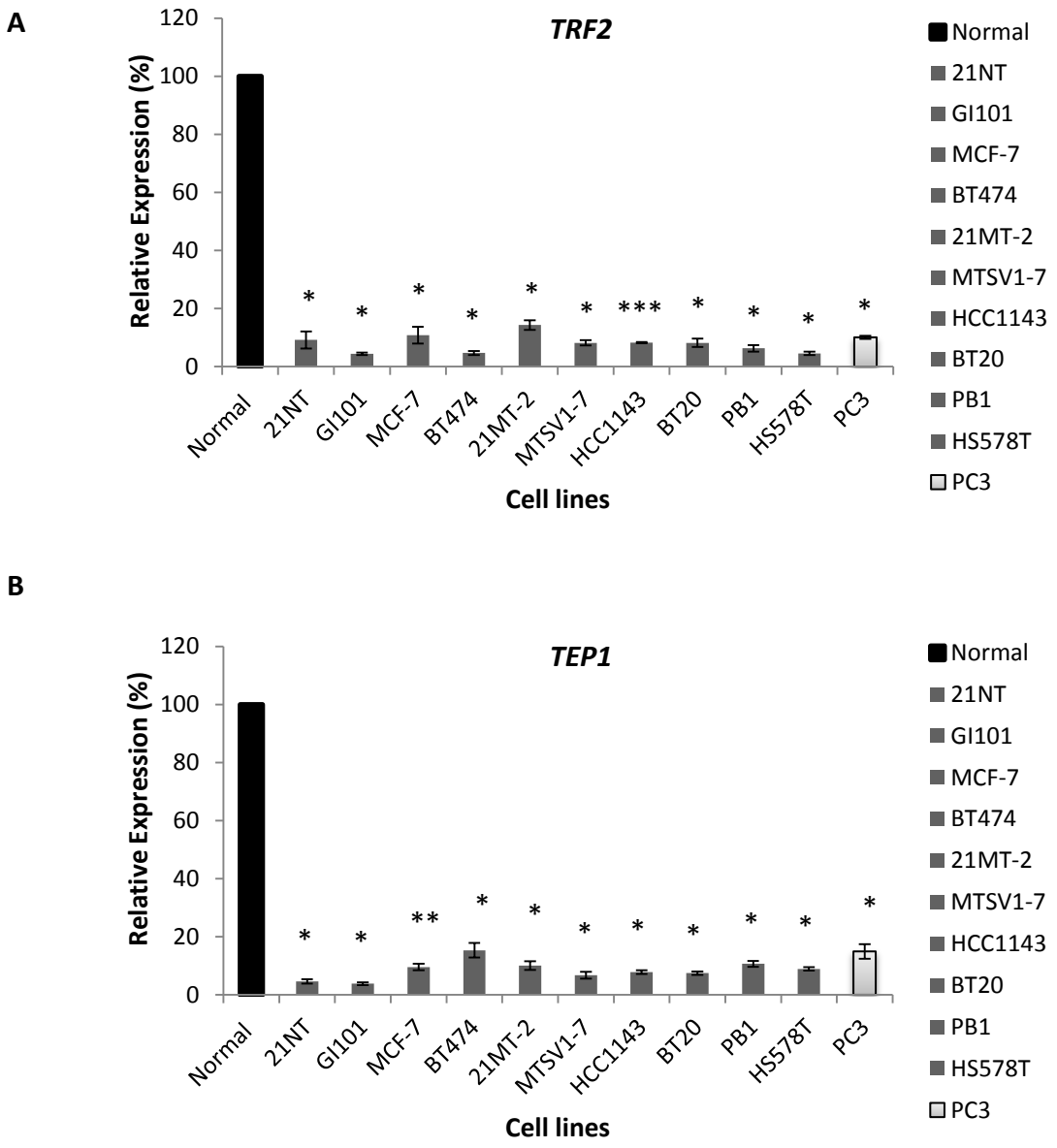

Figure 3.8-*TRF2* and *TEP1* mRNA transcription levels in tumour cell lines and normal tissue. The image **(A)** and **(B)** illustrate qRT-PCR analysis of *TRF2* and *TEP1* mRNA isolated from cancer cell lines. **A)** *TRF2* and **B)** *TEP1* expression in breast cancer, prostate cancer, and normal tissue. Normal breast tissue (cDNA) was used as the calibrator. Error bars represent SEM, **P<0.05, **P<0.01, ***P<0.001.*

3.4.2-POT1 and TPP1 mRNA and protein expression in normal breast epithelial (HMEC) cells and cancer cell lines in culture

3.4.2.1-Gene expression of *POT1* and *TPP1* in breast cancers and the human mammary epithelial strain (HMEC1)

As shown in previous section (3.4.1), all Shelterin and Shelterin-associated genes, except *TPP1*, were down-regulated in breast cancer cell lines in comparison with a normal breast tissue control. Previous work by Salhab *et al.* (2008), showed that levels of *POT1* mRNA were significantly lower in malignant breast tissues in comparison with normal tissues (P=0.0008 and P=0.038 respectively). Moreover, with regard to the hypothesis of a critical role of *POT1* and *TPP1* in telomere length maintenance (Wang F 2007), reanalysis of these genes with a normal mammary epithelial culture cell strain (HMEC1) was warranted.

Human tissues are organized communities of several different cell types that work together to control the function of individual organs. Therefore, these cells may vary at the mRNA and/or protein level in order to carry out their specific functions. In this way, cellularly heterogeneous tissue samples taken for analysis may perhaps exhibit highly varied gene expression or protein levels, compared with individual pure cell strains (Bryant and Mostov 2008). In order to further validate the obtained results, a normal breast mammary epithelial cell strain (HMEC1) was analysed for mRNA levels of *POT1* and *TPP1*.

Based on the results depicted in Figure 3.9-A, it is evident that, the transcription levels of *POT1* in malignant cell lines was substantially lower (P<0.05 and P<0.01 respectively) compared with non-malignant breast tissue. In addition, the mRNA levels of *POT1* in normal mammary cell strains were approximately 20-fold lower than normal breast

tissue control. Therefore, in order to validate obtained results, the graph was re-plotted. As shown in Figure 3.9-B, it is evident that all malignant cell lines expressed substantially lower levels of *POT1* in comparison with HMEC1 ($P<0.05$ and $P<0.01$ respectively).

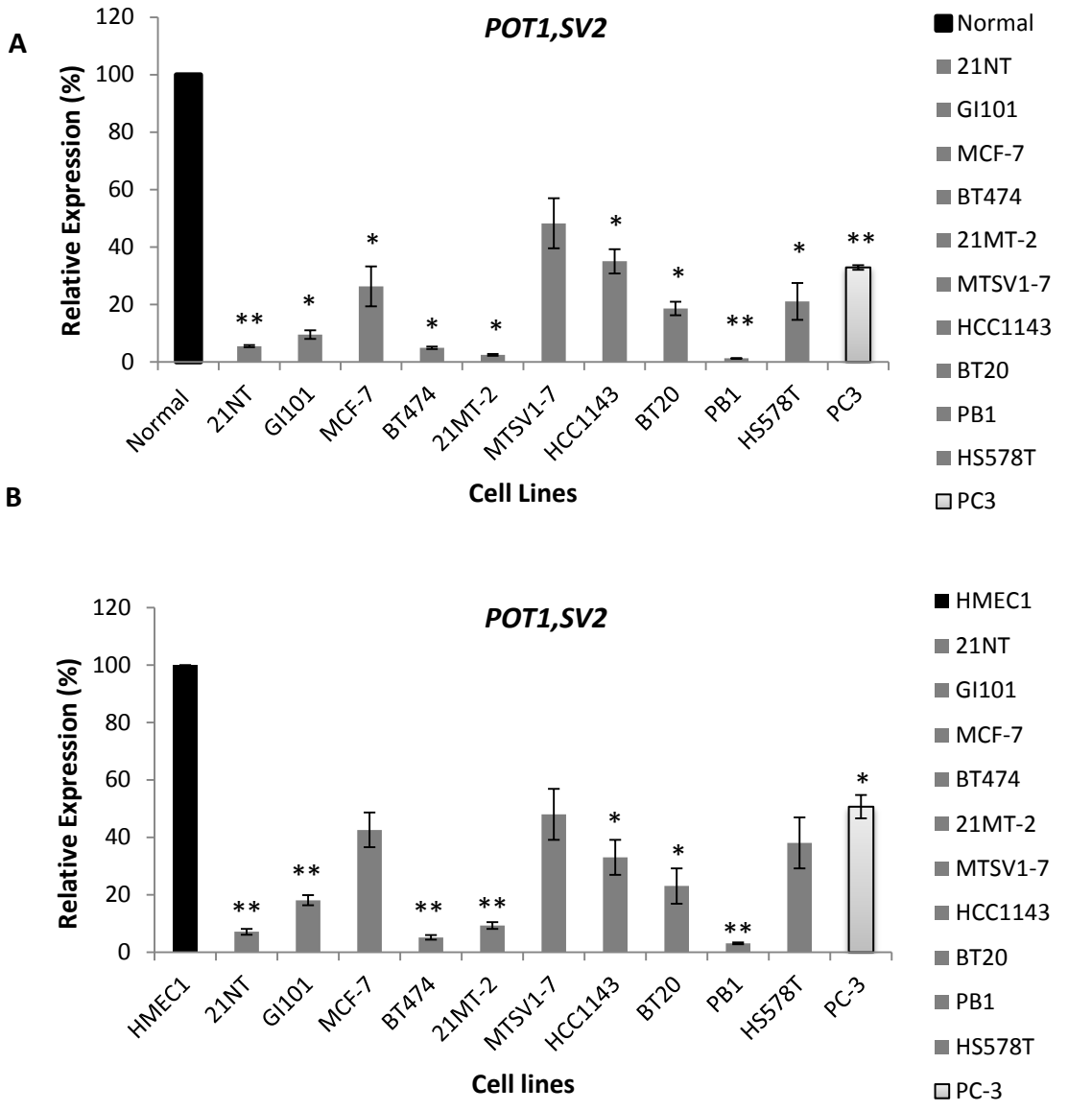

Figure 3.9-Expression patterns of *POT1 SV2* in normal and cancer cell lines. The level of *POT1* mRNA determined by qRT-PCR in breast, prostate cancer cell lines, and normal human epithelial cell (HMEC1) and normal tissue. **A)** Normal breast tissue (cDNA) was used as the calibrator. **B)** Normal mammary epithelial cell strain (HMEC1) was used as the calibrator. Error bars represent SEM, **P*<0.05, ***P*<0.01.

As shown in Figure 3.10-A, the mRNA expression of *TPP1* in PC-3, MTSV1-7, MCF-7, BT-20 and PB1 was over-expressed compared with normal control tissue ($P<0.05$ and $P<0.01$ respectively). In fact, all tumour samples except HS578-T expressed high levels of *TPP1* in comparison with HMEC1 ($P<0.05$ and $P<0.01$ respectively) (Figure 3.10-B).

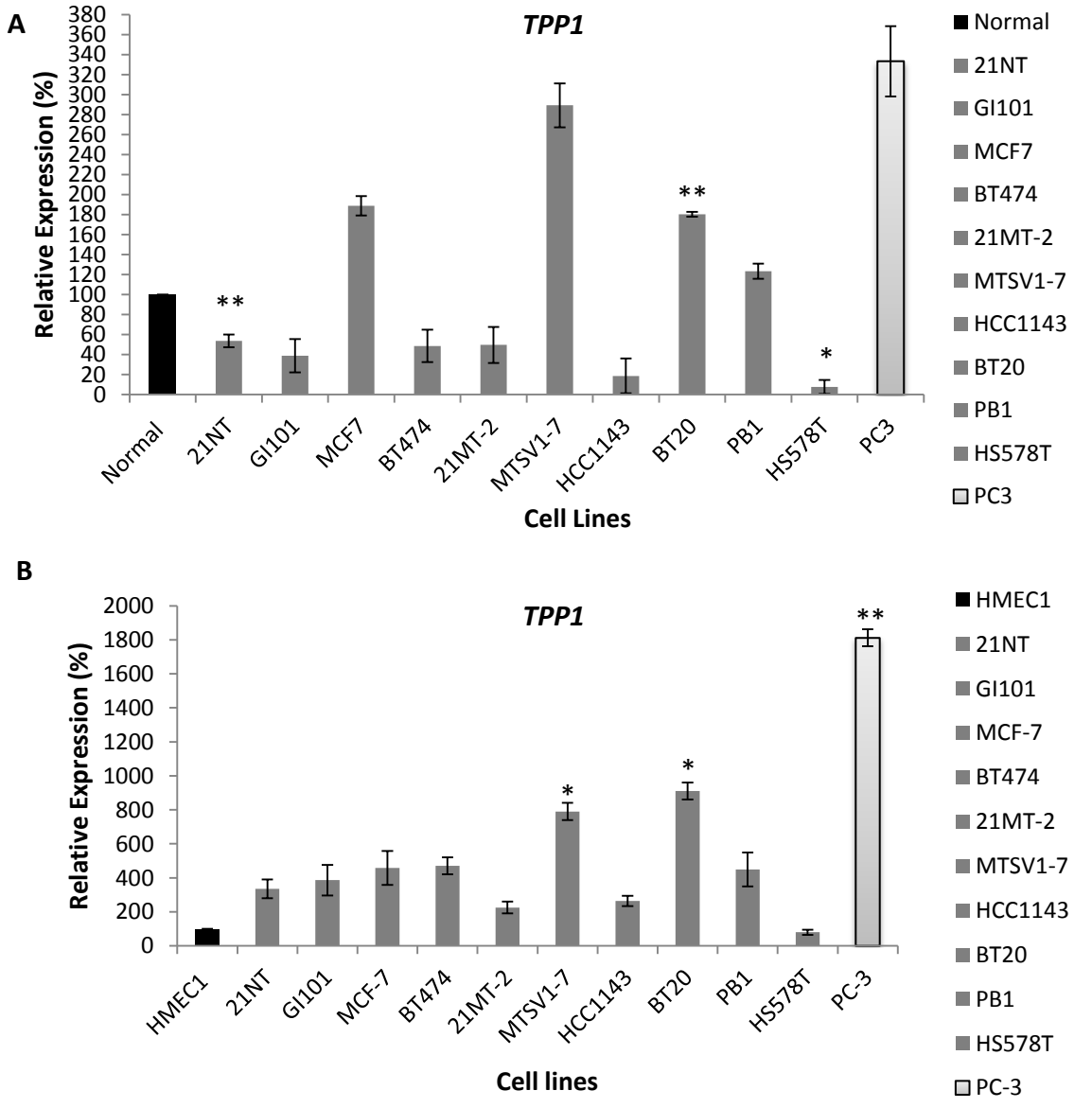

Figure 3.10-Expression patterns of *TPP1* in all normal and cancer cell lines. The mRNA levels of *TPP1* determined by qRT-PCR in breast, prostate cancer cell lines, HMEC1 and normal breast tissue (cDNA). **A)** Normal tissue (cDNA) was used as a calibrator. **B)** HMEC1 was used as the calibrator. Error bars represent SEM, * $P<0.05$, ** $P<0.01$.

3.4.2.2-Protein analysis of POT1 and TPP1 in breast cancer cell lines and HMECs control

An attempt was made to corroborate qRT-PCR results with western blot analysis on a panel of eight human breast cancer cell lines and a normal primary mammary epithelial cell strains at different passage numbers. The western blot analysis was carried out using POT1 rabbit monoclonal antibody (Abcam) and TPP1 rabbit polyclonal antibody (Abcam) and the values were normalised using β-Actin rabbit antibody (Sigma). The imageQuant 5.0 densitometry was used for densitometry analysis. The protein expression of POT1 and TPP1 was normalised to total β-Actin as a housekeeping gene expression and optical density values are presented in all figures. A 71-KD band (Abcam) was evident in each samples corresponding to POT1 (Figure 3.11-A). Figure 3.11 indicates that the POT1 protein levels were similar in BT20, GI101, HCC1143, BT-474 and MCF-7 breast cancer cell lines in comparison with HMEC1. This data was not completely consistent with the qRT-PCR results. However, 21NT, 21MT-2 and HS578-T expressed considerably high levels of POT1 protein compared with HMEC1 which was not in line with the gene expression data (Figures 3.9-B and 3.11).

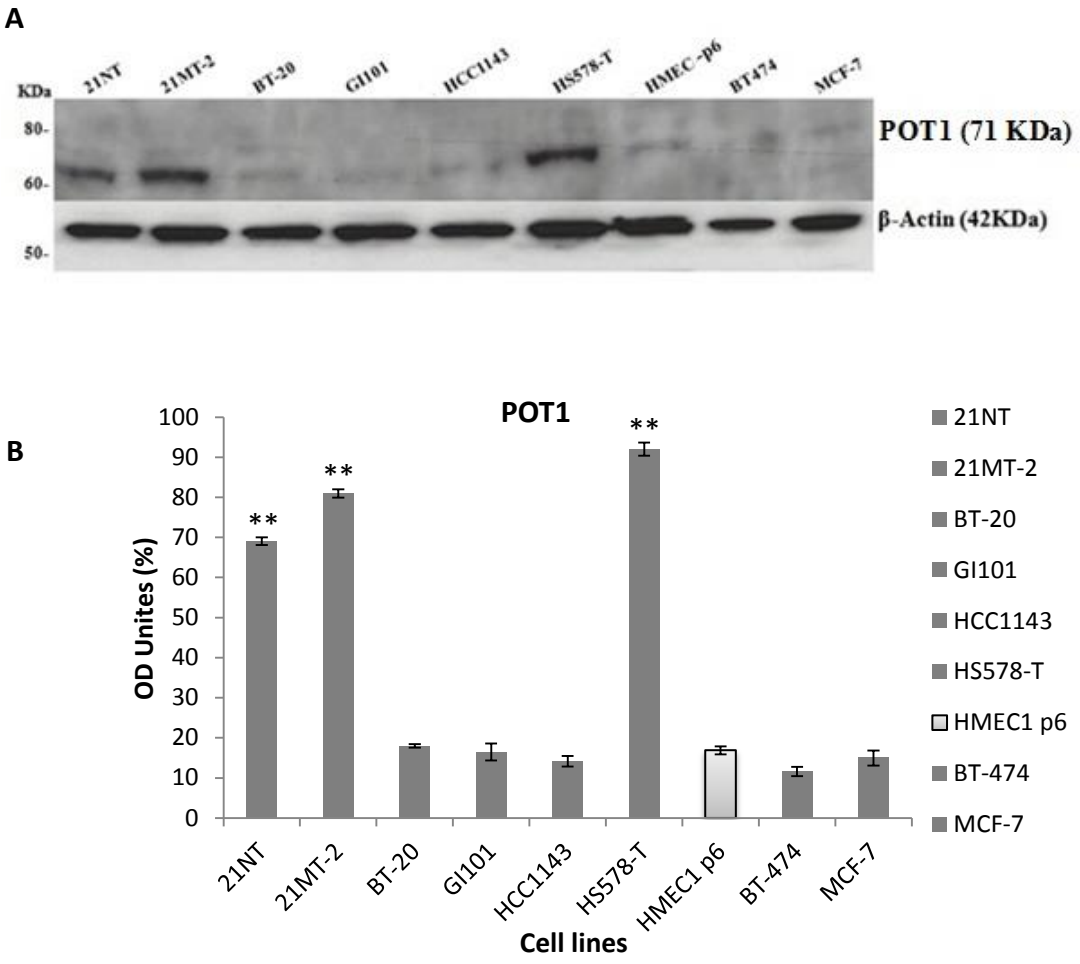

Figure 3.11-Western blot analysis of POT1 protein levels in normal mammary epithelial (HMEC1) and breast cancer cell lines. A) A 12% SDS-PAGE gel indicating POT1 protein expression and β-Actin ratio levels in western blots of all 8 breast cancers and normal mammary epithelial cell strain (HMEC1). **B)** Densitometric analysis of POT1 protein normalised to total β-Actin protein and reported as optical densitometry (OD) unites. Error bars represent SEM, ***P*<0.01.

In order to determine effect of passage number of normal mammary epithelial cell strains on protein level of POT1, different passage numbers of HMECs from two disease-free patients were analysed by western blot. As the protein expression level of 21NT cells was higher than expected, several passages of HMECs was used to compare with 21NT cells. In addition, all passage numbers were different due to the availability of the cell lines.

Western blot analysis showed higher levels of POT1 in patient 1 (HMEC1) at passage 6 in comparison with the other passages (HMEC1-p8 and HMEC1-p10). However, POT1 levels reduced significantly in all patients compared with 21NT cells (P<0.05, P<0.01, P<0.001 and correspondingly). Moreover, no substantial differences of POT1 protein levels have been observed between each passage numbers in patient two (HMEC 2) (Figure 3.12).

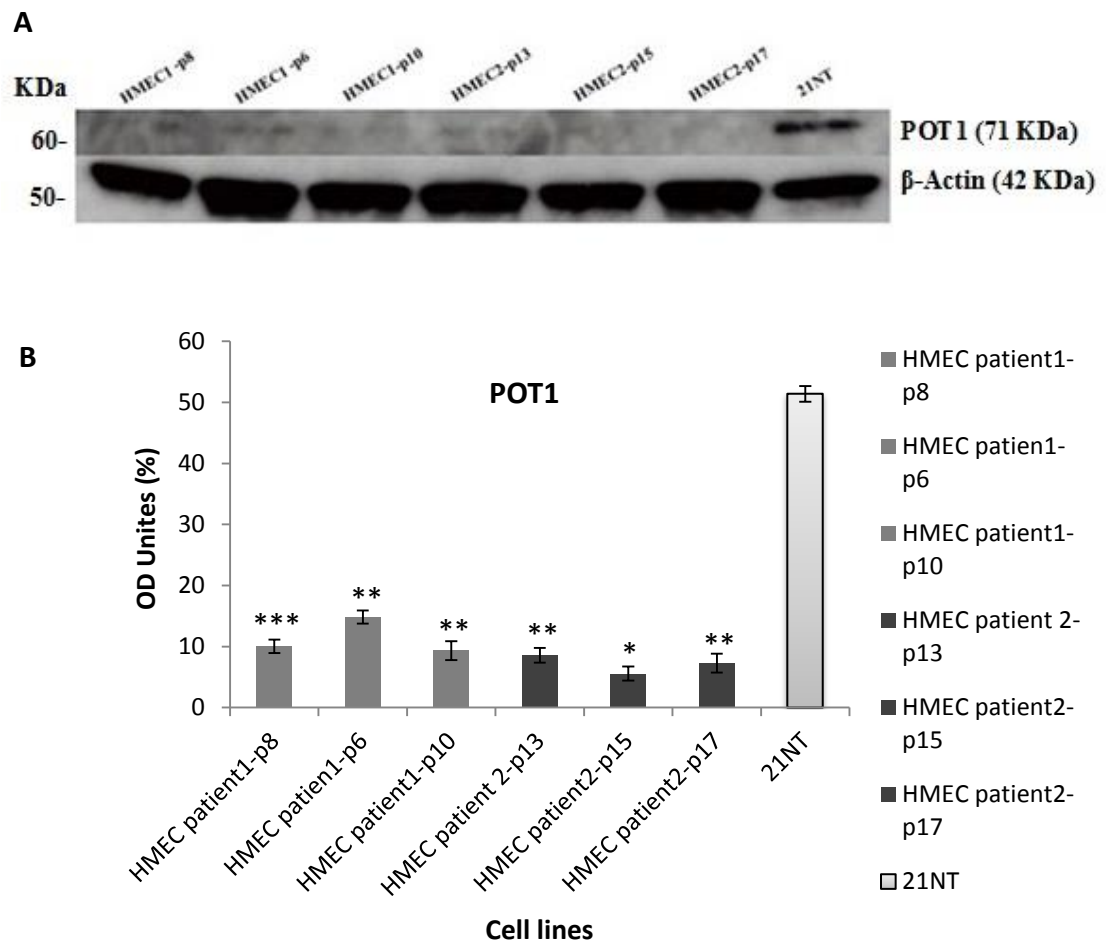

Figure 3.12-Western blot analysis of POT1 protein levels in normal mammary epithelial cell strain (HMECs) at different passage numbers and 21NT breast cancer cells. A) A 12% SDS-PAGE gel showing POT1 protein expression and β-Actin ratio levels of two different patients of normal mammary cell strains and 21NT. **B)** Densitometric analysis of POT1 protein was performed, normalised to total β-Actin protein and reported as optical densitometry (OD) unites. Error bars represent SEM, *P<0.05, **P<0.01 and ***P<0.001, compared with 21NT control.

Western blot analysis revealed a 58-KD band (Abcam) of TPP1 protein levels in normal and breast cancer cell lines (Figure 3.13-A). After imageQuant 5.0 densitometry analysis, the highest expression of TPP1 protein was detected in BT-474 in comparison with HMEC1 (P<0.05). The level of TPP1 protein was lower in 21NT and 21MT-2 cells than the HMEC1 strain control, which was not in line with the gene expression (mRNA) data (Figures 3.10-B and 3.13).

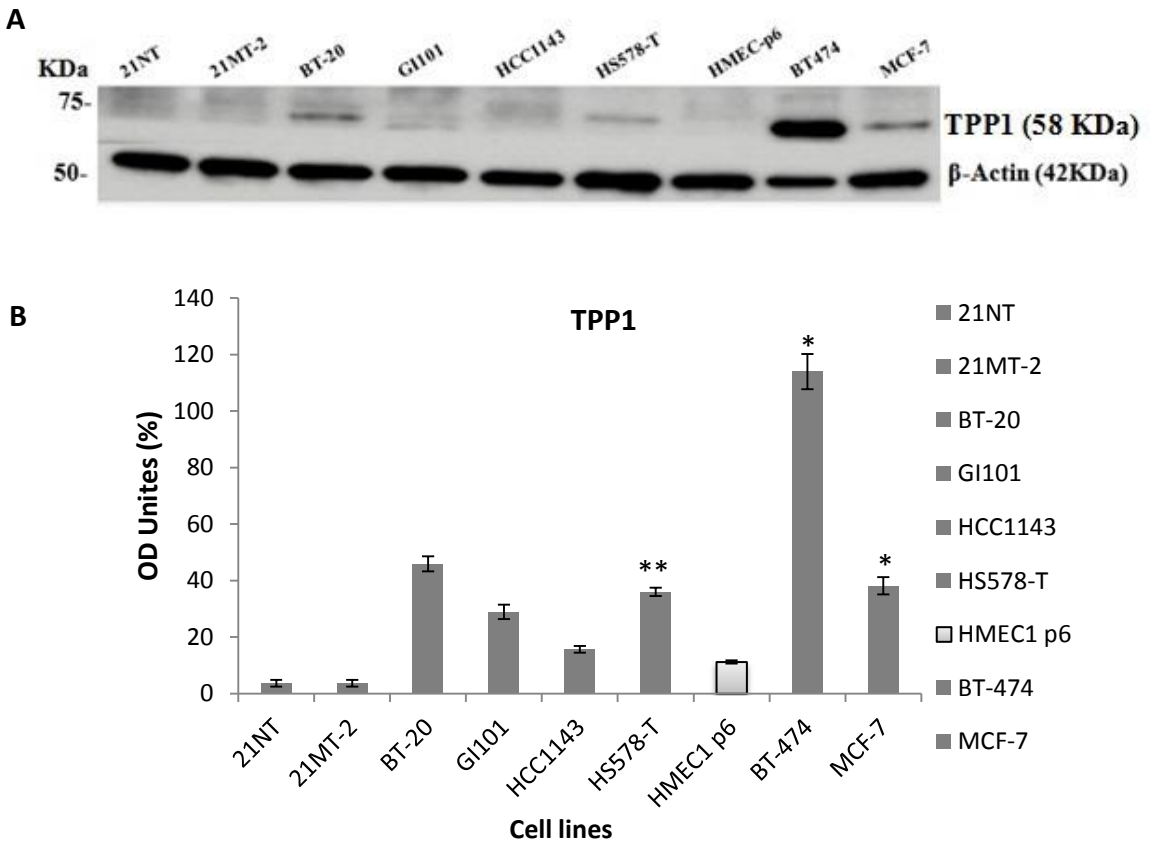

Figure 3.13-Western blot analysis of TPP1 expression in normal mammary epithelial cell strain and breast cancer cell lines. A) A 12% SDS-PAGE gel indicating TPP1 protein expression and β-Actin ratio levels in western blots of all 8 breast cancers and normal mammary epithelial cell strain (HMEC1). **B)** Densitometric analysis of TPP1 protein normalised to total β-Actin protein and reported as optical densitometry (OD) unites. Error bars represent SEM, *P<0.05, **P<0.01.

However, surprisingly, the TPP1 protein levels in HS578T cells were approximately 3-fold higher than HMEC1 (P<0.01) which was not consistent with the qRT-PCR results. Furthermore, BT20, GI101, HCC1143 and MCF-7 expressed high levels of TPP1 protein compared with HMEC1 which were also observed by qRT-PCR results (P<0.05) (Figures 3.10-B and 3.13).

As with POT1, to address increasing passage numbers possibly causing changes in the protein levels of TPP1, HMECs at different passage numbers from two patients were examined by western blot. The 21NT breast cancer cell line was also utilized as a control to compare with each different passage of HMECs. The results (Figure 3.14) showed little difference in TPP1 protein expression in HMEC1 from p10, to HMEC2 p13, p15 and p17 in comparison with 21NT cells. However, the protein levels of TPP1 in patient 1 (HMEC1) at passage 8 was approximately 2-fold higher than that 21NT cells (P<0.01) (Figure 3.14). Moreover, no substantial differences of TPP1 protein levels have been observed between HMEC1 at passage 6 and 21NT cells.

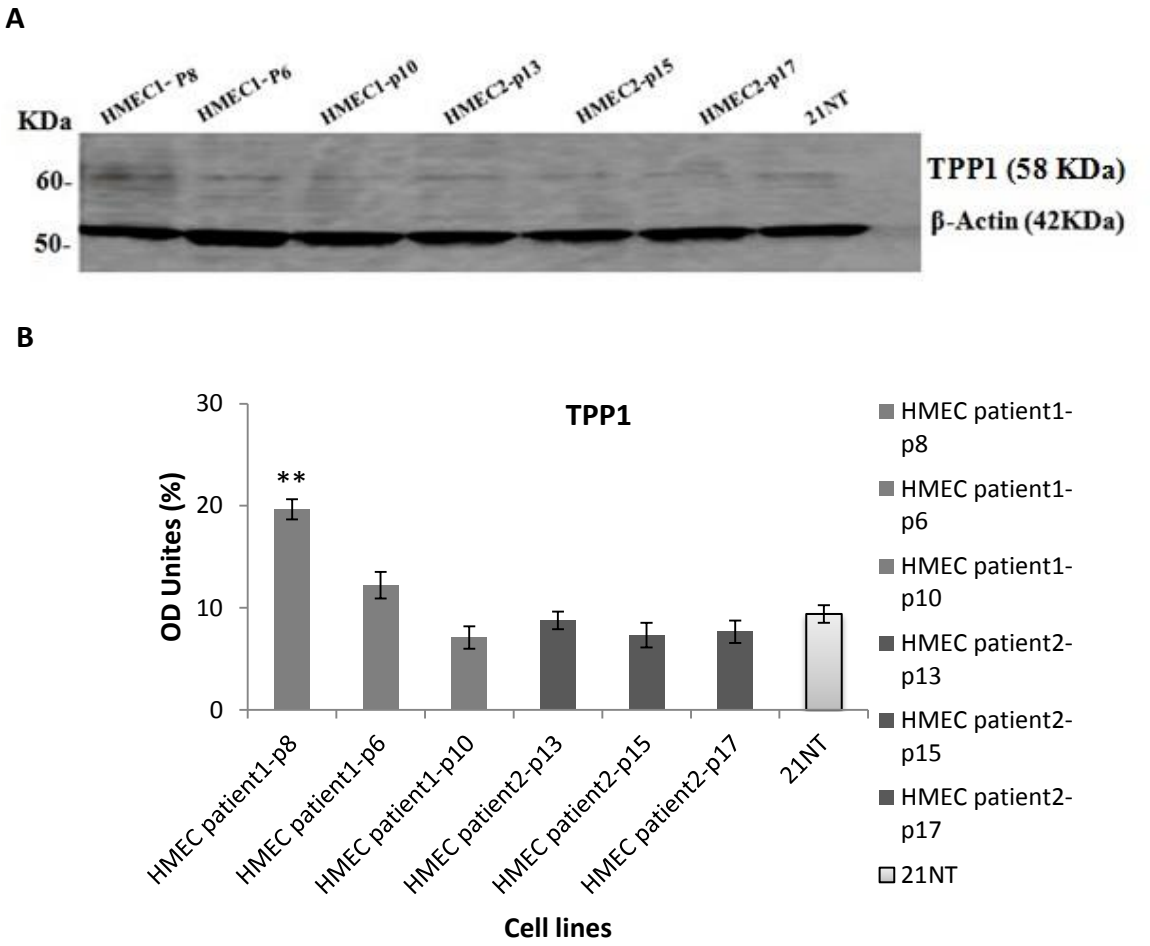

Figure 3.14-Western blot analysis of TPP1 expression in normal mammary epithelial cell strains (HMECs) at different passage numbers and 21NT breast cancer cell line. A) A 12% SDS-PAGE gel showing TPP1 protein expression and β-Actin ratio levels of two different patients of normal mammary epithelial cell strains and 21NT. **B)** For quantitative representation, densitometric analysis of TPP1 protein was performed, normalised to total β-Actin protein and reported as optical densitometry (OD) unites. Error bars represent SEM, ***P*<0.01, compared with 21NT control.

3.5-Discussion

Previous work carried out by Salhab *et al.* (2008), Cookson *et al.* (2009) and Lu *et al*. (2011), reported different expression levels of Shelterin and Shelterin-associated genes in different human cancers (Salhab, Jiang *et al.* 2008; Cookson and Laughton 2009; Lu, Zhang *et al.* 2011). Salhab *et al.* (2008) indicated over-expression of *TNKS1*, *hTERT*, *EST1*, and *TEP1* and down-regulation of *TNKS2* and *POT1* mRNA levels in breast cancer tissues compared with normal breast tissues. Moreover, the lower expression of *TRF1* and *TRF2* was found to be associated with the development and progression of breast cancer. However, findings by Hu *et al*. (2010) in other cancers appeared to be contradictory to this. They demonstrated significant over-expression of *TRF1*, *TRF2*, and *TIN2* in precancerous lesions, gastric cancer tissues, and lymph node metastase in comparison with normal gastric mucosa tissues (Hu, Zhang *et al.* 2010). In addition, recently published data by Lu *et al*. (2011), showed over-expression of *POT1* mRNA levels in gastric cancer tissues.

The aim of the work described in this chapter in relation to the published data was to determine the expression level of each Shelterin and Shelterin-associated genes in ten breast cancer cell lines, commercially available normal human breast tissue (cDNA), together with two different passage number of normal mammary epithelial cell strains (HMEC1 and 2) and the prostate cancer (PC-3) cell line by qRT-PCR. Additionally, based on the potential role of *TPP1* and *POT1* on telomere length maintenance (Hwang, Buncher *et al.* 2012) re-analysis of these genes using HMECs, as an additional normal controls, was further quantified at both gene expression (mRNA) and protein levels.

Human tissues are made up of several different cell types that work together to control the function of individual organs. Therefore, these cells may vary at the transcriptomic and/or proteomic level in order to carry out their specific functions (Bryant and Mostov 2008). In this way, cellularly heterogeneous tissue samples taken for analysis may exhibit highly varied gene expression or protein levels, in comparison with individual normal cell strains. In order to validate results obtained when using commercial breast tissue samples as a normal control, a normal mammary epithelial cell strain (HMECs) was therefore used.

As described in the Results section, in Figures 3.2 and 3.9, it was evident that *POT1* SV1 and SV2 were significantly down-regulated at the mRNA level in breast cancer cell lines compared with normal breast tissue and the pure HMEC1 cell strains ($P<0.5$ and $P<0.01$ respectively). Among the other Shelterin and Shelterin-associated genes implicated in telomere maintenance, the expression of *TRF1* (SV1 and SV2) and *TRF2*, along with *SMG6*, *TIN2* (SV1 and SV2), *TEP1*, *TNKS1*, *TNKS2*, and *RAP1* in normal tissue and breast cancer cell lines were quantified. The results indicated that these genes were down-regulated in breast tumor cell lines compared with breast normal tissue (Figures 3.3, 3.4, 3.5 3.6, 3.7 and 3.8). The marked contrast, the findings revealed that *TPP1* mRNA levels were higher in most breast cancer cell lines compared with HMEC1 and normal tissue controls. The exception was, HS578-T which expressed low levels of *TPP1* compared with HMEC1 and normal tissue controls (Figure 3.10).

Alterations in the expression of telomere binding proteins (TBPs) in cancers may disrupt the capping complex, resulting in telomere degradation and shortening independently of the telomerase status (Yamada, Tsuji *et al.* 2002). The fact that short

telomeres are observed in the vast majority of breast and other epithelial cancers may at least in part be attributable to this.

In order to confirm the results obtained from qRT-PCR, western blot analysis was performed. The POT1 protein levels did not positively associate with mRNA levels in BT20, GI101, HCC1143, BT-474 and MCF-7 breast cancer cell lines in comparison with HMEC1. These tumour cells showed that the POT1 protein levels were similar in comparison with HMEC1 which were not observed by qRT-PCR results. However, 21NT, 21MT-2 and HS578-T expressed considerably high levels of POT1 protein compared with HMEC1 which was not also in line with the gene expression data (P<0. 01) (Figures 3.9-B and 3.11).

The TPP1 protein levels showed a positive correlation with mRNA expression levels in BT-20, GI101, MCF7 and BT474 breast cancer cells. These tumour cell lines showed up-regulation of mRNA levels of TPP1 in comparison with the normal HMEC1 which was consistent with protein level (Figures 3.10-B and 3.13). As shown in Figure 3.13, the highest TPP1 protein level was detected in BT-474 in comparison with HMEC1. However, the protein level of TPP1 was lower in 21NT and 21MT-2 cells compared with HMEC1. In addition, high TPP1 protein levels and low mRNA expression were observed in HS578-T in comparison with HMEC1 which was not consistent with qRT-PCR (Figures 3.10-B and 3.13).

To determine whether different passage culture of the HMECs may impact on TPP1 and POT1 protein levels, different passage numbers of HMECs (HMEC1 and 2) from two patients were examined at low (p6) and high (p17) passage by western blot. The result showed a slight difference in TPP1 expression at different passages. The difference was relatively small. However, approximately 2-fold increase of TPP1 was observed in HMEC1 p8 compared with 21NT cells (Figure 3.14). Moreover, the effect of different passage numbers

on POT1 expression was also studied. As the protein expression level of 21NT cells was higher than expected, several passages of HMECs was used to compare with 21NT. Western blot analysis showed substantially lower levels of POT1 in all patients in comparison with 21NT cells (P<0. 05, P<0. 01 and P<0. 001 respectively). As shown in Figure 3.12, HMEC1, cells from sixth passage had higher protein level of POT1 than cells of the tenth and eighth passage. Furthermore, no substantial difference in POT1 level was detected in HMEC2 p13, p15, and p17 (Figure 3.12).

The lack of correlation between protein and mRNA levels could be due to transcriptional splicing, post-transcriptional splicing, translational modifications, translational regulation, and protein complex formation, which might have an effect on the relative quantities of mRNA and protein (Hartwell, Hopfield *et al.* 1999; Brett, Pospisil *et al.* 2002; Brockmann, Beyer *et al.* 2007; Glisovic, Bachorik *et al.* 2008). Most research assumes that protein concentrations are generally proportional to mRNA concentration. However, since publication of the complete human genome sequence in 2004, many papers have proved this hypothesis wrong. For instance, Tian *et al.* (2004) mapped the abundance ratio of 425 proteins to their corresponding mRNA expression levels in multipotent mouse EML cells and their differentiated progeny, MPRO cells. Over all they identified 150 signature genes which showed significant alterations at their protein and/or mRNA level between the two cell types. In total 19% of genes showed reasonable correlation between mRNA and protein levels; 45% showed significant difference at the mRNA level but not at the protein level, 35% represented significant changes at the protein but not at the mRNA level. Surprisingly, the mRNA and protein levels were inversely correlated in two genes. Furthermore, the expression of the c-kit receptor kinase protein and its mRNA varied seven-

fold and nine-fold respectively between the two cell lines, while the c-kit ligand protein showed a five-fold higher expression level in the EML cell line with no change in the mRNA level. The expression levels of nine mitochondrial proteins were significantly lower in MPRO cell lines compared to EML cells, while the expression of their corresponding mRNA was higher or similar (Tian, Stepaniants *et al.* 2004). Going further, Schwanhausser *et al.* (2011) used NIH3T3 mouse fibroblast to analyse the correlation between expression levels of protein and mRNA (Schwanhausser, Busse *et al.* 2011). They quantified 5279 unique proteins and measured their half-lives along with their mRNAs. Consequently, they reported a median half-life of 46 hours for proteins and 9 hours for mRNA, hence showing proteins to be on average five times more stable than their mRNAs. Furthermore, they divided genes and proteins into three different groups based on their function and looked at their protein-mRNA stability. Looking at their results, the housekeeping genes (i.e., genes coding for ribosomal and glycolytic proteins) showed stable mRNA and protein. The chromatin modifying enzymes, cell-cycle associated genes, and transcription factors have unstable mRNA and proteins. The last group showed stable mRNA and unstable protein, comprising of RNA-processing proteins, genes encoding kinsases, proteases and integrin mediated pathways (Schwanhausser, Busse *et al.* 2011). Looking at these two papers and other published data, it is evident that only 40% of protein levels in cultured mammalian cells are correlated with mRNA levels. Also there is further evidence suggesting that the mRNA levels may be correlated with protein levels only in housekeeping genes with both stable mRNA and protein. On the other hand, the mRNA level may be a poor surrogate for protein levels in genes with stable mRNA and unstable protein e.g. transcription factors and genes

encoding proteases and kinases (Tian, Stepaniants *et al.* 2004; Lundberg, Fagerberg *et al.* 2010; Vogel, Abreu Rde *et al.* 2010; Schwanhausser, Busse *et al.* 2011).

The relationship described between mRNA and protein in these 4 papers is also evident in our results; the Shelterin protein encoding gene *TPP1* had high mRNA levels and low protein levels in 21NT cells, suggesting more stable mRNA compared to protein. However, there is an expression pattern observed in our results which has not been observed and/or explained previously. Based on our results, the Shelterin protein encoding gene *POT1* has low mRNA and high protein levels in 21NT cells (Figures 3.9 and 3.11). Looking at the control cell lines HMECs, the POT1 encoded protein level is less than that of the 21NT breast cancer cells. This suggests that POT1 encoded protein is more stable than its mRNA.

Previous work by Marks *et al.* (1991) found that a mutation in the *p53* gene lead to high expression of the p53 protein in ovarian cancer cells (Marks, Davidoff *et al.* 1991). Therefore, it may be possible that the POT1 protein within 21NT cells is mutated and non-functional. This may explain the higher protein levels observed within 21NT breast cancer cells in comparison with HMECs. To test this hypothesis, further investigation were carried out to look at mutational and epigenetic changes involving the *POT1* gene as described in the following chapter (V).

CHAPTER IV

EPIGENETIC REGULATION OF SHELTERIN AND SHELTERIN-ASSOCIATED GENES AS A MECHANISM FOR ALTERED EXPRESSION IN CANCER CELLS

4.1-Introduction

Down-regulation of some Shelterin genes and up-regulation of *TPP1* in breast cancer cell lines could be due to a number of factors including mutation, DNA methylation, single allele deletions, chromatin remodelling, and haploinsufficiency of the genes. To address the question of whether mutations in Shelterin genes may cause down-regulation of their expression, the literature was consulted. Salhab *et al.* (2008) reported that *POT1* was significantly down-regulated in malignant breast tissues in comparison with normal tissues. Moreover, according to our findings presented in the previous chapter (III), *POT1* was one of the most down-regulated of the Shelterin genes in breast cancer cell lines. Therefore, this gene was selected for further investigation. Previous results demonstrated that human *POT1* is most commonly mutated in a wide range of cancers, such as: papillary thyroid (Cantara, Capuano *et al.* 2012), breast (Shen, Gammon *et al.* 2010) and leukaemia (Poncet, Belleville *et al.* 2008). Further studies revealed single nucleotide polymorphisms (SNPs) of *POT1* in breast cancer (Savage, Chanock *et al.* 2007). Moreover, mutation of *POT1* was observed in approximately 5% chronic lymphocytic Leukaemia (CLL) (Ramsay, Quesada *et al.* 2013). In addition, mutations in *POT1* exon12 were detected in human carcinoma cell strains (HeLa and HO8910-PM) (Hou, Huang *et al.* 2006). However, in 2009, according to the COSMIC database (Catalogue of Somatic Mutations in Cancer, Sanger centre UK http://www.sanger.ac.uk); no mutation was identified in the genomic sequence of the Shelterin genes, including the *POT1* gene, in cancer. Therefore, based on the published data (Hou, Huang *et al.* 2006). It was important to screen the *POT1* gene for existence of exon12 mutation in breast cancer cells.

Epigenetic modifications such as abnormal DNA methylation play an important role in cancer development, for example, by facilitating carcinogenesis and tumour apoptosis (Lund and van Lohuizen 2004). DNA hypermethylation is mediated by DNA methyltransferase enzymes (DNMTs) on cytosine residues in the 5'-CG-3' sequence. DNA hypermethylation within these regions inhibits gene expression via recruitment of repressive proteins such as: methyl-CpG binding protein 1 (MeCP1), MeCP2, and Methyl-binding domain proteins 1, 2, 3, and 4. Transcription is hindered by these proteins via the recruitment of the nucleosome remodelling complex (Mossman, Kim *et al.* 2010).

In chapter III we presented data that demonstrated Shelterin and Shelterin-associated genes were down-regulated in breast cancer cell lines compared with normal breast tissue and HMEC1 strain controls. A DNA methyltransferase inhibitor, 5-aza-2'-deoxycytidine (5-aza-CdR), and a histone deacetylation inhibitor, Trichostatin A (TSA), were used to demethylate DNA and deacetylate histones, respectively, and to induce the expression of silenced genes. It is well established that 5-aza-CdR can repress the growth of numerous tumours *in vitro*, including lung cancer, melanoma, and breast cancer (Mirza, Sharma *et al.* 2010) cells. Therefore, the effect of these drugs on Shelterin and Shelterin-associated genes was investigated in 21NT breast cancer cell line. Moreover, the effect of these drugs on cytosine methylation in the promoter region of *POT1* was investigated.

4.2 -Materials and methods

4.2.1- Mutation at exon12 of *POT1*

DNA was isolated from breast cancer cell lines as previously described in Section 2.7. 50ng of double stranded DNA was utilised in experiments and a pair of primers was synthesized covering exon12 of *POT1* gene (Table 4.1).

Table 4.1-Primer sequences of *POT* exon12

Primers	Sequence (5´⟶3´)	Product size (bp)	Reference
POT1 Ex12 Forward	GCAAAAGGAGTATTCTAACAAAACAG	300	(Hou, Huang *et al.* 2006)
POT1 Ex12 Reveres	TCACGCTTACACCAAAATCG		

PCR was performed using 1.1x Reddy Mix and 10µM of the Forward and Reverse primer, respectively. The reaction mixture volume was 25µl and was incubated in a thermo cycler at 94°C for 5 minutes, followed by 35 cycles of 94°C for 45s, 60°C for 45s, and 72°C for 45s and then a final extension at 72°C for 5 min.

4.2.1.1-PCR product purification using QIAquick™ PCR Purification Kit

Five volumes of PB buffer were added to one volume of PCR reaction and mixed thoroughly. The entire mixture was transferred to a QIAquick spin column placed in a 2ml collection tube and centrifuged for 1 minute at 16,000*rcf*. The flow-through was discarded and the QIAquick spin column was placed back in the same collection tube. About 750µl of PE wash buffer was added to the QIAquick column and centrifuged for 1 minute at 16,000*rcf*. The flow-through was also discarded and QIAquick column was placed back in the same collection tube. The column was centrifuged once more to remove residual ethanol. The QIAquick column was placed in a clean 1.5ml micro-centrifuge tube and 15µl of elution buffer EB (pH 7.0-8.5) was added to the centre of QIAquick column membrane and

centrifuged for 1 minute at 16,000*rcf*. All DNA sequencing reactions were carried out using 8µl DTCS Quick Start Master Mix (Beckman Coulter Kit), approximately 3µl of purified DNA, and 10µM of the Forward primer (Table 4.1). Amplification was carried out using a thermal cycler with the following conditions:

- 96°C – 20 seconds
- 50°C – 20secs
- 60°C – 4minutes

} 30 cycles

4.2.1.2-Precipitation of DNA from sequencing reactions

DNA was precipitated by adding, 2µl of Sodium Acetate (pH5.2), 2µl of 100mM Na_2-EDTA (pH 8.0) and 1µl of 20mg/ml of glycogen to the sequencing reaction mix. Then 60µl of cold 95% ethanol was added to the samples. Samples were immediately centrifuged at 16000*rcf* for 15 minutes at 4°C. Then the DNA pellet was washed twice with 200µl of cold 70% ethanol. For each rinse, samples were centrifuged immediately at 16000*rcf* for 2 minutes at 4°C. After centrifugation, all of the supernatant was carefully removed and then allowed to completely evaporate at room temperature for 10 minutes. Samples were re-suspended in 40µl of sample loading solution (Beckman Coulter). The re-suspended samples were transferred to a 96-well plate and one drop of mineral oil (provided in the Kit) was added to each sample. The samples were loaded to the instrument to start sequencing.

4.2.2-Promoter methylation analysis of the *POT1*

In this technique, DNA is denatured and treated with sodium bisulphite. This causes unmethylated CpG dinucleotides in the promoter region of the genome to convert to uracils whereas methylated cytosines remain unchanged (Figure 4.1).

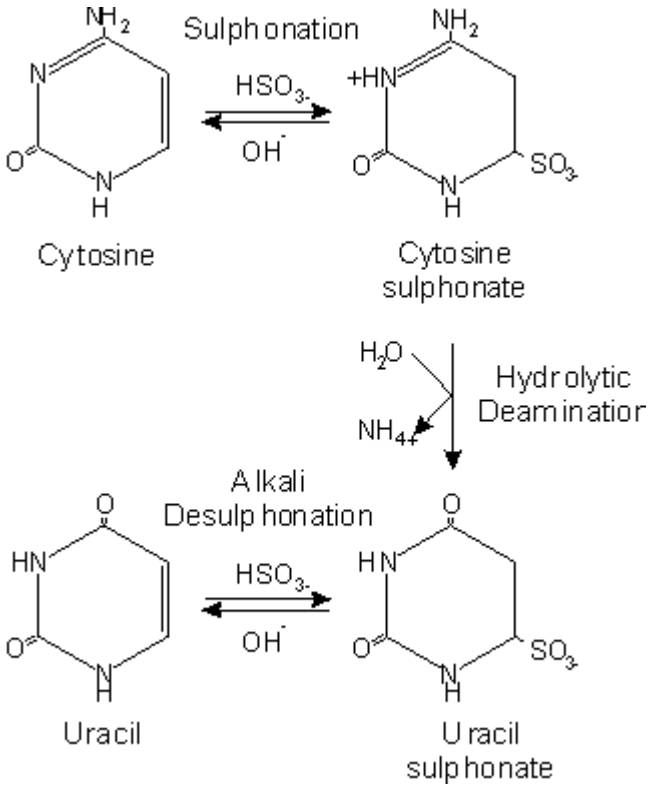

Figure 4.1-Chemical schemes for the conversion of cytosine to uracil. Unmethylated cytosine residues converted to uracil after treatment with sodium bisulphite. After bisulphite PCR amplification, uracil residues converted to thymidine. Image obtained from http://www.methods.info/Methods/DNA_methylation/Bisulphite_sequencing.html website.

4.2.2.1-Bisulphite treatment of DNA samples

Genomic DNA was isolated from breast cancer cell lines, using the Wizard™ Genomic DNA Kit protocol (Promega) (see Section 2.7). Methylcode™ Bisulphite conversion Kit

(Invitrogen) was used for bisulphite treatment of DNA-samples. According to the manufacturer's instructions, CT conversion reagent was prepared by adding 900µl of sterile water, 50µl of Resuspension Buffer, and 300µl of Dilution Buffer directly to one tube of CT Conversion Reagent. Then, the tube was mixed by vortexing for 10 minutes. A mixture of 2µg of genomic DNA samples (total volume 20µl) and CT conversion reagent mix (130µl) was added to the PCR tube. After thorough mixing, the bisulphite treatment was performed using a thermal cycler with the following conditions:

- 98°C for 10 minutes (DNA denaturing step)
- 64°C for 2 hours and 30 minutes (Bisulphite conversion step)
- 4°C storage for up to 20 hours

After completion of bisulphite treatment, the samples were cleaned up by placing them in collection tube and 600µl of Binding Buffer was added to each column. The mixture was inverted several times and centrifuged at full speed (≥9,000*rcf*) for 30 seconds. The flow-through was discarded and 100µl of wash buffer (prepared with ethanol) was added to the column followed by centrifugation at full speed for 30 seconds. After discarding the flow-through, desulphonation was performed by adding 200µl of desulphonation buffer and incubating columns for 15 minutes at room temperature. When the incubation was completed, the columns were centrifuged at full speed for 30 seconds. The flow-through was again discarded and the columns were washed twice with 200µl of wash buffer prepared with ethanol. To remove residual liquid, the columns were placed in new 2ml collection tubes after the second wash, and centrifuged at full speed for 30 seconds. The elution of bisulphite-treated DNA was performed by placing the columns in clean 1.5ml micro-centrifuge tubes and adding 16µl of Elution Buffer to the centre of the membrane.

The bisulphite-treated DNA was eluted by centrifugation at full speed for 30 seconds. The samples containing bisulphite-treated DNA were stored in -20°C until further processing.

4.2.2.2-Primer design for bisulphite sequencing

The bisulphite-treated DNA was amplified by PCR in which the primers were specifically designed for methylated and unmethylated DNA products. MethPrimer program was used to identify CpG islands within a given sequence and assist in designing methylated and unmethylated primers (Figures 4.2-A and 4.2-B).

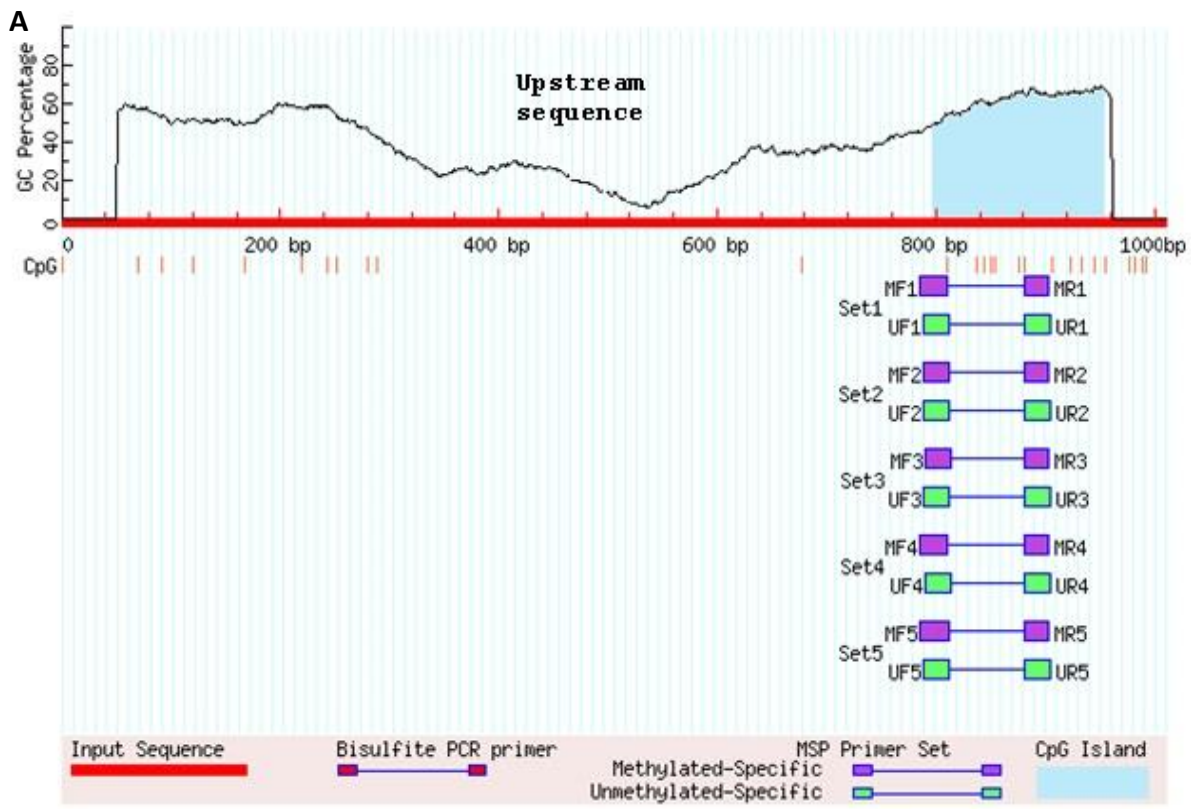

Figure 4.2-A) MethPrimer program for *POT1* CpG Island. Thick horizontal "blue shaded area" indicates CpG Island with individual CpG dinucleotides (seventeen vertical red lines). To assist designing methylated and unmethylated primers, CpG Island Searcher program was used. Image obtained from http://www.urogene.org/cgi-bin/methprimer/methprimer.cgi website**.**

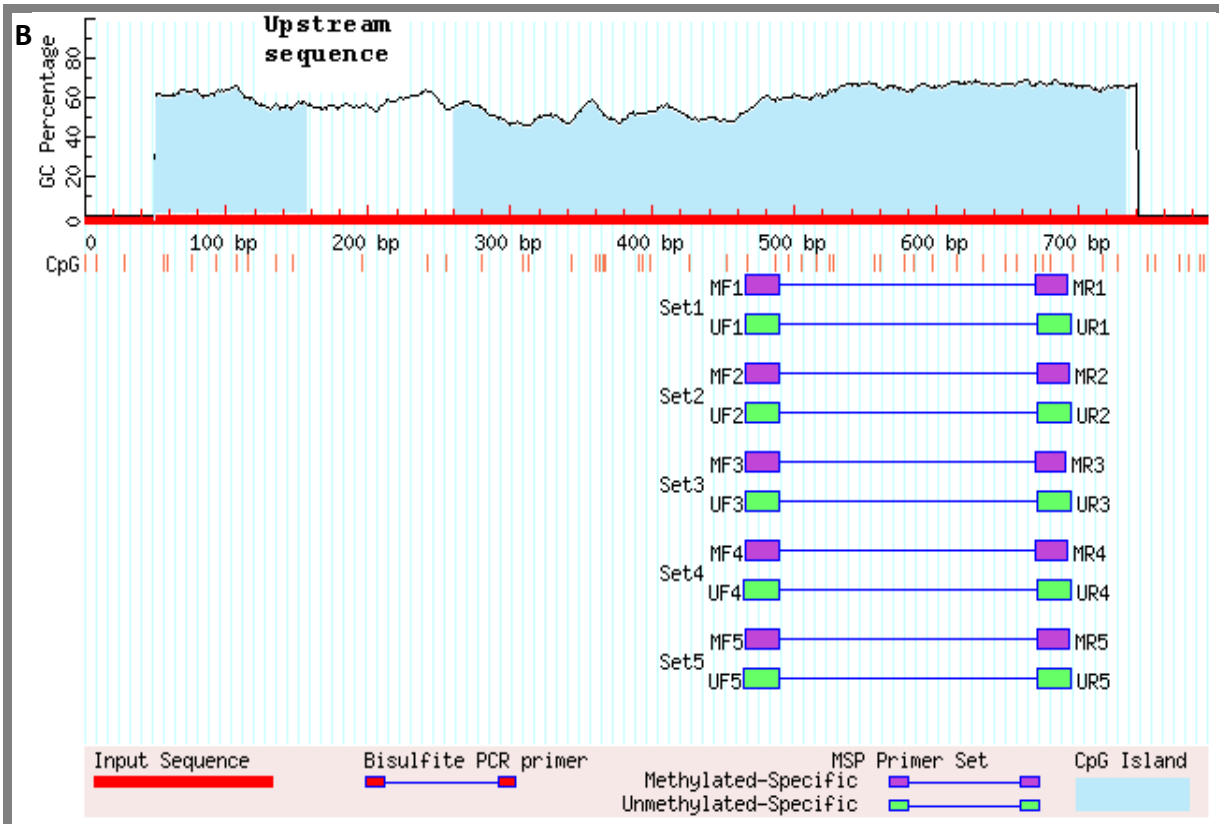

Figure 4.2.B) MethPrimer program for *TIN2* CpG Island. Thick horizontal "blue shaded area" indicates CpG Islands with individual CpG dinucleotides (twenty vertical red lines). To assist designing methylated and unmethylated primers, CpG Island Searcher program was used for this purpose. Image obtained from http://www.urogene.org/cgi-bin/methprimer/methprimer.cgi website.

The methPrimer program was used to identify 5' promoter regions of all six Shelterin genes. This website recognised the promoter regions of *POT1*, *TIN2* and *RAP1*. To define the position of *POT1* and *TIN2* promoter region, approximately 700 base pair upstream of the first exon from http://www.ncbi.nlm.nih.gov/genome/ website was pasted into the http://www.urogene.org/cgi-bin/methprimer/methprimer.cgi website. PCR-primers selected for each gene and its promoter region are presented in Table 4.2 below. The regions chosen for each gene were based upon the density of CpG-sites.

Table 4.2-MSP primer sequences for PCR-products

Gene / Assay	Forward primer (5´⟶3´)	Reverse primer (5´⟶3´)	Product size (bp)
POT1-M*	AGAAAGGTTTTGTTTATAGGAGT	CCAATAACTTTCCAACTTTCGTA	118
POT1-U*	AAGGTTTTGTTTATAGGAGTTTT	CCCAATAACTTTCCAACTTTCAT	116
TIN2-M*	AAAGTAAGGTTGGGAGGATTTAG	ACAAAAAAAACCGTAACGATACG	161
TIN2-U*	AAAGTAAGGTTGGGAGGATTTAG	ACCACAAAAAAAACCATAACAAT	164

***Methylated, ***Unmethylated**

4.2.2.3-Detection of DNA methylation in *POT1* promoter region

In order to generate the 118 base pair and a 116 base pair methylated and unmethylated product, PCR was performed using 1.1x Reddy Mix, 1µg (2µl) of DNA (see Section 4.2.2.1), 25µM of the Forward and Reverse primer, respectively. A negative control was included in every PCR performed. The reaction mixture volume was 25µl and was incubated in a thermo cycler at 94°C for 5 min, followed by 50 cycles of 94°C (denaturation) for 45s, 56°C for 45s (annealing), and 72°C for 45s (extension) and then a final extension at 72°C for 5 min. Then, the PCR products were purified as mentioned in Section 4.2.1.1.

4.2.2.4-Sequencing and analysis of POT1 data

The concentration of DNA was adjusted and the methylated and unmethylated PCR products were sent for sequencing (Beckman Coulter Company).

4.2.3-Effects of 5-aza-CdR and TSA on 21NT breast cancer cell line

4.2.3.1-Drug optimization and cell viability assay (Trypan Blue Assay)

Careful preliminary experiments were performed to determine the optimal drug doses. Briefly, $3x10^5$ cells were seeded into 6-well plate to a total volume of 3ml media per well. Each experiment was carried out in duplicate with different drug concentrations. Twenty-four hours after cell plating, the cells were randomly assigned into control, TSA (Sigma biochemical), 5-aza-CdR (Sigma, St. Louis, MO) and mixed 5-aza-CdR/TSA treatment groups. TSA and 5-aza-CdR were dissolved in dimethylsulphoxide (DMSO). Aliquot of stock solution of 5-aza-CdR (5µM) and TSA (5, 15, 25, 50, and 100ng/ml) were prepared and stored at -20°C. The culture medium was replaced with culture medium containing 5, 15, 25, 50, and 100ng/ml of TSA. Following optimization, cells were treated with the same concentrations of TSA, followed by the addition of 5µM of 5-aza-CdR (was optimized by Dr H Yasaei, personal communication). Cells that were treated with 5-aza-CdR and TSA at different concentrations were cultured and trypsinized with trypsin/EDTA and a cell suspension was made with Alpha modification MEM medium. Then the cell suspension was taken into a fresh Eppendorf tube and stained with Trypan blue (Invitrogen). Stained blue cells were scored as dead cells and unstained bright cells as viable cells. The stained cells were then counted immediately under a microscope by using a haemocytometer and their viability was determined by the following formula:

$$\text{Viability (\%)} = \left(\frac{\text{No of Viable Cells}}{\text{Total no. of cells}} \right) \text{X } 100$$

4.2.3.2-Cell culture, maintenance and treatment

The 21NT cell line was cultured at 37 °C, 5 % CO_2 as previously described. Cells were plated at a density of $1x10^5$ in p100 dish. Twenty-four hours after cell plating, the cells were randomly assigned into treatment and control groups. In treatment groups, the culture medium was replaced with fresh medium containing TSA (50ng/ml) or 5-aza-CdR (5µM) separately. Cells were also treated with both drugs concomitantly. Thereafter, 5µM 5-aza-CdR was added for 48 hours, TSA (50ng/ml) added only during the last 16 hours of treatment. For control groups, two plates were treated with and without 0.02% DMSO. The purpose of these treatments was based on the published data (Pryzbylkowski, Obajimi *et al.* 2008). Moreover, the short-term and long-term effects of the drugs on the mRNA levels of Shelterin and Shelterin associated genes were examined in order to compare the difference between each time points of the treatment. At the end of the experiment, four groups of cells were treated for: 24hrs, 48hrs, 72hrs, 96hrs, 120hrs, 144hrs, 7 days, 3 weeks, 6 weeks and 2 month plus 72 hours retreatment period. At each time point, samples were taken for further experiments. Twenty-four hours later, the medium containing drugs or DMSO-treated was removed and replaced with fresh media. After 2 months of treatment, the cells were retreated again with the same concentrations of 5-aza-CdR and TSA for 72 hours in

order to examine the effects of a double-dose treatment on 21NT cells. Then cells were harvested for RNA, DNA and protein extraction.

4.2.4-RNA isolation and quantitative RT-PCR analysis

RNA was extracted by Trizol reagent (Invitrogen) as described in Section 2.2.2 after different time point treatment of the 21NT cells. Invitrogen SuperScript III Reverse Transcriptase was used to synthesize cDNA. The forward and reverse primers sequences of all Shelterin genes and amplification length are detailed in Table 2.2. qRT-PCR was performed using SYBR green PCR Master Mix (Applied Biosystems). All of the PCR reactions were performed in triplicate and independently repeated three times depending on the experiment. Results are shown as SEM and significance was calculated by using paired *t*-test. A *p* value of less than 0.05 was considered significant.

4.3-Results

4.3.1-Mutation analysis of *POT1* in breast cancer cell lines

Previous work by Hou, Huang *et al.* (2006) showed that *POT1* gene within the exon12 region was mutated in human carcinoma cell lines. Therefore, mutation in the *POT1* exon12 gene was screened in ten breast cancer cell lines. The PCR products on 2% agarose gel showed an intense band between 200bp and 300bp for all human breast cancer cell lines which was consistent with the product size. After checking the product size (Figure 4.3), the exon12 PCR product of *POT1* was sequenced in Beckman Coulter (CEQ™8000 Genetic Analysis System) machine to detect the presence of mutations in all the lines. The results revealed no evidence of mutations in any of the breast cancer cell lines within the exon12 (data not shown, see also Figure S1).

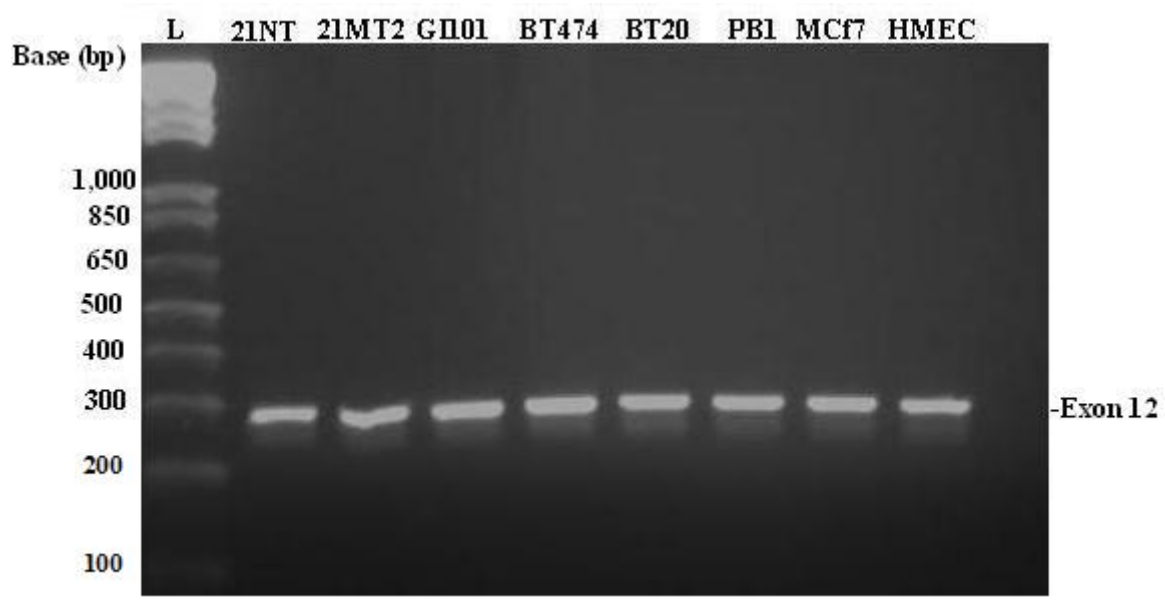

Figure 4.3-The PCR Results of *POT1* Exon12 in cancer and normal (HMEC1) cell lines. Representative agarose electrophoresis image of *POT1* exon12 PCR. Each lane indicates breast cancer cell lines and HMEC1 strain.

4.3.2-Detection of DNA methylation of *POT1* and *TIN2* promoter regions in breast cancer cell lines

Based on the results presented in Chapter III showing down-regulation of Shelterin genes in certain breast cancer cell lines, it is possible that the expression of these genes has been modulated by DNA methylation. To confirm this hypothesis we set out to identify evidence of DNA methylation in the promoter of *POT1* and *TIN2* (in the normal mammary epithelial cell strains (HMEC1) and the breast tumour cell lines, 21NT, BT474, BT-20, MCF-7, GI101, 21MT2, PB1 and HS578-T). To this end the methPrimer (http://www.urogene.org/cgi-bin/methprimer/methprimer.cgi) program was used to identify the 5' promoter regions of all six Shelterin genes. This website recognised the promoter regions of *POT1*, *TIN2*, and *RAP1*.

In this section, we only analysed the promoter region of *POT1* and *TIN2* as these two genes demonstrated a significant up-regulation of gene expression following 5-aza-CdR and 5-aza-CdR/TSA treatment in comparison with the other Shelterin genes (Section 4.3.5). The promoter regions of *POT1* and *TIN2* genes were analysed in all untreated (i.e., not exposed to 5-aza-CdR and TSA) breast cancer cell lines. As shown in Figure 4.4, partial methylation was present in *POT1* and *TIN2* promoter regions in breast cancer cell lines. The results indicated that the *POT1* promoter contains more methylated DNA in breast cancer cells 21NT, BT474, 21MT-2 and PB1. These cell lines also have unmethylated DNA. This is based on the level of intensity of the PCR band on the agarose gel. Moreover, BT20, GI101, and HS578-T have more unmethylated DNA which is consistent with the control (HMEC1). More evidence of *POT1* methylation in 21NT, BT474, 21MT-2, and PB1 cells in comparison with

HMEC1 was observed. However, no significant differences of *TIN2* were observed in methylated and unmethylated lanes (Figure 4.4).

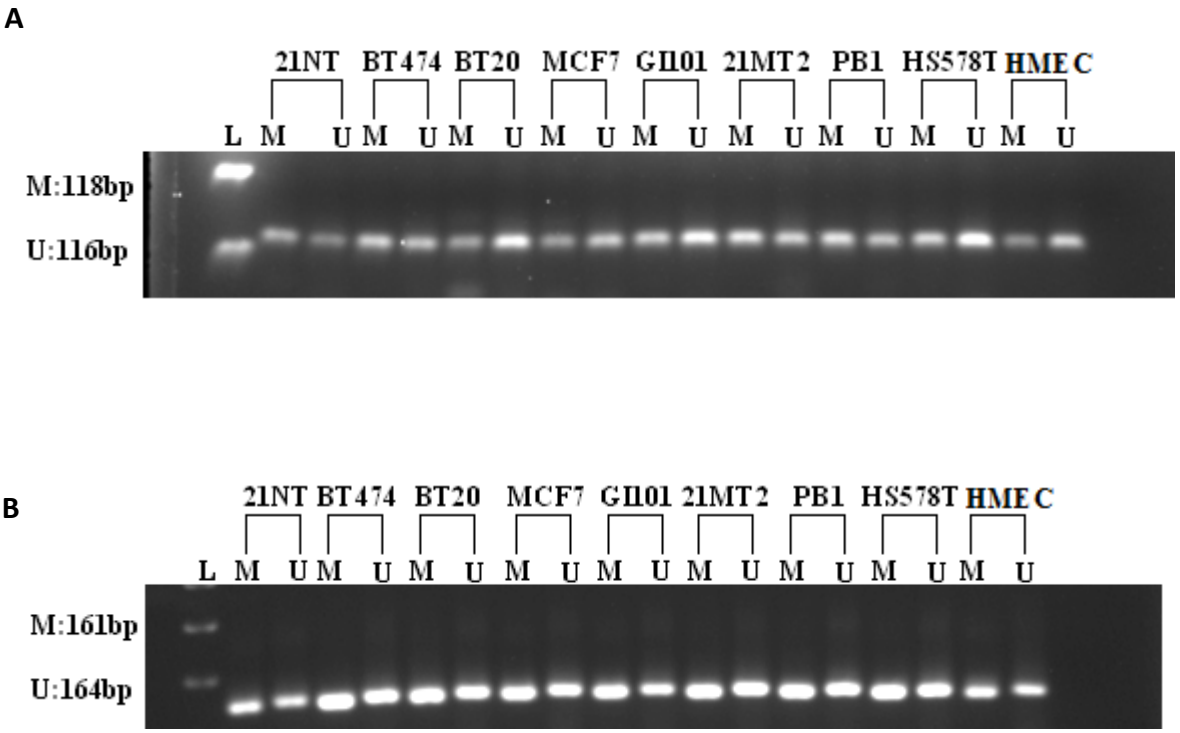

Figure 4.4-Methylation Specific PCR (MSP) analysis of *POT1* (A) and *TIN2* (B) genes in breast cancer cell lines and normal mammary epithelial cell strain (HMEC1). A) *POT1* panel viewed from left to right in breast cancer cell lines. Lane 1 is the ladder, M specifies the presence of methylated DNA, and U demonstrates unmethylated. **B)** *TIN2* panel viewed from left to right shows a ladder, the presence of methylated and unmethylated DNA in breast cancer cell lines.

4.3.3-Sequence analysis of *POT1* promoter region in breast cancer cell lines

As described in the previous section (4.3.2), *POT1* appeared to be more methylated in 21NT and 21MT-2 cell lines in comparison with HMEC1 control. In contrast, the GI101 showed a stronger unmethylated signal in the same promoter region of *POT1*. Therefore, these cell lines were examined more in detailed for *POT1* promoter methylation. To identify precisely where in the promoter region of *POT1* methylation occurs in breast cancer cell lines and normal epithelial cell strains. Genomic DNA from 21NT, 21MT-2, GI101, and HMEC1 were prepared for bisulphite sequencing.

A fragment with a length of 118 base pairs from the *POT1* gene promoter region was utilized for the bisulphite direct sequencing. For this purpose, breast cancer cell lines (21NT, 21MT-2, and GI101) and the normal epithelial cell strains (HMEC1) were sequenced. Figure 4.5 indicates that 21MT-2 and GI101 breast cancer cell lines were unmethylated in the upstream promoter region of the *POT1* CpG Island. Bisulphite sequencing also showed that the methylation ratio in 21NT was about 30%, which showed frequent methylation in the amplified region. However, no methylation in this region was observed in HMEC1 control (Figure 4.5). The sequencing chromatograms also showed that all of the CpG Island in 21MT-2 and GI101 was unmethylated, as about all cytosine was converted to thymidine (Figure 4.5) (Figure S2). As shown in Figure 4.6, 11 possible CpG sites upstream of *POT1* exon1 were analysed. The degree of hypermethylation varied from 3/11 CpG sites in 21NT to 0/11 CpG sites in 21MT-2, GI101, and the HMEC1 control.

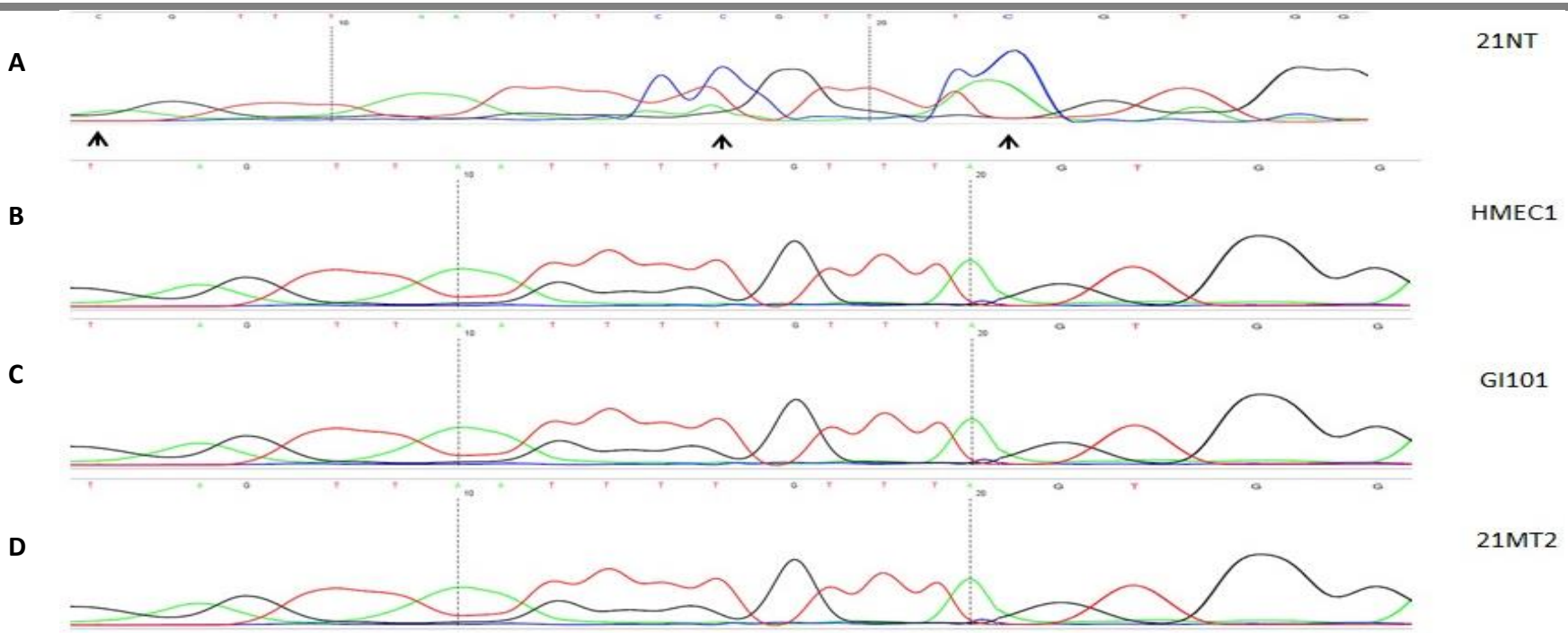

Figure 4.5-*POT1* methylation analysis of the normal mammary epithelial cell strain (HMEC1), 21NT, 21MT-2 and GI101. A) The top panel is upstream promoter region in 21NT cells. **B)** The second panel is 5' CpG Island in HMEC1. **C)** The third panel is upstream promoter region in GI101 and **D)** is 5' CpG Island in 21MT-2 using bisulphite sequencing directly from PCR products. The comparison is based on the percentage of CpG Islands. The chromatogram shows the location of CpG Islands which appears to be partially methylated in 21NT cell line whereas no CpG is methylated in the *POT1* promoter region of HMEC1 cell strain, 21MT-2 and GI101 breast cancer cells. Each colour represents nucleotides T: thimidine, C: cytosine, G: guanine. Arrows indicate CpG dinucleotide which is methylated and the rest remained unmethylated.

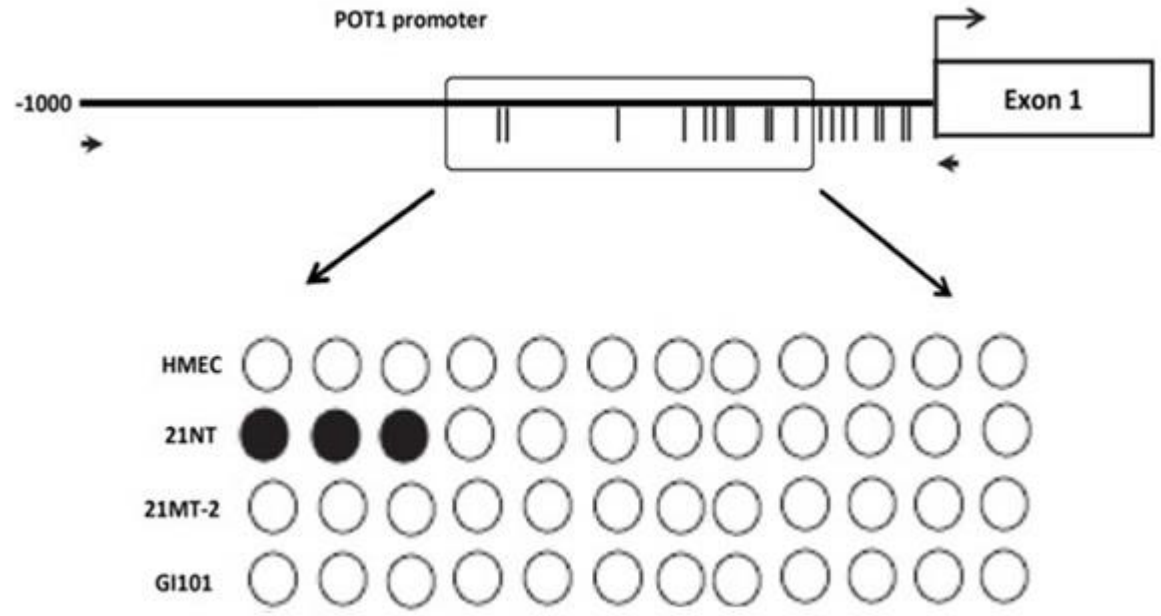

Figure 4.6-CpG methylation status of the *POT1* promoter. About 118 base pair upstream of exon1 was analysed by bisulphite sequencing. The *POT1* promoter region was identified and the rectangular area represents CpG regions. Three breast cancer cell lines and HMEC1 cell strains control were analysed. The black symbols show methylated CpGs and white symbols sites of unmethylated CpGs.

4.3.4-Attempts to reactivate full *POT1* expression by treatment of 21NT breast cancer cells with TSA and 5-aza-CdR

4.3.4.1-Optimization of TSA and 5-aza-CdR concentrations on 21NT cells

The effect of 5-aza-CdR and TSA concentrations on *POT1* expression in 21NT cells was investigated as it was found to be down-regulated in 21NT cancer cells (Chapter III). In this way, the optimization of 5-aza-CdR and TSA was carried out. Figure 4.7-B shows that there is seemingly a very gradual dose dependent increase up to a threshold of 50ng/ml followed by an abrupt step-change between 50 and 100ng/ml. Significantly increased expression levels of *POT1* were observed at the highest concentration of TSA (100ng/ml). However, cell viability was reduced to 61% with single-agent treatment (TSA) at the highest dose (100ng/ml) when compared with untreated control (Figure 4.7-A). As shown in Figure 4.8-A, treatment with TSA at 50 and 100ng/ml with 5µM 5-aza-CdR increased the percentage of cell survival compared with TSA alone (Figure 4.7-A). The highest up-regulation levels of *POT1* were observed at the concentration of 50 and 100ng/ml of TSA with 5µM 5-aza-CdR (Figure 4.8-B). Reduced cell survival after treatment with the highest concentration of TSA indicates cytotoxioty (an inhibition of cell growth /division and all death). The results showed an average cell viability and maximum expression of *POT1* at TSA concentration of 50ng/ml along with 5µM 5-aza-CdR in 21NT cells. Therefore, this suggests that 50ng/ml was the best concentration of TSA to be used.

A

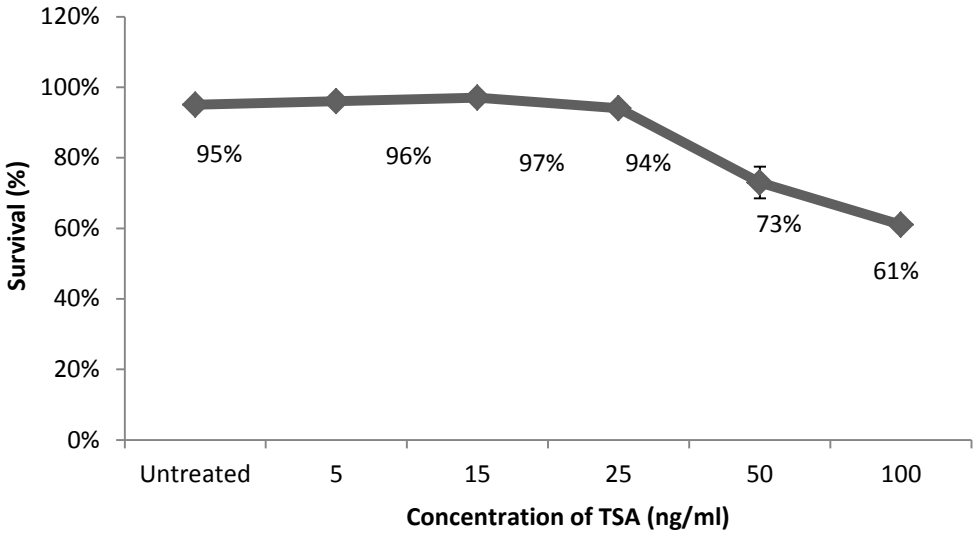

B

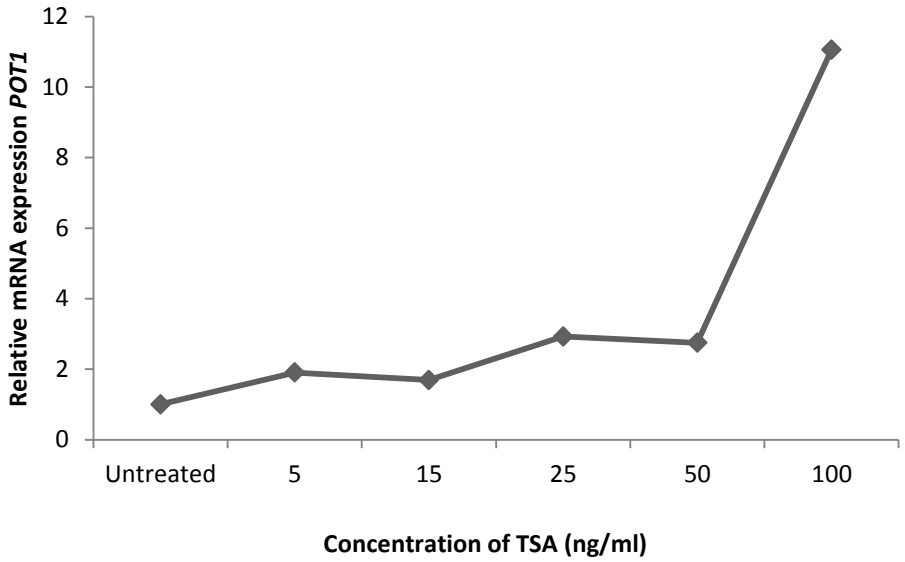

Figure 4.7-The changes in cell viability (A) and expression level of *POT1* (B) after treatment with TSA. The 21NT cell line was treated with TSA for 48 hours at different concentrations. **A)** The cell viability assay was performed to determine cell survival. **B)** qRT-PCR results show changes in *POT1* expression levels in 21NT cell after treatment with TSA at different concentrations. Untreated 21NT was used as the calibrator.

A

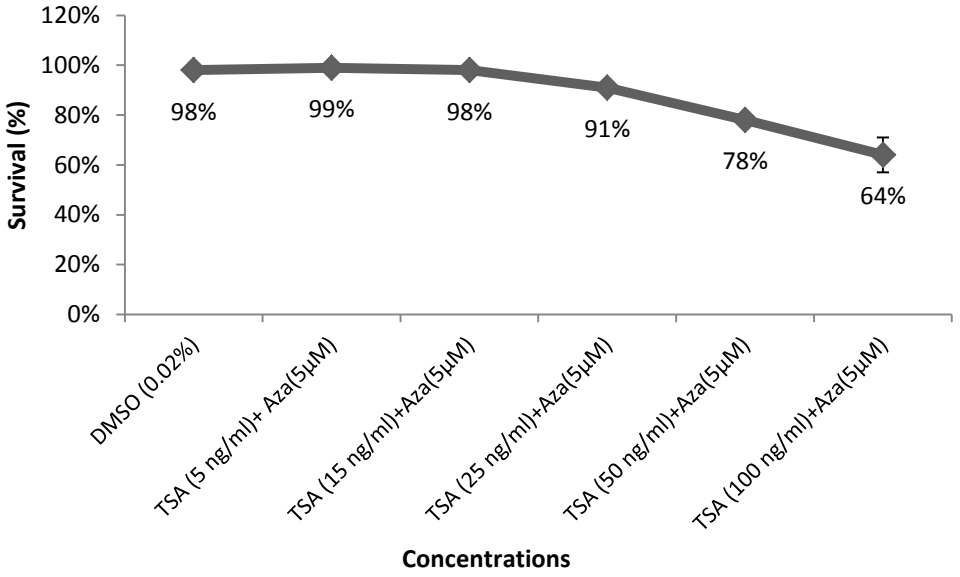

B

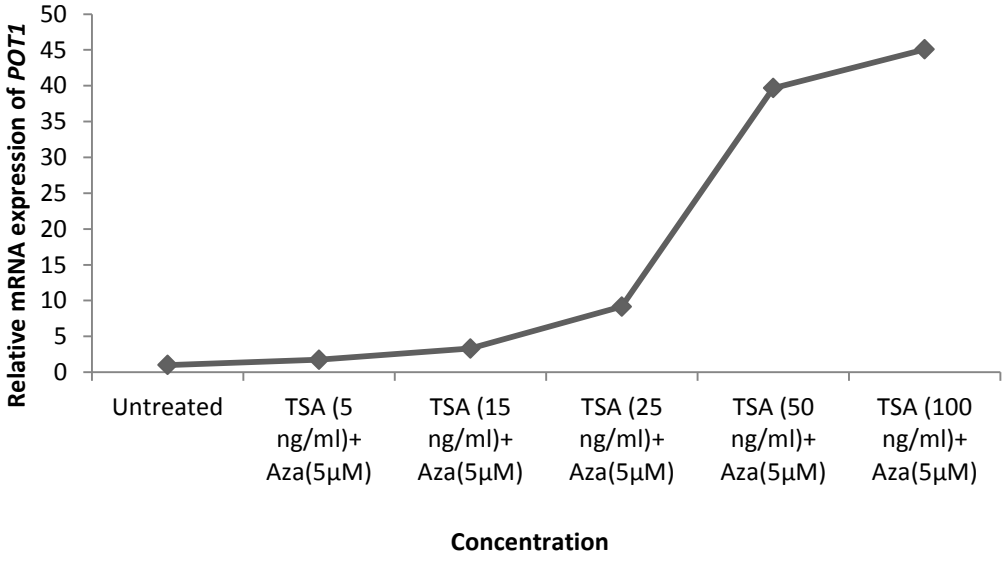

Figure 4.8-The changes in breast cancer cell viability (A) and expression level of *POT1* (B) after treatment with TSA and 5-aza-CdR. 21NT cells was treated with TSA at different concentration and with a single concentration (5µM) of 5-aza-CdR. **A)** The cell viability assay was performed to determine cell survival. **B)** qRT-PCR results show changes in *POT1* expression levels in 21NT cells after treatment with TSA at different concentrations and 5-aza-CdR.

4.3.4.2- Effect of TSA and 5-aza-CdR in 21NT cells at different time points

To determine the effect of TSA and 5-aza-CdR on the 21NT cell lines, cells were treated with both drugs individually or together at different time points (Table 4.3). Since the first replication takes 24 hours, it was decided to compare *POT1* gene expression at 24 and 48 hours to examine the effect of each drug. Cells were treated with two different concentrations of TSA (50 and 100ng/ml) whereas the concentration of 5-aza-CdR was kept constant at 5µM throughout the experiment. In treatments 1-4 (Table 4.3), 21NT cells were treated twice with TSA and 5-aza-CdR with 8 hours gap between each treatment (Ghoshal, Datta *et al.* 2005). The cells were collected either at 24 (1 and 2) or 48 hours post treatment (3 and 4) for further analysis. In treatments 5-8, 21NT cells were treated twice with TSA and 5-aza-CdR with 4 hours gap between each treatment (Ghoshal, Datta *et al.* 2005). The cells were collected either at 24 (5 and 6) or 48 hours post treatment (7 and 8) for further analysis. In treatments 9 and 10 21NT cells were treated with 5µM 5-aza-CdR for 48 hours. TSA at concentrations of 50ng/ml and 100ng/ml, were added to the cell cultures (9 and 10 respectively) for the last 16 hours of treatment (Pryzbylkowski, Obajimi *et al.* 2008; Mirza, Sharma *et al.* 2010). As depicted in Figure 4.9, treatment 9 consisting of 5µM 5-aza-CdR and 50ng/ml of TSA (for the last 16 hours of treatment) had the highest effects on mRNA expression levels of *POT1*. Therefore, 21NT cells were treated with the same regimen for further analysis of effect on other Shelterin and Shelterin-associated genes.

Table 4.3-Regimens for treating 21NT cells with different concentration of TSA (50 or 100ng/ml) and 5µM of 5-aza-CdR at different time points

No of Experiment	TSA Concentration (ng/ml)	5-aza-CdR Concentration(µM)	Time in Culture treated with TSA/5-aza-CdR	Total Time in Culture
1	50	5	8h twice	24h
2	100	5	8h twice	24h
3	50	5	8h twice	48h
4	100	5	8h twice	48h
5	50	5	4h twice	24h
6	100	5	4h twice	24h
7	50	5	4h twice	48h
8	100	5	4h twice	48h
9	50	5	48h with AZA* 16h with TSA	48h
10	100	5	48h with AZA 16h with TSA	48h

***AZA: 5-aza-CdR**

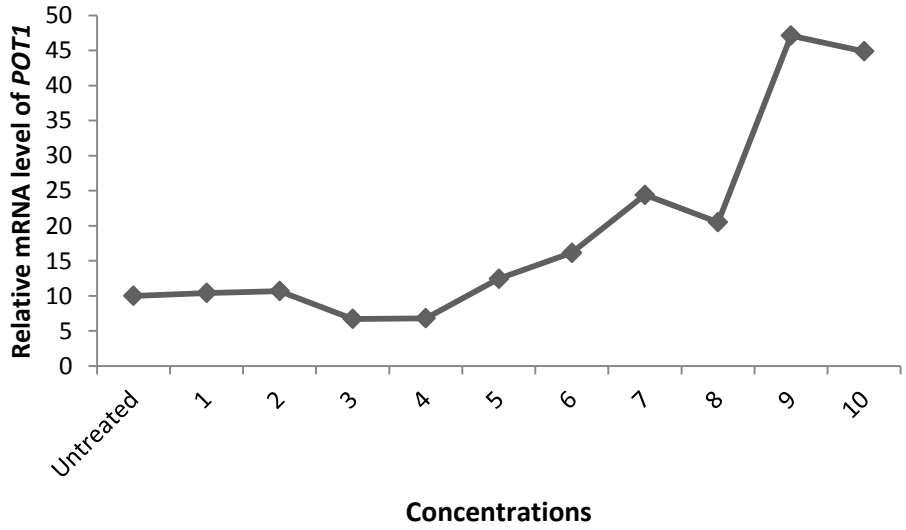

Figure 4.9-Effect of 5-aza-CdR and TSA on expression levels of *POT1*. The qRT-PCR results show changes in *POT1* expression levels in 21NT cells after treatment with 50 and 100ng/ml of TSA with 5-aza-CdR at different time points. Untreated 21NT cells were used as the calibrator.

4.3.5-Up-regulation of Shelterin and Shelterin-associated genes by 5-aza-2'-deoxycytidine (5-aza-CdR) and Trichostatin A (TSA)

To further understand the mechanisms controlling epigenetic regulation of Shelterin genes in breast cancer cells, the effects of 5-aza-CdR and TSA individually and 5-aza-CdR/TSA together on all Shelterin and Shelterin-associated gene expression were investigated in 21NT cells after 48 hours treatment (Figure 4.10). These cells were chosen for analysis because they were available at an earlier passage compared to the other breast cancer cell lines included in this study.

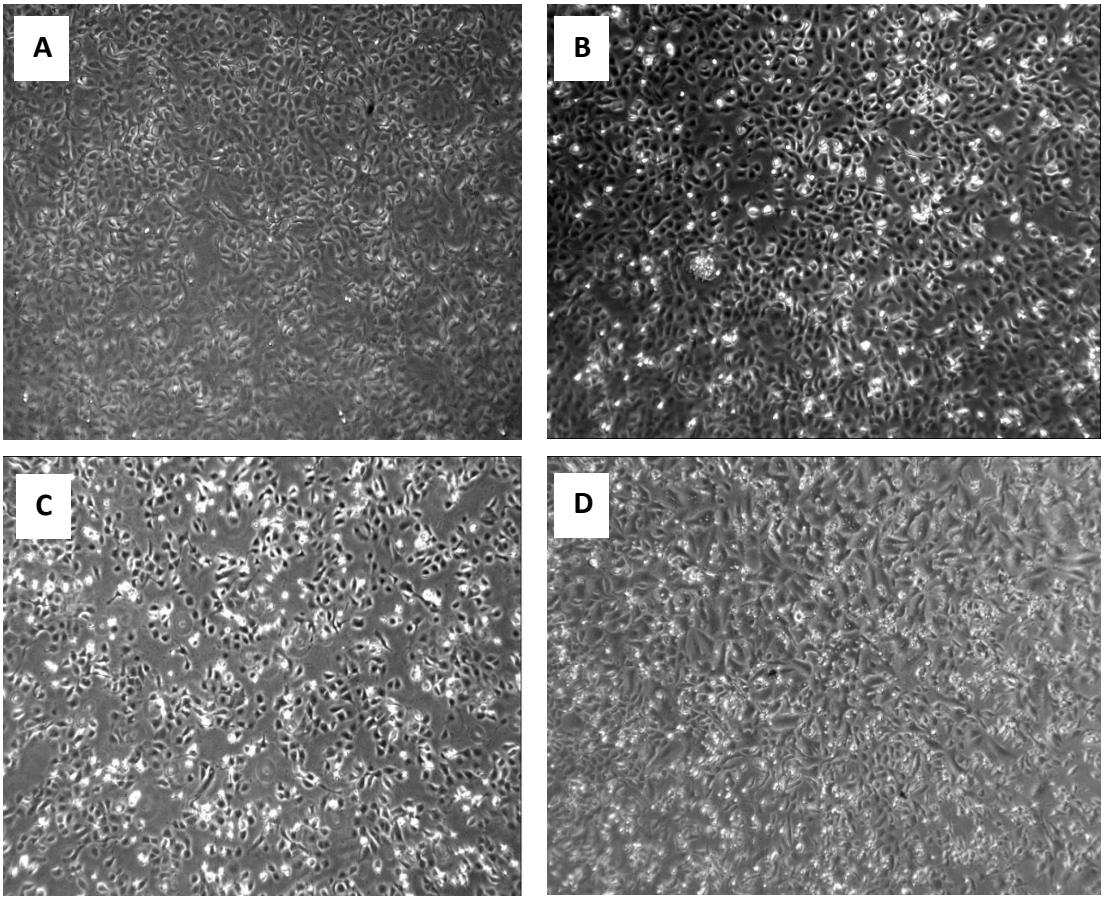

Figure 4.10-Representative images showing an example of individual treatment of 21NT cells with 5-aza-CdR and TSA at x5 magnification. A) 21NT cells containing 0.02% DMSO-treated control and cultured for 48 hours, **B)** 21NT cells containing 5µM 5-aza-CdR and cultured for 48 hours, **C)** 21NT cells containing 5µM 5-aza-CdR and 50ng/ml TSA cultured for 48 hours, **D)** 21NT cells containing 50ng/ml TSA cultured for 48 hours. Each treatment of 21NT cells appears to have rounded cell shape and no difference between each treated cells shape have been observed.

To explore whether the down-regulation of genes encoding members of the Shelterin and Shelterin-associated genes observed in this study, is due to DNA or histone modifications, the 21NT cells was treated with 5-aza-CdR and TSA. Therefore, demethylation of a gene by exposure to 5-aza-CdR and or suppression of the activity of HDAC by TSA should result in removal of a mechanism which should in theory lead to restoration of normal expression the relevant Shelterin and Shelterin-associated genes.

The expression of Shelterin and Shelterin-associated genes was detected using qRT-PCR normalised with endogenous *GAPDH*. Treatment of 21NT cells in combination with 5-aza-CdR and TSA, lead to increased expression of *POT1* and *TIN2* (Figures 4.11-A and 4.13-A) as compared with the DMSO sample (p<0.05). In contrast, the up-regulation of *TNKS2*, *TRF1*, *TRF2*, and *RAP1* did not reach the statistical significance (Figures 4.11-B, 4.12-A, 4.12-B, and 4.13-B). However, 21NT cells treated solely by TSA, did not show up-regulation of *TNKS2*, *TRF2* and *RAP1* (Figures 4.11-B, 4.12-A, 4.13-B). Treatment with 5-aza-CdR alone resulted in up-regulation of all the above genes (except *TRF1)* and there was a significant up-regulation of *POT*1, *TIN2* and *TPP1* mRNA in 5-aza-CdR/TSA and 5-aza-CdR treated samples (p<0.05) (Figures 4.11-A and 4.13-A, 4.14-A). In addition, in the previous results Chapter (III), it was evident that *TPP1* was over-expressed in 21NT cells in comparison with the HMEC1 (Figure 3.10). However, these trends were not statistically significant. The result in this chapter showed that the expression of *TPP1* after 48 hours of treatment with 5-aza-CdR increased by 4-fold when compared with DMSO and untreated controls (p<0.05) (Figure 4.14-A).

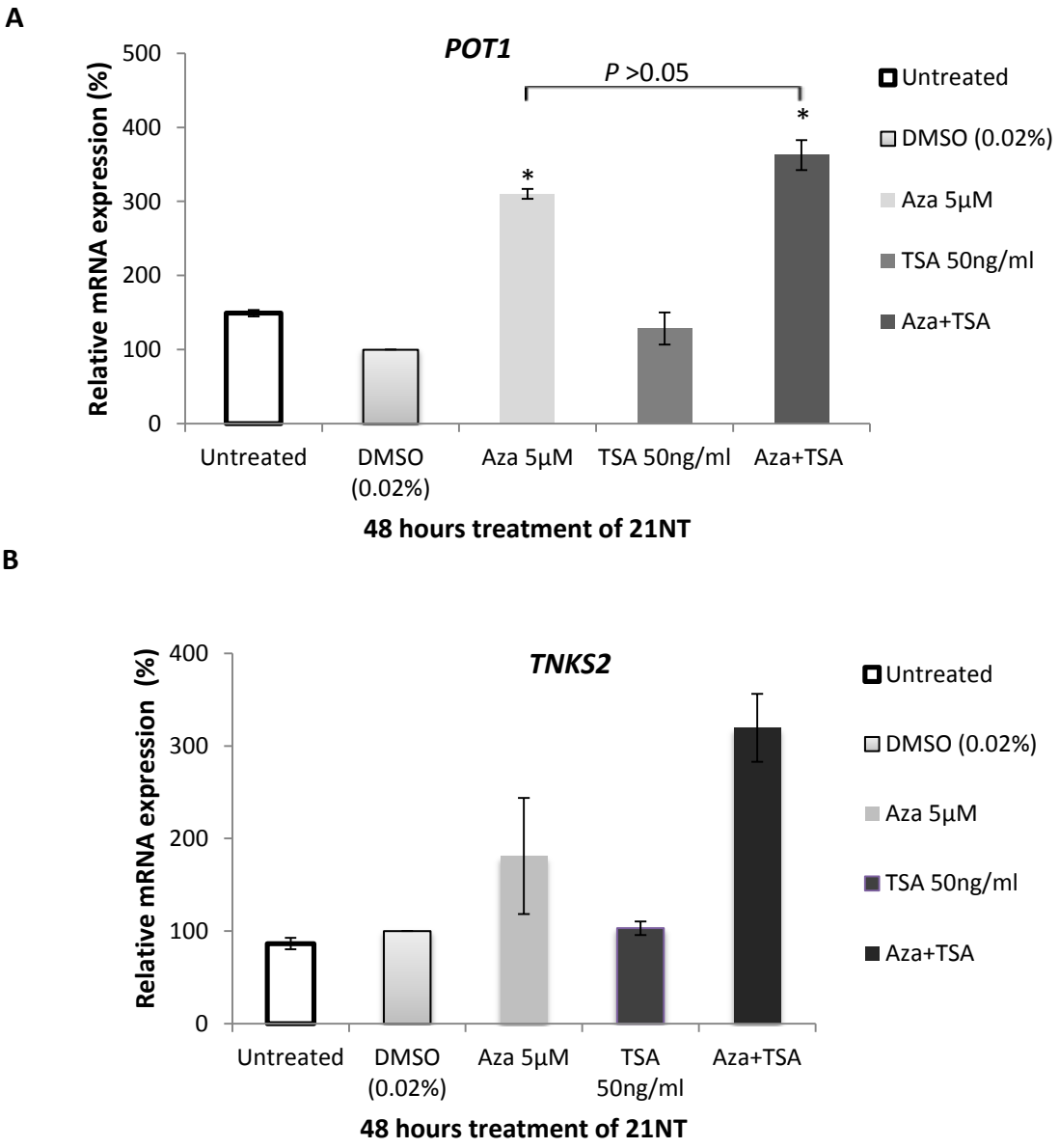

Figure 4.11-Effects of 5-aza-CdR and TSA on the expression of *POT1* and *TNKS2* in the 21NT breast cancer cell line. qRT-PCR analysis of *POT1* **(A)** and *TNKS2* **(B)** mRNA levels following 5-aza-CdR and TSA treatments in 21NT cells for 48 hours. Expression of each gene values were normalised to *GAPDH* mRNA level. DMSO control was used as the calibrator. RQ and error bars indicate relative quantification and SEM. Asterisk indicates significant difference between 21NT treated cells and DMSO-control (**P*<0.05).

A

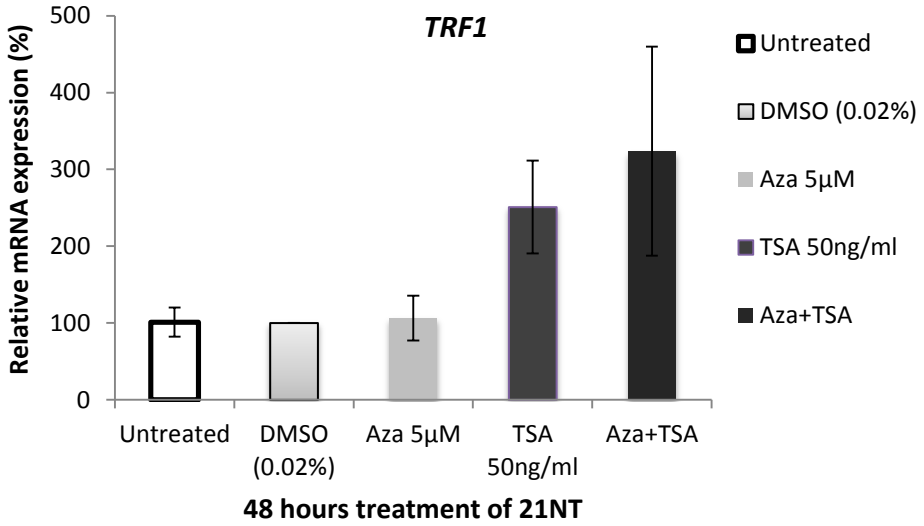

B

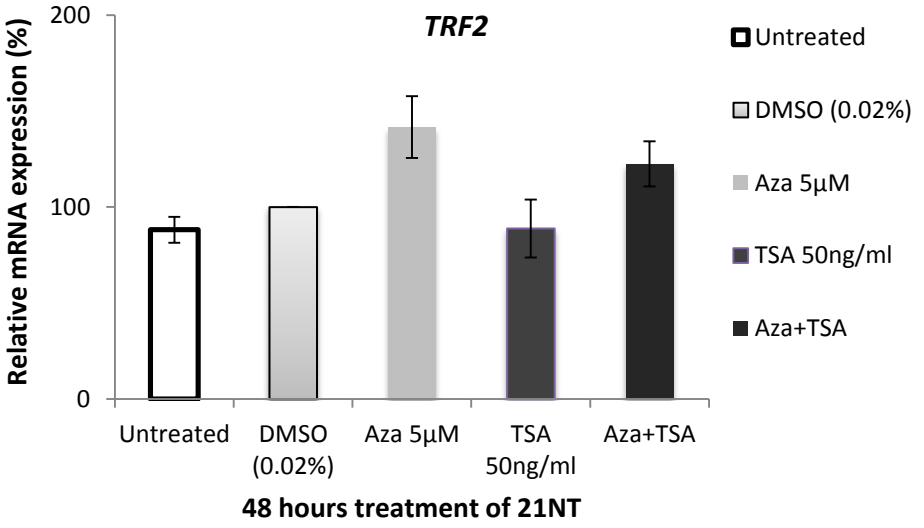

Figure 4.12-Effects of 5-aza-CdR and TSA on the expression of *TRF1* and *TRF2* in the 21NT breast cancer cell line. The image **(A)** and **(B)** represent qRT-PCR analysis of *TRF1* and *TRF2* mRNA isolated from 21NT treated with 5-aza-CdR and TSA for 48 hours. *TRF1* and *TRF2* expression were normalised to the expression of the *GAPDH*. DMSO control was used as the calibrator. RQ and error bars indicate relative quantification and SEM.

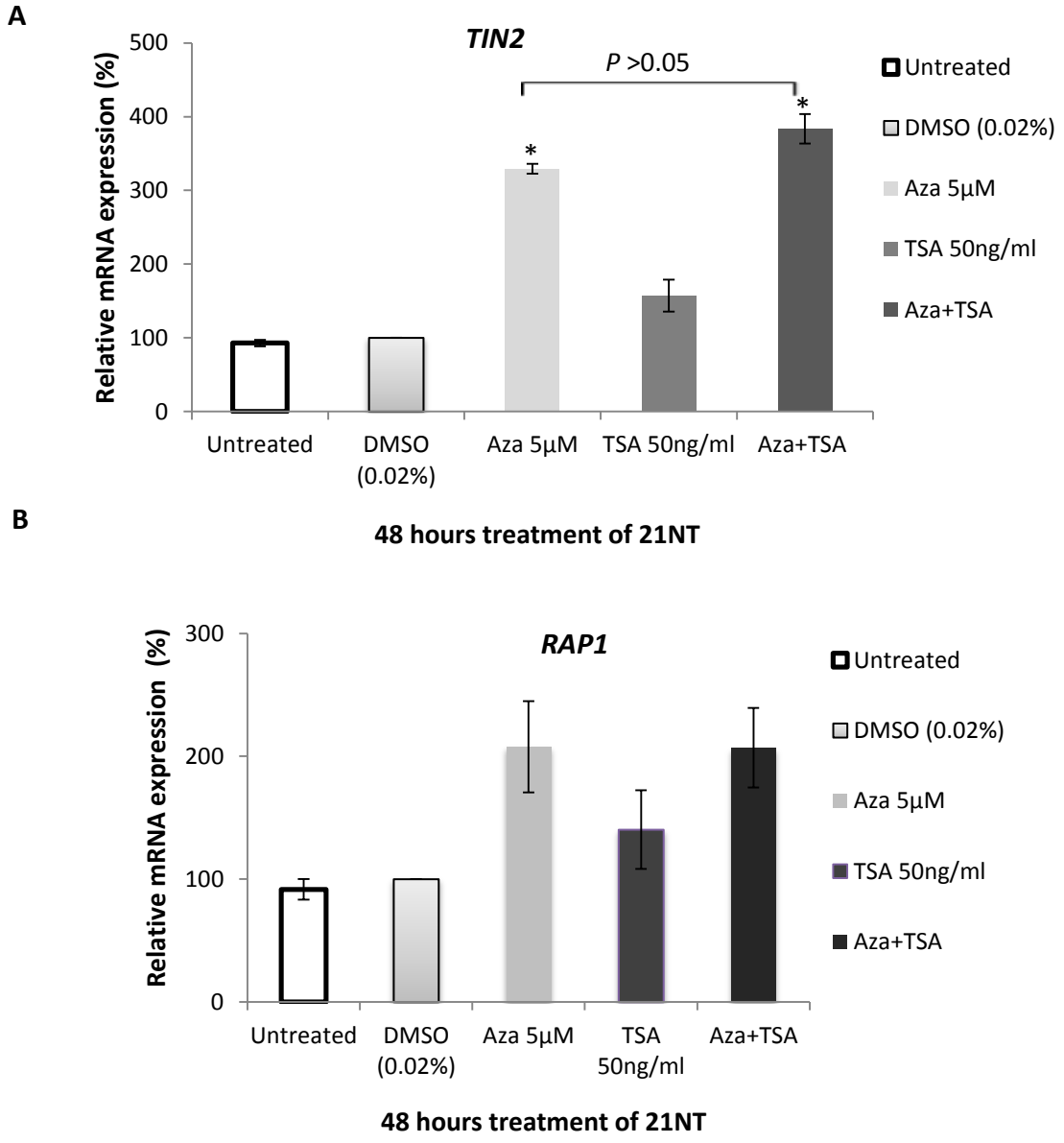

Figure 4.13-Effects of 5-aza-CdR and TSA on the expression of *TIN2* and *RAP1* in the 21NT breast cancer cell line. The graphs (**A** and **B**) represent analysis of mRNA from the 21NT treated cells with qRT-PCR to detect the *TIN2*, *RAP1* and *GAPDH* mRNAs. DMSO control was used as the calibrator. Error bars represent SEM. Asterisk indicates significant difference between 21NT treated cells and DMSO-control (**P*<0.05).

Previous results demonstrated a significant increase in the mRNA levels of *TPP1* in 5-aza-CdR treated samples ($p<0.05$) after 48 hours (Figure 4.14-A). Therefore, 21NT cells were also treated by 5-aza-CdR and TSA individually and in combination with 5-aza-CdR and TSA, for 72 hours or 3 weeks. The long-term (3 weeks) and short-term (72 hours) effect of drugs on levels of TPP1 protein in cultured cells were analysed by western blot. In all samples TPP1 was detectable as a 58 KDa (rabbit polyclonal antibody Abcam) protein (Figures 4.15-A and 4.15-B). The amount of TPP1 protein in 21NT cells treated with 5-aza-CdR/TSA for 72 hours was increased in comparison with the DMSO-control (Figures 4.15 A-B). Thus the protein level of TPP1 was consistent with the qRT-PCR results (Figures 4.14-A and 4.15 A-B). However, the protein level of TPP1 in 21NT cells treated with 5-aza-CdR alone (short-term)

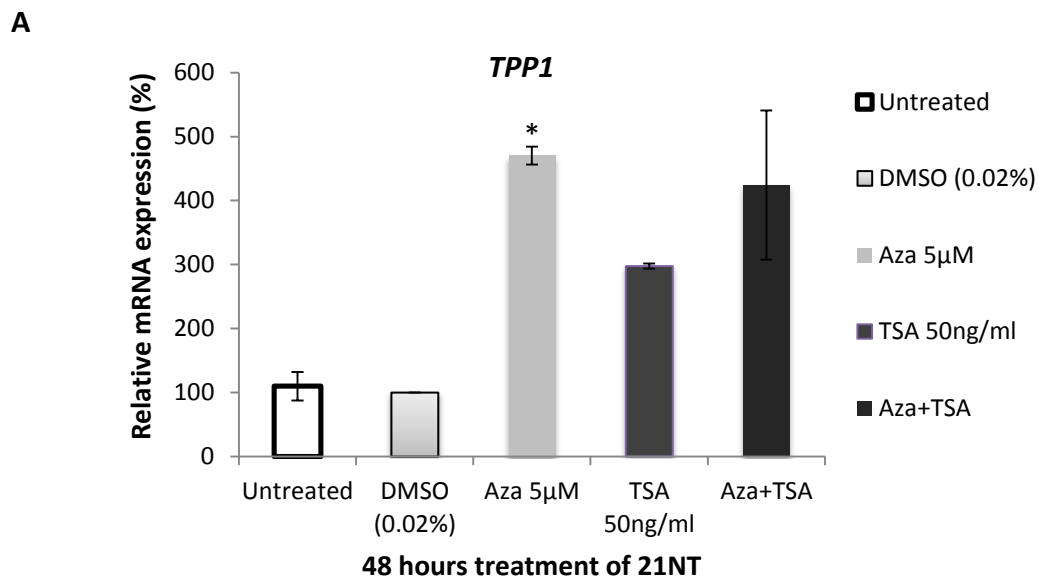

Figure 4.14-Expression of *TPP1* in 21NT treated cell line determined by qRT-PCR. A) The graph represents analysis of transcription level of *TPP1* from the indicated 21NT treated cells with 5-aza-CdR and TSA for 48 hours. All mRNA levels were normalized to the level of *GAPDH* mRNA. Error bars represents SEM. DMSO control was used as the calibrator. Asterisk indicates significant difference between 21NT treated cells and DMSO-control (*$P<0.05$).

was inconsistent with mRNA results. Also, no considerable difference in TPP1 protein level was observed in long-term treated sample compared with short-term treatment (Figure 4.15 B-C).

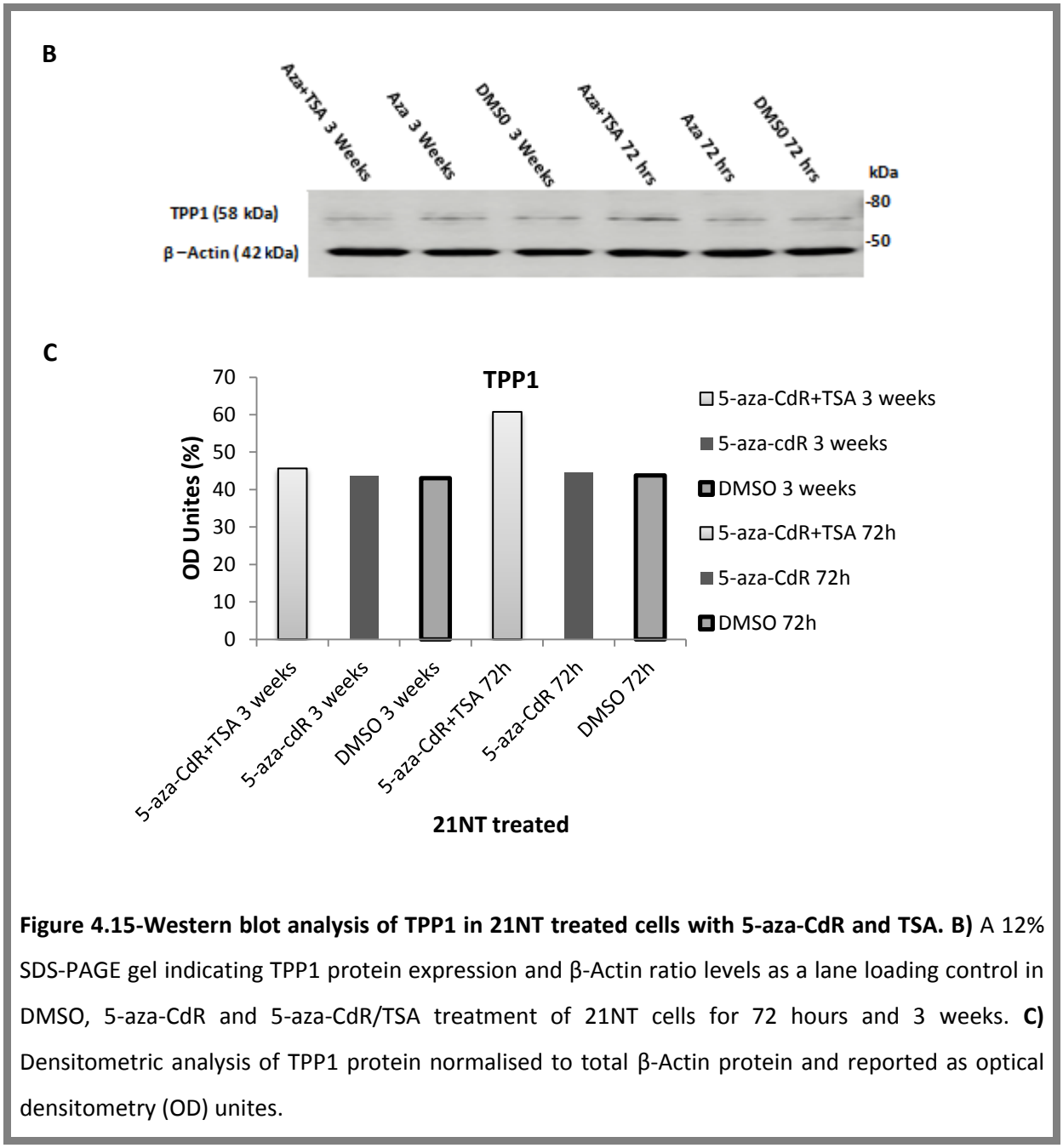

Figure 4.15-Western blot analysis of TPP1 in 21NT treated cells with 5-aza-CdR and TSA. B) A 12% SDS-PAGE gel indicating TPP1 protein expression and β-Actin ratio levels as a lane loading control in DMSO, 5-aza-CdR and 5-aza-CdR/TSA treatment of 21NT cells for 72 hours and 3 weeks. **C)** Densitometric analysis of TPP1 protein normalised to total β-Actin protein and reported as optical densitometry (OD) unites.

4.3.6-Effects of prolonged treatment of 21NT cells with 5-aza-2'-deoxycytidine and Trichostatin A on transcription level of Shelterin genes

As discussed in Section 4.3.5, 5-aza-CdR, TSA and 5-aza-CdR/TSA treatment after 48 hours had differential effects on Shelterin and Shelterin-associated gene expression levels. The preliminary results showed significantly increased expression of *POT1* and *TIN2* mRNA (p<0.05) following 5-aza-CdR and 5-aza-CdR/TSA treatment in the absence of consistent promoter DNA demethylation and histone deacetylation (Figures 4.11-A and 4.13-A). Therefore, we sought to investigate long-term treatment of 21NT cells to identify whether the expression of these genes may possibly change after longer period of exposure. We

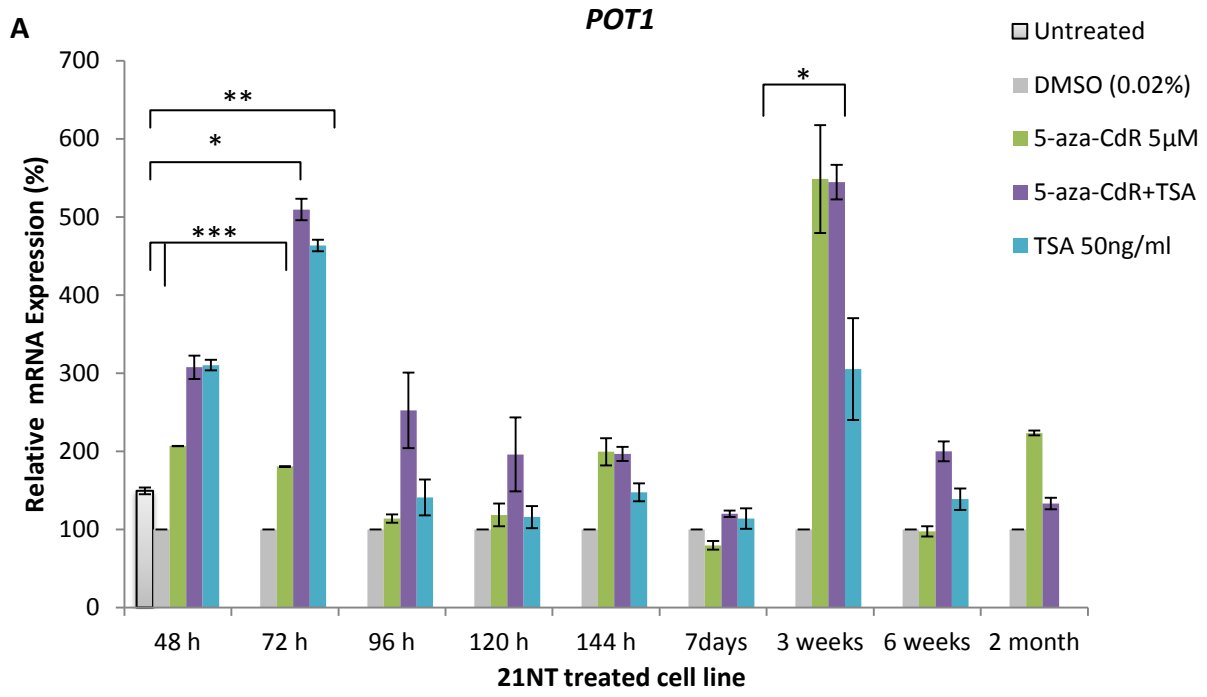

Figure 4.16.A-Expression of *POT1* in 21NT treated cells at different time points. The graph represents analysis of mRNA from the indicated 21NT treated cells by qRT-PCR. 0.02% of DMSO-treated (control) was used as the calibrator. Error bars represent SEM. Asterisk indicates significant differences between 21NT treated cell lines and DMSO-control (*P<0.05, **P<0.01, ***P<0.001).

examined the expression of *POT1* and *TIN2* by 50ng/ml TSA and 5µM 5-aza-CdR treatments for 48h, 72h, 96h, 120h, 144h, 7 days, 3 weeks, 6 weeks and 2 months plus retreatment for 72 hours in 21NT cells. Analysis of each of these genes employed gene-specific primers see Table 2.2. The expression levels of the genes were assessed by qRT-PCR. qRT-PCR was performed in triplicate for each of the cDNA pools. The data showed that treatment of 21NT cells significantly increased transcription levels of *POT1* and *TIN2* upon on treatment with TSA, 5-aza-CdR, and 5-aza-CdR/TSA after different time points. Figure 4.16 shows the expression of *POT1* after 72 hours of treatment with TSA and 5-aza-CdR/TSA was over four-fold higher in the 21NT cells treated than in 21NT untreated cells (*P*<0.05, *P*<0.01 and

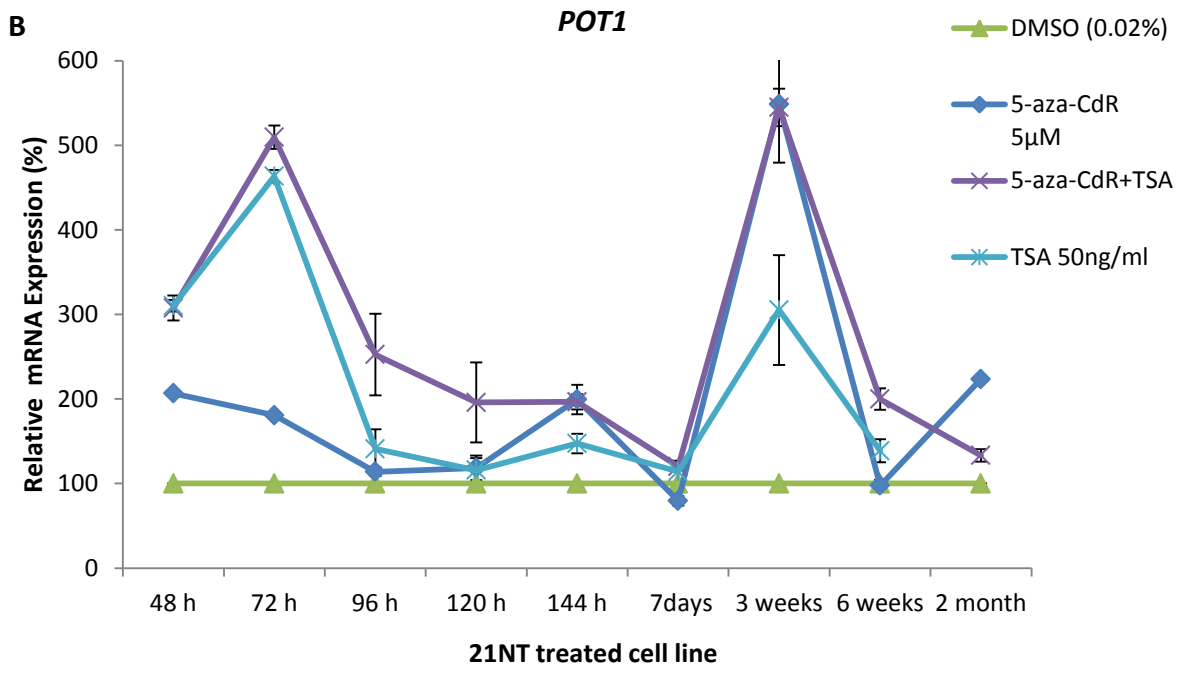

Figure 4.16.B-Expression of *POT1* in 21NT treated cells determined by qRT-PCR. B) The graph represents analysis of transcription levels of *POT1* from the indicated 21NT treated cells with 5-aza-CdR and TSA at different time points. All mRNA levels were normalized to the level of *GAPDH* mRNA. Error bars represent SEM.

P<0.001 correspondingly). In addition, treatment of 21NT cells with 5-aza-CdR and TSA alone, and in combination with 5-aza-CdR and TSA for 48 hours resulted in significant up-regulation of *POT1* (*P*<0.01 and *P*<0.001 correspondingly). Nevertheless, no substantial differences in expression of *POT1* has been observed in 96, 120, 144 hours and 7 days of treatment (Figures 4.16-A and 4.16-B). In addition, the biphasic response of *POT1* and *TIN2* gene expression was seen with an optimal peak at 72 hours, which then declined and the expression was increased significantly again at 3 weeks treatment (correlated with telomere length see Chapter V).

To observe the effects of 5-aza-CdR and TSA on protein levels of POT1 in cultured cells, POT1 protein expression in control (DMSO-treated) and treated cells (5-aza-CdR and TSA) were analysed by western blotting. In all samples, POT1 was detectable as a 71 KDa (rabbit polyclonal antibody, Abcam) protein (Figure 4.16-C). Interestingly, combined treatment with 5-aza-CdR and TSA for 72 hours increased the levels of POT1 protein compared with the single treatment with 5-aza-CdR which was consistent with the qRT-PCR results (Figure 4.16-D). Moreover, less POT1 protein was also expressed in 21NT cells after 3 weeks treatment relative to the DMSO control. The combined use of 5-aza-CdR and TSA for 72 hours treatment had more effect on POT1 protein expression than with 3 weeks of treatment.

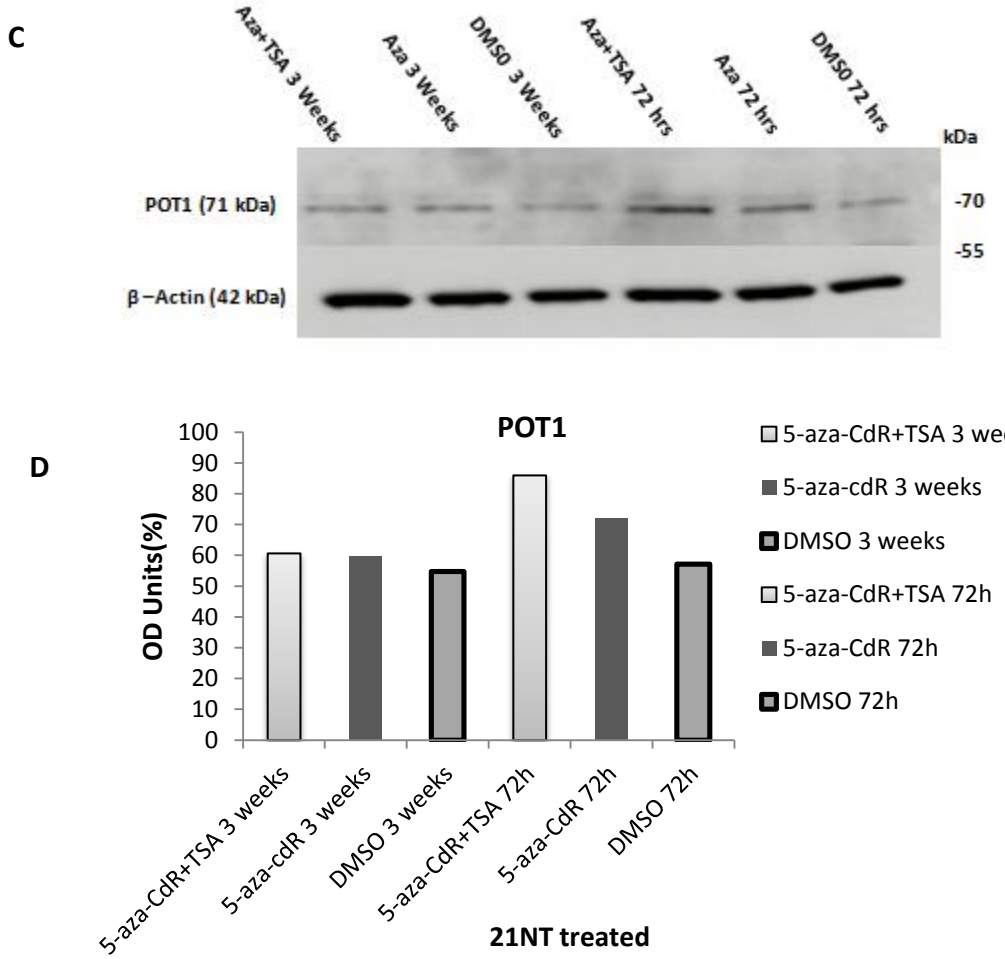

Figure 4.16 C and D-Western blot analysis of POT1 in 21NT treated cell line with 5-aza-CdR and TSA for 7 days and 3 weeks. **C)** 5-aza-CdR and 5-aza-CdR/TSA treatment increased POT1 protein levels in 21NT cells. High levels of POT1 (71 KD) protein was detected by western blotting following 5-aza-CdR and 5-aza-CdR/TSA treatment of 21NT cells for 72 hours. β-Actin utilized as a lane loading control. **D)** Densitometric analysis of POT1 protein normalised to total β-Actin protein and reported as optical densitometry (OD) unites.

As shown in Figures 4.16-A and 4.16-B, *POT1* mRNA levels up-regulated in 5-aza-CdR/TSA treated samples after 6 weeks and 2 month treatments. However, these trends did not reach a statistical significance. Following treatment of 21NT cells with 5-aza-CdR and TSA at different time points, the data suggested that 5-aza-CdR and the combination

treatment of 5-aza-CdR and TSA induced up-regulation of Shelterin genes. Therefore, it is assumed that Shelterin genes are at least in part down-regulated by DNA methylation.

Treatment of 21NT cells also increased mRNA levels of *TIN2* after different time points of treatment. As shown in Figures 4.17-A and 4.17-B, the use of 5-aza-CdR for 120, 144 hours and combined treatment with 5-aza-CdR and TSA for 48, 72, 120, and 144 hours, significantly activated re-expression of *TIN2* in 21NT cells ($P<0.05$ and $P<0.01$ respectively).

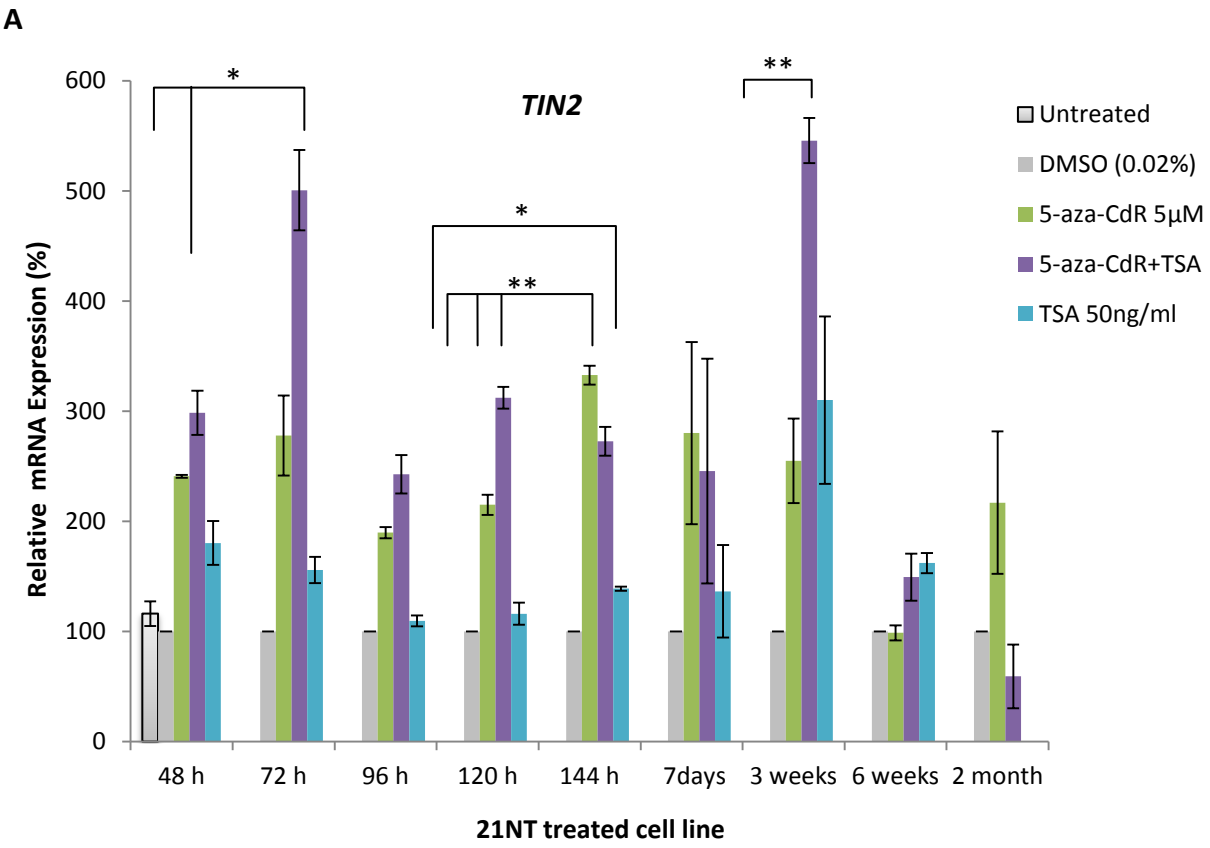

Figure 4.17.A-Expression of *TIN2* in 21NT treated cells at different time points. The graph indicates analysis of mRNA from the indicated 21NT treated cell line by qRT-PCR to detect the *TIN2* and *GAPDH* mRNAs. DMSO control was used as the calibrator. Error bars represent SEM. Asterisk indicates significant differences between 21NT treated cell lines and DMSO-control (*$P<0.05$, **$P<0.01$).

Similar findings were also detected with combined treatment of the drugs after 3 weeks (correlated with telomere length see Chapter V). As evident in Figures 4.17-A and 4.17-B, *TIN2* mRNA levels were significantly up-regulated in 5-aza-CdR/TSA treated samples (P<0.05). Nevertheless, no considerable difference in expression of *TIN2* has been observed in 6 weeks and 2 month retreated samples (Figures 4.17-A and 4.17-B).

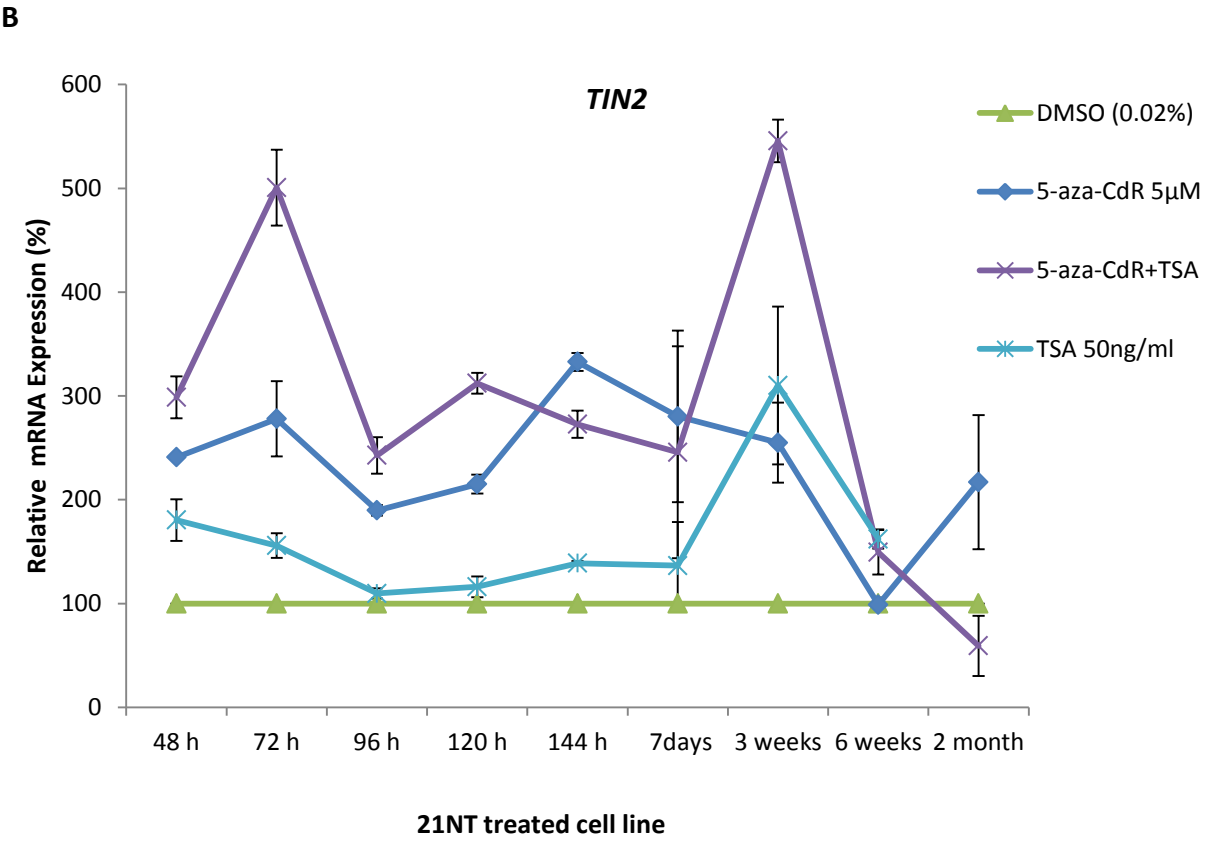

Figure 4.17.B-Expression of *TIN2* in 21NT treated cells at different time points. The graph indicates analysis of mRNA from the indicated 21NT treated cell line by qRT-PCR to detect the *TIN2* and *GAPDH* mRNAs. DMSO control was used as the calibrator. Error bars represent SEM.

4.3.7-*POT1* methylation analysis on genomic DNA of 21NT treated cells

In an effort to investigate whether 5-aza-CdR effects on cytosine methylation levels in the promoter region of *POT1*, the genomic DNA of 21NT treated with DMSO and 5-aza-CdR for 72 hours was examined. As before, a 118 base pair fragment with the length of from the *POT1* promoter region was utilized for the bisulphite direct sequencing method. The 12 possible CpG regions in the promoter region of *POT1* were identified. The results showed that the *POT1* CpG Island in DMSO control was partially methylated whereas 5-aza-CdR treatment had reduced CpG Island methylation at the promoter region (Figure 4.18) (Figure S3). In three of the 12 CpG sites, there was methylation in the DMSO control whereas no methylation was observed after treatment with 5-aza-CdR treatment (Figure 4.19). These data again strongly suggest that *POT1* promoter region at least partly under the control of DNA methylation in 21NT cells.

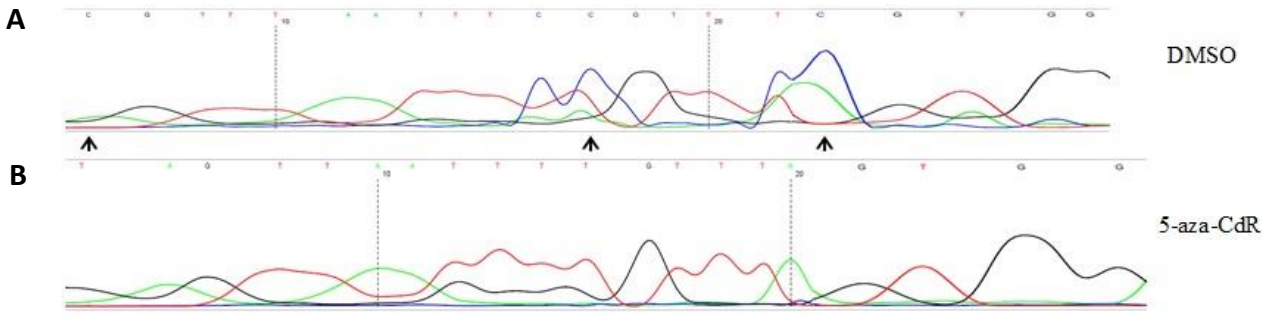

Figure 4.18-Interpretation of methylation sequencing of *POT1* promoter region. A) The upstream promoter region of 21NT cells treated with DMSO **B)** 21NT cells treated with 5-aza-CdR for 72 hours using bisulphite sequencing directly from PCR products. Chromatograms show methylation regions of 21NT treated at different time points. Arrows indicate a CpG methylated dinucleotide and the rest remained unmethylated. The C-picks indicate cytosine which is unmethylated in 21NT treated cells, the T-peaks show thymidine, the A-picks show adenine and the G-picks show guanine.

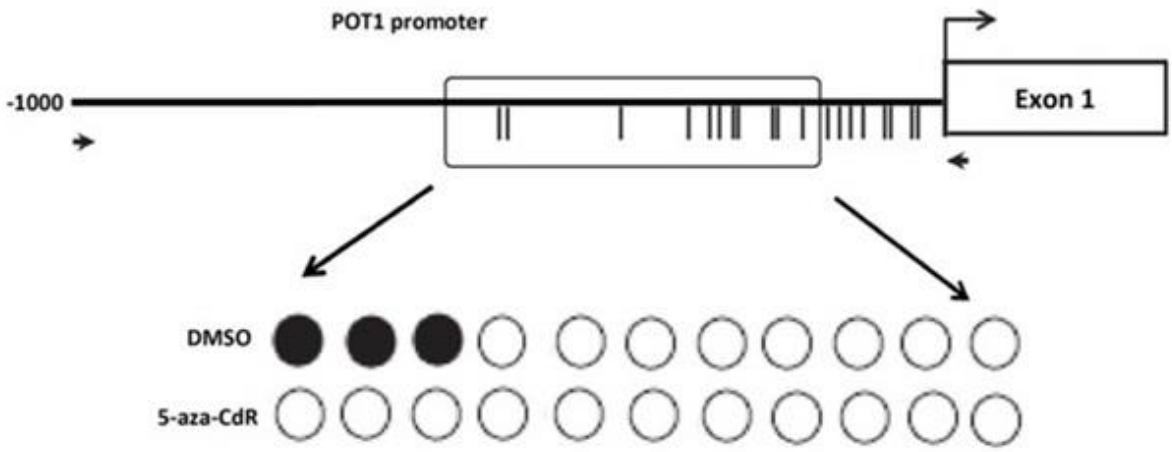

Figure 4.19-CpG methylation status of *POT1* promoter in 21NT breast cancer cells before and after treatment with 5-aza-CdR. About 118 bp upstream of exon1 was analysed by bisulphite sequencing. One CpG promoter region was identified and the rectangular area represents CpG regions. 21NT cells treated with 5-aza-CdR and DMSO control for 72 hours. The black symbols show methylated CpGs and white symbol sites of unmethylated CpGs.

4.4-Discussion

The previous chapter (III) described results from this project providing evidence for altered expression of certain Shelterin genes in breast cancer cell lines. Two main ways in which gene expression can be altered is through mutation or epigenetic modifications. According to the 2009 COSMIC database (Catalogue of Somatic Mutations in Cancer, Sanger Centre UK http://www.sanger.ac.uk) no mutation was identified in the genomic sequence of any Shelterin genes, including *POT1* in breast cancer cell lines. However, currently (2013), the COSMIC database shows over 127 somatic mutations in the *POT1* gene in different cancers, such as breast, skin, and cervix. In addition, Ramsay *et al.* (2013) showed that *POT1* is commonly mutated in multiple myeloma, breast, lung, squamous cells, and hepatocellular carcinomas. However, at the time this project started, only one somatic mutation in exon12 of *POT1* had been discovered in HeLa and HO8910-PM cells (Hou, Huang *et al.* 2006). Based on these findings, genomic DNAs were isolated from the breast cancer cell lines and DNA sequencing of exon12 was carried out to identify a possible genetic mechanism that might lead to reduction of *POT1* expression in these cell lines. Sequence analysis of exon12 showed that no mutation was present in the panel of 10 breast cancer cell lines studied in this project. However, it remains possible that mutations exist in other exons of *POT1*. It was not possible to sequence all exons of the *POT1* gene in all breast cancer cell lines due to lack of time and resources.

Gene expression can be regulated both by DNA methylation and by histone modifications (such as acetylation, methylation, phosphorylation, and ubiquitination) through specific chromatin modifying enzymes (Jaenisch and Bird 2003; Bannister and Kouzarides 2011). In order to account for the observed reduction in Shelterin gene

expression, these genes may possibly be silenced by DNA methylation in some breast cancer cells. Abnormal DNA methylation and histone modification are thought to play an essential role in carcinogenesis and apoptosis (Kondo, Shen *et al.* 2003). It has been previously reported that the combined treatment of breast cancer cell lines with 5-aza-CdR and TSA resulted in alteration of the expression level of estrogen receptor alpha (ER) (Pryzbylkowski, Obajimi *et al.* 2008). In addition, findings by Meng *et al*. (2008) showed that treatment of an ovarian cancer cell line with 5-aza-CdR and TSA resulted in DNA demethylation of *hMLH1* gene (Meng, Dai *et al.* 2008).

The work described in this chapter, a powerful DNA methylation inhibitor, 5-aza-CdR, and a histone deacetylase inhibitor, TSA, used to address the possible mechanism for down-regulation of Shelterin and Shelterin-associated genes in 21NT breast cancer cells. The qRT-PCR results revealed that Shelterin genes were transcriptionally repressed through methylation and/or deacetylation as their mRNA expression was up-regulated in 21NT cell lines after 48 hours treatment with the drugs (Figures 4.11, 4.12, 4.13 and 4.14-A). The mRNA expression of *POT1*, *TIN2*, and *TPP1* was significantly increased in treated 21NT cells compared with untreated and DMSO-treated controls ($P<0.05$). The transcription levels of *TNKS2*, *TRF1*, *TRF2* and *RAP1* appeared higher in 21NT cells after treatment (compared with untreated and DMSO controls). However, these trends did not reach a statistical significance. With TSA as a single agent approximately a 2-fold up-regulation in *TRF1*, *RAP1* and *TPP1* was observed in comparison with untreated and DMSO-treated controls. Nevertheless, no substantial up-regulation of *TNKS2* and *TRF2* were observed after TSA treatment. This suggests that *TRF2* and *TNKS2* genes are marginally up-regulated by promoter demethylation rather than histone modifications (Figures 4.11, 4.12, 4.13 and

4.14-A). With the other Shelterin genes taken together, the results in this section indicated that Shelterin and Shelterin-associated genes were up-regulated due to the synergistic effects of 5-aza-CdR in combination with TSA treatment at 48 hours in 21NT cells. Based on the preliminary results, a significant increase in the expression of *POT1* and *TIN2* ($p<0.05$) could be observed following 5-aza-CdR and 5-aza-CdR/TSA treatment in 21NT cells. The effect of drugs at different time points was examined in order to investigate the expression of *POT1* and *TIN2* genes affected by 5-aza-CdR and 5-aza-CdR/TSA treatment of 21NT cells. To evaluate changes in these genes, the expression levels of *POT1* and *TIN2* were compared at each different time points ranging from 48 hours to 2 month treatment. The results showed that 5-aza-CdR and TSA only affected *TIN2* and *POT1* mRNA levels at short-term (48 and 72 hour) and 3 weeks exposure. In addition, the biphasic response of *POT1* and *TIN2* gene expression was seen with an optimal peak at 72 hours, which then declined and the expression was increased significantly again at 3 weeks treatment (correlated with telomere length see Chapter V). Nonetheless, no considerable differences in the expression of these genes were observed in 2 months cells retreated for 72 hours. Collectively the results indicated that 5-aza-CdR and TSA lose their effectiveness at the longest time points of treatment (6 weeks and 2 month retreatment) (Figures 4.16 and 4.17). Therefore, treatment is not permanent and reversible.

The effects of 5-aza-CdR and TSA treatment on 21NT cells at different time points on *POT1* and *TIN2* mRNA levels, had not been studied in the project to date. Enzymes known as DNA methyltransferases (DNMTs) carry out DNA methylation at the 5 position of CpG dinucleotides. These enzymes regulate DNA methylation by catalysing the transfer of a methyl group from S-adenosyl-L-methionin (SAM) to a cytosine (Bestor 2000). DNMT1 is the

main methylation maintenance enzyme that methylates hemi-methylated DNA during the process of DNA replication (Pradhan, Bacolla *et al.* 1999; Kim, Samaranayake *et al.* 2009). Since many tumour suppressor genes are known to be inhibited through the DNA methylation process during carcinogenesis, 5-aza-CdR has been used to reactive these genes through inhibiting DNMTs. 5-aza-CdR which is incorporated into gDNA during replication, and thereby inhibits DNA methylation via irreversible covalent binding to DNMT1 (Maslov, Lee *et al.* 2012). By this mechanism, it could be argued that the lowest mRNA levels of *POT1* and *TIN2* between 72 hours and 3 weeks may perhaps resulted from an increase in the expression of the DNA methyltransferase 1 enzyme, leading to hypermethylation of *POT1* and *TIN2* after several replications.

Recent work by Kang *et al.* (2013) demonstrated that Runt-related transcription factor 3 (*RUNX3*), a tumour suppressor gene, was hypermethylated in MCF-7, breast cancer cell line. They showed that 5-aza-CdR induces apoptosis and inhibits cell proliferation by demethylating the promoter region of *RUNX3* and reactivating its expression (Kang, Dai *et al.* 2013). Therefore, based on previous investigations, it should be noted that 5-aza-CdR is a chemotherapeutic drug, which causes cell death via induction of apoptosis pathways. Consistent with this observation, approximately 72 hours after treatment with 5-aza-CdR, a significant reduction in 21NT cell number was observed. Therefore, by 7 days of treatment, cells which have become resistance to the treatment but retained the unmethylated status will start to grow and continue to grow up to 3 weeks accompanied by an increase in gene expression.

POT1 appears to bind directly to the 3' overhang of single stranded telomeric DNA. This protein interacts with TIN2 via TPP1 protein to become part of the Shelterin complex

(Takai, Kibe *et al.* 2011). Hence, TPP1 is the only protein that is directly bound to POT1 and TIN2. qRT-PCR results showed significant up-regulation of *TPP1* after 48 hours treatment of 21NT cells with 5-aza-CdR treatment ($p<0.05$). We then investigated the protein levels of TPP1 and POT1 on short-term (72 hours) and long-term (3 weeks) treatment of the 21NT cells to examine whether the expression of these genes at the protein level might perhaps change after longer period of treatment. Western blot analysis was performed using POT1 rabbit monoclonal antibody (Abcam) and TPP1 rabbit polyclonal antibody (Abcam) and the values was normalised using β-Actin rabbit antibody (Sigma). These confirmed previous results obtained with qRT-PCR and revealed that 5-aza-CdR and the combined treatment of 5-aza-CdR and TSA induced the protein levels of POT1 after 72 hours treatment in comparison with DMSO-treated control. However, no significant increase was detected in long-term treatment (Figures 4.16-C and 4.16-D). Furthermore, no substantial difference in TPP1 protein level was observed in long-term treated sample compared to the short-term treatment (Figure 4.15). As shown in section 4.3.6, *POT1* and *TIN2* were significantly up-regulated in 21NT cells after being treated with 5-aza-CdR and TSA at different time points in comparison with DMSO and untreated controls. Therefore, our data indicated that promoter regions of *POT1* and *TIN2* genes may possibly be under the control of DNA methylation. Consequently, Methylation specific PCR (MSP) was used to examine the promoter regions of *POT1* and *TIN2* genes. Methylation specific PCR indicated that the promoter region of *POT1* was partially methylated in untreated (i.e., not exposed to 5-aza-CdR and TSA) breast cancer cell lines (21NT, 21MT-2 and GI101). However, no significant differences in the promoter region of *TIN2* were observed in methylated and unmethylated lanes compared with the control (HMEC1) (Figure 4.4).

The upstream promoter region of *POT1* was analysed for methylation in 21N, 21MT-2 and GI101 breast cancer cell lines, using bisulphite sequencing. Contrary to expectation, bisulphite sequencing data showed that no CpG region was methylated in 21MT-2 and GI101 breast cancer cell lines (Figure 4.5). However, 21NT cells was about 30% methylated in the upstream promoter region of *POT1* in comparison with HMEC1 (Figure 4.6). The product obtained from bisulphite PCR was sequenced and 100bp of error-free sequence was obtained. This was not enough to get an accurate estimation of the methylation pattern within the promoter region of *POT1*. Therefore, further sequence analysis should be carried out encompassing a larger region of the *POT1* promoter region.

In the current study, we determined the effects of these drugs on cytosine methylation levels in the promoter regions of *POT1*. The 21NT cells were treated with these drugs for 72 hours to investigate the reduction of cytosine methylation at *POT1* promoter region. Bisulphite sequencing data showed that 5-aza-CdR treatment removed all methylation sites of CpG dinucleotide in comparison with DMSO-treated as all cytosine residues were converted to thymidine (Figures 4.18 and 4.19). This finding is consistent with the earlier results showing up-regulation of Shelterin genes. In light of the new data discussed above, both DNA methylation and histone deacetylation appear to be implicated in the silencing of Shelterin and Shelterin-associated genes in breast cancer cell lines. The results presented here suggest that the synergistic effect of 5-aza-CdR may perhaps reduce DNA methylation in association with gene reactivation. It has been hypothesized that 5-aza-CdR and TSA treatments enhance gene transcription by opening promoter region to increased accessibility of assembling transcription factor complexes (Yang, Phillips *et al.* 2001; Margueron, Duong *et al.* 2004). Since these two agents have individually been able to

induce gene expression, they might be expected synergistically have a more potent effect on the gene expression than either alone.

Chapter V

ANALYSIS OF TELOMERE LENGTHS IN THE BREAST CANCER CELL LINE 21NT FOLLOWING EPIGENETIC CHANGES TO THE SHELTERIN GENES

5.1-Introduction

As has been mentioned in early chapters, telomeres consist of repetitive TTAGGG sequences found at the end of mammalian chromosomes, and play an important role in maintaining genomic integrity (Jacobs 2013). Telomeres are maintained by two main processes: (i) a telomere-specific DNA polymerase called telomerase (the primary mechanism), and (ii) the secondary alternative lengthening of telomeres mechanism known as ALT (a rare mechanism found in some tumours) (Conomos, Pickett *et al.* 2013). The telosomal proteins encoded by Shelterin genes play a part in protecting the ends of telomeres (de Lange 2002). The reverse transcriptase enzyme telomerase is responsible for the addition of hexanucleotide repeats TTAGGG, onto the 3'-end of a telomere, and consequently counter the process of replication-associated telomere shortening (Bryan 1995). The six protein complex Shelterin packages (caps) the ends of chromosomes preventing them from being recognised as a site of DNA damage during DNA replication (Liu, O'Connor *et al.* 2004; de Lange 2005). In view of the fact that a capacity for limitless replication is a sign of cancer, telomerase or ALT must be activated to overcome the process of telomere erosion (Hanahan and Weinberg 2000). Contrary to normal somatic cells, 85-90% of tumour cells express high levels of telomerase which is responsible for maintaining the 2-3kb telomere length of most cancer epithelial cells (carcinomas) (Kim, Piatyszek *et al.* 1994).

The role of telomerase activation in human cancer development has been widely studied (Donate and Blasco 2011) and it is important to understand how telomerase activation occurs in breast cancer. It has been reported that the up-regulation of telomerase

is associated with cell immortalization and malignancy (Salhab, Jiang *et al.* 2008). There is a strong body of evidence suggesting that short telomeres in breast cancer cells precipitate telomere dysfunction and this may be in part related to Shelterin proteins and their level of expression in breast cancer cells (Butler, Hines *et al.* 2012).

In the previous chapter (IV), we have shown that treatment of the 21NT cells with the DNA demethylating agent 5-aza-CdR and the histone deacetylase inhibitor TSA at different time point results in up-regulation of Shelterin genes mRNA expression. The transcription levels of *POT1*, *TIN2*, and *TPP1* were significantly increased in treated 21NT cells compared with untreated and DMSO controls ($P<0.05$). The resulting effect of the two agents on telomere length was a question of a considerable interest. The primary aim of this section of the work was to investigate if the up-regulation of Shelterin gene expression had an effect on telomere length. Therefore, changes in telomere length in short-term (72 hours) and long-term (3 weeks, 6 weeks, and 2 months plus retreat for 72 hours) treatment of 21NT cells was examined (Table 5.1).

The assessment of telomere dynamics is critically dependent on the telomere length measurement techniques used. Several techniques are available to measure telomere length; these include Southern blot analysis (Terminal restriction fragment (TRF)), quantitative fluorescence *in situ* hybridisation (Q-FISH), flow-FISH, the hybridisation protection assay (HPA), quantitative PCR, and single telomere length analysis (STELA). Each method has its benefits and disadvantages. For instance, Southern blot and flow-FISH can determine the average telomere length, while Q-FISH provides information about telomere lengths of individual chromosomes. Quantitative polymerase chain reaction (q-PCR) is another technique to measure telomere length. However, the lack of an appropriate primer

binding site can hamper this method (Forstemann, Hoss *et al.* 2000; Cawthon 2002). Therefore, an important subsidiary aim of this section of the project was to compare the aforementioned techniques in terms of reliability and accuracy.

5.2-Materials and methods

5.2.1-Interphase Quantitative Fluorescent *in situ* hybridization (i-QFISH)

For interphase analysis, samples were produced according to standard cytogenetic methods, with exception of colcemid treatment.

5.2.1.1-Prehybridization washes

Cells that were treated with 5-aza-CdR and TSA at different time points (see Section 4.2.3 and Table 5.1) were trypsinized with Trypsin/EDTA. The cell suspension was centrifuged at 12000*rcf* for 5 minutes. Cells were then treated with 10ml of hypotonic buffer (75mM of KCl) for 30 minutes in a 37°C water bath (this causes cells to swell with water and to burst to release DNA content). The samples were then centrifuged at 1000*rcf* for 5 minutes. The process of fixation was carried out by removing KCl and adding methanol and glacial acidic acid (3:1) solution. Cell suspensions were dropped onto clean glass slides and aged at 55°C overnight. After 24 hours, microscope slides containing samples were washed with phosphate-buffered saline (PBS) for 5 minutes on the shaker. Subsequently, the samples were treated with 4% formaldehyde for 2 minutes and washed in PBS for 3 times for 5 minutes each. In order to remove unwanted proteins, the cells were treated with 1mg/ml pepsin solution (50ml of water acidified with 0.5ml of 1M HCl, pH 2.0, containing 10% pepsin (Sigma)) for 10 minutes at 37°C in water bath. The slides were then washed 2 times with PBS for 2 minutes each on a shaker platform and then fixed with 4%

formaldehyde for 2 minutes. Afterwards, the samples were washed three times with PBS for 5 minutes each then dehydrated in the 70%, 90%, 100% ethanol for 5 minutes each. Slides were left to dry at room temperature.

Table 5.1-Represents different time point of 21NT treated cells with 5-aza-CdR, TSA or DMSO

Cell type	Period of time under treatment with			Period of time after treatment				
	5µM of 5-aza-CdR	50ng/ml of TSA	0.02 % of DMSO					
Treated 21NT	48hrs	16hrs	48hrs	72hrs	7 days	3 weeks	6 weeks	2 months

5.2.1.2-Hybridization

20µl of the synthetic oligonucleotide PNA (**P**eptide **N**ucleic **A**cid) specific for the telomeric DNA sequence $(CCCTAA)_{3,}$ labelled with FITC, was added to the slides. Slides were then placed on the heating block for 2 minutes at 70-75°C and left in a dark humidified chamber for 2 hours at room temperature. Stock hybridization mixture (1ml) for the telomeric probe was made up of 700µl deionised formamide, 5µl blocking reagent (10% in maleic acid), 50µl $MgCl_2$ buffer (2.5M $MgCl_2$, 9 mM Na_2HPO_4, pH 7.0), 10µl Tris (1M, pH 7.2), 152µl ddH_2O and 83µl of PNA solution (6 µl/ml FITC or Cy3-conjugated PNA) (peptide nucleic acid, Applied Biosystems, MA, USA).

5.2.1.3-Post hybridization washes

After hybridization, the samples were washed twice in 70% formamide solution for 15 minutes each. Then the slides were washed 3 times with PBS for 5 minutes in the dark on a shaker. Slides were then dehydrated in 70%, 90%, and 100% ethanol for 5 minutes each. 15µl of Vectra-shield with fluorescence DAPI mounting medium (Vector, Vectashield) was

added to each slide and covered with a 22x50mm coverslip before sealing with a clear nail varnish.

5.2.1.4-Image capture and telomere length analysis

Images of interphase cells was acquired on a digital fluorescence microscope (Zeiss Axioskop 2) equipped with CCD camera (Photometrics) and Smart Capture software (Digital Scientific, Cambridge, UK) using fixed time exposure of 0.5 sec and magnification of 63x. IP lab software (Digital Scientific), (Figure 5.1) was used to analyse telomere fluorescence intensity per cell. The average signal was calculated as the total intensity of the telomeric signal utilizing the area under curve minus the background signal. The experiment was repeated at least twice and each time 100 cells were quantified for each sample.

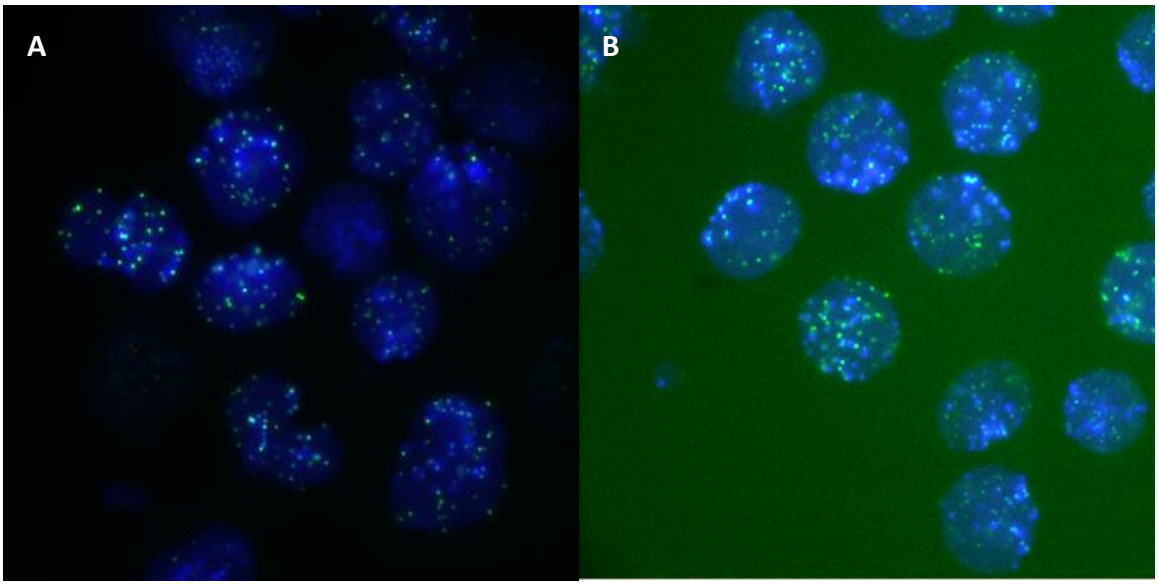

Figure 5.1-Representative images of **A)** LY-R (radio-resistant) and **B)** LY-S (radio-sensitive) interphase cells after hybridization with telomeric PNA oligonucleotides.

5.2.2-Telomere length determination by flow-FISH

The *in vitro* measurement of telomere length can be done via different high throughput techniques. One such technique is called flow-FISH, and is based on flow-cytometry. It works by utilizing a fluorescence tag hybridized to the telomeric repetitive sequence of $(C3TAA)_3$. A modified version of this method first described by Cabuy *et al.* (2004) was utilized in this work (Cabuy, Newton *et al.* 2004).

Cells were grown as described previously. Pellets containing $5x10^5$ cells were re-suspended and fixed in 1ml of 70% ethanol. To avoid cellular aggregation, fixative was added drop by drop under continuous shaking. Thereafter, the cells were incubated at 4°C overnight. All the centrifugations between the washing steps were performed at 0.8*rcf* for 5 minutes. The cell pellets were washed by adding 1ml of PBS, centrifuged, and then the supernatant was discarded carefully. 500µl of hybridization mixture containing 70% formamide, 10mM Tris-HCl pH 7.0, 1% BSA made in PBS, and 0.3µg/ml of fluorescein isothiocyanate (FITC) conjugated peptide nucleic acid (PNA) probe $(C3TAA)_3$ was added to the cell pellet and the mixture was heated at 80°C for 10 minutes in the dark to denature the DNA. The cells were left to hybridise for two hours in the dark at room temperature. Samples without the PNA telomeric probe were used as negative controls. After the hybridization step, pellets were spun down and supernatant was discarded carefully. Post-hybridization washes were carried out to ensure that excess and unbound probe was washed away, therefore reducing the background fluorescence. This was done by adding 500µl of wash solution containing 70% formamide, 10mM Tris buffer (pH 7), 0.1 % BSA and PBS to the cells. The pellet was suspended in the wash solution and the samples were centrifuged at 0.8*rcf* to collect cells and supernatants were discarded. A second wash was

done again twice using a 500µl of a solution containing PBS and 0.1% BSA; the cells were then centrifuged at 0.8*rcf*. A second incubation was done with propidium iodide (PI) (Sigma) to quantitatively assess the DNA content of cells. PI is a widely used fluorescence dye that binds directly to DNA by intercalating between the bases. In addition, PI binds to RNA therefore it is important to digest all RNA in the sample by treating it with RNaseA (Invitrogen). The cell pellet obtained above was re-suspended in a solution contained PBS, 0.1% BSA, 10µg/ml of RNase A, and 0.1µg/ml of PI. The tubes were then stored in the dark for one hour at 4°C. After incubation, the samples were centrifuged and supernatant was discarded. The tubes were kept on ice all prior to the measurement with the flow cytometer.

FACSCoulter EPICS XL (Becton Dickinson) was calibrated using flow-check fluorospheres (Beckman Coulter) to check laser alignment on all four channels; this step was performed before each measurement. The instrument was calibrated to measure the FITC telomeric signal on the FL1 channel, and the PI signal on FL3 channel. After calibration, cells were electronically gated for the G0/G1 phase of the cell cycle form the FL3 histogram window. The telomeric fluorescence intensity (TFI) of cells in the G0/G1 stage was recorded. In order to remove the background reading, TFI from the negative control cells was also measured and subtracted from the main sample reading. The experiment was carried out at least three times, and each time TFI readings from a minimum of 5,000 cells and a maximum of 20,000 cells were recorded (Figure 5.2).

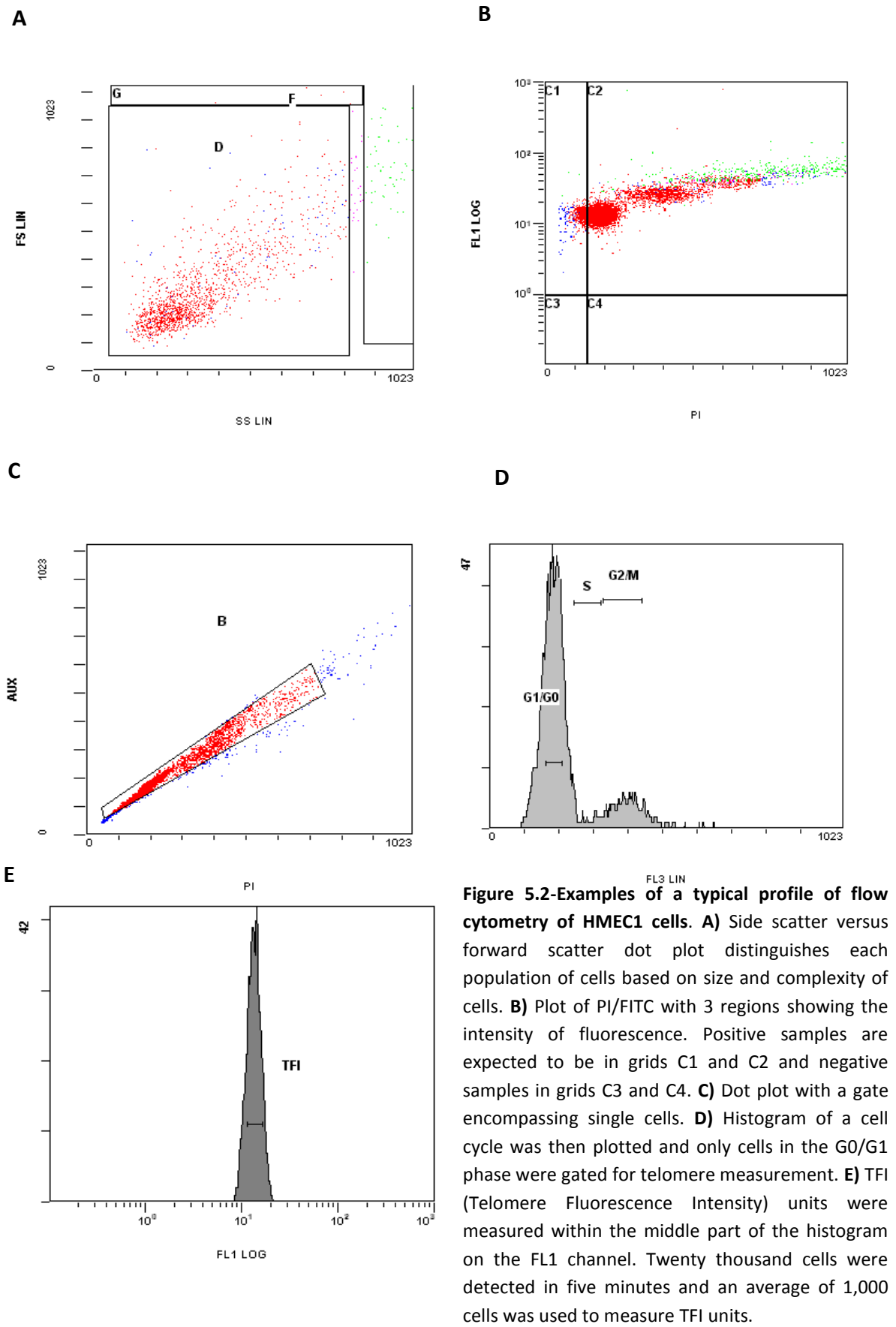

Figure 5.2-Examples of a typical profile of flow cytometry of HMEC1 cells. **A)** Side scatter versus forward scatter dot plot distinguishes each population of cells based on size and complexity of cells. **B)** Plot of PI/FITC with 3 regions showing the intensity of fluorescence. Positive samples are expected to be in grids C1 and C2 and negative samples in grids C3 and C4. **C)** Dot plot with a gate encompassing single cells. **D)** Histogram of a cell cycle was then plotted and only cells in the G0/G1 phase were gated for telomere measurement. **E)** TFI (Telomere Fluorescence Intensity) units were measured within the middle part of the histogram on the FL1 channel. Twenty thousand cells were detected in five minutes and an average of 1,000 cells was used to measure TFI units.

5.2.3-Terminal restriction fragment (TRF) telomere length analysis

5.2.3.1-Overview

Mammalian telomeric hexanucleotide repeats (T2AG3) and some sub-telomeric DNA sequences do not include restriction sites. Therefore, genomic DNA can be digested with restriction enzymes such as *Hinf I* and *Rsa I* to cut genomic DNA into small fragments, while the terminal chromosome fragment remains intact. Digested DNA fragments, including an undisclosed length of sub-telomeric DNA and the terminal section of *TTAGGG* repeats is called the terminal restriction fragment (TRF). Agarose gel electrophoresis separates the average size of the TRF which can be measured by Southern blotting. It includes hybridisation to a digoxigenin (DIG)-labelled probe precise for hexameric repeats and incubation with a specific DIG-antibody covalently linked to alkaline phosphate (Roche). Alkaline phosphate (AP) is used to visualize the immobilized telomere probe metabolising CDP-*Star*, a highly sensitive chemiluminescence substrate. During DNA replication, telomeric DNA is eroded which appears as a smear when analysed, showing the characteristically heterogeneous telomere population. This method is commonly used to determine difference in telomere length.

5.2.3.2-TRF Telomere Length Assay

$5x10^5$ cells were harvested and washed with sterile PBS, pelleted and re-suspended in fresh PBS. Genomic DNA from treated 21NT cell was extracted as described in Section 2.7. TRF length measurement was performed utilizing the Telomere Length Assay (Roche Diagnosis). Approximately 3µg of DNA was digested for 2 hours at 37°C using a mixture of restriction enzymes *Hinf I* and *Rsa I* in a concentration of 20U/µl for each enzyme. The reaction was stopped by adding 5µl of gel electrophoresis loading buffer. The digested genomic DNA was loaded on to 0.8% 1x TAE buffer agarose gel. The same amount of DNA from each sample was carefully loaded in every lane. A DIG labelled molecular weight marker was loaded on either side of the respective samples. The gel was run at 5V/cm in 1x TAE buffer until the bromophenol blue tracking marker reached about 10 centimetres from the starting wells (total run 2-4 hours depending on tank size) (Figure 5.3). The gel was then left for 10 minutes in 0.25M HCI until the bromophenol blue stain changed colour to yellow. Then the gel was rinsed twice with sterile water and was denatured for 30 minutes in 0.5M NaOH, 1.5M NaCl followed by two more rinses. The gel was then neutralized for 30 minutes in 0.5M Tris-HCI, 3M NaCl (pH 7.5). All incubation steps were performed at room temperature with gentle agitation. Southern blotting of the digested DNA was done by capillary transfer using 20x Saline-Sodium Citrate (SSC) onto Hybond N^+ membranes (Amersham) overnight.

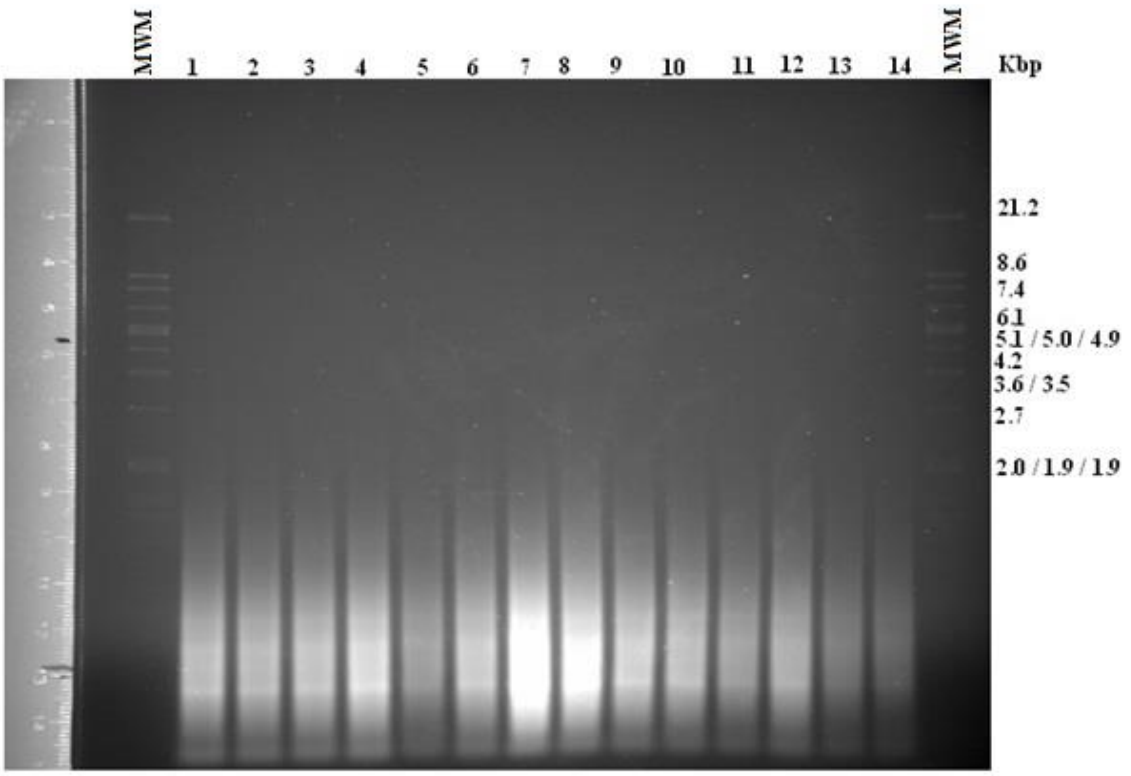

Figure 5.3-Image of a typical agarose gel after electrophoresis showing smears of gDNA following digestion with restriction enzymes. The gel was then southern blotted and hybridised to the telo-*TTAGGG* probe. Representative result of TRF analysis for telomere length measurement in 21NT treated with 5-aza-CdR and TSA at different time points and control (HMEC1) cells using telomere length Assay. The lanes on the left and right sides show the molecular size marker. Lane1) Untreated, Lane2) DMSO 72hrs, Lane3) 5-aza-CdR 72hrs, Lane4) 5-aza-CdR/TSA 72hrs, Lane5) 5-aza-CdR 3weeks, Lane6) 5-aza-CdR/TSA 3weeks, Lane7) 5-aza-CdR 6weeks, Lane8) 5-aza-CdR/TSA 6weeks, Lane9) DMSO, Lane10) 5-aza-CdR 2 months, Lane11) 5-aza-CdR/TSA 2 months, Lane 12) HMEC1 p5, Lane13) HMEC1 P20, Lane14) The positive control DNA from immortal cell line (Telomere length Assay) respectively. The genomic DNA was digested with *Hinf I* and *Rsa I* enzymes and hybridized with a telomere-specific, digoxigenin (DIG)-labelled hybridization probe. The size markers are indicated on the right.

5.2.3.3-Southern hybridization

After Southern transfer, the membrane was washed in 2x SSC. Pre-hybridization was carried out by adding 18ml of pre-warmed DIG Easy Hyb Granules solution to the membrane for 30 minutes at 42°C with gentle agitation. Before hybridization, the telomere probe was added to the pre-warmed DIG-Easy Hyb Granules solution. The membrane was then hybridized for 3 hours at 42°C in a mixture of DIG-Easy Hyb and Telomere probe (Roche) with gentle agitation. Low stringency washes were carried out by discarding the hybridization solution and washing the membrane two times for 5 minutes in 2x SSC, 0.1% SDS at room temperature. High stringency washes were done twice for 20 minutes at 50°C in pre-warmed 0.2x SSC, 0.1% SDS with gentle agitation. Then, the membrane was washed with 100ml of washing buffer (provided by the kit). In order to pre-block the membrane, 100ml 1x blocking solution was added to the membrane and incubated for 30 minutes at room temperature with gentle agitation. The membrane was then incubated in anti-DIG-AP solution (Roche) for 30 minutes at room temperature with gentle agitation and subsequently washed twice in 100ml of washing buffer. The membrane was then incubated for 5 minutes at room temperature with a detection buffer (Roche), followed by the addition of the substrate solution (CDP-*Star*) for 5 minutes before exposure to an X-ray film (Amersham Hyperfilm™ ECL) for 5 minutes at room temperature.

5.2.3.4-Densitometry

The average TRF value was calculated by evaluating the telomeric signal (smear) relative to molecular weight standard supplied with the Roche Kit. The exposed X-ray film was scanned with densitometer (a desk scanner G2710, HP) and using ImageQuant software 5.2 (Amersham Biosciences, USA). It showed telomere lengths as smears ranging from 2 to

more than 21 kb. Each sample lane of the scanned image was overlaid with a grid. Then, the telomeric signal in each lane was quantified as a grid object, described as a single column with 30 rows (Figure 5.5). The resolution of the TRF length calculation was determined by the highest of the individual squares of the grid. This grid was placed over the lanes corresponding to the molecular size markers and telomere lane. Afterwards, the data was transferred to a spread-sheet (Microsoft) to quantitate integrate volume. Interpolating molecular sizes for each row were determined by plotting the row number 1-30 against the molecular size ladder and fitting a best (least squares) line. The average labelled TRF length in each lane was calculated in Excel as the mean of the optical density above background (Figure 5.4).

A

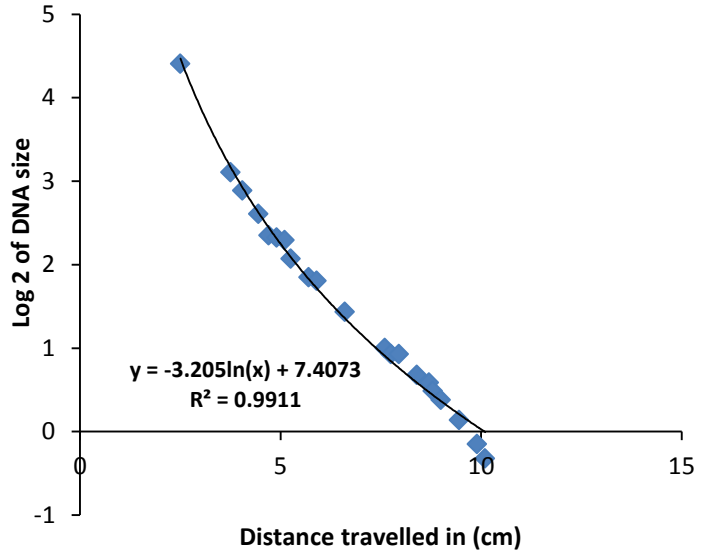

B

Ladder kb	Log2 MW
21.2	4.405992
8.6	3.104337
7.4	2.887525
6.1	2.608809
5.1	2.350497
5.0	2.321928
4.9	2.292782
4.2	2.070389
3.6	1.847997
3.5	1.807355
2.7	1.432959
2.0	1.0
1.9	0.925999
1.9	0.925999
1.6	0.678072
1.5	0.584963
1.4	0.485427
1.3	0.378512
1.1	0.137504
0.9	-0.152
0.8	-0.32193

Figure 5.4-Southern blot analysis of telomere length in 21NT treated cells and controls (HMECs). A) Standard curve used to calculate absolute telomere length measured by Southern blots of TRFs. Y-axis represents log2 of DNA ladder and X-axis represents distance travelled in gel. Correlation coefficient calculated is 0.991. **B)** Numbers showing converted log2 values of DNA ladder size in kb used in the analysis.

The mean TRF length was defined according to the following formula: TRF = Σ (OD_i)/Σ (OD_i/L_i). For each square lane that contains DNA, OD_i is the chemiluminescent signal and L_i is the lengths of the TRF at position i on the gel image. Then the mean TRF length was calculated using the above formula.

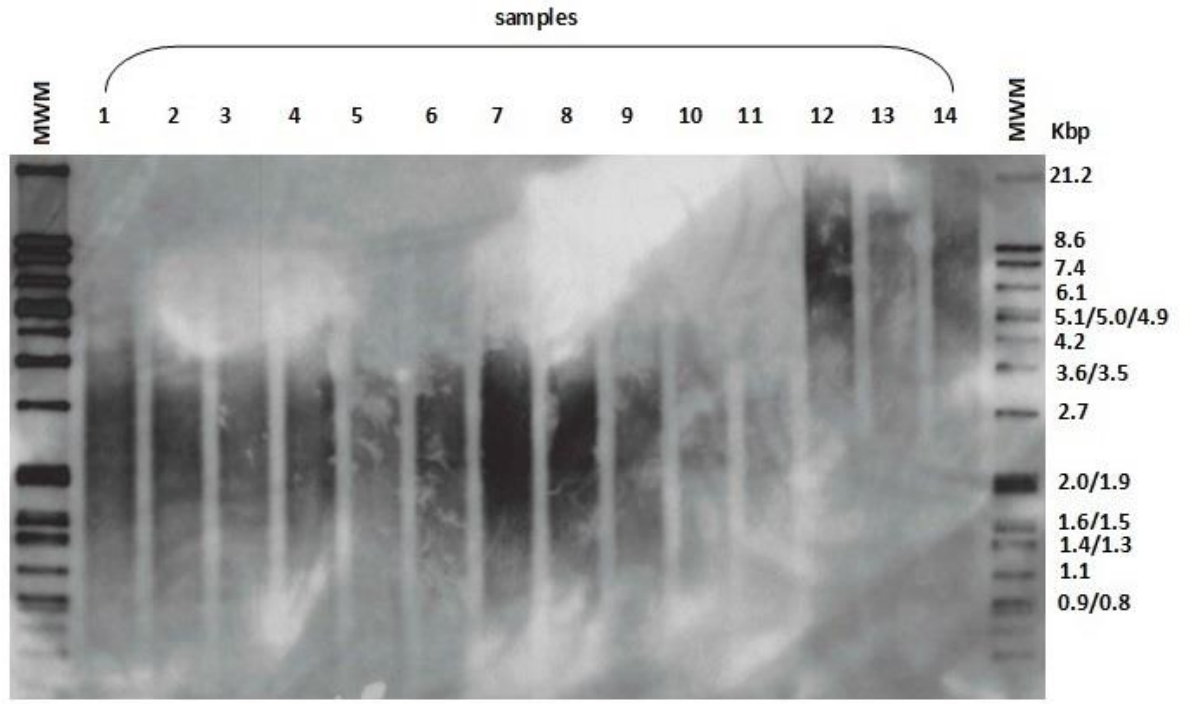

Figure 5.5-Chemiluminescent detection of TRFs. The lane on the both sides shows the molecular size marker. Lane 1) Untreated, Lane 2) DMSO-treated 72hrs, Lane 3) 5-aza-CdR 72hrs, Lane 4) 5-aza-CdR/TSA 72hrs, Lane 5) 5-aza-CdR 3weeks, Lane 6) 5-aza-CdR/TSA 3weeks, Lane 7) 5-aza-CdR 6weeks, Lane 8) 5-aza-CdR/TSA 6weeks, Lane 9) DMSO-treated, Lane 10) 5-aza-CdR 2 months, Lane 11) 5-aza-CdR/TSA 2 month, Lane 12) HMEC1 p5, Lane 13) HMEC1 P20, Lane 14) The positive control DNA from immortal cell line (Telomere length Assay) respectively. Gel profiles were read in a densitometer and gained in a grid and data were analysed in Excel spread sheet. Telomeric sizes are then calculated as explained.

5.2.4-Telomere length measurement by quantitative real time PCR

In order to determine telomere length, a real-time PCR technique was used. The relative telomere length was compared with that of a single copy gene. A single copy gene (SCG) control was used for amplification of each sample, and to determine genome copies per sample. We used 36B4 as a single copy gene which encodes the acidic ribosomal phosphoprotein PO (O'Callaghan and Fenech 2011). Genomic DNA was extracted from 21NT treated cells (see Section 4.2.3) and the normal human mammary epithelial cell strain (HMEC1) using the Wizard™ Genomic DNA Kit as described in Section 2.7 (Chapter II). Telomere and single copy gene master mixes were prepared separately. Briefly, two q-PCR master mixes were prepared, one with the telomere primer pair and the other with the single copy gene primer pair (36B4). 10µl of 2x Power SYBER® Green PCR Master Mix (Applied Biosystems); 2µM forward primer (Telomere-F or 36B4-F) (Sigma, Table 5.2); 2µM reverse primer (Telomere-R or 36B4-R) (Sigma, Table 5.2), 4µl of 5ng/µl DNA sample; and nuclease free water up to 20µl were added to the templates.

Telomere and single copy gene q-PCRs were performed in separate 96-well plates. 20µl of telomere master mix was added to each sample well containing 5ng/µl DNA samples, standard well (2µl of the telomere standard) and no template control (NTC) of the first plate. The second plate was 20µl of single copy gene master mix containing 5ng/µl DNA samples, standard well (2µl of the single copy gene standard) and no template control (NTC). A telomere standard curve was established by serial dilutions of the telomere standard (1018400 kb through to 10184 kb dilution) and was used to measure the content of telomeric sequence per sample in kb (Figure 5.6).

A single copy gene (36B4) was used as a control for amplification of every sample performed and to determine genome copies per sample. A single copy gene standard curve was generated by performing serial dilutions of the 36B4 standard (6125000 kb through to 6.125 kb dilution). Plasmid DNA (*pBR322*) was also added to each standard to maintain a constant 20ng of total DNA per reaction tube. After setting up the reactions, the plate was sealed with a real time plate sealer (MicroAmp, Applied Biosystems) and then centrifuged for one minute at 1000*rcf* to bring all the contents to the bottom of the well. Real-time PCR runs were performed in triplicate for each of the DNA pools. Each experiment was performed at least three times ensuring the reproducibility and accuracy of the results. The real time PCR reactions were run using the following reaction conditions for both telomere and 36B4 amplifications followed by the construction of a dissociation (or melt) curve:

- 95.0°C for 10 minutes (DNA denaturing step)
- 95.0°C for 15 seconds (DNA denaturing step) } 40 Cycles
- 60.0°C for 1 minute (DNA Annealing step)
- 95.0°C for 15 seconds
- 60.0°C for 15 seconds } Dissociation Step
- 95.0°C for 15 seconds

The values (kb/reaction for telomere and genome copies for single copy gene) were exported to an Excel file and used to calculate total telomere length in kb per human diploid genome. The telomere kb length per reaction value was then divided by diploid genome copy number to give a total telomeric length in kb per human diploid genome.

Table 5.2-Oligomers used for telomere length assay in 21NT treated and normal cells (O'Callaghan and Fenech 2011)

Oligomer Name	Oligomere Sequence (5´ ⟶ 3´)	Amplicon size (bP)
Telomere Standard (Human/Rodent)	$(TTAGGG)_{14}$	84
36B4 Standard (Human)	CAGCAAGTGGGAAGGTGTAATCCGTCTCCACAGACAAGGCCA GGACTCGTTTGTACCCGTTGATGATAGAATGGG	75
Telo-F (Human/Rodent)	CGGTTTGTTTGGGTTTGGGTTTGGGTTTGGGTTTGGGTT	>76
Telo-R (Human/Rodent)	GGCTTGCCTTACCCTTACCCTTACCCTTACCCTTACCCT	>76
36B4-F (Human)	CAGCAAGTGGGAAGGTGTAATCC	75
36B4-R(Human)	CCCATTCTATCATCAACGGGTACAA	75

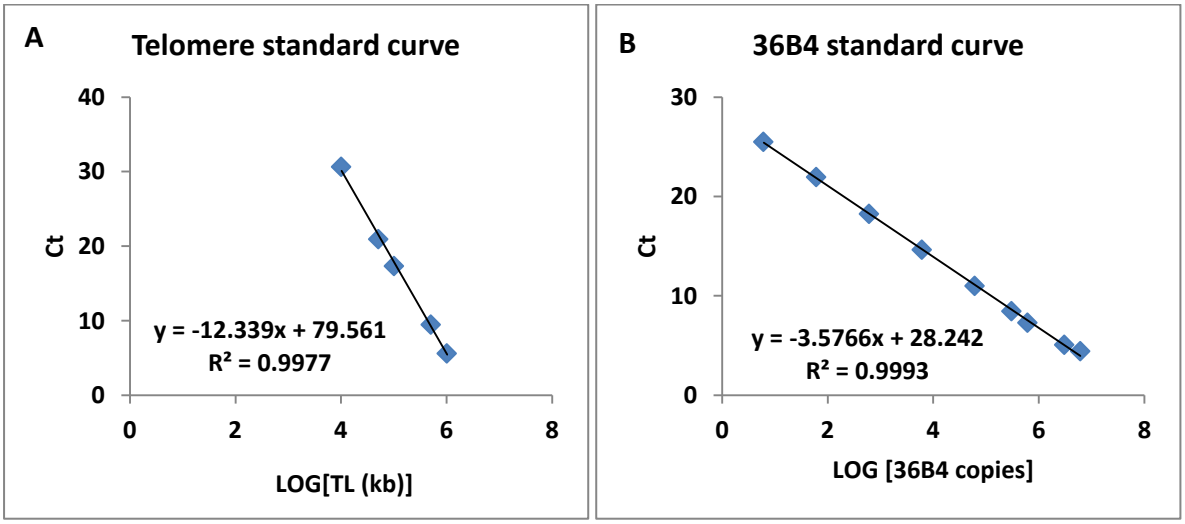

Figure 5.6-Standard curve used to calculate absolute telomere length. A) Standard curve for calculating length of telomere sequence per sample: X-axis demonstrates amount of telomere sequence in kb per reaction with correlation coefficient of 0.997. **B)** Standard curve for calculating genome copies using 36B4 copy number: correlation coefficient was 0.999.

5.3-Results

5.3.1-Telomere length analysis by Interphase Quantitative Fluorescent *in situ* Hybridization in 21NT breast cancer cells

The breast cancer epithelial cell line, 21NT, treated with the demethylating agent, 5-aza-CdR and the histone deacetylation inhibitor, TSA, showed up-regulation of expression of Shelterin genes (described in Chapter IV). The aim of the work described in this chapter was to analyse telomere lengths in 21NT cells before and after treatment with demethylating agents. The reasoning behind this was to analyse if up-regulation of some of the Shelterin genes such as *POT1* and *TPP1* has an effect on average telomere length. As the first method of telomere length measurement we used iQ-FISH. The average length of the telomeres in interphase stage was measured by Smart Capture software.

The average telomere fluorescence intensities (TFI) of 21NT cells treated with 5-aza-CdR and a combination treatment with 5-aza-CdR and TSA at short-term (72 hours) and long-term (3 weeks, 6 weeks and 2 months plus retreated for 72 hours) was measured and compared with those of normal human epithelial cell strain (HMEC1), untreated 21NT and DMSO-treated (the term DMSO treated control refers to 21NT cells that received the solvent DMSO-treated at final concentration of 0.02%) controls. Two mouse lymphoma LY-R (radio-resistant) and LY-S (radio-sensitive) cells were also used as calibration standards with known telomere lengths of 49kb and 7kb respectively (McIlrath, Bouffler *et al.* 2001). A total 100 interphase cells per cell line were analysed by iQ-FISH to examine the telomere fluorescence intensity for each cell line. Figure 5.7 shows different telomere fluorescence intensity signals in DMSO-treated control, treated 21NT cells and HMEC1 cell strains.

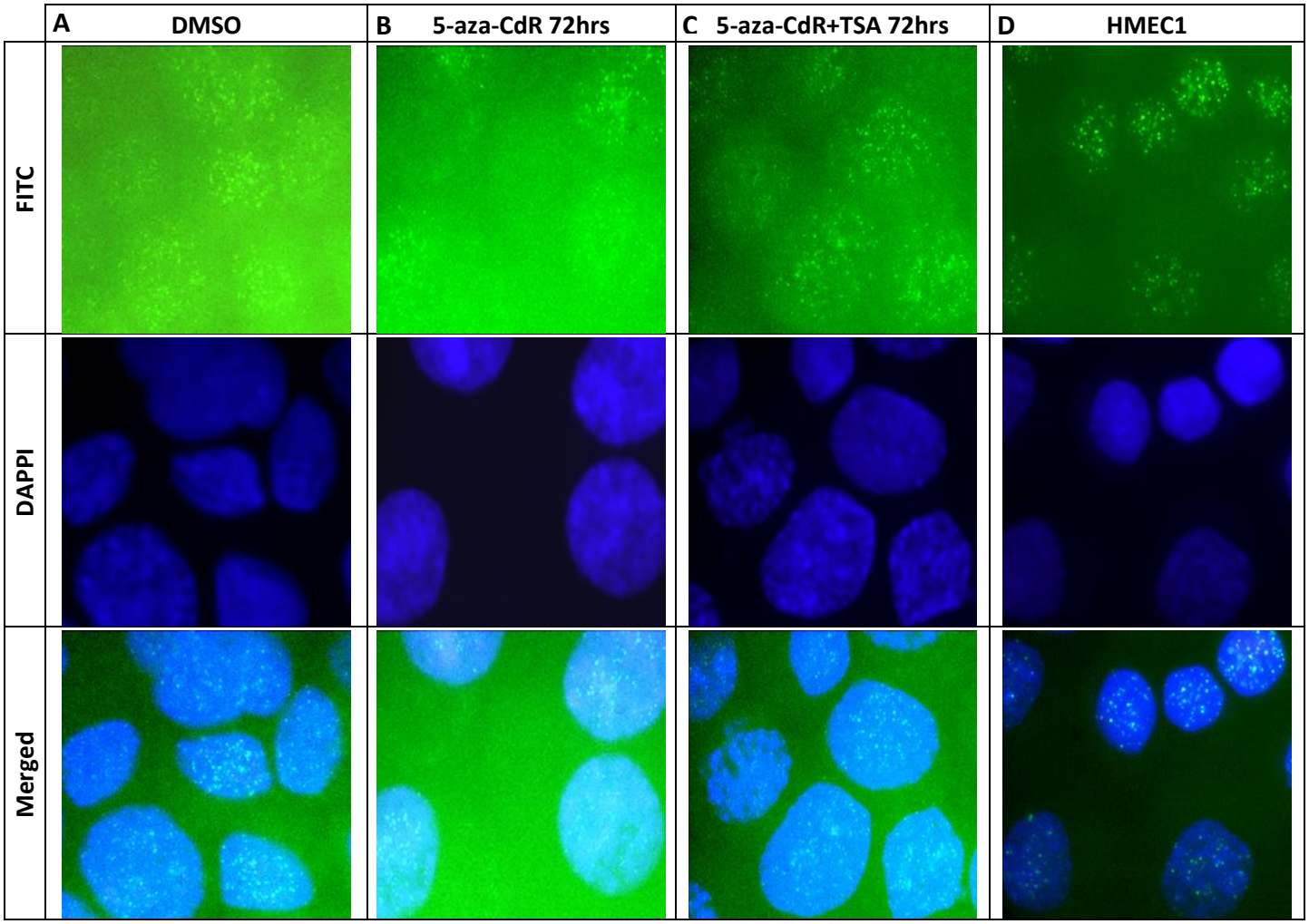

Figure 5.7-Digital image of iQ-FISH. A) DMSO-treated, **B and C)** 21NT treated with 5-aza-CdR and TSA for 72 hours, **D)** Normal mammary epithelial cell strain (HMEC1). Telomeres were labelled by PNA-FITC (green) and nuclei were labelled by DAPI (blue). As shown, different samples give different signals and clear signals have been observed in 5-aza-CdR and TSA treatment compared with DMSO-treated control. Magnifications of the images are x65.

Following treatment of the 21NT cells with demethylating agents significantly higher total telomere fluorescence intensity was observed in treated 21NT cells compared with DMSO-treated control (*P*<0.001) (Figure 5.8). The analysis revealed that 21NT treated cells with 5-

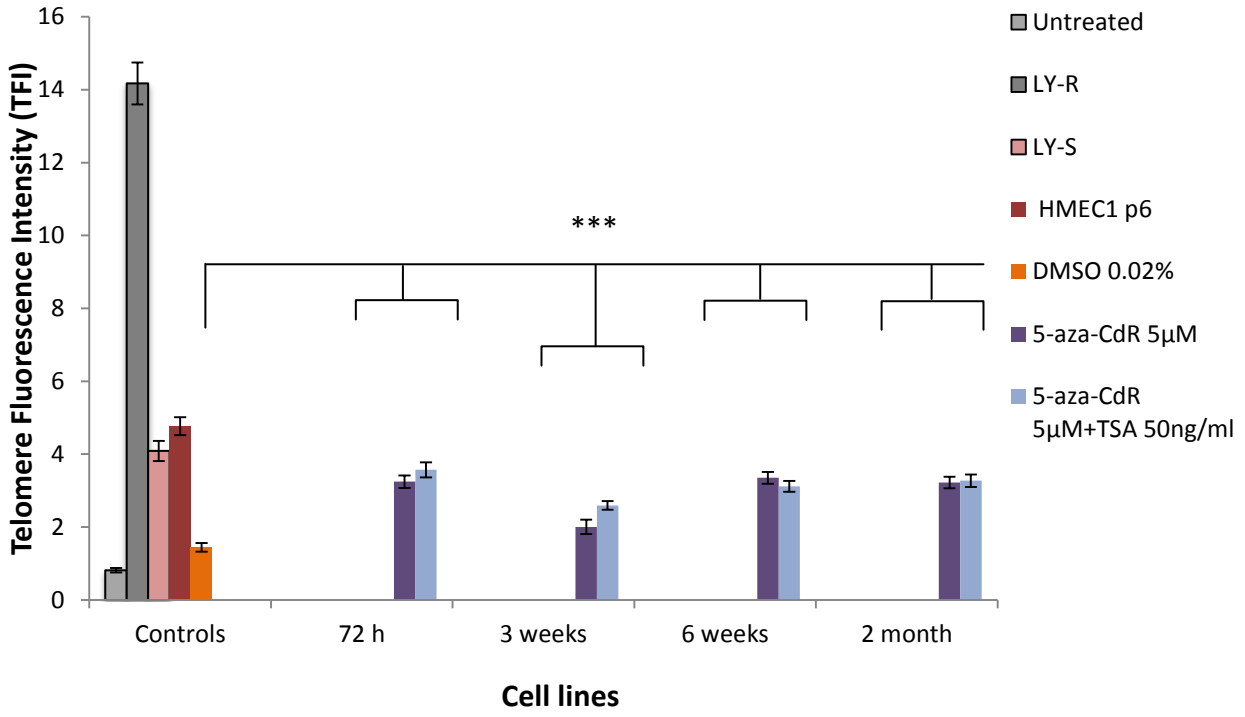

Figure 5.8-Telomere length measurement by iQ-FISH. Comparison of the mean TFI in 21NT treated and control cell lines. The telomere fluorescence intensity is shown in normal human epithelial cell strain (HMEC), LY-R, LY-S, un-treated 21NT, DMSO-treated and 21NT treated with 5-aza-CdR and a combination treatment with 5-aza-CdR and TSA at 72 hrs, 3 weeks, 6 weeks and 2 months + retreatment for 72 hours. The analysis was performed using untreated 21NT with the lowest TFI compared to 21NT treated at different time points and controls; HMEC1 p6, LY-R, and LY-S. The experiment was repeated at least twice and each time 100 cells were quantified for each sample. Error bars represent SEM. Asterisk indicates difference between DMSO-treated cells and the 21NT treated cell lines (***P<0.001).

aza-CdR and a combination treatment with 5-aza-CdR and TSA at different time points, showed approximately a 2-fold increase in telomere fluorescence intensity compared with DMSO-treated and untreated 21NT cells (*P*<0.001) (Figure 5.8). However, 3 weeks treatment showed shorter TFI than the 72 hours, 6 weeks and two month treatment.

5.3.2-Telomere length analysis by flow-FISH in 21NT treated and control cell lines

Results obtained from iQ-FISH showed a significant increase in telomere fluorescence intensity when the human breast cancer cell line 21NT was treated with 5-aza-CdR and TSA at different time points. To confirm these results, we set out to measure the observed telomere elongation using a high-throuput flow cytometry method. We have therefore measured the telomere length intensity by flow-FISH in all of 21NT treated, untreated, DMSO-treated and HMEC1 cells. Telomere fluorescence intensity was measured in the G0/G1 phase of the cell cycle to make sure data were consistent with those obtained using iQ-FISH. Flow cytometry provides the flexibility to gate cells in different cell cycle (Figure 5.9). Since DNA content is doubled in S-phase, the telomere length measurement is gated in G0/G1. In comparing both methods we sought to confirm that the increase in telomere length observed when cells were treated with 5-aza-CdR and TSA was a reliable result.

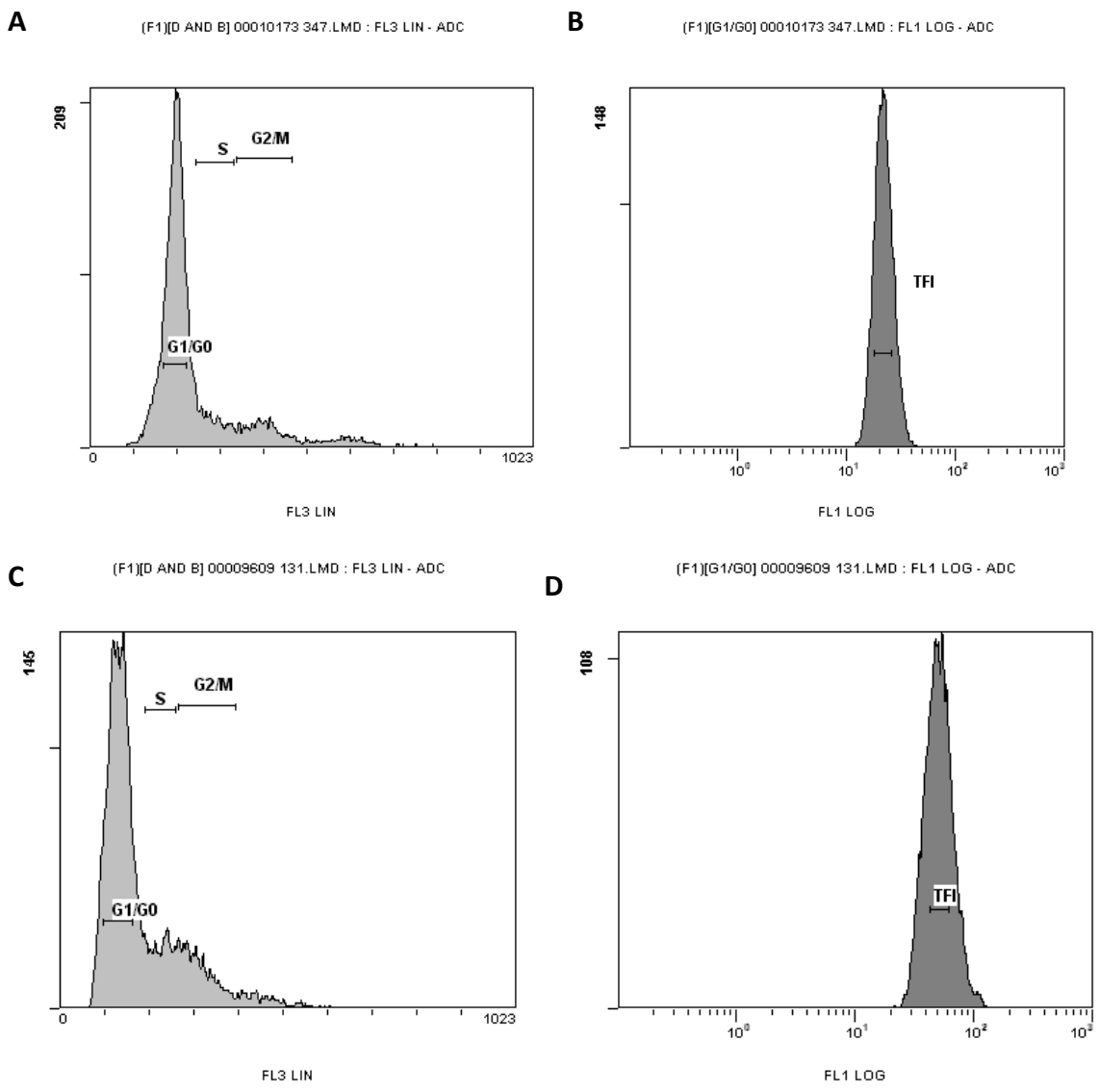

Figure 5.9-Example of cell cycle and actual TFI in different cell lines. A and **B)** represent the histogram window of the cell cycle of DMSO-treated control and TFI, **C** and **D)** represent the cell cycle of 21NT treated with 5-aza-CdR for 72 hours and TFI.

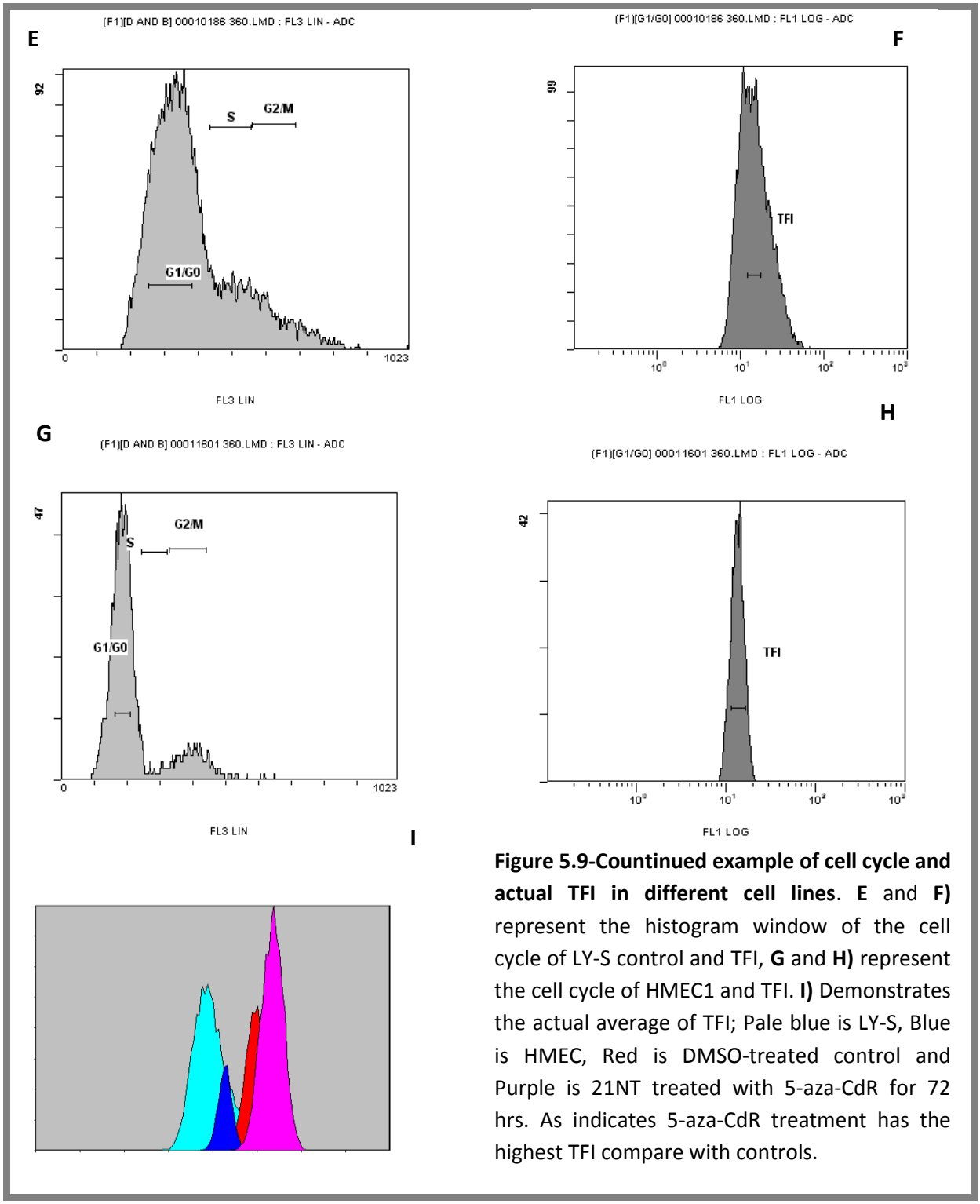

Figure 5.9-Countinued example of cell cycle and actual TFI in different cell lines. **E** and **F)** represent the histogram window of the cell cycle of LY-S control and TFI, **G** and **H)** represent the cell cycle of HMEC1 and TFI. **I)** Demonstrates the actual average of TFI; Pale blue is LY-S, Blue is HMEC, Red is DMSO-treated control and Purple is 21NT treated with 5-aza-CdR for 72 hrs. As indicates 5-aza-CdR treatment has the highest TFI compare with controls.

Data generated from flow-FISH experiments are shown in Figure 5.10. Interestingly, telomere fluorescence intensity of 21NT treated cells significantly increased after 72 hours, and 3 weeks when compared with DMSO-treated control (**P<0.01,***P<0.001

respectively). However, these trends did not reach statistical significance after 6 weeks treatment. No higher impact was observed after 2 months post treatment of 21NT cells compared with DMSO-treated control (Figure 5.10).

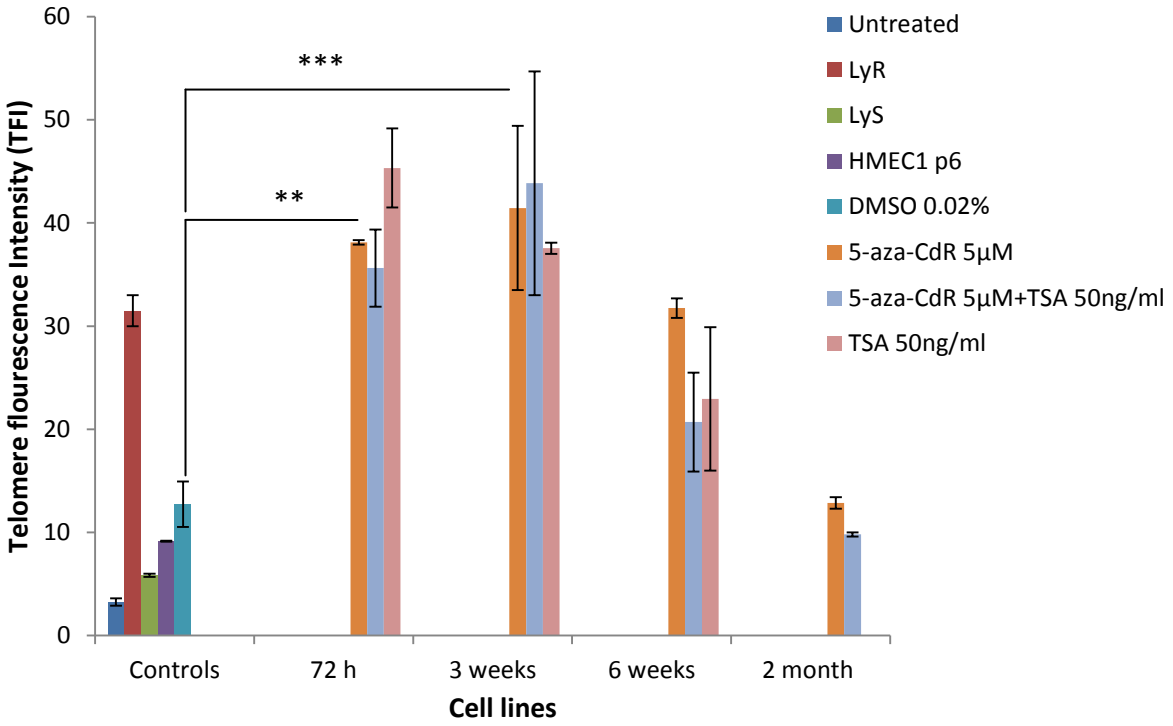

Figure 5.10-Telomere length measurement by flow-FISH. Comparison of the mean Telomere Fluorescence Intensity (TFI) in 21NT treated and control cell lines. The telomere fluorescence intensity is shown in HMEC1, LY-R, LY-S, untreated 21NT (controls), DMSO-treated and 21NT treated with 5-aza-CdR and a combination treatment with 5-aza-CdR and TSA at 72 hrs, 7 days, 3 weeks and 2 months plus retreatment for 72 hours. Error bars represent SEM. Asterisk indicates difference between DMSO-treated cells and the 21NT treated cell lines (**P<0.01, ***P<0.001).

Based on the results obtained from iQ-FISH and flow-FISH methods used for telomere length estimation, flow-FISH proved to be least accurate in comparison with iQ-FISH. Our data revealed that there was low correlation between these two methods (Table 5.3). Although, the increases telomere lengths in treated samples were observed using both

methods, this increase was not expected from untreated samples. Therefore, there are some advantages and disadvantages with each of the two methods that may influence the results. For instance, in the flow-FISH technique, cell clumping, crude experimental processor and fixation method might affect the results (Derradji, Bekaert *et al.* 2005). Furthermore, with this method, it seems that the probe cannot bind properly to the samples with pellet clumping which can influence the accuracy of the telomere fluorescence intensity. Flow-FISH and iQ-FISH provide the values of fluorescence intensity per cells. However, with both techniques it is not possible to measure the telomere fluorescence intensity signals corresponding to each individual chromosome end.

Table 5.3-Comparison of flow-FISH and iQ-FISH results. TFI values represent the telomere fluorescence intensity; *P values indicate the difference between all the treated and untreated samples. HMEC1, LY-R and LY-S cells were used as a positive control.

Samples	TFI (flow-FISH)	T-test (flow-FISH)	TFI (iQ-FISH)	T-test (iQ-FISH)
Untreated	3.25		0.81	
DMSO-treated	12.75		1.44	
HMEC1 p6	9.15		4.7	
LY-R	31.5		3.9	
LY-S	5.85		2.0	
5-aza-CdR 72hrs	**38.12	0.017	3.24	***1.8E-15
5-aza-CdR/TSA 72hrs	35.62	0.269744	3.57	***1.2E-15
5-aza-CdR 3weeks	***41.45	0.001801	2.0	***0.001
5-aza-CdR/TSA 3weeks	43.85	0.216611	2.59	***7.6E-11
5-aza-CdR 6weeks	31.75	0.174331	3.34	***9.5E-18
5-aza-CdR/TSA 6weeks	20.7	0.363277	3.11	***8.6E-16
5-aza-CdR 2months	12.85	0.61155	3.22	***3.1E-16
5-aza-CdR/TSA 2months	9.8	0.025613	3.27	***1.4E-15

5.3.3-Telomere length analysis by terminal restriction fragment (TRF) in 21NT treated and control cell lines

The initial observation of increased telomere length in treated 21NT cells was unexpected but in the line with our hypothesis. Could up-regulation of some of the Shelterin genes stabilise telomere lengths and even elongate them in the presence of telomerase enzyme. In order to be more confident of the initial data, we set out to confirm the above findings using other methods of telomere length measurement (Terminal Restriction Fragment, TRF).

The result from the analysis of the 13 samples in Figure 5.11 is shown in Table 5.4. LY-R and LY-S samples were not considered as the enzymes used in the assay do not cut the mouse DNA samples. The data showed that there was the most increase in telomere length for 21NT cells treated with 5-aza-CdR at 3 weeks and the combination with 5-aza-CdR and TSA treatment for 72 hours (as compared with their respective DMSO-treated and untreated 21NT controls). Samples from short-term (72 hours) treatment with 5-aza-CdR yielded telomere length approximately the same size as those with long-term treatment with combination of 5-aza-CdR and TSA (3 weeks) treatment. However, only minimal differences were observed in 6 weeks and 2 months treatment groups. Therefore, it seems that the drugs lose their effectiveness over long term treatment period (2 months) (Figure 5.11). The telomere length in the positive DNA control from an immortal cell line was 10.18 kb which was consistent with the size recommended in the kit (Roche). A 1.13 kb difference in telomere size was observed in HMEC1 controls at different passages. It could be hypothesized that telomere shortening is correlated with increasing the passage number.

Table 5.4-Changes in telomere length (kb) determined by TRF analysis in control and treated samples

Samples	Telomere length (kb)
HMEC1 p5	8.95
HMEC1 p20	7.82
Positive control DNA	10.18
untreated 21NT	1.45
DMSO-treated	1.35
5-aza-CdR 72hrs	2.33
5-aza-CdR/TSA 72hrs	3.30
5-aza-CdR 3 weeks	4.56
5-aza-CdR/TSA 3 weeks	2.45
5-aza-CdR 6 weeks	2.36
5-aza-CdR/TSA 6 weeks	2.32
5-aza-CdR 2 months / retreat	1.94
5-aza-CdR +TSA 2 months /retreat	1.55

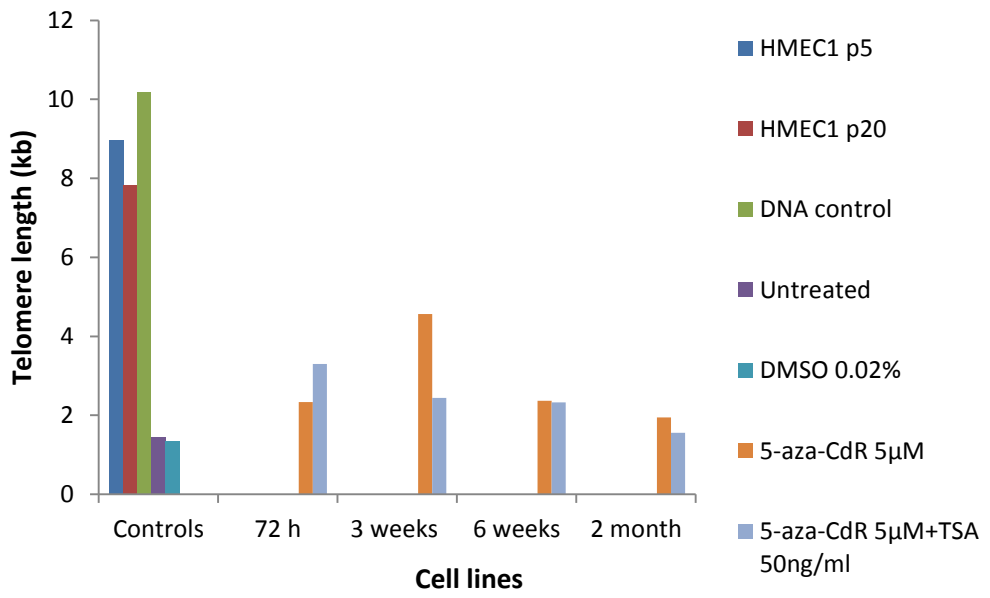

Figure 5.11-Telomere length measurement by telomere restriction fragment length (TRF). Comparison of the telomere length in 21NT treated and control cell lines. The telomere length is shown in normal human epithelial cell strain (HMEC1 p5 and P20), the positive control DNA from immortal cell line (Roche), untreated 21NT cells , DMSO-treated, and 21NT treated with 5-aza-CdR and a combination treatment with 5-aza-CdR and TSA at 72hrs, 3 weeks, 6 weeks and 2 months plus retreatment for 72 hours. The analysis was performed with untreated 21NT cells with the lowest telomere length (kb) compared with 21NT treated cells at different time points and to the adjacent controls; HMEC1 p5, HMEC1 p20, and positive control DNA.

5.3.4-Telomere length analysis by quantitative real time PCR in 21NT treated and control cells

In order to confirm results obtained from TRF, iQ-FISH, and flow-FISH, the q-PCR technique was also performed. The average telomere length was measured by q-PCR in treated 21NT cells at different time points, untreated 21NT cells, DMSO-treated and HMEC1 controls. As shown in Figure 5.12, HMEC1 showed a mean telomere lengths of around 7.3 kb. In comparison with untreated and DMSO-treated controls, the short-term (72 hrs) and 3 weeks treatment of 21NT cells with 5-aza-CdR showed increase telomere lengths ranging from 4.5 kb to 4.7 kb. The average telomere length in untreated 21NT cells was approximately 2.5 kb which was consistent with published results (Cuthbert, Bond *et al.* 1999). The mean telomere length of the combination treatment of 21NT cells with 5-aza-CdR and TSA for 72 hours and 3 weeks had a significant telomere length increase of about 3.4 kb and 3.7 kb, respectively ($P<0.05$). However, no higher impact was observed with 6 weeks and 2 month treatment of 21NT cells with 5-aza-CdR and 5-aza-CdR/TSA in comparison with 72 hours and 3 weeks treatment (Figure 5.12).

Comparing the results obtained using TRF showed that 21NT treated cells had the highest increase in telomere length at 3 weeks of treatment with 5-aza-CdR (~4.56 kb) which was similar to the q-PCR result (~4.61kb) described earlier in this chapter (Figures 5.11 and 5.12).

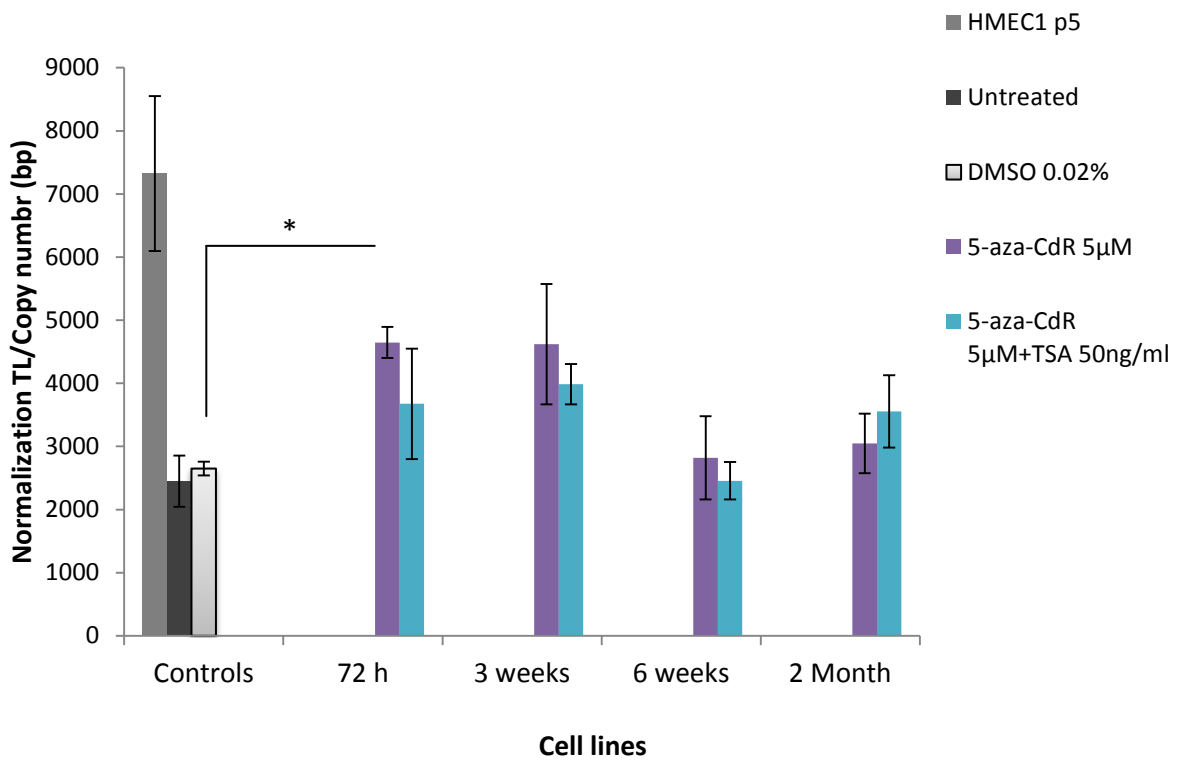

Figure 5.12-Telomere length measurement by q-PCR. Comparison of the telomere length in 21NT treated and control cell lines. The telomere length is shown in the normal human epithelial cell line (HMEC1 p5), untreated 21NT , DMSO-treated, and 21NT treated with 5-aza-CdR and a combination treatment with 5-aza-CdR and TSA at 72 hrs, 3 weeks, 6 weeks and 2 months plus retreatment for 72 hours. The analysis was performed with untreated 21NT and DMSO-treated with the lowest telomere length (kb) compared with 21NT treated at different time points and to the adjacent controls; HMEC p5, untreated 21NT and DMSO-treated controls. Error bars represent SEM. Asterisk indicates difference between DMSO-treated cells and 21NT treated cell lines (*P<0.05).

Results from using the q-PCR and TRF techniques for telomere length measurement were approximately similar and showing an increase in telomere length (Table 5.5). However, there are some differences between two methods. Like q-PCR, the TRF method was performed using genomic DNA to measure telomere length. However, unlike with q-PCR, the TRF assay requires larger amounts of DNA. A significant drawback of the TRF method versus the q-PCR analysis is the fact that TRF estimates the length of telomeric

sequences that also contain subtelomeric repeats. These can vary in length based on the last restriction site at a given chromosome arm. Therefore increasing the TRFs heterogeneity influences the length of subtelomeric repeats and this prevents detection of the true length of telomere repeats (Vera and Blasco 2012). Previous findings by Steinert *et al.* (2004) showed that the mean length of subtelomeric portions is about 2 to 4 kb of sequence that is resistant to enzymatic digestion (Steinert, Shay *et al.* 2004). Unlike q-PCR and TRF methods, there was a considerable discrepancy between flow-FISH and iQFISH. Consequently, these two methods seem to be not as reliable and accurate as q-PCR and TRF. However, it appears that TRF and q-PCR techniques have both their benefits and disadvantages; it seems that molecular analyses in comparison with cytogenetic techniques are more quantitative and can measure changes in telomere length with better accuracy. The q-PCR method, in comparison with all the other methods used here, appears to be most accurate and reliable technique.

Table 5.5-Comparison of TRF and q-PCR results. This table represents the differences in telomere length measurements by TRF and q-PCR methods.

Samples	TRF (kb)	q-PCR (kb)
Untreated	1.45	2.44
DMSO-treated	1.35	2.64
HMEC1 p5	8.95	7.32
5-aza-CdR 72hrs	2.33	4.64
5-aza-CdR/TSA 72hrs	3.30	3.67
5-aza-CdR 3 weeks	4.56	4.61
5-aza-CdR/TSA 3 weeks	2.43	3.98
5-aza-CdR 6 weeks	2.36	2.81
5-aza-CdR/TSA 6 weeks	2.32	2.45
5-aza-CdR 2 months	1.94	3.04
5-aza-CdR/TSA 2 months	1.55	3.55

5.4-Discussion

Telomere length dysregulation plays a major role in cancer development (Butler, Hines *et al.* 2012). Telomeric attrition is involved in genomic instability and in early events in tumorigenesis. Maintaining telomere structure and function relies on the interaction between telomere length and the Shelterin complex (Hu, Zhang *et al.* 2010). It has been shown in several independent studies that regulating the expression of telomere proteins can be implicated in telomere length regulation in cancer (Gao, Zhang *et al.* 2011; Butler, Hines *et al.* 2012). For instance, one previous study in gastric cancer (and precancerous gastric lesions) reported that over-expression of *TRF1*, *TRF2*, *TIN2*, and *TERT* was associated with the reduction of telomere length (Hu, Zhang *et al.* 2010). Additionally, recent findings by Butler *et al.* (2012) observed that the over-expression of *POT1*, *TIN2*, *TRF1*, and *TRF2* in breast cancers was associated with a decrease in mean telomere length.

Since the 21NT cells has shorter telomeres (~ 3kb) (Cuthbert, Bond *et al.* 1999) than normal HMECs (~ 8kb) (Sputova, Garbe *et al.* 2013), we asked the question whether the increase in telomere length in 21NT cells treated with 5-aza-CdR and TSA could be due to demethylation and/or chromatin remodelling leading to an increase in Shelterin gene expression. This might suggest a mechanism linking telomere shortening and down-regulation of Shelterin genes in breast cancer cell lines.

The assessment of telomere dynamics is critically dependent on the telomere length measurement techniques chosen. In this study four different methods: TRF, iQ-FISH, flow-FISH and q-PCR were used to measure telomere length.

Two main lines of investigations were covered in the work described this chapter. First, the telomere length measurements were obtained from 21NT cells treated over a time course ranging from 72 hours to 2 months using the four different methodologies; all four methods were compared in terms of reliability and accuracy.

The telomere fluorescence intensity (TFI) of 21NT cells treated with 5-aza-CdR and TSA at different time points were measured by iQ-FISH and flow-FISH. The iQ-FISH results showed the TFI of 21NT treated cells was significantly higher in comparison with control (DMSO-treated) cells ($P<0.001$). No substantial difference in telomere lengths observed between 72 hours, 6 weeks and 2 month of treatment (Figure 5.8). We have also measured the telomere fluorescence intensity of 21NT treated, untreated, control (DMSO-treated) and HMEC1 cells in G0/G1 phase of cell cycle by flow-FISH. During the G0/G1 phase the cells stopped dividing; hence, before telomeres replication in late S phase, the average telomere fluorescence intensity in G0/G1 was examined. The average TFI of 21NT treated cells increased after 72 hours, 3 weeks and 6 weeks in comparison with the DMSO-treated control ($P<0.01$ and $P<0.001$ respectively). Nonetheless, it was observed that at 2 months following initial treatment of the 21NT cells, no difference in TFI was observed compared with the DMSO-treated control (Figure 5.10). The average telomere length determined by TRF showed that the telomere length in 21NT cells treated with 5-aza-CdR for 3 weeks had a higher increase in comparison with 72 hours, 6 weeks and 2 months treatment. However, the telomere length after short-term treatment (72hrs) increased compared with the DMSO-treated and untreated controls (Figure 5.11). Results of q-PCR showed approximately a two-fold increase in telomere length of 21NT cells for 72 hours and 3 weeks which were similar in comparison with TRF technique (Figure 5.12). No substantial differences in

telomere length have been observed in 6 weeks and 2 months retreated samples in comparison with 72 hours and 3 weeks treatment. The same trend held true when we looked at the expression levels of *POT1* and *TIN2* at different time points (previously discussed in Chapter IV). These results indicated that 5-aza-CdR and TSA lose their effectiveness in the longest time point of treatment (6 weeks and 2 months retreatment) (Figure 5.12). In other words, 5-aza-CdR treatment is reversible and not permanent.

All these findings support an emerging view that Shelterin genes *POT1, TIN2* and *TPP1* positively and negatively regulate telomere length elongation by telomerase. The TPP1-POT1 complex is presumably activating telomerase processivity under the certain circumstances. This complex covers the 3' overhang of single stranded telomeric DNA and inhibits binding of the telomere to telomerase (Wang, Podell *et al.* 2007). Moreover, disruption of this complex (TPP1-POT1) results in inhibition of POT1 to localize to telomeric DNA (Liu, Safari *et al.* 2004). It is moreover likely that the association of POT1-TPP1-TIN2 is important for recruitment of telomerase to the telomere. The data in this chapter have demonstrated that up-regulation of Shelterin genes through demethylation of their promoters co-operate with an effect on telomere length.

mRNA expression of Shelterin genes was silenced in breast cancer cell lines by DNA methylation and histone deacetylation. As discussed earlier, (Chapter IV), *POT1*, *TIN2* and *TPP1* were significantly induced in 21NT cells treated with DNA methylation inhibitor 5-aza-CdR and the histone deacetylation inhibitor, TSA ($P<0.05$). This further supports the hypothesis that these genes were silenced by DNA methylation and histone deacetylation. The results suggest that after treatment with 5-aza-CdR and TSA, Shelterin gene expression was increased. Correlation between 5-aza-CdR and TSA induced Shelterin gene expression

and increased telomere length. However, it is recognised that 5-aza-CdR and TSA will affect expression of many genes. Nonetheless, the possible association shown here is of interest.

Chapter VI

OVER-EXPRESSION OF HUMAN *POT1* IN 21NT BREAST CANCER CELL LINE REGULATES TELOMERE LENGTH ELONGATION

6.1-Introduction

Earlier in this project (Chapter IV), when the 21NT breast cancer cell line was treated with 5-aza-CdR and TSA, evidence for up-regulation of Shelterin genes was observed. Significant re-expression of *POT1* and *TIN2* was seen after short-term and long-term treatment of 21NT cells. Moreover, previous results showed that up-regulation of Shelterin genes was positively correlated with increased telomere length.

The telomere binding proteins (TBPs) have been proposed to regulate telomerase enzyme activity at the chromosome level. POT1 is the only protein that is able to bind directly to the 3′ single strand of telomeric DNA via its oligonucleotide/oligosaccharide-binding (OB) fold domain (Baumann and Cech 2001; Lei, Podell *et al.* 2004; Loayza, Parsons *et al.* 2004; Gao, Zhang *et al.* 2011). It has been found that TPP1 recruits POT1 to telomeres. Moreover, the amino terminus of TPP1 has a telomerase-interacting domain, signifying that TPP1 plays a role in the recruitment of telomerase to chromosome ends (Tejera, Stagno d'Alcontres *et al.* 2010). Additionally, in the present of POT1, the Shelterin components RAP1, TRF1, and TRF2 localise to the telomere. Therefore, the Shelterin complex may require POT1 in order to maintain telomere length (Ramsay, Quesada *et al.* 2013) and it seems that POT1 is implicated in telomere length maintenance. Therefore, this gene was chosen for further analysis to investigate the effect of *POT1* in telomere length elongation. In this connection, our working hypothesis was that ectopic over-expression of *POT1* in 21NT breast cancer cells may regulate telomere length.

6.2-Materials and methods

6.2.1-Transformation of POT1 cDNA into bacterial cells

The full length of human *POT1* gene (2kb, variation 1) was cloned into the plasmid vector pcDNA/FRT/V5-His-TOPO (a kind gift from Roger Reddel (Colgin, Baran *et al.* 2003)). This vector contains hygromycin for selection in mammalian cells. For amplification, 100ng of plasmid pcDNA5-POT1 was added into a vial of One Shot® TOP10 Chemically Component *E. coli* and incubated on ice for 30 minutes. The sample was heat-shocked at 42^{o}C for 30 seconds and then incubated on ice for 2 minutes. After that, 250µl of SOC medium was added to the tube. The tube was capped tightly and shakes horizontally in a Gallenkamp orbital shaker at 200rpm at 37^{o}C for one hour. Afterwards, 200µl of SOC medium was spread on pre-warmed LB-agar (Sigma) plate containing 50µg/ml ampicillin. Plates were incubated at 37^{o}C overnight. Then, 6 single ampicillin resistant bacteria clones were picked and used to inoculate 5ml of LB-Broth (Sigma) media containing 50µg/ml ampicillin. The cultures were grown overnight in an orbital shaker at 200rpm at 37^{o}C.

6.2.1.1-Isolation of plasmid DNA with Alkaline Protease Solution

Samples were purified from cultured transformed bacteria using Wizard® *Plus* SV Minipreps DNA purification Kit (Promega). The bacterial cells were collected by centrifugation at 16000*rcf* for 5 minutes. The supernatant was removed and the pellet was re-suspended by adding 250µl of Cell Re-suspension Solution. Then 250µl of Cell Lysis Solution was added to each sample and mixed by inverting it 4 times. Afterwards, 10µl of Alkaline Protease Solution was added to the tubes, mixed by inversion, incubated at room temperature for 5 minutes. 350µl of Neutralization Solution was then added and mixed.

Subsequently, the tubes were spun at 16000*rcf* at room temperature for 10 minutes. The entire mixture was transferred into Spin Column and centrifuged at top speed for 1 minute at room temperature. The flow-through was discarded and spin column was placed back in the same collection tube. The columns were washed twice with 750µl of Wash Solution prepared with ethanol and centrifuged at 16000*rcf* for 1 minute. The elution of plasmid DNA was performed by placing the columns in clean 1.5ml micro-centrifuge tubes and adding 100µl of Nuclease-Free Water to the centre of the membrane. The sample was eluted by centrifugation at full speed for 1 minute. Then, the tubes containing plasmid DNA were stored at -20°C until further processing. The concentration of plasmid DNA was adjusted. Then, for plasmid confirmation by restriction enzyme analysis, 1µg of extracted plasmid DNA were cut in a 20µl of reaction volume containing 2µl of BamH1, 2µl of Buffer, 0.1 µl of Bovine serum albumin (BSA) and made up to 20µl with sterile distilled water. The reaction mixture was incubated at 37°C for 2 hours. After digestion, DNA samples were run on 0.8% agarose gel for 2 hours (Figure 6.1).

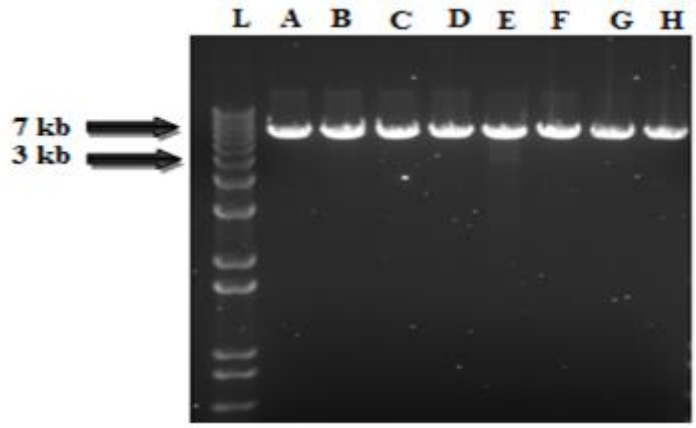

Figure 6.1-Image of a typical 0.8% of agarose gel electrophoresis with digested plasmid DNA to check the size of plasmid. The lane on the left side shows the molecular size marker. The 7kb band seen on the gel represents of *POT1* gene attached to the 5kb plasmid vector.

6.2.1.2-QIAGEN® plasmid purification Maxi-prep Kit

The Maxiprep purification was carried out to obtain the most pure form of DNA and was used according to the manufacturer's instructions. Briefly, a single transformed bacterial colony, which was confirmed as having the POT1 insert, was grown in 5ml of LB-Broth media containing 50µg/ml ampicillin on an orbital shaker at 200rpm overnight at 37°C. Then, 2ml of cultured media was added to 100ml of LB-Broth media containing 50µg/ml ampicillin and was placed in an orbital shaker at 200rpm overnight at 37°C. The bacterial cell pellets were collected by centrifugation at 16000*rcf* for 15 minutes at 4°C. The cell pellet was re-suspended in 10ml of Buffer PI (50mM Tris-HCl pH 8, 10mM EDTA, and 100µg/ml RNase A). 10ml of Buffer P2 (200 mM NaOH, 1% SDS) was added to the samples and mixed thoroughly by inversion 4 to 6 times, and incubated at room temperature for 5 minutes. After that, 10ml of chilled Buffer P3 (3M potassium acetate pH 5.0) was added to the tubes and mixed by vigorously inverting 6 times. The lysate was poured into the barrel of a QIAfilter Cartridge and then were incubated at room temperature for 10 minutes. The cap was removed from the QIAfilter Cartridge outlet nozzle and the plunger was gently inserted into the QIAfilter Cartridge. Afterwards, the cell lysate was filtered into the equilibrated QIAGEN-tip. The supernatant was loaded into a QIAGEN-tip column previously equilibrated with 10ml of Buffer QBT (750mM NaCl, 50mM MOPS pH 7.0, 15% iso-propanol, 0.15% TritonX-100) and allowed to empty by gravity flow. The columns were washed twice with 10ml of Buffer QC (1.0M NaCl, 50mM MOPS pH 7.0, 15% iso-propanol) and the plasmid DNA was eluted with 5ml of Buffer QF (1.25M NaCl, 50mM Tris-HCl pH 8.5, 15% iso-propanol). Plasmid DNA was precipitated by adding 3.5ml of iso-propanol and centrifuged at 16.1*rcf* for 30 minutes at 4°C. The supernatant was carefully decanted DNA pellet was

washed with 2ml of room-temperature 70% ethanol and spun down at 16.000*rcf* for 10 minutes. The DNA was dried and re-suspended in 200µl of DNase-free water. The samples were kept on ice for 30 minutes and the concentration of plasmid DNA was measured.

6.2.1.3-Transfection procedure using GeneJuice®

One day prior to transfection, $15x10^5$ 21NT cells still in the exponential phase of growth were seeded into p100 tissue culture dish. The cells grew overnight to reach about 80% confluency. For each 100-mm dish to be transfected, 800µl of serum free modified Eagle medium was placed into a sterile 1.5ml tube. 18µl of GeneJuice®Transfection Reagent (Novagen) was dropped directly to the serum-free medium. The tube was mixed thoroughly by vortexing and incubated at room temperature for 5 minutes. Three tubes were prepared; one was a transfection reagent control (GeneJuice reagent/serum-free medium), another was POT1 plasmid and the final tube was an empty vector control (pcDNA3.1/hygro 5.6kb plasmid kindly provided by Dr Evgeny Makarov). After that, 10µg of POT1 plasmid and 10µg of pcDNA (control) were added to each tube of GeneJuice reagent/serum-free medium mixture by gentle pipetting and incubated at room temperature for 15 minutes. The cells were washed with PBS and 10ml of fresh culture medium was added. Then, prepared precipitates were added to each plate and incubated for 24 hours. After incubation for overnight, the culture medium was aspirated and divided in 10 plates. For the purposes of this study, we wanted to isolate stable clones that over-expressed *POT1*. To do this, 21NT transfected cells were routinely cultured in modified Eagle's medium with 400U/ml Hygromycin B as a selection marker. This selection marked that only clones which have picked up the vector carrying the selectable marker will grow. Cells that do not contain the

vector will die after several weeks in culture. Subsequently the incubation was continued for 3 to 4 weeks, allowing for growth and selection of 21NT-transfected colonies.

6.2.1.4-Picking of cell colonies

In preparation for picking cell colonies, cloning cylinders of varying sizes were cleaned and sterilised by submersing them in 100% pure ethanol (Hayman) for one day prior to use. The position of colonies was identified under a microscope and colonies well separated from one other were chosen for isolation. Each clone was marked by a permanent marker on the bottom of the plate. The media was removed and washed with pre-warmed PBS. After gentle swirling and aspiration of PBS, an appropriately sized cloning cylinder was removed from 100% pure ethanol solution with sterile forceps and firmly pressed into pre-autoclaved Vaseline to create a thick layer on the bottom of the cylinder. The cloning cylinder was placed carefully over the colony based on the circle drawn on the bottom of the dish and presses down firmly to form a tight seal. Then 100-250µl of TrypLE Express (depending on the cylinder size) was pipetted into the cylinder. This process was repeated if several colonies were to be isolated from the same plate, and the cells were incubated at 37^{o}C for 3 minutes. After incubation, the cells were checked under the microscope to make sure that they were detached. Subsequently, the cells were retro-pipetted several times and transferred to a 12 well-plate containing 1ml of pre-warmed complete medium. This step was repeated several times until all colonies had been picked and transferred to the 12 well-plates. Each clone was cultured until the cells reached 90% confluence; they were then harvested and transferred to a P60 plate. Once the cells had reached 90% confluence on a P100 dish they were used for further analysis.

6.2.2-Quantification of telomerase activity using RQ-TRAP assay

6.2.2.1-Protein isolation

Cell lines to be analysed were grown to 80-90% confluence on a P100 dish. At this point cells were harvested and total cell number was determined. The cell pellet was obtained by centrifuging at 15,000*rcf* for 5 minutes. The supernatant was aspirated and the pellet was washed once with pre-warmed PBS. Sample pellets were left on wet ice and 200µl CHAPS lysis buffer (TRAPEZE®1x CHAPS MILLIPORE Company) per 10^5-10^6 cells was used to re-suspend the pellets. All samples were retro-pipetted several times and the cell suspension was transferred to a fresh tube. The suspension was incubated on wet ice for 30 minutes before centrifugation at 12,000*rcf* for 20 minutes at 4^{o}C. 150µl of the supernatant was transferred into a fresh tube and determined the protein concentration for all the samples including the one was going to be used as the standard curve. The remaining extract was aliquoted and immediately stored at -80^{o}C until required.

6.2.2.2-Determination of protein concentration

The protein concentration of samples was determined using the Pierce™ BCA Protein Assay Kit (Thermo Scientific). Pierce BCA Protein Assay is a detergent-compatible formulation based on bicinchoninic acid (BCA) for the colorimetric detection and quantitation of total protein. The assay was performed according to manufacturer's guidelines. A standard calibration curve was set up using bovine serum albumin (BSA) diluted in CHAPS lysis buffer, ranging from concentrations 0-2µg/ml (Figure 6.2). All unknown sample protein concentrations were measured against the standard curve (Table 6.1).

Table 6.1-Preparation of diluted BSA standards for BCA analysis

Tube	Volume of dH_2O	Volume of BSA	Final BSA concentration (µg/ml)
A	100	0	0
B	90	10	0.2
C	80	20	0.4
D	70	30	0.6
E	60	40	0.8
F	50	50	1
G	25	75	1.5
H	0	100	2

200µl of Working Reagent (BCA protein assay reagent A/B diluted 50:1) was prepared for each aliquot of protein extract and BSA protein standard concentration. To each 5µl of protein lysate, 200µl of the Working Reagent was added and the samples were vortexed thoroughly on a shaker for 30 second. The tube was incubated at 37°C for 30 minutes in water bath and then allowed to cool at room temperature. Subsequently, 100µl of each sample was added to 96-well plate. The A562 of the standards and protein lysates was then measured using a plate reader (BP800, BioHit). A standard curve was prepared by plotting the blank-corrected measurement for each BSA standard against its concentration. The standard curve was then used to determine the protein concentration of each study sample.

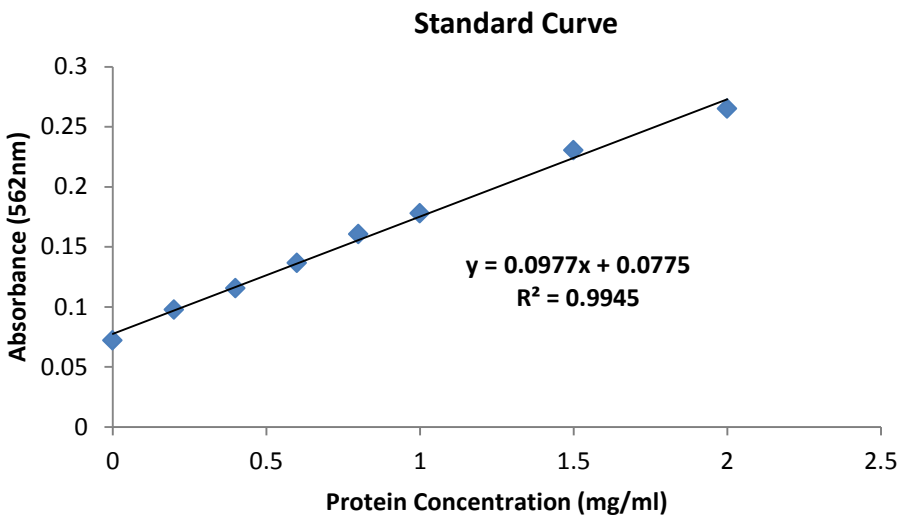

Figure 6.2-Standard curve used in protein quantification.

6.2.2.3-Quantitative telomere-repeat amplification (TRAP) Assay

Telomerase activity was measured using a quantitative TRAP assay (Paraskeva, Atzberger *et al.* 1998). Bench-top surfaces and pipettes were cleaned with RNAse Zap (Ambion) in preparation for the assay. Samples to be analysed were thawed on wet ice and diluted to a final concentration of 250ng/µl in CHAPS lysis buffer. Stock solutions were immediately quick-frozen and stored at -80^{o}C to prevent protein degradation. Reaction mixtures for each of the samples to be analysed were made up using the following components and volumes:

-12.5µl of standard iTaq™ Universal Syber®-green (BIO-RAD)

-1µl telomerase primer (ACX primer) (0.05µg/µl) (5'-GCGCGG (CTTACC) 3CTAACC-3')

-1µl telomerase primer (TS Primer) (0.1µg/µl) (5'-AATCCGTCGAGCAGAGTT-3')

-1µl protein samples

-15.5µl nuclease free water

-Total volume = 25µl

Reaction mixtures were thawed on ice to prevent protein degradation, vortexed and centrifuged briefly. Samples were assayed in triplicate and each assay run included a telomerase positive, negative and non-template control. As an additional negative control, 10µl of each target sample was heat-treated to inactivate the enzyme by incubating at 85^{o}C for 10 minutes. The microtitre plate was then loaded into the thermocycler block and PCR amplification parameters were carried out with the following reaction conditions. The reaction mixture was first incubated at 25°C for 20 minutes to allow the telomerase in the protein extracts to elongate to TS primer by adding TTAGGG repeat sequence. PCR was then started at 95°C for 10 minutes to activate Taq polymerase followed by a two-step PCR amplification of 35 cycles at 95°C for 30s and 60°C for 90s. Telomerase activity is reported as standard cell equivalents. To quantify telomerase activity, a standard curve was generated from serially diluted telomerase positive prostate cell line; PC-3/hTERT extracts (10^6-10^2). The threshold cycle values (C_t) of the unknown samples were read off against the standard curve, which gives the level of telomerase activity compared with PC-3/hTERT cells. All RQ-TRAP reactions were analyzed in triplicate and error bars created using standard error.

6.3-Results

6.3.1-*POT1* over-expression facilitates telomere length elongation on 21NT cells

POT1 is one of a six proteins which makes up the Shelterin complex that specifically binds to the G-rich single strand tail of mammalian chromosomes. POT1 function in cancer cells has been extensively studied in order to understand how this protein maintains telomere function and regulates the telomerase enzyme activity in disease states. Previous work by Colgin *et al.* (2003) showed that the over-expression of full length *POT1* in telomerase positive HT1080 cells increased telomere length in over-expressed cloned cells. Therefore, based on these findings we hypothesized that over-expression of *POT1* in 21NT cells might positively regulate telomere length.

6.3.2-Determination of relative *POT1* mRNA levels in 21NT transfected clones

In order to evaluate the effects of *POT1* (variation 1) over-expression in 21NT cancer cells, these cells were transfected with human *POT1*. cDNA from two stable clones plus non-transfected 21NT cells, and ten vector control clones were synthesized from total RNA (Figure 6.3).

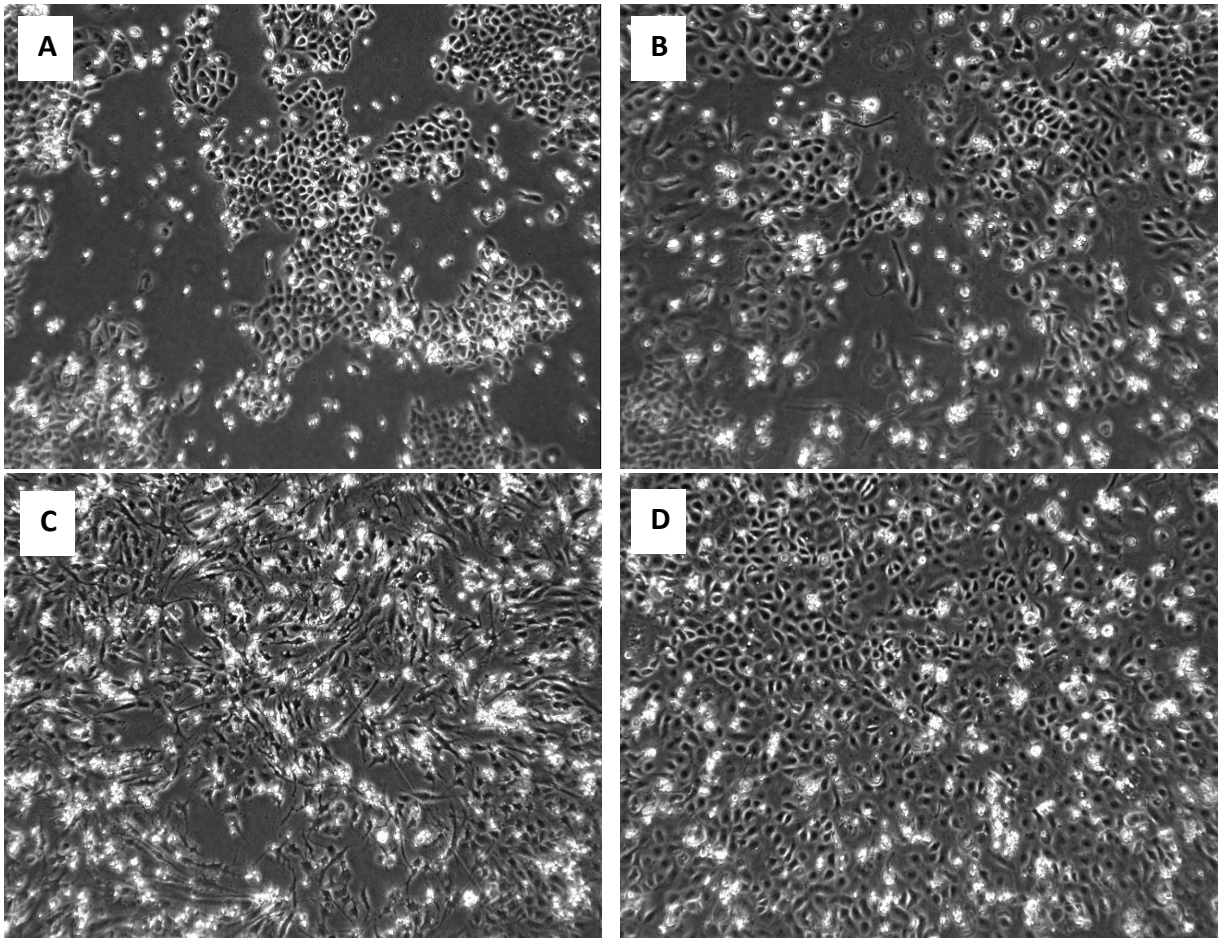

Figure 6.3-Images of 21NT transfected clones at 10x magnification. Representative images of 21NT transfected clones growing after 3-4 weeks in selection before being picked and cultured as a separate cell line. **A)** Image of POT1-1/pcDNA5, **B)** POT1-3/pcDNA5, **C)** POT1-4/pcDNA5, **D)** empty vector control clone (pcDNA3.1-1). *POT1* transfected cells appeared to grow more slowly in comparison with empty vector control clone.

The expression levels of *POT1*, in 21NT transfected cells were quantified using qRT-PCR and normalized against endogenous *GAPDH*. As shown in Figure 6.4, *POT1* mRNA levels were elevated 3-4 fold in the POT1-1/pcDNA5 and POT1-3/pcDNA5 compared with non-transfected 21NT cells. This difference was statistically significance when compared with the level in non-transfected 21NT cells (P<0.5). There were no substantial differences in expression of *POT1* in vector control clones (pcDNA3.1-1) in comparison with 21NT control cells (Figure 6.4).

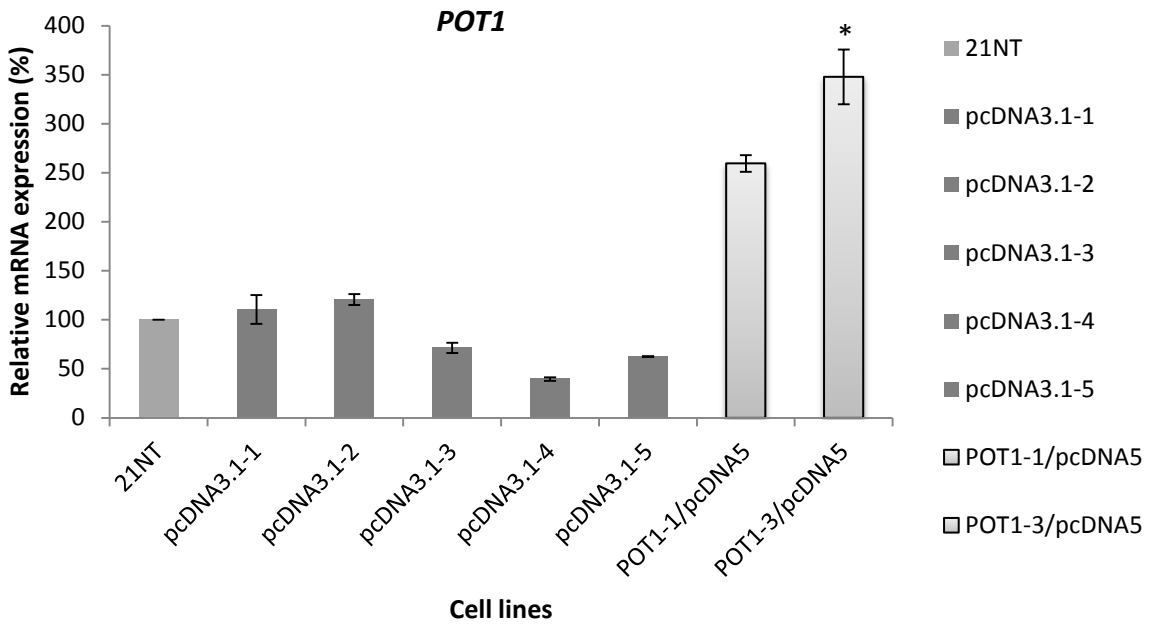

Figure 6.4-Over-expression of *POT1* (variation 1) after transfection of 21NT cells. Data shows the average expression level of *POT1* in 21NT non-transfected control, 5 vector control clones and two clones after *POT1* transfection, relative to *GAPDH*. The non-transfected 21NT cells were used as the calibrator. RQ indicates relative quantification and Error bars represent SEM. Asterisk indicates significant difference between 21NT cells and transfected cells (*P<0.05).

6.3.3-Western blot analysis

In order to confirm over-expression of POT1 in transfected 21NT cells at the protein level, western blot analysis was performed. The western blot analysis was carried out using POT1 rabbit monoclonal antibody (Abcam) and the values were normalised using β-Actin rabbit antibody. A 71-KD band which corresponds to the size of the POT1 protein was evident in non-transfected 21NT cells, two vector control clones, PC-3 included for comparison, and normal mammary epithelial cell strain (Figure 6.5-A). After imageQuant 5.0 densitometry analysis, the POT1 protein levels were found to be elevated more than 30% in the 21NT cells over-expressing POT1 compared with vector controls, 21NT cells, PC-3 cells,

and normal mammary epithelial cell strain (HMEC1) controls which was broadly in line with the qRT-PCR results (Figures 6.4 and 6.5-B).

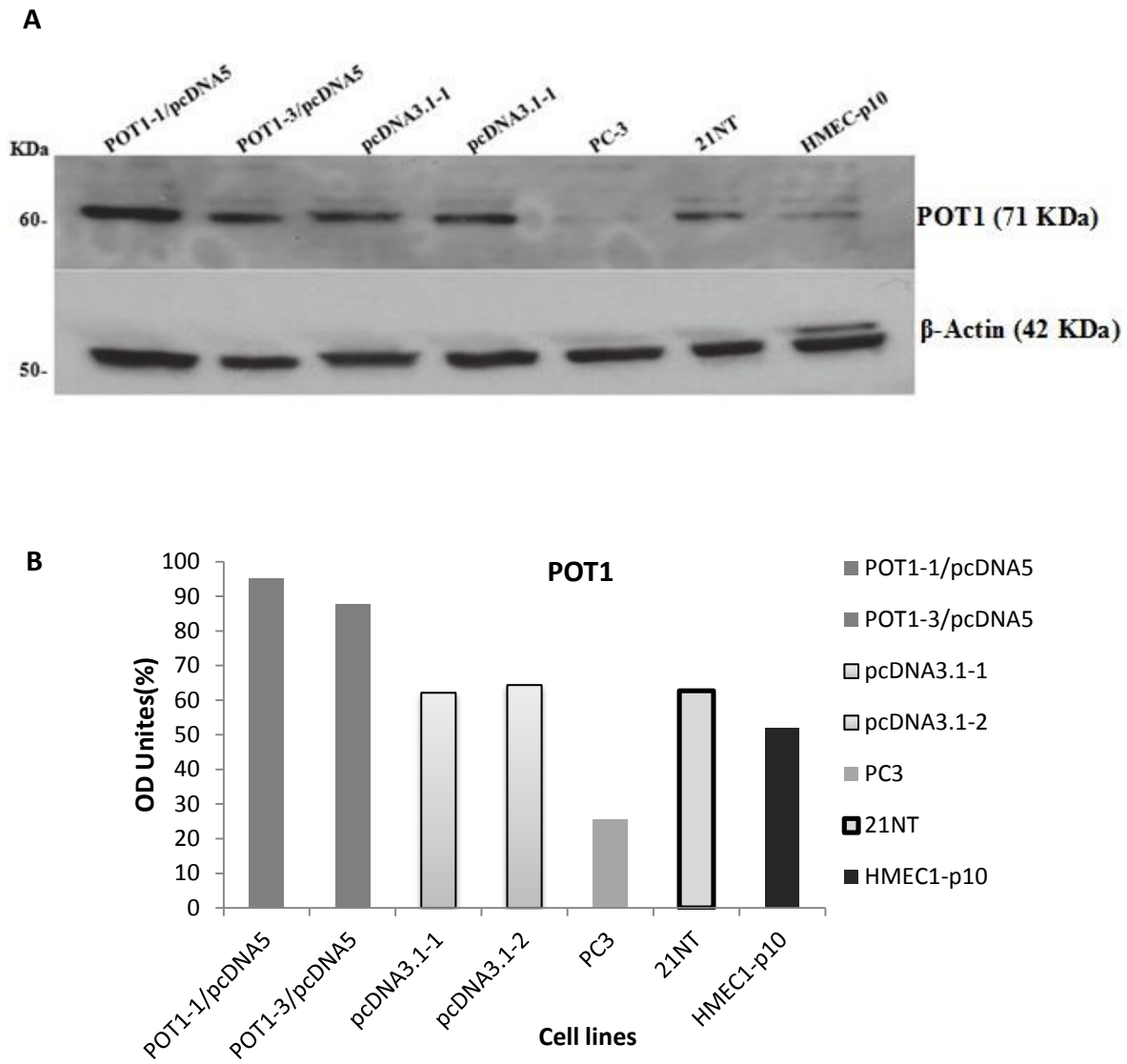

Figure 6.5-Western blot analysis of POT1 expression in 21NT transfected and control cell lines. A) A 12% SDS-PAGE gel indicating POT1 protein expression and β-Actin ratio levels in western blots of transfected 21NT cells, two vector controls, PC-3, non-transfected 21NT and normal mammary epithelial cell strain (HMEC-p10). **B)** Densitometric analysis of POT1 protein normalised to total β-Actin protein and reported as optical densitometry (OD) unites.

In order to investigate the interaction between *TPP1* and *POT1*, the mRNA levels of *TPP1* in *POT1* over-expressing 21NT cloned was quantified. The mRNA expression of *TPP1* was increased in the POT1-1/pcDNA5 and POT1-3/pcDNA5 in comparison with vector controls and non-transfected 21NT. However, these increased did not reach a statistical significance (Figure 6.6).

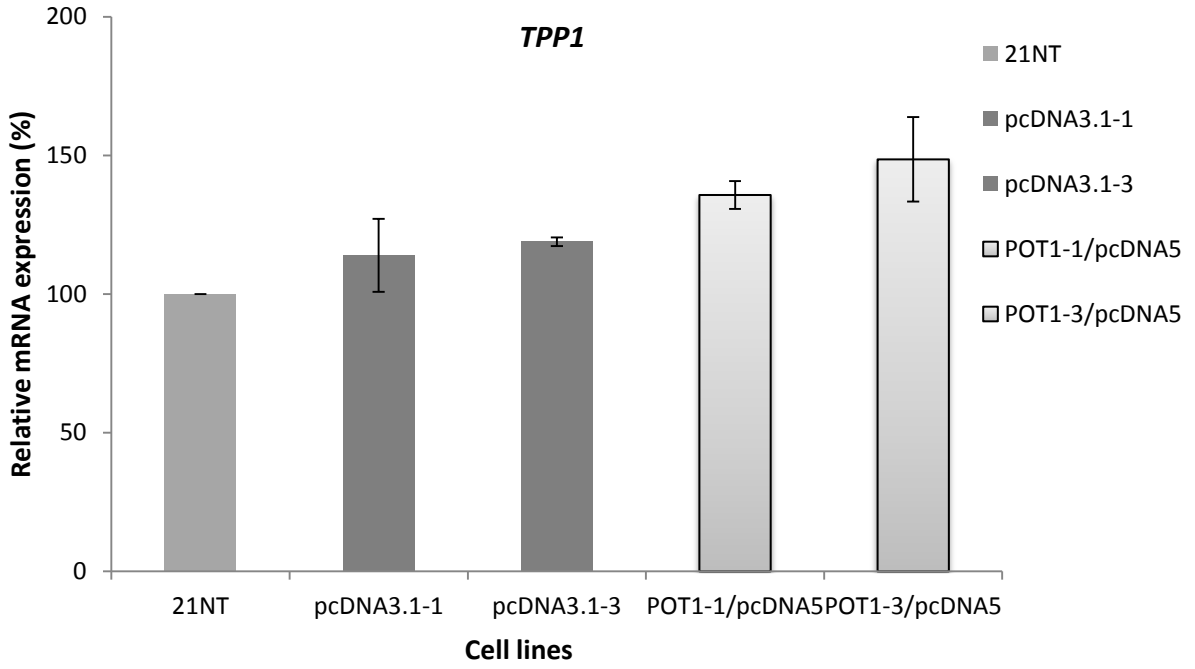

Figure 6.6-Represents comprehensive expression levels of *TPP1* after over-expression of *POT1* in transfection of 21NT cells. Data shows the average expression of *TPP1* in 21NT un-transfected control, two vector control clones and two clones of *POT1* transfection relative to *GAPDH*. The un-transfected 21NT cells were used as the calibrator. RQ indicates relative quantification and error bars represent SEM.

6.3.4-Telomere length analysis of 21NT transfected cells

Previous studies by Colgin *et al.* (2003) showed that over-expression of *POT1* in telomerase-positive HT1080 cells results in increased telomere length. In addition, subsequent studies have confirmed that reduction of *POT1* by RNA interference (RNAi) causes loss of telomeric single-stranded overhangs and induces chromosomal instability and apoptosis (Yang, Zheng *et al.* 2005).

In order to obtain a better and clear understanding of the exact role and function of POT1 in protection and maintenance of telomeres in human breast cancer, we needed to determine whether over-expression POT1 may play a role in telomere length maintenance. For this analysis the q-PCR technique was used as it was the most accurate and quickest (Chapter V) to measure telomere length. After about 4 weeks, genomic DNA was extracted from two stable clones, non-transfected 21NT cells, two vector control clones, PC-3 was included for comparison and a normal mammary epithelial cell strain (HMEC1) using Wizard^{TM} Genomic DNA Kit as described in Section 2 (Chapter II). As shown in Figure 6.7, PC-3 and HMEC1 controls showed telomere length ranging from 4.5 to 7.2 kb respectively. The average telomere length of 21NT non-transfected and empty vector control clones ranged from 2.5 to 3 kb, while the *POT1* over-expressing clones were between 4 to 5 kb. This represents an increase in telomere length of approximately 2kb around 4 weeks after transfection. Overall, the results showed that telomeres were elongated in two clones whereas no elongation was observed in the two vector control clones (Figure 6.7). Therefore, it seems that POT1 is a positive regulator of telomere length.

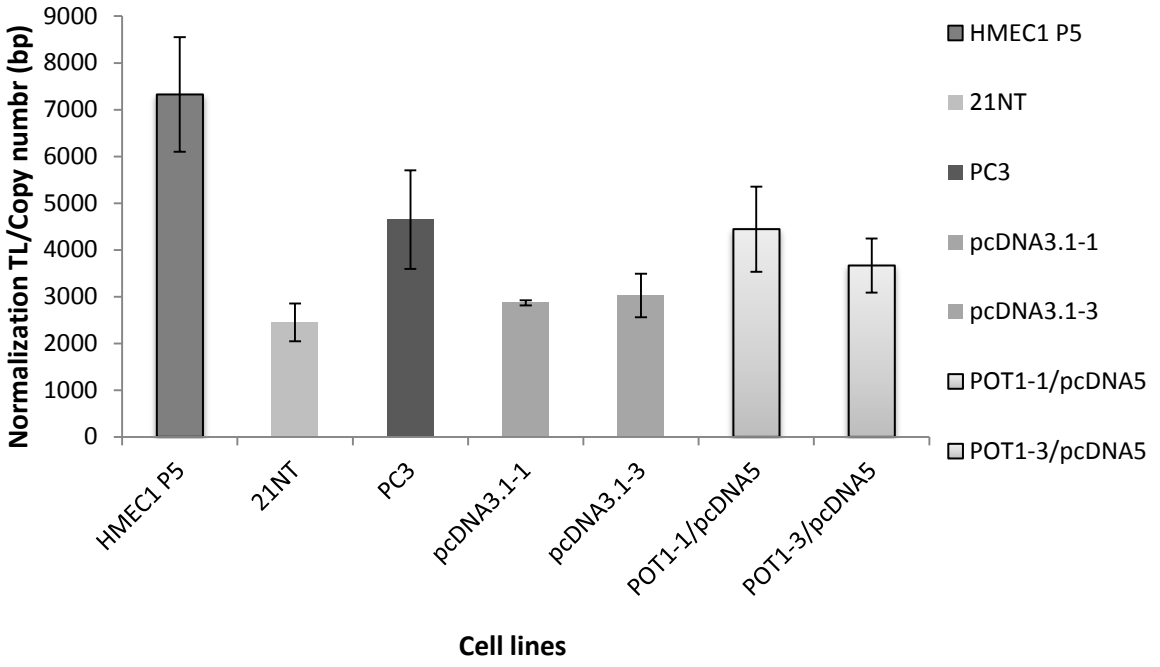

Figure 6.7-Telomere length measurement by q-PCR. Comparison of the telomere length in 21NT transfected and control cell lines. The telomere length is shown in normal human epithelial cell line (HMEC p5), non-trasnfected 21NT, and two vectors control clones, PC-3 and two stable colons. The analysis was performed with non-transfected 21NT and two vector control clones with the lowest telomere length (kb) compared with two stable clones to the adjacent controls; HMEC1 p5 and PC-3 controls. Error bars represent SEM.

6.3.5-Analysis of telomerase enzyme activity

Telomerase activity within stable clones was measured in order to search for a link between telomerase activity and increased telomere elongation. The quantitative TRAP assay was carried out using PC-3/hTERT as a positive control (provided by Dr Terry Roberts). This cell line expressed high levels of exogenous *hTERT* and as a result has high telomerase enzyme activity, telomerase positive non-transfected 21NT cells, and the telomerase negative HMEC1 cell strain; all were used as control samples. To quantify telomerase activity, PC-3/hTERT control was serially diluted and the relevant standard curve plotted.

Based on the equation obtained, the mean C_t values for unknown samples calculated and telomerase activity was calculated relative to the telomerase positive control (Figure 6.8). Negative controls for each individual sample to determine heat-sensitivity, were also included by heat-treating (HT) an extract of each sample.

The results, presented in Figure 6.8, show that approximately two-fold reduction in telomerase enzyme activity was observed in two stable clones compared with 21NT cells, non-transfected, and PC-3/hTERT controls. Our data suggested that telomere elongation by POT1 is not mediated by increased telomerase activity.

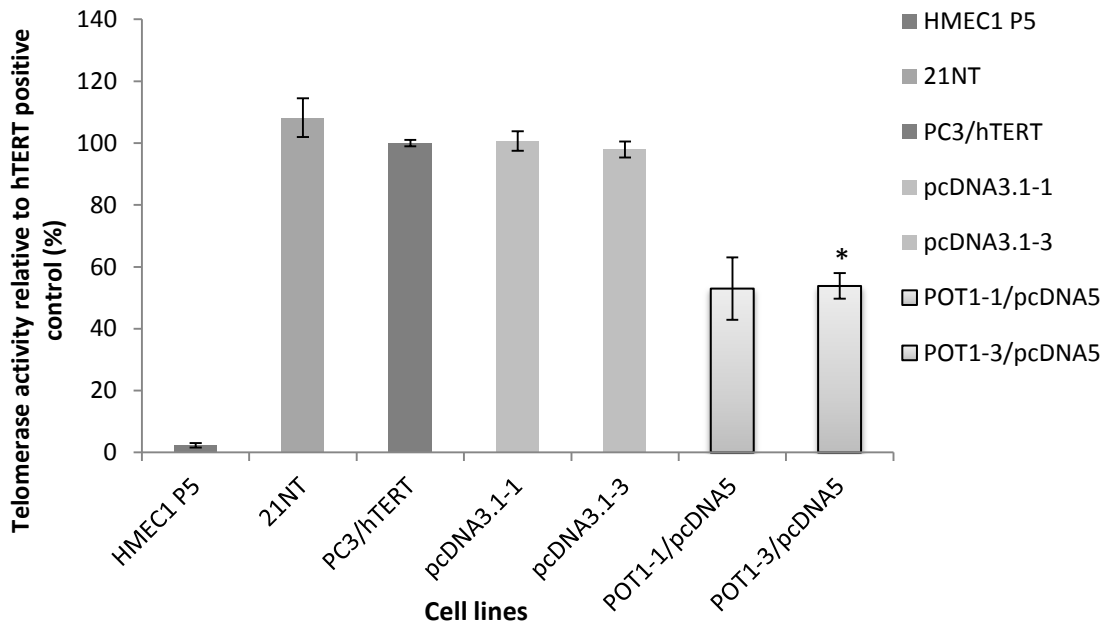

Figure 6.8-Quantitative telomerase activity. All values were acquired based on C_t values. Relative telomerase enzyme activity was obtained utilizing a standard curve generated by the serial dilution of PC-3/hTERT. The telomerase enzyme activity is shown in normal human epithelial cell line (HMEC1 p5) as a negative control, non-transfected 21NT, PC-3/hTERT as a positive control, two vector control clones and 21NT POT1 expressing clones. The analysis was performed with the highest telomerase enzyme activity assigned to the PC-3/hTERT sample and the activity in the unknown worked out as a percentage PC-3/hTERT sample. Error bars represent SEM. Asterisk indicates significant difference between 21NT cells and transfected cells (* P<0.05).

6.4-Discussion

Based on the results obtained from work described in Chapter V, which showed a significant increase in telomere length after 72 hours and 3 weeks treatment of 21NT cells with 5-aza-CdR and TSA, it was of interest to explain whether any one of the Shelterin proteins may play a role in this phenomenon. In other words could forced over-expression of any of the Shelterin genes stabilise telomere length in breast cancer cells? Or conversely could reduced expression of Shelterin genes lead to telomere lengthening (Yang, Zheng *et al.* 2005). It was previously reported that after each cell division, the 3' single stranded telomeric DNA becomes approximately 50 to 100bp shorter in the absence of telomerase activity (Stewart, Ben-Porath *et al.* 2003). Therefore, it has been suggested shortening of telomeric DNA occurs at the 3' overhang. It has been shown that POT1 is the only Shelterin protein that binds directly to the G-rich tail of telomeric DNA (Martinez and Blasco 2010). Therefore, it can be considered that POT1 is possibly one of the most important candidates within the Shelterin complex to participate in telomere elongation in breast cancer cells. The role of POT1 in telomere length regulation has been the subject of intense investigation. For instance, Kendellen *et al.* (2009) showed that deletion of the OB fold of the *POT1* domain induces telomere elongation (Kendellen, Barrientos *et al.* 2009). However, findings by Colgin et al. (2003) appeared to be contradictory to this. They observed that over-expression of *POT1* in telomerase-positive cells resulted in telomere length elongation.

Based on the relevant publications highlighted above, and the work described in the Chapter V, showing that significant re-expression of *POT1* in 21NT cells was observed after treatment with 5-aza-CdR and TSA (see Chapter IV), we set out to find what effect over-expression of *POT1* has on telomere length. To test whether over-expression of *POT1*

induces telomere lengthening, 21NT cells were stably transfected with human *POT1* (variation 1) cDNA. The mRNA levels of *POT1* increased more than three-fold compared with the empty vectors and non-transfected 21NT controls. The over-expression of POT1 at the protein levels was confirmed by western blotting. POT1 protein levels were elevated approximately 40% in the 21NT stable transfectants in comparison with controls which were broadly consistent with the qRT-PCR.

In order to determine the effect of over-expression of *POT1* on the function of *TPP1*, the mRNA levels of *TPP1* was quantified. The expression levels of *TPP1* were increased in the POT1-1/pcDNA5 and POT1-3/pcDNA5 compared with empty vector controls and non-transfected 21NT cells. However, these increases did not reach a statistical significance. TPP1 has been previously identified as a partner of POT1 and binds directly to TIN2 and form a part of Shelterin protein complex (Takai, Kibe *et al.* 2011). Consistent with these observations, over-expression of *POT1* may perhaps play an important role to elevate the expression of *TPP1* in 21NT transfected cells. Therefore, it seems that the interaction of POT1 and TPP1 regulates telomere lengthening and enhance POT1 affinity for 3' single stranded telomeric DNA.

To investigate the effect over-expression of *POT1* has on telomere length elongation; the average telomere length was examined by q-PCR. The results showed that the average telomere length of the *POT1* over-expressing clones was about 2 to 3 kb longer in comparison with 21NT non-transfected and empty vector control clones. The same trend held true when we looked at telomere length at different time point treatments (previously discussed in Chapter V).

Based on these results we asked the question whether the increased telomere length was the results of telomerase activity? Therefore, telomerase enzyme activity was assessed by a quantitative TRAP assay. Surprisingly, there was about a 2-fold reduction in telomerase activity in the *POT1* transfected clones which had increased telomere length when compared with non-transfected 21NT cells and empty vector controls. As expected, telomerase activity in normal diploid HMEC1 cells was extremely low.

The result showed that telomere elongation by over-expressing *POT1* (variation 1) is not due to a direct effect of the telomerase enzyme. These results are interesting in light of and consistent with the previous finding by Colgin *et al.* (2003) showing that telomere elongation by over-expression of *POT1* was not accompanied by an increase in telomerase activity. In addition, Yang *et al.* (2007) observed a significant increase in telomere length following over-expression of *POT1* (variation 1) in the HT1080 human fibrosarcoma cell line. They reported that this telomere lengthening was likely to be telomerase dependent as they did not observe an increase telomere length in telomerase negative human fibroblasts (Yang, Zhang *et al.* 2007).

It has been found that POT1 inhibits telomerase activity presumably by obstructing access to the 3' overhang (Colgin, Baran *et al.* 2003). However, this does not mean that POT1 completely inhibits activation of telomerase at the 3' telomeric overhang. Hence, it seems likely that POT1 negatively regulates telomerase access to the telomere (Colgin, Baran *et al.* 2003; Yang, Zhang *et al.* 2007). It is conceivable that telomere length may be regulated by the interaction of POT1 with TPP1 complex. Moreover, it is possible that the interaction of POT1-TPP1 complex with telomeric single-stranded DNA regulates telomere elongation, suggesting this association appears to play a fundamental role in the capping

function of POT1. In addition, the interaction of POT1 with TPP1 is necessary for telomerase dependent telomere lengthening as TPP1 can directly correlate with one of the catalytic subunit of telomerase enzyme, i.e. hTERT (Yang, Zhang *et al.* 2007).

Two theories about the function of telomere regulation have been described; “open” and “closed” states. It is argued that the “closed” conformation protects telomeric DNA from end-to-end fusion, implying that this condition is possibly implicated in the T-loop model. However, in the “open” state the telomere allows telomerase to access to the chromosome end (Colgin, Baran *et al.* 2003). This hypothesis leads to speculation that one possible prominent role for POT1 is to bind directly the 3' overhang of telomeric DNA and stabilize telomeres in the “open” state. Therefore, it is conceivable that over-expression of *POT1* displaces the T-loop formation and helps telomeres remaining in the “open” conformation (Colgin, Baran *et al.* 2003). Thus, according to this theory, we can assume that POT1 may allow telomerase access to telomere which results in increased telomere length. Collectively, according to our finding, it could be hypothesized that POT1 may perhaps be a negative regulator of telomerase activity to regulate telomere length (Colgin, Baran *et al.* 2003). It seems that POT1 may possibly regulate a localized activation of telomerase at the telomere end in telomerase-positive cancer cell lines. Taken together, it is interesting to speculate that POT1 may be a useful target for developing anti-cancer therapeutic agents against cancer.

Chapter VII

GENERAL DISCUSSION AND FUTURE DIRECTIONS

Maintenance and regulation of chromosome ends, at the telomere is fundamental for genome stability. Telomeres are made up of hexameric repeats to which Shelterin proteins bind in order to protect chromosome ends from end-to-end fusion, thus preventing them from being recognised as sites of DNA double strand breaks (Butler, Hines *et al.* 2012). Telomere dysfunctions have been implicated in most epithelial carcinomas. For instance, in 150 cases of breast tumours, more than 50% had significantly altered (mainly shorter) telomere lengths in comparison with normal breast tissues (Meeker, Hicks *et al.* 2004). The relationship between telosomal DNA-binding proteins and telomere length maintenance has become a popular area of interest recently. Butler *et al.* (2012) demonstrated that the mRNA levels of *TRF1*, *TRF2*, *TIN2* and *POT1* were correlated with telomere length in breast tumours. Furthermore, earlier investigations had shown that down-regulation of *POT1* correlates with telomere length dysfunction in gastric carcinoma (Kondo, Oue *et al.* 2004). Based on the advances highlighted above, this project aimed to examine whether the expression of Shelterin and Shelterin-associated genes is altered in breast cancer cell lines and if so whether telomere length maintenance is affected. Answers to distinct questions relating to the evaluation of changes in telomere length in breast cancer cell lines were sought. First, we asked whether there is up-regulation or down-regulation of Shelterin and Shelterin-associated genes in breast cancer cell lines. To answer this, the mRNA and protein levels of these genes in a panel of ten breast cancer cell lines were quantified (Chapter III). Second, in an attempt to understand the causes and consequences of any observed alteration in the regulation of Shelterin and Shelterin-associated genes in breast cancer cell lines, the epigenetic regulation of these genes were assessed (Chapter IV). Third, changes in telomere length in breast cancer cell lines following epigenetic changes were measured with

different techniques (Chapter V). Finally, and most importantly, the aim was to identify a single Shelterin gene (*POT1*) to study in greater detail. Ectopic over-expression of *POT1* in the 21NT breast cancer cell lines was performed in order to understand more about the molecular mechanisms that may possibly contribute to alterations in telomere length regulation (Chapter VI).

Previous work done by Salhab *et al.* (2008) demonstrated an increase in the mRNA levels of *TNKS1*, *hTERT*, *EST1*, and *TEP1* in breast cancer tissues whereas *TNKS2* and *POT1* were down-regulated in comparison with normal breast tissue. More recently, Gao *et al*. (2011) reported over-expressed levels of *POT1* in gastric cancer tissues. Furthermore, *TRF1*, *TRF2* and *TIN2* were significantly over-expressed in precancerous lesions, gastric cancer tissues, and lymph node metastases in comparison with normal gastric mucosa tissues (Hu, Zhang *et al.* 2010; Gao, Zhang *et al.* 2011). Different patterns of mRNA expression of Shelterin and Shelterin-associated genes may result in telomere length dysfunction in breast cancer cell lines. Therefore, the focus of the first set of experiment (Chapter III) in this study was to quantify mRNA and protein levels of these genes in different breast and prostate cancer cell lines. Some of the Shelterin genes have different splice variants. Therefore, in order to investigate a difference between each splice varient, their mRNA levels were quantified by qRT-PCR (Chapter III).

Results showed that *POT1* splice variant (SV) 1 and 2, *TRF1* (SV1 and SV 2) and *TRF2*, *SMG6* (SV1), *TIN2* (SV1 and SV2), *TEP1*, *TNKS2*, and *RAP1* were significantly down-regulated at the mRNA level in breast cancer cell lines in comparison with RNA extracted from normal mammary breast tissue. However, interestingly, *TPP1* mRNA levels were higher in most breast cancer cell lines compared with normal breast tissue. Tissues are mixed populations

of tightly connected cells. Gene expression can vary from one cell to another dependent on their distinct function. Therefore, differences in the expression of Shelterin and Shelterin-associated genes between individual tissues and cells may be observed. Hence, in order to validate telosomal gene expression results further, a normal breast mammary epithelial cell strain (HMEC1) was analysed for mRNA levels of *POT1* and *TPP1*. The mRNA levels of *POT1* were considerably lower in all cancer cell lines in comparison with HMEC1. The protein levels of Shelterin genes were next examined and it was found that 21NT, 21MT2 and HS578-T expressed considerably higher levels of POT1 protein compared with HMEC1 which was not in agreement with the mRNA expression data. As expected, TPP1 protein was over-expressed in most breast cancer cell lines compared with HMEC1 (Chapter III). However, the level of TPP1 protein was lower in 21NT and 21MT-2 than HMEC1 control, which again did not correlate with the mRNA expression data.

It is commonly believed that mRNA expression levels correlate with protein levels within cells but clearly this is not always the case. For instance, Schwanhausser *et al.* (2011) quantified protein and mRNA levels of 5279 unique proteins in NIH3T3 mouse fibroblast to analyse the correlation between expression levels of protein and mRNA. These investigations found proteins to be on average five times more stable than their mRNAs. Moreover, Tian *et al.* (2004) used multipotent mouse EML cells and their differentiated progeny MPOR cells to map the abundance ratios of 425 proteins and compared them to the amount of their corresponding mRNAs. They showed that 150 genes have alterations at their protein and/or mRNA levels between the two cell types. In addition, the EML cells showed a 5-fold higher level of c-kit ligand protein (aka stem cell factor) but no change in mRNA levels. Thus, based on these two papers and other published data from independent

researchers, it could be concluded that the concentration of proteins and their mRNA is not always proportional to each other and concentration of one cannot be used universally to estimate the concentration of the other. In contrast to the findings of the above cited studies is that mRNA and protein levels of housekeeping genes are generally stable.

The observed relationship between the mRNA and protein levels of TPP1 may be explained by the above reasoning. TPP1 was expressed at high mRNA and low protein levels. However, there is also an unexpected relationship observed in these results; POT1 had a high level of protein and low level of mRNA in most breast cancer cell lines compared with HMEC1. Furthermore, the POT1-encoded protein had lower expression levels in the normal control HMECs compared with 21NT cancer cell line. Previous work by Marks *et al.* (1991) showed that high p53 protein levels were associated with inactivating mutations in ovarian cancer cells (Marks, Davidoff *et al.* 1991). In addition, the results from a recent study indicated recurrent somatic mutations in the *POT1* gene in cancer cells (Ramsay, Quesada *et al.* 2013). Therefore, the observed discrepancy in our results may be explained by stable mutant forms of the POT1 protein within 21NT cells. Furthermore, despite the higher protein content of POT1 in 21NT cells, this mutated POT1 protein may not be capable of binding to the other Shelterin components properly which leads to telomere dysfunction. This may explain the higher protein levels observed within 21NT breast cancer cells in comparison with HMECs.

Several cellular factors (i.e., mutation, DNA methylation, histone acetylation, chromatin remodelling, etc.) in theory could affect the expression of Shelterin and Shelterin-associated genes in breast cancer cell lines. Based on previous published data and our

results presented in Chapter III, *POT1* mRNA was found to be significantly down-regulated in malignant breast tissues and cancer cell lines (Salhab, Jiang *et al.* 2008). Moreover, it had been previously reported that *POT1* was the most mutated Shelterin gene in a wide range of cancers such as; gastric, papillary thyroid, breast and leukaemia cancer cell lines (Poncet, Belleville *et al.* 2008; Shen, Gammon *et al.* 2010; Wan, Tie *et al.* 2011; Cantara, Capuano *et al.* 2012). Prior studies have shown that POT1 is the only Shelterin protein which is able to bind directly to the G-strand telomeric single strand DNA sequence overhang via its OB fold and plays a critical role in regulating telomere length (Lei, Podell *et al.* 2004; Yang, Zhang *et al.* 2007). Additionally, in the presence of POT1, the Shelterin components TIN2, TRF1, and TRF2 localises to the telomeres. As a result of that, Shelterin proteins may require the POT1 component to maintain telomere length (Ye, Hockemeyer *et al.* 2004; Wang, Podell *et al.* 2007).

Currently, the catalogue of somatic mutations in cancer (COSMIC) database shows over 127 somatic mutations in *POT1*, 41 in *TPP1*, and 249 in *RAP1*. However, at the time part of this study was carried out in 2009, the COSMIC database did not report any mutations within *POT1* and any other Shelterin genes. Hou *et al.* (2006) reported a single mutation within exon12 of *POT1* in HeLa and HO8910-PM cells. Therefore, the first focus of the work described in Chapter IV was to screen for exon12 mutations within breast cancer cell lines. The results revealed that no mutations within exon12 of the *POT1* gene were present in any of 10 breast cancer cell lines. This finding does not of course exclude mutations which may be present in other exons of *POT1*. A more comprehensive study to look for mutations within all Shelterin genes within the breast cancer cell lines would have been useful.

However, the scale of such a study would have been too large to accommodate in this project.

Epigenetic alterations to DNA and histones can results in silencing of genes (Kondo, Shen *et al.* 2003). The down-regulation of Shelterin genes in breast cancer cell lines (Chapter III) could be due to epigenetic modification (methylation) of the promoter of these genes or histone acetylation/deacetylation of chromatin at this locus. To study this, the promoter regions of *POT1* and *TIN2* genes in breast cancer cell lines were analysed. Methylation Specific PCR (MSP) showed that *POT1* was partially methylated in untreated breast cancer (i.e., not exposed to 5-aza-CdR and TSA) cell lines. However, in *TIN2* no significant differences were observed in methylated and unmethylated lanes in all breast cancer cell lines. These results provided insight into a plausible mechanism to explain the observed expression data based on DNA hypermethylation in the breast cancer cell lines.

A previous study by Zemliakova *et al.* (2003) looked at promoter methylation of five genes which were methylated in breast cancer tissues. They found that the promoter region of *p16* (56%), *RB1* (17%), *CDH1* (79%), *P15* (2%) and *MGMT* (8%) were methylated in breast cancer tissues (Zemliakova, Zhevlova *et al.* 2003). In addition, it was reported that *BRCA1* was hypermethylated in breast and ovarian cancers (Esteller, Silva *et al.* 2000). Furthermore, a previous study showed that the *RECK* gene was hypermethylated in hepatocellular carcinoma (HCC) in comparison with non-tumour tissues. It has been also reported that hypermethylation of the *RECK* promoter may be associated with silencing of *RECK* mRNA expression. Indeed, it was implied that the expression of *RECK* was likely regulated by DNA

methylation in the promoter region of the gene in hepatocellular carcinoma tissues (Zhang, Ling *et al.* 2012).

Based on published studies highlighted above, the 21NT cell line was then used as a model system for treatment with 5-aza-CdR and TSA, two epigenetic modifying agents. If Shelterin genes expression were silenced through promoter methylation/histone modification, the treatments should reactivate them.

The National Cancer Institute database reported that these epigenetic modification agents have been used as anti-cancer drugs in about 100 clinical trials (Ghoshal, Datta *et al.* 2005). The drugs have been used to treat different types of leuckemia, sickle cell anemia and β-thalassemia (Saunthararajah, Hillery *et al.* 2003). Work by Mirza *et al.* (2010) showed that *p53* and *p21* were up-regulated in MCF-7 breast cancer cells treated with 5-aza-CdR. Demethylation of *p53* and *p21* promoters in MCF-7 cells after treatment with 5-aza-CdR resulted in an up-regulation of these genes. It was found that the mRNA levels of *POT1*, *TIN2*, and *TPP1* were significantly increased in 21NT cells treated with both agents in comparison with DMSO-treated control.

The novel findings described in this project showed that 5-aza-CdR and TSA were most effective on modulating *TIN2* and *POT1* mRNA levels after relatively short term (48 and 72 hour) treatment and again after 3 weeks treatment of 21NT cells. In addition, the biphasic response of *POT1* and *TIN2* gene expression was seen with an optimal peak at 72 hours, which then declined and the expression was increased significantly again at 3 weeks treatment (correlated with telomere length see Chapter V). However, these agents together were found to lose their effectiveness during long term treatment (6 weeks and 2 month

retreatment) as no substantial difference was observed at these time points. Thus, the treatment was not permanent and is reversible. It is well established that the process of DNA methylation is carried out by DNA methyltransferases (DNMTs) enzymes. These enzymes catalyse the transfer of a methyl group from S-adenosyl-L-methionine (SAM) to the 5 position of cytosine (Robertson 2001). DNMT1, the main methylation maintenance enzyme, preferentially methylates hemi-methylated DNA during the process of DNA replication. In this scenario, 5-aza-CdR is incorporated exclusively into DNA as a cytidine analogue, and thereby inhibits DNA methylation via irreversible covalent binding to DNMT1 (Maslov, Lee *et al.* 2012). By this mechanism, it could be argued that the lowest expression of *POT1* and *TIN2* between 72 hours and 3 weeks may have resulted from an increase in the expression of DNA methyltransferases 1 enzyme, leading to hypermethylation of *POT1* and *TIN2* after several replications. Further investigations will be required to examine which factors are involved to decrease the transcription levels of *POT1* and *TIN2* in the interval between 72 hours and 3 weeks treatment. For instance, if this assay were to be repeated in the future, the expression of DNMT1 could be analysed along with *POT1* and *TIN2*.

It has been reported in several independent studies that 5-aza-CdR has therapeutic value for cancer treatment (Venturelli, Armeanu *et al.* 2007; Cai, Kohler *et al.* 2011; Liu, Zhang *et al.* 2012). Recent work by Kang *et al.* (2013) reported that Runt-related transcription factor 3 (*RUNX3*), a tumour suppressor gene, was hypermethylated in MCF-7 (breast cancer cell line). The work reported that 5-aza-CdR induces apoptosis and inhibits cell proliferation by demethylating the promoter region of *RUNX3* and reactivating its expression (Kang, Dai *et al.* 2013). Therefore, based on previous investigations, it should be noted that, used as a chemotherapeutic drug, 5-aza-CdR causes cell death via induction of

apoptosis pathways. Consistent with these observations, approximately 72 hours after treatment with 5-aza-CdR, a significant reduction in 21NT cell number was observed. Therefore, theoretically by 7 days of treatment, cells which have become resistant to apoptosis but retained the unmethylated status will start to grow out of the population and continue to grow up to 3 weeks accompanied by an increase in gene expression. Further studies *in vitro* will be required to determine which factors are involved in the modulation of gene expression. For instance, the Terminal deoxynucleotidyl transferase dUTP Nick End Labeling (TUNEL) assay may be a useful method to detect apoptotic programmed cell death.

In order to support the results described in this thesis, the promoter region of *POT1* was analysed for CpG demethylation in DNA samples from 5-aza-CdR treated 21NT cells. The bisulphite sequencing data obtained was entirely consistent with the results showing up-regulation of *POT1*, as all potential methylation sites within the CpG Island were demethylated after the treatment of 21NT cells with 5-aza-CdR. These data confirmed that 5-aza-CdR inhibits epigenetic mechanisms including DNA methylation. This appears to have the effect of reversing the silencing of Shelterin and Shelterin-associated genes in breast cancer cell lines. It is suggested that 5-aza-CdR and TSA enhance gene transcription by opening promoter regions to increase accessibility of assembling transcription factor complexes (Yang, Phillips *et al.* 2001; Margueron, Duong *et al.* 2004). It should be stressed that 5-aza-CdR in combination with TSA reactivated expression of Shelterin and Shelterin-associated genes, while TSA alone mostly had little effect on the expression of aforementioned genes. However, prior studies by others showed that TSA reactivates the expression of estrogen receptor (ER) in breast cancer cell lines (Yang, Ferguson *et al.* 2000). It is therefore, likely that the combined effect of 5-aza-CdR with TSA on gene expression has

dual activity on DNA demethylation and histone acetylation respectively. Since these two agents were individually shown to enhance gene expression, they seem to act synergistically. We can speculate that silencing of these genes is controlled by epigenetic modifications. The findings described in Chapter IV open up interesting avenues for future work. In the first instance, the promoter regions of other Shelterin and Shelterin-associated genes should be examined in all breast cancer cell lines. A second experimental approach should focus on delineating histone modifications such as acetylation of lysine residues on histone H3 and H4, together with the methylation of lysine 9 on histone H3, H9, H27 and H3K36 as well as the role of histone methylation (Wozniak, Klimecki *et al.* 2007). The application of chromatin immunoprecipitation (ChIP) technology followed by real-time PCR to quantify the degree of histone methylation in 21NT cells and other breast cancer cell lines would be central to such work.

Results obtained thus far demonstrated an up-regulation of some Shelterin genes when breast cancer cells were treated with epigenetic modulators. How does this affect telomere length maintenance? Previous studies indicated that dysregulation of Shelterin genes expression can result in telomere length dysfunction in a variety of cancers, including breast cancer (Butler, Hines *et al.* 2012). For instance, Hu *et al.* (2010) showed that over-expression of *TRF1*, *TRF2* and *TIN2* in gastric cancer tissues were correlated with a reduction in telomere length. Moreover, deficiencies in Shelterin regulation have recently been implicated in telomere length dysfunction during liver carcinogenesis (El Idrissi, Hervieu *et al.* 2013). However, the majority of studies have shown only that altered expression of Shelterin proteins affects telomere length, but they have not pinpointed a mechanism. To date, no previous investigations have reported effects of 5-aza-CdR and TSA treatment on

telomere length maintenance in cancer cells. Hence, following telomere length measurement by several reliable methods, it was clear that short-term (72 hrs) and 3 weeks treatment of 21NT cells with 5-aza-CdR resulted in an increase telomere lengths around of 4.7 kb. Therefore, it would seem that, in cancer, Shelterin expression is down-regulated through epigenetic modification of DNA and histone proteins. Up-regulation of Shelterin genes, through the use of epigenetic modifying agents, are directed towards the telomeres where they influence telomere length elongation. Indeed, our data may suggest that the regulation of the Shelterin protein complex is needed to maintain telomere length regulation in breast cancer cell lines.

The POT1-TPP1 complex covers the single strand 3' overhang and prevents binding of the telomere to telomerase (Wang, Podell *et al.* 2007). It remains likely that the association of POT1-TPP1-TIN2 plays a key role in recruiting telomerase to the telomere. Therefore, our results clearly showed that Shelterin genes particularly *POT1*, *TIN2* and *TPP1*, were significantly induced in 21NT cells following treatment with the DNA methylation inhibitor, 5-aza-CdR and the histone deacetylation inhibitor, TSA. This further supports the hypothesis in this thesis that demethylation of the Shelterin genes *TIN2*, *POT1* and *TPP1*, stabilises the Shelterin complex that functions to regulate and maintain telomere length elongation.

Based on results discussed above, three of the Shelterin proteins were significantly up-regulated after treatment with 5-aza-CdR and TSA; this ultimately led to telomere elongation. In the final Chapter of the thesis, it was attempted to identify the most important gene of the three. In this respect it was previously reported that the single-stranded 3' in the absence of telomerase DNA becomes approximately 50 to 100 bases

shorter after each cell division (Stewart, Ben-Porath *et al.* 2003). This may well be linked with POT1 as it is the only Shelterin protein that directly binds to the 3' ends of telomere (Baumann and Price 2010).

Previous noteworthy studies showed that reduction of *POT1* by RNAi results the loss of the 3' overhangs (Yang, Zheng *et al.* 2005). Furthermore, it had also been observed that over-expression of *POT1* in telomerase-positive cells resulted in telomere length elongation (Colgin, Baran *et al.* 2003; Yang, Zhang *et al.* 2007). Therefore, based on the results from previous Chapters, it was concluded that over-expression of *POT1* in 21NT cells may provide an improved understanding of telomere regulation in cancer cell lines. Thus, the full length of human *POT1* (variation 1) gene was over-expressed in 21NT cells to determine the effect on telomere length elongation. The results revealed that the average telomere length of the *POT1* over-expressing clones was 2 to 3 kb longer in comparison with 21NT non-transfected and empty vector control clones. However, increased telomere length by ectopic over-expression of *POT1* is not likely to be due to a direct effect on telomerase enzyme activity since the latter was not increased.

Based on a previous finding by Colgin *et al.* (2003) telomere length elongation by over-expressing *POT1* did not show an increase in telomerase activity. Such a result may validate our hypothesis and could support the finding that telomere elongation by *POT1* is not accompanied by an increase in telomerase activity. However, this does not exclude the possibility that POT1 completely inhibits activation of telomerase at the chromosome ends. Furthermore, our results showed approximately a 2-fold decrease in telomerase activity in transfected 21NT cells. Therefore, it is likely that POT1 initially allows telomerase to synthesise telomeres and leads to telomere length elongation up to 2kb, after a certain

length is reached, subsequently inhibits telomerase access and prevents further elongation. Therefore, it could be argued that POT1 negatively regulates the access of telomerase to the telomeres (Colgin, Baran *et al.* 2003). In order to further examine the role of telomerase activity and POT1-mediated telomere lengthening, *POT1* over-expression should be carried out within a telomerase-negative HMEC cell strain.

Two models of telomere length regulation have been described. The “open” state permits the access of telomere to telomerase and the “closed” conformation shields telomere DNA from end-to-end fusion (Colgin, Baran *et al.* 2003). With an “open” conformation, POT1 may possibly stabilise the telomere, via binding to the 3' overhang of the telomere end. Therefore, POT1 could be a negative regulator of telomerase activity in order to maintain telomere length. However, it is also possible that POT1 controls a localised activation of the telomerase enzyme at the telomere end. Our data highlights the importance of a potential fundamental role for POT1 in regulating Shelterin genes stability. It is likely that the interaction of POT1 with TPP1 form a part of the Shelterin complex via by binding TIN2. This develops the concept that, by virtue of these interactions, such a complex appears to form a stable sub-complex to interact with other Shelterin genes to protect and maintain telomere length.

In the past, several studies used genetically modified mice and cultured human cell lines to investigate the role of Shelterin genes in telomere length maintenance in aging and cancer (Martinez and Blasco 2010; Lu, Wei *et al.* 2013). For instance, inhibition of the expression of Shelterin genes, or over-expression of dominant negative forms of these proteins, (in cultured human cell lines) or knockout of Shelterin component (in mouse embryonic fibroblasts (MEFs)) results in telomere loss, T-loop recombination and telomere

fusion (Lu, Wei *et al.* 2013). In addition, conditional knockout of *Rap1*, *Tpp1*, and *Trf1* in mice showed high incidence of oncogenesis and deletion of *Pot1* induces mouse dyskeratosis congenita (DKC) (Hockemeyer, Palm *et al.* 2008; Martinez and Blasco 2010). Depletion of Shelterin components in mice pinpointed telomere dysfunction as the major driving force which leads to a more rapid pathological aging phenotype in comparison with those induced by telomerase deficiency. Moreover, genetic variation in the Shelterin complex has been observed in human pathological aging and cancer (Lu, Wei *et al.* 2013). Taken together, these observations indicated that, Shelterin proteins in telomere biology and disease play fundamental role in the context of the mammalian organism.

Results obtained in this thesis have shown that the use of chemotherapeutic epigenetic modifying drugs, such as 5-aza-CdR and TSA, induce and increase the expression of several Shelterin and Shelterin-associated genes in breast cancer cell lines. Up-regulation of these genes ultimately leads to an increase in telomere length. The effect of 5-aza-CdR and TSA on mammalian telomeres has not been widely reported in the literature to-date making the results presented here novel. We can now speculate on how the use of therapeutic agents such as 5-aza-CdR and TSA to increase telomere lengths of cancer cells may benefit clinical outcome. Research into the role of Shelterin and telomerase in cancer has found that telomerase re-activation functions to maintain telomeres at a critically short length (Low and Tergaonkar 2013). Telomeres in this unstable state are still prone to genetic damage via end-to-end fusions and translocations. This will have the effect of damaging the genome of the cancer cell further giving rise to further clonal evolution and a more advanced disease. If drugs such as 5-aza-CdR and TSA are used to treat cancer, they could induce telomere lengthening. This may have the effect of stabilizing the telomere and

reducing the amount of genetic damage the cell will undergo thereby stopping the clonal evolution of the cancer cell population. These tumours may be more susceptible to further treatment as a result. Drugs such as 5-aza-CdR and TSA are non-specific and cause global cellular demethylation/deacetylation which in the context of this work can be considered off-target effects. In order to specifically target telomere maintenance, it may be better to concentrate one or more Shelterin components rather than telomerase itself.

It is conceivable that targeting telomere length and telomerase will be an effective pharmaceutical strategy for cancer treatment. Manipulating telomere length (e.g. by controlling expression of telomerase components such as hTERT) might be expected to be beneficial for treating aging related diseases and cancer (Holysz, Lipinska *et al.* 2013; Lu, Wei *et al.* 2013). In addition, targeting Shelterin protein components may possibly more effective that targeting telomerase, especially POT1 which is implicated to regulate telomere length and capping (Martinez and Blasco 2010; Lu, Wei *et al.* 2013).

We observed that the over-expression of *POT1* negatively affected telomerase activity and resulted telomere lengthening. Increases in telomere length may stabilize cancer cells and render them less prone to telomeric fusion. As a result the clonal evolution of cancer cell populations may be reduced and making them more susceptible to further drug treatment. Therefore, targeting *POT1* in breast cancer cells allows for simultaneous investigation of telomere length and regulates the access of telomerase to telomere.

Gene therapy is the use of DNA as a drug to treat disease by delivering therapeutic DNA into a patient's cells. The most common form of gene therapy involves using DNA that encodes a functional, therapeutic gene to replace a mutated gene potentially in cancers. This relies on the efficient transfer of a nucleic acids which encodes a therapeutic protein,

into cells by a number of methods using viral vectors. Viruses such as retrovirus, lentivirus and adenovirus can be used *in vivo* to introduce genetic material into their host cell as a part of their replication process (Roth and Cristiano 1997; Cross and Burmester 2006). For instance, in clinical trials, the *in vivo* strategy involves the direct delivery of DNA (usually via a viral vector) to resident cells of the target tissue. There are two requirements for such a strategy: firstly, that target cells be easily accessible for infusion or injection of virus, and secondly, that the transfer vector readily and specifically infects, integrates, and then expresses the therapeutic gene in target cells and not surrounding cells at effective levels for extended time periods (Selkirk 2004). Thus, gene therapy can be used to deliver *POT1* into cells may be considered as a potential mechanism to treat breast cancer.

References

Aapola, U., K. Kawasaki, et al. (2000). "Isolation and initial characterization of a novel zinc finger gene, DNMT3L, on 21q22.3, related to the cytosine-5-methyltransferase 3 gene family." Genomics **65**(3): 293-298.

Abel, T. and R. S. Zukin (2008). "Epigenetic targets of HDAC inhibition in neurodegenerative and psychiatric disorders." Curr Opin Pharmacol **8**(1): 57-64.

Allred, D. C. (2010). "Ductal carcinoma in situ: terminology, classification, and natural history." J Natl Cancer Inst Monogr **2010**(41): 134-138.

Ancelin, K., M. Brunori, et al. (2002). "Targeting assay to study the cis functions of human telomeric proteins: evidence for inhibition of telomerase by TRF1 and for activation of telomere degradation by TRF2." Mol Cell Biol **22**(10): 3474-3487.

Arpino, G., V. J. Bardou, et al. (2004). "Infiltrating lobular carcinoma of the breast: tumor characteristics and clinical outcome." Breast Cancer Res **6**(3): R149-156.

Assmus, B., C. Urbich, et al. (2003). "HMG-CoA reductase inhibitors reduce senescence and increase proliferation of endothelial progenitor cells via regulation of cell cycle regulatory genes." Circ Res **92**(9): 1049-1055.

Autexier, C. and N. F. Lue (2006). "The structure and function of telomerase reverse transcriptase." Annu Rev Biochem **75**: 493-517.

Ballestar, E. (2011). "Epigenetic alterations in autoimmune rheumatic diseases." Nat Rev Rheumatol **7**(5): 263-271.

Band, V., D. Zajchowski, et al. (1990). "Tumor progression in four mammary epithelial cell lines derived from the same patient." Cancer Res **50**(22): 7351-7357.

Bannister, A. J. and T. Kouzarides (2011). "Regulation of chromatin by histone modifications." Cell Res **21**(3): 381-395.

Baumann, P. and T. R. Cech (2001). "Pot1, the putative telomere end-binding protein in fission yeast and humans." Science **292**(5519): 1171-1175.

Baumann, P. and C. Price (2010). "Pot1 and telomere maintenance." FEBS Lett **584**(17): 3779-3784.

Bestor, T. H. (2000). "The DNA methyltransferases of mammals." Hum Mol Genet **9**(16): 2395-2402.

Bhanot, M. and S. Smith (2012). "TIN2 stability is regulated by the E3 ligase Siah2." Mol Cell Biol **32**(2): 376-384.

Bianchi A (1997). "TRF1 is a dimer and bends telomeric DNA." **16**: :1785–1794.

Bianchi, A., S. Smith, et al. (1997). "TRF1 is a dimer and bends telomeric DNA." EMBO J **16**(7): 1785-1794.

Biglia, N., L. Mariani, et al. (2007). "Increased incidence of lobular breast cancer in women treated with hormone replacement therapy: implications for diagnosis, surgical and medical treatment." Endocr Relat Cancer **14**(3): 549-567.

Bilaud, T., C. Brun, et al. (1997). "Telomeric localization of TRF2, a novel human telobox protein." Nat Genet **17**(2): 236-239.

Blackburn, E. a. S., J, (2006). "Telomere Extension By Telomerase."

Blander, G. and L. Guarente (2004). "The Sir2 family of protein deacetylases." Annu Rev Biochem **73**: 417-435.

Bochkarev, A. and E. Bochkareva (2004). "From RPA to BRCA2: lessons from single-stranded DNA binding by the OB-fold." Curr Opin Struct Biol **14**(1): 36-42.

Botha, J. L., F. Bray, et al. (2003). "Breast cancer incidence and mortality trends in 16 European countries." Eur J Cancer **39**(12): 1718-1729.
Brett, D., H. Pospisil, et al. (2002). "Alternative splicing and genome complexity." Nat Genet **30**(1): 29-30.
Broccoli, D., A. Smogorzewska, et al. (1997). "Human telomeres contain two distinct Myb-related proteins, TRF1 and TRF2." Nat Genet **17**(2): 231-235.
Brockmann, R., A. Beyer, et al. (2007). "Posttranscriptional expression regulation: what determines translation rates?" PLoS Comput Biol **3**(3): e57.
Brohet, R. M., M. E. Velthuizen, et al. (2013). "Breast and ovarian cancer risks in a large series of clinically ascertained families with a high proportion of BRCA1 and BRCA2 Dutch founder mutations." J Med Genet.
Bryan, T. M. (1995). "Telomere elongation in immortal human cells without detectable telomerase activity." 4240–4248.
Bryant, D. M. and K. E. Mostov (2008). "From cells to organs: building polarized tissue." Nat Rev Mol Cell Biol **9**(11): 887-901.
Butler, K. S., W. C. Hines, et al. (2012). "Coordinate regulation between expression levels of telomere-binding proteins and telomere length in breast carcinomas." Cancer Med **1**(2): 165-175.
Byrnes, G. B., M. C. Southey, et al. (2008). "Are the so-called low penetrance breast cancer genes, ATM, BRIP1, PALB2 and CHEK2, high risk for women with strong family histories?" Breast Cancer Res **10**(3): 208.
Cabuy, E., C. Newton, et al. (2004). "Identification of subpopulations of cells with differing telomere lengths in mouse and human cell lines by flow FISH." Cytometry A **62**(2): 150-161.
Cai, F. F., C. Kohler, et al. (2011). "Epigenetic therapy for breast cancer." Int J Mol Sci **12**(7): 4465-4487.
Campisi, J. (2005). "Senescent cells, tumor suppression, and organismal aging: good citizens, bad neighbors." Cell **120**(4): 513-522.
Cantara, S., S. Capuano, et al. (2012). "Lack of mutations of the telomerase RNA component in familial papillary thyroid cancer with short telomeres." Thyroid **22**(4): 363-368.
Canudas, S., B. R. Houghtaling, et al. (2007). "Protein requirements for sister telomere association in human cells." EMBO J **26**(23): 4867-4878.
Catteau, A., W. H. Harris, et al. (1999). "Methylation of the BRCA1 promoter region in sporadic breast and ovarian cancer: correlation with disease characteristics." Oncogene **18**(11): 1957-1965.
Cawthon, R. M. (2002). "Telomere measurement by quantitative PCR." Nucleic Acids Res **30**(10): e47.
Celli, G. B. and T. de Lange (2005). "DNA processing is not required for ATM-mediated telomere damage response after TRF2 deletion." Nat Cell Biol **7**(7): 712-718.
Chen, C. L., N. S. Weiss, et al. (2002). "Hormone replacement therapy in relation to breast cancer." JAMA **287**(6): 734-741.
Chen, Y., Y. Yang, et al. (2008). "A shared docking motif in TRF1 and TRF2 used for differential recruitment of telomeric proteins." Science **319**(5866): 1092-1096.
Chiang, Y. J., M. L. Nguyen, et al. (2006). "Generation and characterization of telomere length maintenance in tankyrase 2-deficient mice." Mol Cell Biol **26**(6): 2037-2043.

Chong, L., B. van Steensel, et al. (1995). "A human telomeric protein." Science **270**(5242): 1663-1667.
Chu, K. C., R. E. Tarone, et al. (1996). "Recent trends in U.S. breast cancer incidence, survival, and mortality rates." J Natl Cancer Inst **88**(21): 1571-1579.
Colgin, L. M., K. Baran, et al. (2003). "Human POT1 facilitates telomere elongation by telomerase." Curr Biol **13**(11): 942-946.
Cong, Y. S., W. E. Wright, et al. (2002). "Human telomerase and its regulation." Microbiol Mol Biol Rev **66**(3): 407-425, table of contents.
Conomos, D., H. A. Pickett, et al. (2013). "Alternative lengthening of telomeres: remodeling the telomere architecture." Front Oncol **3**: 27.
Cook, B. D., J. N. Dynek, et al. (2002). "Role for the related poly(ADP-Ribose) polymerases tankyrase 1 and 2 at human telomeres." Mol Cell Biol **22**(1): 332-342.
Cookson, J. C. and C. A. Laughton (2009). "The levels of telomere-binding proteins in human tumours and therapeutic implications." Eur J Cancer **45**(4): 536-550.
Couch, F. J., L. M. Farid, et al. (1996). "BRCA2 germline mutations in male breast cancer cases and breast cancer families." Nat Genet **13**(1): 123-125.
Cross, D. and J. K. Burmester (2006). "Gene therapy for cancer treatment: past, present and future." Clin Med Res **4**(3): 218-227.
Cuthbert, A. P., J. Bond, et al. (1999). "Telomerase repressor sequences on chromosome 3 and induction of permanent growth arrest in human breast cancer cells." J Natl Cancer Inst **91**(1): 37-45.
D'Souza, B., F. Berdichevsky, et al. (1993). "Collagen-induced morphogenesis and expression of the alpha 2-integrin subunit is inhibited in c-erbB2-transfected human mammary epithelial cells." Oncogene **8**(7): 1797-1806.
Das, P. M. and R. Singal (2004). "DNA methylation and cancer." J Clin Oncol **22**(22): 4632-4642.
de Lange, T. (2002). "Protection of mammalian telomeres." Oncogene **21**(4): 532-540.
de Lange, T. (2005). "Shelterin: the protein complex that shapes and safeguards human telomeres." Genes Dev **19**(18): 2100-2110.
de Lange T., L., V. & Blackburn, E (2006). "Mammalian telomeres." Cold Spring Harbor Laboratory Press.
Deb, S., H. Do, et al. (2013). "PIK3CA mutations are frequently observed in BRCAX but not BRCA2 -associated male breast cancer." Breast Cancer Res **15**(4): R69.
Derradji, H., S. Bekaert, et al. (2005). "Comparison of different protocols for telomere length estimation by combination of quantitative fluorescence in situ hybridization (Q-FISH) and flow cytometry in human cancer cell lines." Anticancer Res **25**(2A): 1039-1050.
Diefenbach, J. and A. Burkle (2005). "Introduction to poly(ADP-ribose) metabolism." Cell Mol Life Sci **62**(7-8): 721-730.
Diotti, R. and D. Loayza (2011). "Shelterin complex and associated factors at human telomeres." Nucleus **2**(2): 119-135.
Donate, L. E. and M. A. Blasco (2011). "Telomeres in cancer and ageing." Philos Trans R Soc Lond B Biol Sci **366**(1561): 76-84.
Drummond, D. C., C. O. Noble, et al. (2005). "Clinical development of histone deacetylase inhibitors as anticancer agents." Annu Rev Pharmacol Toxicol **45**: 495-528.
Egger, G., G. Liang, et al. (2004). "Epigenetics in human disease and prospects for epigenetic therapy." Nature **429**(6990): 457-463.

Eisenhauer, P. B., P. Chaturvedi, et al. (2001). "Tumor necrosis factor alpha increases human cerebral endothelial cell Gb3 and sensitivity to Shiga toxin." Infect Immun **69**(3): 1889-1894.

El Idrissi, M., V. Hervieu, et al. (2013). "Cause-specific telomere factors deregulation in hepatocellular carcinoma." J Exp Clin Cancer Res **32**(1): 64.

Elizabeth H Blackburn (2006). "Telomeres and telomerase: the path from maize,Tetrahymena and yeast to human cancer and aging." NATURE MEDICINE **12**.

Esteller, M., P. G. Corn, et al. (2001). "A gene hypermethylation profile of human cancer." Cancer Res **61**(8): 3225-3229.

Esteller, M., J. M. Silva, et al. (2000). "Promoter hypermethylation and BRCA1 inactivation in sporadic breast and ovarian tumors." J Natl Cancer Inst **92**(7): 564-569.

Fairall L (2001). "Structure of the TRFH dimerization
domain of the human telomeric proteins TRF1 and TRF2." **8:**: 351–361.

Feldser, D. M., J. A. Hackett, et al. (2003). "Telomere dysfunction and the initiation of genome instability." Nat Rev Cancer **3**(8): 623-627.

Ferlay, J., E. Steliarova-Foucher, et al. (2013). "Cancer incidence and mortality patterns in Europe: estimates for 40 countries in 2012." Eur J Cancer **49**(6): 1374-1403.

Flotho, C., R. Claus, et al. (2009). "The DNA methyltransferase inhibitors azacitidine, decitabine and zebularine exert differential effects on cancer gene expression in acute myeloid leukemia cells." Leukemia **23**(6): 1019-1028.

Forstemann, K., M. Hoss, et al. (2000). "Telomerase-dependent repeat divergence at the 3' ends of yeast telomeres." Nucleic Acids Res **28**(14): 2690-2694.

Gao, J., J. Zhang, et al. (2011). "Expression of telomere binding proteins in gastric cancer and correlation with clinicopathological parameters." Asia Pac J Clin Oncol **7**(4): 339-345.

Garbe, J. C., S. Bhattacharya, et al. (2009). "Molecular distinctions between stasis and telomere attrition senescence barriers shown by long-term culture of normal human mammary epithelial cells." Cancer Res **69**(19): 7557-7568.

Gazdar, A. F., V. Kurvari, et al. (1998). "Characterization of paired tumor and non-tumor cell lines established from patients with breast cancer." Int J Cancer **78**(6): 766-774.

Gelmini, S., S. Quattrone, et al. (2007). "Tankyrase-1 mRNA expression in bladder cancer and paired urine sediment: preliminary experience." Clin Chem Lab Med **45**(7): 862-866.

Gensch, C., Y. P. Clever, et al. (2007). "The PPAR-gamma agonist pioglitazone increases neoangiogenesis and prevents apoptosis of endothelial progenitor cells." Atherosclerosis **192**(1): 67-74.

Ghoshal, K., J. Datta, et al. (2005). "5-Aza-deoxycytidine induces selective degradation of DNA methyltransferase 1 by a proteasomal pathway that requires the KEN box, bromo-adjacent homology domain, and nuclear localization signal." Mol Cell Biol **25**(11): 4727-4741.

Girault, I., S. Tozlu, et al. (2003). "Expression analysis of DNA methyltransferases 1, 3A, and 3B in sporadic breast carcinomas." Clin Cancer Res **9**(12): 4415-4422.

Glisovic, T., J. L. Bachorik, et al. (2008). "RNA-binding proteins and post-transcriptional gene regulation." FEBS Lett **582**(14): 1977-1986.

Goffin, J. and E. Eisenhauer (2002). "DNA methyltransferase inhibitors-state of the art." Ann Oncol **13**(11): 1699-1716.

Gotzsche, P. C. and M. Nielsen (2011). "Screening for breast cancer with mammography." Cochrane Database Syst Rev(1): CD001877.

Graff, J. R., J. G. Herman, et al. (1995). "E-cadherin expression is silenced by DNA hypermethylation in human breast and prostate carcinomas." Cancer Res **55**(22): 5195-5199.

Greider, C. W. (1996). "Telomere length regulation." Annu Rev Biochem **65**: 337-365.

Griffith, J., A. Bianchi, et al. (1998). "TRF1 promotes parallel pairing of telomeric tracts in vitro." J Mol Biol **278**(1): 79-88.

Griffith, J. D., L. Comeau, et al. (1999). "Mammalian telomeres end in a large duplex loop." Cell **97**(4): 503-514.

Ha, G. H., H. S. Kim, et al. (2012). "Tankyrase-1 function at telomeres and during mitosis is regulated by Polo-like kinase-1-mediated phosphorylation." Cell Death Differ **19**(2): 321-332.

Hackett, A. J., H. S. Smith, et al. (1977). "Two syngeneic cell lines from human breast tissue: the aneuploid mammary epithelial (Hs578T) and the diploid myoepithelial (Hs578Bst) cell lines." J Natl Cancer Inst **58**(6): 1795-1806.

Hanahan, D. and R. A. Weinberg (2000). "The hallmarks of cancer." Cell **100**(1): 57-70.

Hanaoka (2005). "Comparison between TRF2 and TRF1 of their telomeric

DNA-bound structures and DNA-binding activities." **14:**: 119–130.

Harley, C. B., A. B. Futcher, et al. (1990). "Telomeres shorten during ageing of human fibroblasts." Nature **345**(6274): 458-460.

Hartwell, L. H., J. J. Hopfield, et al. (1999). "From molecular to modular cell biology." Nature **402**(6761 Suppl): C47-52.

Hayflick, L. and P. S. Moorhead (1961). "The serial cultivation of human diploid cell strains." Exp Cell Res **25**: 585-621.

He, H., A. S. Multani, et al. (2006). "POT1b protects telomeres from end-to-end chromosomal fusions and aberrant homologous recombination." EMBO J **25**(21): 5180-5190.

Hockemeyer, D., W. Palm, et al. (2007). "Telomere protection by mammalian Pot1 requires interaction with Tpp1." Nat Struct Mol Biol **14**(8): 754-761.

Hockemeyer, D., W. Palm, et al. (2008). "Engineered telomere degradation models dyskeratosis congenita." Genes Dev **22**(13): 1773-1785.

Hockemeyer, D., A. J. Sfeir, et al. (2005). "POT1 protects telomeres from a transient DNA damage response and determines how human chromosomes end." EMBO J **24**(14): 2667-2678.

Holliday, R. (1991). "Mutations and epimutations in mammalian cells." Mutat Res **250**(1-2): 351-363.

Holysz, H., N. Lipinska, et al. (2013). "Telomerase as a useful target in cancer fighting-the breast cancer case." Tumour Biol **34**(3): 1371-1380.

Hou, G., D. N. Huang, et al. (2006). "Human pot1 gene exon12 mutation screening in cultured human carcinoma cell strains (lines)." J South Med Univ **26**(7): 991-993.

Houghtaling BR, C. L., Chang W, Smith S (2004). "A dynamic molecular link between the telomere length regulator TRF1 and the chromosome end protector TRF2." **14**: 1621–1631.

Houghtaling, B. R., L. Cuttonaro, et al. (2004). "A dynamic molecular link between the telomere length regulator TRF1 and the chromosome end protector TRF2." Curr Biol **14**(18): 1621-1631.

Hsiao, S. J. and S. Smith (2008). "Tankyrase function at telomeres, spindle poles, and beyond." Biochimie **90**(1): 83-92.
Hu, H., Y. Zhang, et al. (2010). "Expression of TRF1, TRF2, TIN2, TERT, KU70, and BRCA1 proteins is associated with telomere shortening and may contribute to multistage carcinogenesis of gastric cancer." J Cancer Res Clin Oncol **136**(9): 1407-1414.
Hwang, H., N. Buncher, et al. (2012). "POT1-TPP1 regulates telomeric overhang structural dynamics." Structure **20**(11): 1872-1880.
Isabelle, M., X. Moreel, et al. (2010). "Investigation of PARP-1, PARP-2, and PARG interactomes by affinity-purification mass spectrometry." Proteome Sci **8**: 22.
Jacobs, J. J. (2013). "Loss of telomere protection: consequences and opportunities." Front Oncol **3**: 88.
Jacot, W., S. Thezenas, et al. (2013). "BRCA1 promoter hypermethylation, 53BP1 protein expression and PARP-1 activity as biomarkers of DNA repair deficit in breast cancer." BMC Cancer **13**(1): 523.
Jaenisch, R. and A. Bird (2003). "Epigenetic regulation of gene expression: how the genome integrates intrinsic and environmental signals." Nat Genet **33 Suppl**: 245-254.
Jirtle, R. L. and M. K. Skinner (2007). "Environmental epigenomics and disease susceptibility." Nat Rev Genet **8**(4): 253-262.
Johnson, S. M., J. A. Shaw, et al. (2002). "Sporadic breast cancer in young women: prevalence of loss of heterozygosity at p53, BRCA1 and BRCA2." Int J Cancer **98**(2): 205-209.
Jones, P. A. and S. B. Baylin (2007). "The epigenomics of cancer." Cell **128**(4): 683-692.
Jurkowski, T. P. and A. Jeltsch (2011). "On the evolutionary origin of eukaryotic DNA methyltransferases and Dnmt2." PLoS One **6**(11): e28104.
Kaighn, M. E., K. S. Narayan, et al. (1979). "Establishment and characterization of a human prostatic carcinoma cell line (PC-3)." Invest Urol **17**(1): 16-23.
Kaminker, P. G., S. H. Kim, et al. (2001). "TANK2, a new TRF1-associated poly(ADP-ribose) polymerase, causes rapid induction of cell death upon overexpression." J Biol Chem **276**(38): 35891-35899.
Kang, H. F., Z. J. Dai, et al. (2013). "RUNX3 gene promoter demethylation by 5-Aza-CdR induces apoptosis in breast cancer MCF-7 cell line." Onco Targets Ther **6**: 411-417.
Karlseder, J., D. Broccoli, et al. (1999). "p53- and ATM-dependent apoptosis induced by telomeres lacking TRF2." Science **283**(5406): 1321-1325.
Kass, S. U., D. Pruss, et al. (1997). "How does DNA methylation repress transcription?" Trends Genet **13**(11): 444-449.
Kelleher, C., I. Kurth, et al. (2005). "Human protection of telomeres 1 (POT1) is a negative regulator of telomerase activity in vitro." Mol Cell Biol **25**(2): 808-818.
Kendellen, M. F., K. S. Barrientos, et al. (2009). "POT1 association with TRF2 regulates telomere length." Mol Cell Biol **29**(20): 5611-5619.
Kenemans, P., R. A. Verstraeten, et al. (2004). "Oncogenic pathways in hereditary and sporadic breast cancer." Maturitas **49**(1): 34-43.
Kibe, T., G. A. Osawa, et al. (2010). "Telomere protection by TPP1 is mediated by POT1a and POT1b." Mol Cell Biol **30**(4): 1059-1066.
Kim, J. K., M. Samaranayake, et al. (2009). "Epigenetic mechanisms in mammals." Cell Mol Life Sci **66**(4): 596-612.

Kim, M. K. and S. Smith (2013). "Persistent telomere cohesion triggers a prolonged anaphase." Mol Biol Cell.
Kim, N. W., M. A. Piatyszek, et al. (1994). "Specific association of human telomerase activity with immortal cells and cancer." Science **266**(5193): 2011-2015.
Kim, S. H., C. Beausejour, et al. (2004). "TIN2 mediates functions of TRF2 at human telomeres." J Biol Chem **279**(42): 43799-43804.
Kim, S. H., A. R. Davalos, et al. (2008). "Telomere dysfunction and cell survival: roles for distinct TIN2-containing complexes." J Cell Biol **181**(3): 447-460.
Kim, S. H., P. Kaminker, et al. (1999). "TIN2, a new regulator of telomere length in human cells." Nat Genet **23**(4): 405-412.
Kondo, T., N. Oue, et al. (2004). "Expression of POT1 is associated with tumor stage and telomere length in gastric carcinoma." Cancer Res **64**(2): 523-529.
Kondo, Y., L. Shen, et al. (2003). "Critical role of histone methylation in tumor suppressor gene silencing in colorectal cancer." Mol Cell Biol **23**(1): 206-215.
Kouzarides, T. (2007). "Chromatin modifications and their function." Cell **128**(4): 693-705.
Kuilman, T., C. Michaloglou, et al. (2010). "The essence of senescence." Genes Dev **24**(22): 2463-2479.
Labarge, M. A., J. C. Garbe, et al. (2013). "Processing of human reduction mammoplasty and mastectomy tissues for cell culture." J Vis Exp(71).
Lacey, J. V., Jr., S. S. Devesa, et al. (2002). "Recent trends in breast cancer incidence and mortality." Environ Mol Mutagen **39**(2-3): 82-88.
Lasfargues, E. Y., W. G. Coutinho, et al. (1978). "Isolation of two human tumor epithelial cell lines from solid breast carcinomas." J Natl Cancer Inst **61**(4): 967-978.
Lasfargues, E. Y. and L. Ozzello (1958). "Cultivation of human breast carcinomas." J Natl Cancer Inst **21**(6): 1131-1147.
Latrick, C. M. and T. R. Cech (2010). "POT1-TPP1 enhances telomerase processivity by slowing primer dissociation and aiding translocation." EMBO J **29**(5): 924-933.
Lee, M. E., S. Y. Rha, et al. (2008). "Variation of the 3' telomeric overhang lengths in human cells." Cancer Lett **264**(1): 107-118.
Lehtio, L., R. Collins, et al. (2008). "Zinc binding catalytic domain of human tankyrase 1." J Mol Biol **379**(1): 136-145.
Lei, M., E. R. Podell, et al. (2004). "Structure of human POT1 bound to telomeric single-stranded DNA provides a model for chromosome end-protection." Nat Struct Mol Biol **11**(12): 1223-1229.
Lei, M., A. J. Zaug, et al. (2005). "Switching human telomerase on and off with hPOT1 protein in vitro." J Biol Chem **280**(21): 20449-20456.
Levitus, M., Q. Waisfisz, et al. (2005). "The DNA helicase BRIP1 is defective in Fanconi anemia complementation group J." Nat Genet **37**(9): 934-935.
Levy, M. Z., R. C. Allsopp, et al. (1992). "Telomere end-replication problem and cell aging." J Mol Biol **225**(4): 951-960.
Lewis, K. A. and D. S. Wuttke (2012). "Telomerase and telomere-associated proteins: structural insights into mechanism and evolution." Structure **20**(1): 28-39.
Li, C. I., N. S. Weiss, et al. (2000). "Hormone replacement therapy in relation to risk of lobular and ductal breast carcinoma in middle-aged women." Cancer **88**(11): 2570-2577.

Lin, Y. S., A. Y. Shaw, et al. (2011). "Identification of novel DNA methylation inhibitors via a two-component reporter gene system." J Biomed Sci **18**: 3.
Litman, R., M. Peng, et al. (2005). "BACH1 is critical for homologous recombination and appears to be the Fanconi anemia gene product FANCJ." Cancer Cell **8**(3): 255-265.
Liu, D., M. S. O'Connor, et al. (2004). "Telosome, a mammalian telomere-associated complex formed by multiple telomeric proteins." J Biol Chem **279**(49): 51338-51342.
Liu, D., A. Safari, et al. (2004). "PTOP interacts with POT1 and regulates its localization to telomeres." Nat Cell Biol **6**(7): 673-680.
Liu, J., Y. Zhang, et al. (2012). "5-Aza-2'-deoxycytidine induces cytotoxicity in BGC-823 cells via DNA methyltransferase 1 and 3a independent of p53 status." Oncol Rep **28**(2): 545-552.
Liu, Y., B. E. Snow, et al. (2000). "Telomerase-associated protein TEP1 is not essential for telomerase activity or telomere length maintenance in vivo." Mol Cell Biol **20**(21): 8178-8184.
Loayza D, d. L. T. (2003). "POT1 as a terminal transducer of TRF1 telomere length control." **424**: 1013–1018.
Loayza, D., H. Parsons, et al. (2004). "DNA binding features of human POT1: a nonamer 5'-TAGGGTTAG-3' minimal binding site, sequence specificity, and internal binding to multimeric sites." J Biol Chem **279**(13): 13241-13248.
Loayza, D. a. D. L., T (2003). "POT1 as a terminal transducer of TRF1 telomere length control." Nature **424**: 1013-1018.
Loveday, C., C. Turnbull, et al. (2011). "Germline mutations in RAD51D confer susceptibility to ovarian cancer." Nat Genet **43**(9): 879-882.
Low, K. C. and V. Tergaonkar (2013). "Telomerase: central regulator of all of the hallmarks of cancer." Trends Biochem Sci **38**(9): 426-434.
Lu, L., C. Zhang, et al. (2011). "Telomerase expression and telomere length in breast cancer and their associations with adjuvant treatment and disease outcome." Breast Cancer Res **13**(3): R56.
Lu, Y., B. Wei, et al. (2013). "How will telomeric complex be further contributed to our longevity? - the potential novel biomarkers of telomere complex counteracting both aging and cancer." Protein Cell **4**(8): 573-581.
Lund, A. H. and M. van Lohuizen (2004). "Epigenetics and cancer." Genes Dev **18**(19): 2315-2335.
Lundberg, E., L. Fagerberg, et al. (2010). "Defining the transcriptome and proteome in three functionally different human cell lines." Mol Syst Biol **6**: 450.
Ly, D., D. Forman, et al. (2013). "An international comparison of male and female breast cancer incidence rates." Int J Cancer **132**(8): 1918-1926.
Makarov, V. L., Y. Hirose, et al. (1997). "Long G tails at both ends of human chromosomes suggest a C strand degradation mechanism for telomere shortening." Cell **88**(5): 657-666.
Maldonado, E., M. Hampsey, et al. (1999). "Repression: targeting the heart of the matter." Cell **99**(5): 455-458.
Mangia, A., A. Malfettone, et al. (2011). "Old and new concepts in histopathological characterization of familial breast cancer." Ann Oncol **22 Suppl 1**: i24-30.

Margueron, R., V. Duong, et al. (2004). "Histone deacetylase inhibition and estrogen receptor alpha levels modulate the transcriptional activity of partial antiestrogens." J Mol Endocrinol **32**(2): 583-594.
Marks, J. R., A. M. Davidoff, et al. (1991). "Overexpression and mutation of p53 in epithelial ovarian cancer." Cancer Res **51**(11): 2979-2984.
Martin, M. (2006). "Molecular biology of breast cancer." Clin Transl Oncol **8**(1): 7-14.
Martinez, P. and M. A. Blasco (2010). "Role of shelterin in cancer and aging." Aging Cell **9**(5): 653-666.
Martinez, P., M. Thanasoula, et al. (2010). "Mammalian Rap1 controls telomere function and gene expression through binding to telomeric and extratelomeric sites." Nat Cell Biol **12**(8): 768-780.
Maslov, A. Y., M. Lee, et al. (2012). "5-aza-2'-deoxycytidine-induced genome rearrangements are mediated by DNMT1." Oncogene **31**(50): 5172-5179.
Matsutani, N., H. Yokozaki, et al. (2001). "Expression of telomeric repeat binding factor 1 and 2 and TRF1-interacting nuclear protein 2 in human gastric carcinomas." Int J Oncol **19**(3): 507-512.
McClintock, B. (1941). "The Stability of Broken Ends of Chromosomes in Zea Mays." Genetics **26**(2): 234-282.
McIlrath, J., S. D. Bouffler, et al. (2001). "Telomere length abnormalities in mammalian radiosensitive cells." Cancer Res **61**(3): 912-915.
Meeker, A. K., J. L. Hicks, et al. (2004). "Telomere shortening occurs in subsets of normal breast epithelium as well as in situ and invasive carcinoma." Am J Pathol **164**(3): 925-935.
Meindl, A., H. Hellebrand, et al. (2010). "Germline mutations in breast and ovarian cancer pedigrees establish RAD51C as a human cancer susceptibility gene." Nat Genet **42**(5): 410-414.
Meng, C. F., D. Q. Dai, et al. (2008). "[Effects of 5-Aza-2'-deoxycytidine and trichostatin A on DNA methylation and expression of hMLH1 in ovarian cancer cell line COC1/DDP]." Ai Zheng **27**(12): 1251-1255.
Meyerson, M., C. M. Counter, et al. (1997). "hEST2, the putative human telomerase catalytic subunit gene, is up-regulated in tumor cells and during immortalization." Cell **90**(4): 785-795.
Miller, L. D., J. Smeds, et al. (2005). "An expression signature for p53 status in human breast cancer predicts mutation status, transcriptional effects, and patient survival." Proc Natl Acad Sci U S A **102**(38): 13550-13555.
Mirza, S., G. Sharma, et al. (2010). "Demethylating agent 5-aza-2-deoxycytidine enhances susceptibility of breast cancer cells to anticancer agents." Mol Cell Biochem **342**(1-2): 101-109.
Misra, S., P. V. Mahajan, et al. (2008). "Safety of procedural sedation and analgesia in children less than 2 years of age in a pediatric emergency department." Int J Emerg Med **1**(3): 173-177.
Mossman, D., K. T. Kim, et al. (2010). "Demethylation by 5-aza-2'-deoxycytidine in colorectal cancer cells targets genomic DNA whilst promoter CpG island methylation persists." BMC Cancer **10**: 366.
Muller (1938). "The remaking of chromosomes." Collecting Net **8**: 182-195.

Murata, H., N. H. Khattar, et al. (2002). "Genetic and epigenetic modification of mismatch repair genes hMSH2 and hMLH1 in sporadic breast cancer with microsatellite instability." Oncogene **21**(37): 5696-5703.

Newbold (2005). "Cellular immortalization and telomerase activation in cancer." Oxford University Press: 107-185.

O'Callaghan, N. J. and M. Fenech (2011). "A quantitative PCR method for measuring absolute telomere length." Biol Proced Online **13**: 3.

O'Connor, M. S., A. Safari, et al. (2004). "The human Rap1 protein complex and modulation of telomere length." J Biol Chem **279**(27): 28585-28591.

O'Connor, M. S., A. Safari, et al. (2006). "A critical role for TPP1 and TIN2 interaction in high-order telomeric complex assembly." Proc Natl Acad Sci U S A **103**(32): 11874-11879.

Okano, M., S. Xie, et al. (1998). "Dnmt2 is not required for de novo and maintenance methylation of viral DNA in embryonic stem cells." Nucleic Acids Res **26**(11): 2536-2540.

Olovnikov, A. M. (1973). "A theory of marginotomy. The incomplete copying of template margin in enzymic synthesis of polynucleotides and biological significance of the phenomenon." J Theor Biol **41**(1): 181-190.

Ottaviano, Y. L., J. P. Issa, et al. (1994). "Methylation of the estrogen receptor gene CpG island marks loss of estrogen receptor expression in human breast cancer cells." Cancer Res **54**(10): 2552-2555.

Palm, W. and T. de Lange (2008). "How shelterin protects mammalian telomeres." Annu Rev Genet **42**: 301-334.

Paraskeva, E., A. Atzberger, et al. (1998). "A translational repression assay procedure (TRAP) for RNA-protein interactions in vivo." Proc Natl Acad Sci U S A **95**(3): 951-956.

Pelttari, L. M., J. Kiiski, et al. (2012). "A Finnish founder mutation in RAD51D: analysis in breast, ovarian, prostate, and colorectal cancer." J Med Genet **49**(7): 429-432.

Plentz, R. R., S. U. Wiemann, et al. (2003). "Telomere shortening of epithelial cells characterises the adenoma-carcinoma transition of human colorectal cancer." Gut **52**(9): 1304-1307.

Poncet, D., A. Belleville, et al. (2008). "Changes in the expression of telomere maintenance genes suggest global telomere dysfunction in B-chronic lymphocytic leukemia." Blood **111**(4): 2388-2391.

Pradhan, S., A. Bacolla, et al. (1999). "Recombinant human DNA (cytosine-5) methyltransferase. I. Expression, purification, and comparison of de novo and maintenance methylation." J Biol Chem **274**(46): 33002-33010.

Pryzbylkowski, P., O. Obajimi, et al. (2008). "Trichostatin A and 5 Aza-2' deoxycytidine decrease estrogen receptor mRNA stability in ER positive MCF7 cells through modulation of HuR." Breast Cancer Res Treat **111**(1): 15-25.

Raices, M., R. E. Verdun, et al. (2008). "C. elegans telomeres contain G-strand and C-strand overhangs that are bound by distinct proteins." Cell **132**(5): 745-757.

Rakha, E. A., M. E. El-Sayed, et al. (2008). "Prognostic significance of Nottingham histologic grade in invasive breast carcinoma." J Clin Oncol **26**(19): 3153-3158.

Ramsay, A. J., V. Quesada, et al. (2013). "POT1 mutations cause telomere dysfunction in chronic lymphocytic leukemia." Nat Genet **45**(5): 526-530.

Reichenbach, P., M. Hoss, et al. (2003). "A human homolog of yeast Est1 associates with telomerase and uncaps chromosome ends when overexpressed." Curr Biol **13**(7): 568-574.

Reid, S., D. Schindler, et al. (2007). "Biallelic mutations in PALB2 cause Fanconi anemia subtype FA-N and predispose to childhood cancer." Nat Genet **39**(2): 162-164.

Robertson, K. D. (2001). "DNA methylation, methyltransferases, and cancer." Oncogene **20**(24): 3139-3155.

Rodier, F. and J. Campisi (2011). "Four faces of cellular senescence." J Cell Biol **192**(4): 547-556.

Rosenberg, L. U., C. Magnusson, et al. (2006). "Menopausal hormone therapy and other breast cancer risk factors in relation to the risk of different histological subtypes of breast cancer: a case-control study." Breast Cancer Res **8**(1): R11.

Roth, J. A. and R. J. Cristiano (1997). "Gene therapy for cancer: what have we done and where are we going?" J Natl Cancer Inst **89**(1): 21-39.

Roth, S. Y., J. M. Denu, et al. (2001). "Histone acetyltransferases." Annu Rev Biochem **70**: 81-120.

Royle, N. J., J. Foxon, et al. (2008). "Telomere length maintenance--an ALTernative mechanism." Cytogenet Genome Res **122**(3-4): 281-291.

Rubin, R. L. (2005). "Drug-induced lupus." Toxicology **209**(2): 135-147.

Sado, T., M. H. Fenner, et al. (2000). "X inactivation in the mouse embryo deficient for Dnmt1: distinct effect of hypomethylation on imprinted and random X inactivation." Dev Biol **225**(2): 294-303.

Salhab, M., W. G. Jiang, et al. (2008). "The expression of gene transcripts of telomere-associated genes in human breast cancer: correlation with clinico-pathological parameters and clinical outcome." Breast Cancer Res Treat **109**(1): 35-46.

Sarzi-Puttini, P., F. Atzeni, et al. (2005). "Drug-induced lupus erythematosus." Autoimmunity **38**(7): 507-518.

Saslow, D., C. Boetes, et al. (2007). "American Cancer Society guidelines for breast screening with MRI as an adjunct to mammography." CA Cancer J Clin **57**(2): 75-89.

Sauntharajah, Y., C. A. Hillery, et al. (2003). "Effects of 5-aza-2'-deoxycytidine on fetal hemoglobin levels, red cell adhesion, and hematopoietic differentiation in patients with sickle cell disease." Blood **102**(12): 3865-3870.

Savage, S. A., S. J. Chanock, et al. (2007). "Genetic variation in five genes important in telomere biology and risk for breast cancer." Br J Cancer **97**(6): 832-836.

Sbodio, J. I., H. F. Lodish, et al. (2002). "Tankyrase-2 oligomerizes with tankyrase-1 and binds to both TRF1 (telomere-repeat-binding factor 1) and IRAP (insulin-responsive aminopeptidase)." Biochem J **361**(Pt 3): 451-459.

Schmitz, A. C., D. Gianfelice, et al. (2008). "Image-guided focused ultrasound ablation of breast cancer: current status, challenges, and future directions." Eur Radiol **18**(7): 1431-1441.

Schoeftner, S. and M. A. Blasco (2008). "Developmentally regulated transcription of mammalian telomeres by DNA-dependent RNA polymerase II." Nat Cell Biol **10**(2): 228-236.

Schwanhausser, B., D. Busse, et al. (2011). "Global quantification of mammalian gene expression control." Nature **473**(7347): 337-342.

Seimiya, H., Y. Muramatsu, et al. (2004). "Functional subdomain in the ankyrin domain of tankyrase 1 required for poly(ADP-ribosyl)ation of TRF1 and telomere elongation." Mol Cell Biol **24**(5): 1944-1955.
Selkirk, S. M. (2004). "Gene therapy in clinical medicine." Postgrad Med J **80**(948): 560-570.
Sfeir, A. and T. de Lange (2012). "Removal of shelterin reveals the telomere end-protection problem." Science **336**(6081): 593-597.
Shampay, J., J. W. Szostak, et al. (1984). "DNA sequences of telomeres maintained in yeast." Nature **310**(5973): 154-157.
Sharma, S., T. K. Kelly, et al. (2010). "Epigenetics in cancer." Carcinogenesis **31**(1): 27-36.
Shay, J. W., O. M. Pereira-Smith, et al. (1991). "A role for both RB and p53 in the regulation of human cellular senescence." Exp Cell Res **196**(1): 33-39.
Shay, J. W. and W. E. Wright (2005). "Senescence and immortalization: role of telomeres and telomerase." Carcinogenesis **26**(5): 867-874.
Shen, J., M. D. Gammon, et al. (2010). "Multiple genetic variants in telomere pathway genes and breast cancer risk." Cancer Epidemiol Biomarkers Prev **19**(1): 219-228.
Shippen-Lentz, D. and E. H. Blackburn (1989). "Telomere terminal transferase activity from Euplotes crassus adds large numbers of TTTTGGGG repeats onto telomeric primers." Mol Cell Biol **9**(6): 2761-2764.
Simpson, P. T., T. Gale, et al. (2003). "The diagnosis and management of pre-invasive breast disease: pathology of atypical lobular hyperplasia and lobular carcinoma in situ." Breast Cancer Res **5**(5): 258-262.
Singal, R. and G. D. Ginder (1999). "DNA methylation." Blood **93**(12): 4059-4070.
Smith, S., I. Giriat, et al. (1998). "Tankyrase, a poly(ADP-ribose) polymerase at human telomeres." Science **282**(5393): 1484-1487.
Smogorzewska, A. and T. de Lange (2004). "Regulation of telomerase by telomeric proteins." Annu Rev Biochem **73**: 177-208.
Smogorzewska, A., B. van Steensel, et al. (2000). "Control of human telomere length by TRF1 and TRF2." Mol Cell Biol **20**(5): 1659-1668.
Soohoo, C. Y., R. Shi, et al. (2011). "Telomerase inhibitor PinX1 provides a link between TRF1 and telomerase to prevent telomere elongation." J Biol Chem **286**(5): 3894-3906.
Soule, H. D., J. Vazguez, et al. (1973). "A human cell line from a pleural effusion derived from a breast carcinoma." J Natl Cancer Inst **51**(5): 1409-1416.
Sputova, K., J. C. Garbe, et al. (2013). "Aging phenotypes in cultured normal human mammary epithelial cells are correlated with decreased telomerase activity independent of telomere length." Genome Integr **4**(1): 4.
Spyridopoulos, I., J. Haendeler, et al. (2004). "Statins enhance migratory capacity by upregulation of the telomere repeat-binding factor TRF2 in endothelial progenitor cells." Circulation **110**(19): 3136-3142.
Squires, J. E., H. R. Patel, et al. (2012). "Widespread occurrence of 5-methylcytosine in human coding and non-coding RNA." Nucleic Acids Res **40**(11): 5023-5033.
Stansel, R. M., T. de Lange, et al. (2001). "T-loop assembly in vitro involves binding of TRF2 near the 3' telomeric overhang." EMBO J **20**(19): 5532-5540.
Steinert, S., J. W. Shay, et al. (2004). "Modification of subtelomeric DNA." Mol Cell Biol **24**(10): 4571-4580.
Stewart, S. A., I. Ben-Porath, et al. (2003). "Erosion of the telomeric single-strand overhang at replicative senescence." Nat Genet **33**(4): 492-496.

Stewart, S. A. and R. A. Weinberg (2006). "Telomeres: cancer to human aging." Annu Rev Cell Dev Biol **22**: 531-557.

Stresemann, C., B. Brueckner, et al. (2006). "Functional diversity of DNA methyltransferase inhibitors in human cancer cell lines." Cancer Res **66**(5): 2794-2800.

Suwaki, N., K. Klare, et al. (2011). "RAD51 paralogs: roles in DNA damage signalling, recombinational repair and tumorigenesis." Semin Cell Dev Biol **22**(8): 898-905.

Takai, K. K., T. Kibe, et al. (2011). "Telomere protection by TPP1/POT1 requires tethering to TIN2." Mol Cell **44**(4): 647-659.

Tejera, A. M., M. Stagno d'Alcontres, et al. (2010). "TPP1 is required for TERT recruitment, telomere elongation during nuclear reprogramming, and normal skin development in mice." Dev Cell **18**(5): 775-789.

Theobald, D. L., R. M. Mitton-Fry, et al. (2003). "Nucleic acid recognition by OB-fold proteins." Annu Rev Biophys Biomol Struct **32**: 115-133.

Tian, Q., S. B. Stepaniants, et al. (2004). "Integrated genomic and proteomic analyses of gene expression in Mammalian cells." Mol Cell Proteomics **3**(10): 960-969.

Tischkowitz, M., M. Capanu, et al. (2012). "Rare germline mutations in PALB2 and breast cancer risk: a population-based study." Hum Mutat **33**(4): 674-680.

Turek-Plewa, J. and P. P. Jagodzinski (2005). "The role of mammalian DNA methyltransferases in the regulation of gene expression." Cell Mol Biol Lett **10**(4): 631-647.

van Leth, F., S. Andrews, et al. (2005). "The effect of baseline CD4 cell count and HIV-1 viral load on the efficacy and safety of nevirapine or efavirenz-based first-line HAART." AIDS **19**(5): 463-471.

van Steensel, B. and T. de Lange (1997). "Control of telomere length by the human telomeric protein TRF1." Nature **385**(6618): 740-743.

Venturelli, S., S. Armeanu, et al. (2007). "Epigenetic combination therapy as a tumor-selective treatment approach for hepatocellular carcinoma." Cancer **109**(10): 2132-2141.

Vera, E. and M. A. Blasco (2012). "Beyond average: potential for measurement of short telomeres." Aging (Albany NY) **4**(6): 379-392.

Virnig, B. A., T. M. Tuttle, et al. (2010). "Ductal carcinoma in situ of the breast: a systematic review of incidence, treatment, and outcomes." J Natl Cancer Inst **102**(3): 170-178.

Vogel, C., S. Abreu Rde, et al. (2010). "Sequence signatures and mRNA concentration can explain two-thirds of protein abundance variation in a human cell line." Mol Syst Biol **6**: 400.

Wan, S. M., J. Tie, et al. (2011). "Silencing of the hPOT1 gene by RNA inference promotes apoptosis and inhibits proliferation and aggressive phenotype of gastric cancer cells, likely through up-regulating PinX1 expression." J Clin Pathol **64**(12): 1051-1057.

Wang F (2007). "The POT1-TPP1 telomere complex is a
telomerase processivity factor." Nature **445**: 506-510.

Wang, F., E. R. Podell, et al. (2007). "The POT1-TPP1 telomere complex is a telomerase processivity factor." Nature **445**(7127): 506-510.

Watson, J. D. (1972). "Origin of concatemeric T7 DNA." Nat New Biol **239**(94): 197-201.

Wei, C. and M. Price (2003). "Protecting the terminus: t-loops and telomere end-binding proteins." Cell Mol Life Sci **60**(11): 2283-2294.

Weidner, N., J. P. Semple, et al. (1991). "Tumor angiogenesis and metastasis--correlation in invasive breast carcinoma." N Engl J Med **324**(1): 1-8.

Weigelt, B., H. M. Horlings, et al. (2008). "Refinement of breast cancer classification by molecular characterization of histological special types." J Pathol **216**(2): 141-150.

Wiechmann, L. and H. M. Kuerer (2008). "The molecular journey from ductal carcinoma in situ to invasive breast cancer." Cancer **112**(10): 2130-2142.

Wojtyla, A., M. Gladych, et al. (2011). "Human telomerase activity regulation." Mol Biol Rep **38**(5): 3339-3349.

Wozniak, R. J., W. T. Klimecki, et al. (2007). "5-Aza-2'-deoxycytidine-mediated reductions in G9A histone methyltransferase and histone H3 K9 di-methylation levels are linked to tumor suppressor gene reactivation." Oncogene **26**(1): 77-90.

Wright, W. E., O. M. Pereira-Smith, et al. (1989). "Reversible cellular senescence: implications for immortalization of normal human diploid fibroblasts." Mol Cell Biol **9**(7): 3088-3092.

Wright, W. E. and J. W. Shay (2005). "Telomere-binding factors and general DNA repair." Nat Genet **37**(2): 116-118.

Wyatt, H. D., S. C. West, et al. (2010). "InTERTpreting telomerase structure and function." Nucleic Acids Res **38**(17): 5609-5622.

Xin H, L. D., Wan M, Safari A, Kim H (2007). "TPP1 is a homologue of ciliate TEBP-beta and interacts with POT1 to recruit telomerase." **445**: 559–562.

Xin, H., D. Liu, et al. (2007). "TPP1 is a homologue of ciliate TEBP-beta and interacts with POT1 to recruit telomerase." Nature **445**(7127): 559-562.

Yamada, M., N. Tsuji, et al. (2002). "Down-regulation of TRF1, TRF2 and TIN2 genes is important to maintain telomeric DNA for gastric cancers." Anticancer Res **22**(6A): 3303-3307.

Yang, Q., R. Zhang, et al. (2007). "Functional diversity of human protection of telomeres 1 isoforms in telomere protection and cellular senescence." Cancer Res **67**(24): 11677-11686.

Yang, Q., Y. L. Zheng, et al. (2005). "POT1 and TRF2 cooperate to maintain telomeric integrity." Mol Cell Biol **25**(3): 1070-1080.

Yang, X., A. T. Ferguson, et al. (2000). "Transcriptional activation of estrogen receptor alpha in human breast cancer cells by histone deacetylase inhibition." Cancer Res **60**(24): 6890-6894.

Yang, X., D. L. Phillips, et al. (2001). "Synergistic activation of functional estrogen receptor (ER)-alpha by DNA methyltransferase and histone deacetylase inhibition in human ER-alpha-negative breast cancer cells." Cancer Res **61**(19): 7025-7029.

Ye, J. Z. and T. de Lange (2004). "TIN2 is a tankyrase 1 PARP modulator in the TRF1 telomere length control complex." Nat Genet **36**(6): 618-623.

Ye, J. Z., J. R. Donigian, et al. (2004). "TIN2 binds TRF1 and TRF2 simultaneously and stabilizes the TRF2 complex on telomeres." J Biol Chem **279**(45): 47264-47271.

Ye, J. Z., D. Hockemeyer, et al. (2004). "POT1-interacting protein PIP1: a telomere length regulator that recruits POT1 to the TIN2/TRF1 complex." Genes Dev **18**(14): 1649-1654.

Yoder, J. A. and T. H. Bestor (1998). "A candidate mammalian DNA methyltransferase related to pmt1p of fission yeast." Hum Mol Genet **7**(2): 279-284.

Yu, Y. H., C. Liang, et al. (2010). "Diagnostic value of vacuum-assisted breast biopsy for breast carcinoma: a meta-analysis and systematic review." Breast Cancer Res Treat **120**(2): 469-479.

Zemliakova, V. V., A. I. Zhevlova, et al. (2003). "[Abnormal methylation of several tumor suppressor genes in sporadic breast cancer]." Mol Biol (Mosk) **37**(4): 696-703.

Zhang, C., Y. Ling, et al. (2012). "The silencing of RECK gene is associated with promoter hypermethylation and poor survival in hepatocellular carcinoma." Int J Biol Sci **8**(4): 451-458.

Zhang, F., Li, Qin (2008). "Effects of trichostatin A (TSA) on growth and gene expression in Hela cells." Journal of Clinical Oncology **7**.

Zhong, F. L., L. F. Batista, et al. (2012). "TPP1 OB-fold domain controls telomere maintenance by recruiting telomerase to chromosome ends." Cell **150**(3): 481-494.

Zhong, Z., L. Shiue, et al. (1992). "A mammalian factor that binds telomeric TTAGGG repeats in vitro." Mol Cell Biol **12**(11): 4834-4843.

Zhou, L., X. Cheng, et al. (2002). "Zebularine: a novel DNA methylation inhibitor that forms a covalent complex with DNA methyltransferases." J Mol Biol **321**(4): 591-599.

Zhu, W. G., T. Hileman, et al. (2004). "5-aza-2'-deoxycytidine activates the p53/p21Waf1/Cip1 pathway to inhibit cell proliferation." J Biol Chem **279**(15): 15161-15166.

Zhu, X. D., B. Kuster, et al. (2000). "Cell-cycle-regulated association of RAD50/MRE11/NBS1 with TRF2 and human telomeres." Nat Genet **25**(3): 347-352.

Zinn, R. L., K. Pruitt, et al. (2007). "hTERT is expressed in cancer cell lines despite promoter DNA methylation by preservation of unmethylated DNA and active chromatin around the transcription start site." Cancer Res **67**(1): 194-201.

List of websites

AMERICAN CANCER SOCIETY, 26/02/2013, 2013-last update, Breast Cancer. Available: www.cancer.org/acs/groups/cid/documents/webcontent/003090-pdf.pdf [10/06/2013, 2013].

CANCER RESEARCH UK, (14/05/2013, 2013-last update, About Breast Cancer. Available: http://www.cancerresearchuk.org/cancer-help/type/breast-cancer/about/ [10/06/2013, 2013].

COLLEGE OF AMERICAN PATHOLOGISTS, CAP, 28/05/2013, 2013-last update, Cancer Protocols, Breast Cancer, Invasive Ductal Carcinoma. Available: www.cap.org/apps/docs/reference/myBiopsy/BreastInvasiveDuctalCarcinoma.pdf [10/06/2013, 2013].

Cancer Research UK, 2008 http://www.cancerresearchuk.org/cancer info/cancerstats/types/breast/incidence/

Cancer Research UK, 2010, http://www.cancerresearchuk.org/cancer-info/cancerstats/types/breast/?script=true

Anatomy and physiology of the male and female: http://cnx.org/content/m46392/latest/

National statistic 2013: http://www.cancer.gov/cancertopics/types/breast

National Statistics, http://www.breastcancercampaign.org/about-breast-cancer/breast-cancer statistics?gclid=CPHAl_Xmj74CFQcTwwodTKUAYQ#breast-cancer statistics?gclid=CPHAl_Xmj74CFQcTwwodTKUAYQ&_suid=139912181429208675876083928262

Publication:

Motevalli, A., Yasaei, H., Anjomani Virmouni, S., Slijepcevic, P. and Roberts, T. (2014). “The effect of chemotherapeutic agents on telomere length maintenance in breast cancer cell lines”. Breast Cancer Res. Treat. **145**(1).

Appendix 1:

All sequences of POT1 exon12:

GTTGGAAGCTTTCTTAGAATCTATAGCCTTCATACCAAACTTCAATCAATGAATTCAGAGAATCAGACAATGTT
AAGTTTAGAGTTTCATCTTCATGGAGGTACCAGTTACGGTCGGGGAATCAGGGTCTTGCCAGAAAGTAACTCT
GATGTGGATCAACTGAAAAA

HMEC1

GTTGGAAGCTTTCTTAGAATCTATAGCCTTCATACCAAACTTCAATCAATGAATTCAGAGAATCAGACAATGTT
AAGTTTAGAGTTTCATCTTCATGGAGGTACCAGTTACGGTCGGGGAATCAGGGTCTTGCCAGAAAGTAACTCT
GATGTGGATCAACTGAAAAA

21NT

GTTGGAAGCTTTCTTAGAATCTATAGCCTTCATACCAAACTTCAATCAATGAATTCAGAGAATCAGACAATGTT
AAGTTTAGAGTTTCATCTTCATGGAGGTACCAGTTACGGTCGGGGAATCAGGGTCTTGCCAGAAAGTAACTCT
GATGTGGATCAACTGAAAAA

21MT-2

GTTGGAAGCTTTCTTAGAATCTATAGCCTTCATACCAAACTTCAATCAATGAATTCAGAGAATCAGACAATGTT
AAGTTTAGAGTTTCATCTTCATGGAGGTACCAGTTACGGTCGGGGAATCAGGGTCTTGCCAGAAAGTAACTCT
GATGTGGATCAACTGAAAAA

BT20

GTTGGAAGCTTTCTTAGAATCTATAGCCTTCATACCAAACTTCAATCAATGAATTCAGAGAATCAGACAATGTT
AAGTTTAGAGTTTCATCTTCATGGAGGTACCAGTTACGGTCGGGGAATCAGGGTCTTGCCAGAAAGTAACTCT
GATGTGGATCAACTGAAAAA

BT474

GTTGGAAGCTTTCTTAGAATCTATAGCCTTCATACCAAACTTCAATCAATGAATTCAGAGAATCAGACAATGTT
AAGTTTAGAGTTTCATCTTCATGGAGGTACCAGTTACGGTCGGGGAATCAGGGTCTTGCCAGAAAGTAACTCT
GATGTGGATCAACTGAAAAA

HCC1143

GTTGGAAGCTTTCTTAGAATCTATAGCCTTCATACCAAACTTCAATCAATGAATTCAGAGAATCAGACAATGTT
AAGTTTAGAGTTTCATCTTCATGGAGGTACCAGTTACGGTCGGGGAATCAGGGTCTTGCCAGAAAGTAACTCT
GATGTGGATCAACTGAAAAA

GI101

GTTGGAAGCTTTCTTAGAATCTATAGCCTTCATACCAAACTTCAATCAATGAATTCAGAGAATCAGACAATGTT
AAGTTTAGAGTTTCATCTTCATGGAGGTACCAGTTACGGTCGGGGAATCAGGGTCTTGCCAGAAAGTAACTCT
GATGTGGATCAACTGAAAAA

Figure S1-POT1 exon12 in cancer and control cell lines.

MCF-7
GTTGGAAGCTTTCTTAGAATCTATAGCCTTCATACCAAACTTCAATCAATGAATTCAGAGAATCAGACAATGTT
AAGTTTAGAGTTTCATCTTCATGGAGGTACCAGTTACGGTCGGGGAATCAGGGTCTTGCCAGAAAGTAACTCT
GATGTGGATCAACTGAAAAA

HS578-T
GTTGGAAGCTTTCTTAGAATCTATAGCCTTCATACCAAACTTCAATCAATGAATTCAGAGAATCAGACAATGTT
AAGTTTAGAGTTTCATCTTCATGGAGGTACCAGTTACGGTCGGGGAATCAGGGTCTTGCCAGAAAGTAACTCT
GATGTGGATCAACTGAAAAA

PB1
GTTGGAAGCTTTCTTAGAATCTATAGCCTTCATACCAAACTTCAATCAATGAATTCAGAGAATCAGACAATGTT
AAGTTTAGAGTTTCATCTTCATGGAGGTACCAGTTACGGTCGGGGAATCAGGGTCTTGCCAGAAAGTAACTCT
GATGTGGATCAACTGAAAAA

PC3
GTTGGAAGCTTTCTTAGAATCTATAGCCTTCATACCAAACTTCAATCAATGAATTCAGAGAATCAGACAATGTT
AAGTTTAGAGTTTCATCTTCATGGAGGTACCAGTTACGGTCGGGGAATCAGGGTCTTGCCAGAAAGTAACTCT
GATGTGGATCAACTGAAAAA

Figure S1-POT1 exon12 in cancer cell lines.

Appendix 2:

HMEC1: TAGTTAATTTTGTTTAGTGG

21MT-2: TAGTTAATTTTGTTTAGTGG

GI101: TAGTTAATTTTGTTTAGTGG

21NT: CGTTTAATTTCCGTTTCGTGG

Figure S2-Sequence of POT1 promoter region in untreated cancer and control cell lines.

Appendix 3:

DMSO: CGTTTAATTTCCGTTTCGTGG

5-aza-CdR: TAGTTAATTTTGTTTAGTGG

Figure S3-Sequence of POT1 promoter region in 21NT treated with 5-aza-CdR and DMSO for 72 hours.